Biosynthesis of fluoroacetate and 4-fluorothreonine in Streptomyces cattleya

Amin, Muhammad Ruhul

BIOSYNTHESIS OF FLUOROACETATE AND 4-FLUOROTHREONINE IN *Streptomyces cattleya*

Muhammad Ruhul Amin BSc (Hons)

PhD Thesis

University of Durham

1996

DECLARATION

The work contained in this thesis was carried out in the Department of Chemistry at the University of Durham in collaboration with the Department of Food and Agricultural Chemistry at the Queen's University of Belfast between October 1993 and July 1996. All the work was carried out by the author unless otherwise indicated. Incubation experiments with *S. cattleya* resting cells plus GC-MS analysis were performed at Queen's University. It has not been previously submitted for a degree at this or any other University.

To Amma and family

" Say : If the ocean were ink (wherewith to write out) the words of my Lord,
Sooner would the ocean be exhausted than the words of my Lord,
even if we added another ocean in its aid. "

(Translation of the meaning of Al-Qur'an, 18 : 109)

ACKNOWLEDGEMENTS

I am firstly indebted to my supervisor, David O'Hagan, for his valuable advice and support throughout the course of my PhD. My special thanks go to our collaborators at the Queen's University of Belfast (see photograph below); Prof. Dave Harper for his continued help and support, Cormac Murphy for his enthusiasm, hospitality and expertise with resting cell experiments and my good friend and colleague, Jack Hamilton for his superb GC-MS analyses and overall contribution to this project as a whole. A very special thank you to Ian McKeag for his expertise and patience in running the $^{19}F\{^{1}H\}$-NMR samples (500MHz).

I wish to express my sincere appreciation to BNFL for financial support, and my industrial supervisors (see photograph below); Dr. Harry Eccles, Dr. Roy Bowden and Dr. Peter Binks for the wonderful 'business' dinners and of course their continued support and interest in the project.

A special thank you goes to Dr. Naveed Zaidi, Bhai, for his guidance and exceptional advice with all aspects of practical Organic chemistry. Dr. Jens Nieschalk, with his ever helpful approach regarding synthetic Organic chemistry was very welcomed. Thank you to the technical staff; Dr. Kenwright, Julia Say, Dr. Ray Matthews for service NMR analysis, Dr. Tony Royston for his kind help with computing and of course Joe, Tom, Gordon, Ray and Elizabeth for their hospitality and cheerful character. How could I forget, the Store 'Superintendent', Jimmy, for the countless friendly arguments over the store counter. The generous help of my 'bellringing pseudoacademic' pal Kelvin was much appreciated. Thanks also to Dr. Andreas Batsanov and Janet Moloney for the X-ray crystallography.

Many thanks to the ever growing O'Hagan group; Dr. Jeff White, Dr. Dave Bailey, Dr. Nikki Chesters, Dr. Sarah Rogers, Dr. Jens Fuchser and pending doctors Colin, Adam, Caragh, Chi, Prash, Lee, Steve and Yannis. Thanks also go to my friend Dr. Raju Dasaradhi for his jokes that even made the test-tubes giggle, what a comedian ! 'Nuff Respect' goes out to Raz for his affectionate brothership and 'chilled' attitude.

I would also like to take this opportunity to acknowledge my dear respected brother Mehdi for his words of wisdom, my Qur'an and Arabic teacher Mustafa Tavasli, and my close brothers Dr. Salamat Ali, Dr. Mark Amir Blower, Dr. Rauf Samadi, Abu Ayman, Br. Esam, Br. Azhar, Dr. Said and of course my mates; Arshed, Ismail, Mr. Khan, Kash, Shaqueel and 'rude boy' Zia. My 'A' Level teacher, Mr. Newton, deserves a special mention for teaching Chemistry with such enthusiasm and dedication, thank you !

Last but not least, a big hug goes to my dear mother and father of Molik Pur, Fenchu Ganj, Sylhet in Bangladesh and my sisters, Sabina for her valuable ideas and advice, and Jennifer (or is it Anisa ?)

ABSTRACT

This thesis describes results on the biosynthesis of fluoroacetate and 4-fluorothreonine by the bacterium *Streptomyces cattleya*. Exploratory ^{14}C-radiolabelling experiments, designed to determine the relative incorporation of a range of metabolites into fluoroacetate, demonstrated that substrates such as glucose, glycine and serine were efficient precursors. [2-^{13}C]-Glycolate, [1,2-$^{13}C_2$]-glycolate, [2,2-$^{2}H_2$]-glycolate, DL-[3,4,4,4-$^{2}H_4$]-threonine, DL-[4,4,4-$^{2}H_3$]-threonine, [3,3,3-$^{2}H_3$]-alanine, [3-^{2}H]-fluoropyruvate and [3-^{2}H]-3-fluorolactate were synthesised and characterised. Incorporations of synthesised and commercially available putative precursors, [1-^{13}C]-glycine, [2-^{13}C]-glycine, [1,2-$^{13}C_2$]-glycine, [3-^{13}C]-serine, [1-^{13}C]-pyruvate, [2-^{13}C]-pyruvate, [3-^{13}C]-pyruvate, [2-^{13}C]-acetate, [3-^{13}C]-alanine, [2,3,3-$^{2}H_3$]-aspartate, [2,2,3,3-$^{2}H_4$]-succinate and [2-^{13}C]-glycerol into fluoroacetate and 4-fluorothreonine were assessed. [2-^{13}C]-Glycerol appeared to be the highest incorporated precursor of those tested. The ^{13}C label from [2-^{13}C]-glycerol predominated at C-1 (~56%) of fluoroacetate and C-3 (57%) of 4-fluorothreonine. ^{19}F-NMR emerged as a powerful analytical tool by which to determine the regiospecific incorporation of ^{13}C and ^{2}H into the fluorometabolites.

A conclusion to emerge from this study is that a glycolytic intermediate in *S. cattleya* appears to be a substrate for the bio-fluorination process. Incubation studies with [3-^{2}H]-fluoropyruvate and [3-^{2}H]-3-fluorolactate, tested as possible initial fluorination products, showed low incorporation of deuterium atoms into the fluorometabolites which did not reinforce a role for 2-phosphoglycerate, 3-phosphoglycerate and glycerol-3-phosphate as substrates for the fluorinating enzyme. The incorporations which are almost identical into the two fluorometabolites strongly indicate that the assembly of the carbon skeleton of fluoroacetate and C-3 and C-4 of 4-fluorothreonine involves a common biosynthetic intermediate. Thus the close metabolic relationship between the two fluorometabolites indicates the presence of a single fluorinating enzyme in *S. cattleya*.

A three step route to 4-(*2S,3S*)-fluorothreonine was developed by a modification of Seebach's imidazolidinone methodology for the preparation of L-threonine and is the subject of Chapter 4. An X-ray crystal structure of the synthetic 4-(*2S,3S*)-fluorothreonine assisted in assignment and confirmation of the absolute stereochemistry of the natural product. This modified methodology is amenable to isotope labelling by employing $NaB^{2}H_4$ to generate [3-^{2}H]-4-fluorothreonine. Moreover it offers an alternative route to *threo*-amino acids and has the advantage of using acid chlorides in place of aldehydes when the required aldehyde is unavailable.

ABBREVIATIONS

•	: carbon isotope label (^{13}C)
Ci	: Curie
μCi	: microcurie
Ac	: acetyl
ACP	: acyl carrier protein
ATP	: adenosine triphosphate
B.p.	: boiling point
BuLi	: n-butyllithium
Bz	: benzoyl
CI	: chemical ionisation
CoA	: coenzyme-A
d	: doublet
D	: deuterium atom
DCM	: dichloromethane
d.e.	: diastereomeric excess
DNA	: deoxyribonucleic acid
dt	: double triplet
dp	: double pentet
ee	: enantiomeric excess
EI	: electron ionisation
FAB	: fast atom bombardment
FAS	: fatty acid synthase
GC	: gas chromatography
GC-MS	: gas chromatography-mass spectroscopy
HPLC	: high performance liquid chromatography
IR	: infra red
LDA	: lithium diisopropylamide
LHMDS	: lithium hexamethyldisilazide
Me	: methyl
MES	: N-morpholinoethane sulphonic acid
mM	: millimolar

M.p.	: melting point
MS	: mass spectroscopy
MSTFA	: N-methyl-N-(trimethylsilyl)-trifluoroacetamide
NADH	: nicotinamide adenine dinucleotide, reduced form
NADPH	: nicotinamide adenine dinucleotide phosphate, reduced form
NMR	: nuclear magnetic resonance
m	: multiplet
p	: pentet
Ph	: phenyl
PKS	: polyketide synthase
P	: phosphate group, PO_4^{3-}
q	: quartet
RNA	: ribonucleic acid
s	: singlet
t	: triplet
TCA	: tricarboxylic acid cycle/ Kreb's cycle
THFA	: tetrahydrofolic acid
THF	: tetrahydrofuran
tlc	: thin layer chromatography

CONTENTS

CHAPTER 1

Introduction

CHAPTER 2

Exploratory experiments on fluorometabolite biosynthesis in *S. cattleya*

CHAPTER 3

$^{13}C/^{2}H$ labelling studies on fluorometabolite biosynthesis in *S. cattleya*

CHAPTER 4

Total synthesis of the natural product 4-fluorothreonine

CHAPTER 5

Experimental

APPENDIX A

Crystal Structure Data

APPENDIX B

Conferences, Presentations & Publications

APPENDIX C

Bibliography

CHAPTER 1

Introduction & Background

CHAPTER 1

1. General introduction and background

Time has witnessed humanity's quest in harnessing the natural resources available for its benefit and progress. Human civilisations have always been conscious of the numerous chemicals present in nature. Evidence of their acquaintance with these biomolecules has been manifested through the earliest disciplines in folk medicine, perfumery and the process of dyeing fabrics/ materials. Human awareness of natural poisons invited their use as potential weapons, the ancient Chinese civilisation, for instance, were accustomed to using the arrow poison aconite, while Indian medicine, around 900 BC, was not unfamiliar with arsenic and opium.[1] Many of these natural compounds were derived from crude plant extracts and found their applications in early human cultures as medicines **(1)**, poisons **(2)**, stimulants **(3)**, narcotics **(4)** and perfumes **(5)** [2] (Fig. 1.1).

Such compounds derived from natural sources are termed 'natural products' or secondary metabolites. These products play a critical role in the homeostasis of the ecosystem, functioning as chemical messengers in complex communicative, defensive and attractive interactions[3] between organisms as well as acting as the major source of therapeutic agents for humankind.[4] The interest and excitement generated by the origin of natural products is sufficiently unique that it ranks as a separate discipline in the field of organic chemistry.

Scientists working in the field of biosynthesis are fuelled by the structural curiosity of secondary metabolites plus the intriguing mechanisms and pathways by which they are produced and furthermore by their medicinal and pharmacological applications. It comes as no surprise that a great number of secondary metabolites have been isolated, identified and synthesised in a relatively short period of time. The myriad of known and unknown natural products offers an almost unlimited scope for probing the intricate ways in which nature has been programmed to synthesise these fascinating molecules.

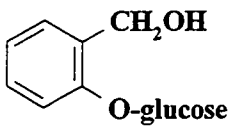

(1)

salicin (from willow bark)

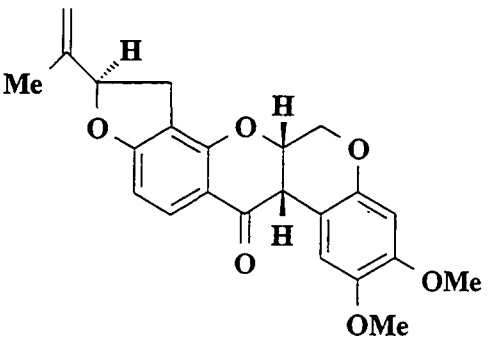

(2)

rotenone (fish poison)

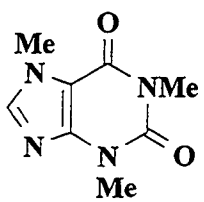

(3)

caffeine

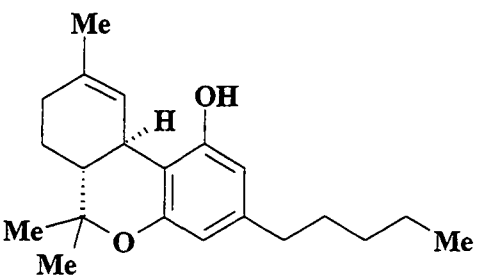

(4) tetrahydrocannabinol

(marijuana, hashish)

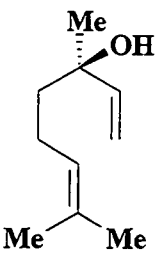

(5) linalol (lavender oil)

Fig. 1.1

1.1 Primary and Secondary Metabolism

Natural products are synthesised (anabolism) and degraded (catabolism) by a series of biochemical reactions catalysed by enzymes. Anabolism and catabolism are the two processes collectively known as metabolism. Primary metabolic pathways operate in all living systems and are responsible for synthesis and utilisation of universal metabolites such as sugars, amino acids, fatty acids, RNA, DNA to sustain the basic functions of all cells. In bacterial batch cultures, these metabolites are formed during the active phase of

cell growth (trophophase), while secondary metabolites usually accumulate after primary metabolite biosynthesis and cell growth has ceased during the period known as the stationary phase (idiophase) that follows the trophophase.[5] Therefore secondary metabolites (sometimes known as idiolytes)[6] are synthesised by non-dividing cells and have no direct function in sustaining normal cell growth. Unlike primary metabolites, secondary metabolites tend to be restricted to individual genera, species or strains and are found mostly in plants and micro-organisms.[7]

1.2 Functions of Secondary Metabolites

Various ideas have been proposed for the functions of secondary metabolites. There has been evidence to suggest that they serve sophisticated roles in the survival strategy of the producer by acting as chemical signals.[8-11] It is now quite clear that many secondary metabolites mediate intra- and inter- specific interactions, i.e. plant-plant interactions (allelopathy),[3,12] plant-insect interactions, plant-micro-organism interactions. These types of interactions generally benefit their producers as poisons and consequently offer a defensive strategy assisting survival of the organism in competitive surroundings.

1.2.1 Plant-plant Signalling

Plant secondary metabolites exhibit inhibitory effects on the seed germination and growth of other plants in the same competitive environment (allelopathy).[13] The leaves and roots are usually responsible for the release of these particularly harmful chemicals either by evaporation into the atmosphere or by leaching through soil.[2] Various types of air-borne monoterpenes and water soluble phenols are used by these plants as 'allelopathic' agents, examples include camphor **(6)** and vanillic acid **(7).**

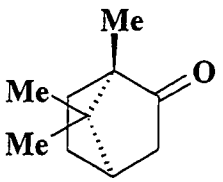

(6)

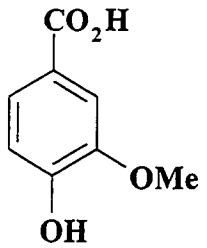

(7)

1.2.2 Plant-insect/ herbivore Signalling

Plants have developed protection and survival strategies by producing offensive substances that act as antifeedants to a wide range of insects and herbivores.[14-18] Two examples include the potent cyanogenic glycosides[19] **(8)** which hydrolyse to the poison HCN in predators, and azadirachtin **(9)** which has been exploited for centuries by the natives of the Indian subcontinent as an insect/ pest repellent.[20]

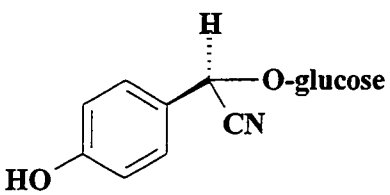

(8)

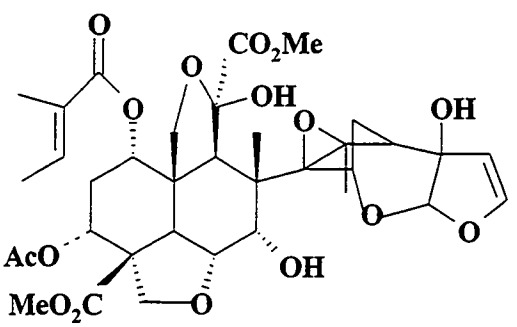

(9) azadirachtin

(isolated from Indian neem tree)

Not all plants, however, produce deterrents, many synthesise chemical attractants which serve to stimulate the visual (colour), olfactory (floral fragrances) and taste senses in host organisms.[21] For example, the odour of the triene **(10)** attracts the honey bee and indirectly assists in the pollination of clovers.[2]

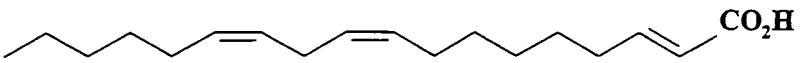

(10)

1.2.3 Insect-insect Signalling

The major function of secondary metabolites in this type of interaction is thought to be in communication through sex or trail pheremones.[22] These communication compounds are typically derivatives of phenols, monoterpenes and fatty acids. Sex pheremones **(11)** serve as chemical attractants for mating and sometimes hunting, *e.g.* the bolas spider is capable of producing female sex pheremones belonging to many species of moth.[2] These phoney pheremones attract male moths which become the victims of the predator.

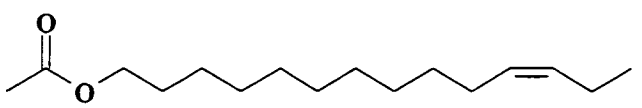

(11)

Natural pheremone of the 'redbanded leaf roller' insect

1.2.4 Animal-animal Signalling

Toxic metabolites used for defence are not simply restricted to insects, many aquatic animals secrete metabolites to deter potential predators, *e.g.* the Pacific sole produces pavoninin **(12)** to repel sharks.[2]

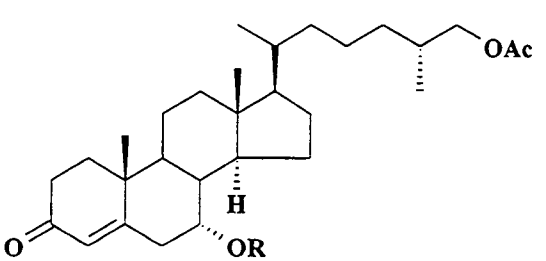

(12) R = Sugar

Tropical frogs have long been known by the natives to produce toxins, *e.g.* the Colombian frog discharges the poison batrachotoxin **(13)** in times of danger.[23]

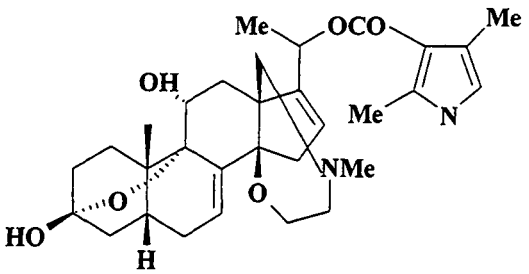

(13)

An alternative suggestion for the functions of secondary metabolites is that they serve to maintain primary metabolism at a time when the products of primary metabolism cannot be used for cell replication, until such time as growth can resume.[24] However, on a general note, secondary metabolite production appears to be prevalent in those organisms, plants and micro-organisms, which appear to lack an immune system.

1.3 Secondary Metabolic Products and Man

We are surrounded by many secondary metabolites in our daily life. Beverages and foodstuffs owe their distinctive aroma and flavour to various secondary products. The balance between good and bad smells and tastes is strongly dependent on the dosage or concentration of the metabolites present.[10] Various complex components are responsible for the characteristic essence of the foodstuffs but some fruits may contain only one such component, *e.g.* ethyl 2-methylbutyrate is responsible for the distinctive aroma of apples and the pungent odour of garlic is due to the chemical diallyldisulphide. A comparison of the flavouring principles in peach (undecalactone) and coconut (α-nonalactone) clearly demonstrates that there are no simple relationships between the chemical structure and flavour of secondary products.[10]

Secondary products are also found as principle components of drugs and medicines and a great number find their applications in the pharmaceutical industry.

Quinine **(14)** acts as an anti-malarial agent and L-scopolamine **(15)** is used as a cerebral sedative, and premedication prior to surgery for limiting saliva secretion.

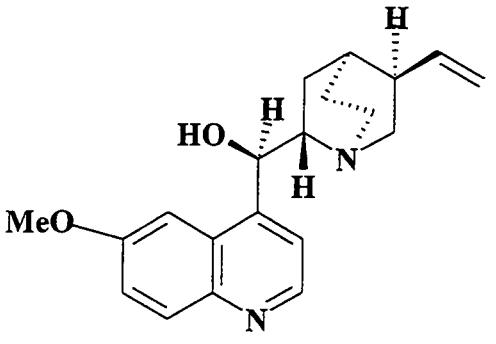

(14)

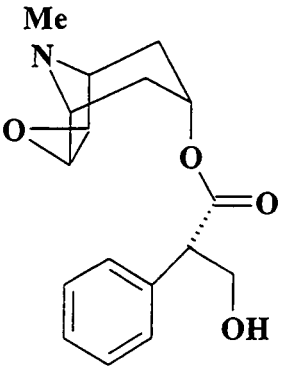

(15)

Antibiotics are by far the major contributors to the treatment of disease *e.g.* penicillins **(16)** and tetracyclines **(17).**

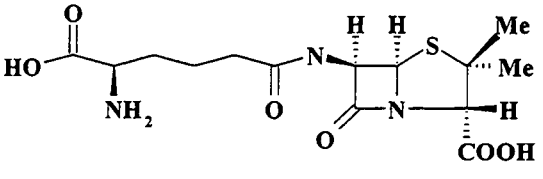

(16) **penicillin N**

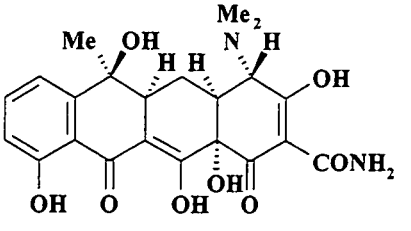

(17)

Stimulants and narcotics are in widespread use in many countries.[25] Examples of these plant based stimulants include nicotine **(18)** a constituent of tobacco leaves, and arecaidine[10] the main ingredient in betel nuts chewed by millions in Southeast Asia. The acute hallucinogenic properties of the narcotic, cocaine **(19)**, have promoted its use and abuse throughout the world and like most narcotics it is able to support an economy of its own.

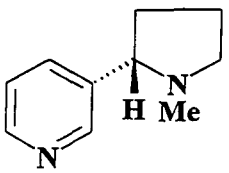

(18)

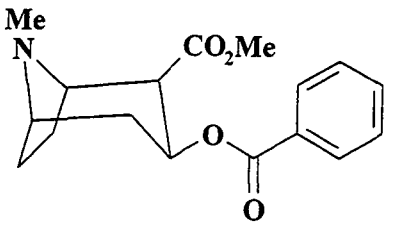

(19)

In contrast to the numerous beneficial aspects of secondary metabolites, many pose a direct threat to human life. Poisonous compounds have presented a widespread problem since the dawn of civilisation. Early humans used these products for hunting (curare alkaloids isolated from plants and frogs) and also for killing other humans, but today these metabolites serve as the toxic constituent of various pesticides.[10] Accidental poisoning from toxic fungi, berries and seeds accounts for a majority of acute poisoning cases[10] and this can only be circumvented by increasing our knowledge of the natural toxins in our environment.

1.4 Biosynthesis of the Major Classes of Natural Products

There are several principal building blocks for the biogenesis of secondary metabolites. These are acetate, mevalonate, shikimate and the amino acids. Acetyl-CoA is the precursor of polyketides (including certain phenols and other aromatics) and fatty acid derived metabolites like the prostaglandins and leukotrienes. Mevalonate is the progenitor of isoprenoids and steroids, while shikimic acid is used in the production of aromatic amino acids and certain polyphenols. Amino acids are the biosynthetic precursors of the alkaloids and peptide antibiotics. However, one must note that many secondary metabolites are of mixed biosynthetic origin.

1.4.1 Fatty acids[26-29]

Fatty acids are primary metabolites formed by the condensation of acetyl-CoA **(20)** units catalysed by fatty acid synthases (FAS) as outlined in Fig. 1.2[30]

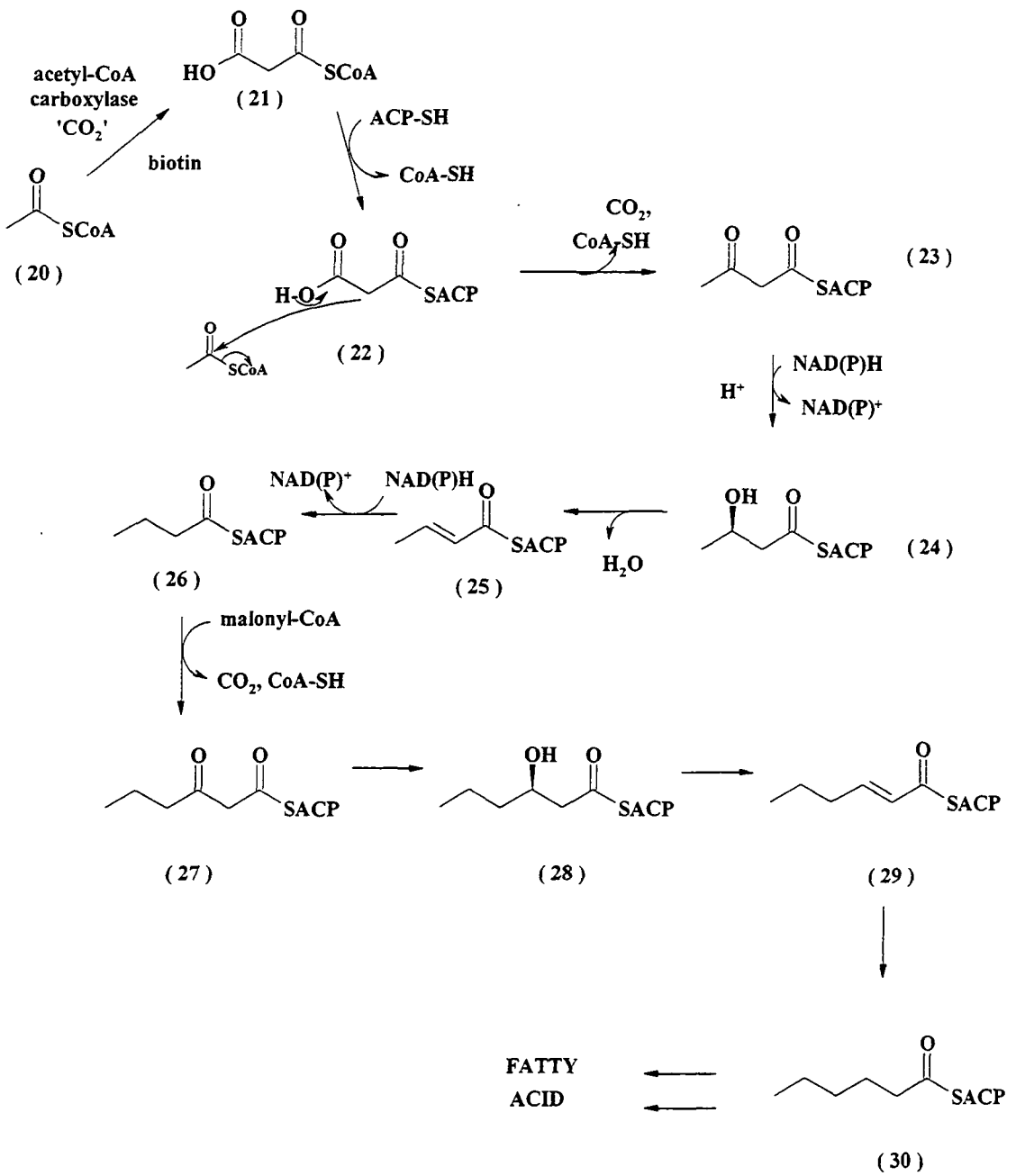

Fig. 1.2

Acetyl-CoA **(20)** is activated to malonyl-CoA **(21)** by acetyl-CoA carboxylase and then malonyl-CoA undergoes transesterification with the ACP of the relevant FAS followed by a decarboxylative condensation to generate a β-keto intermediate. A series of reductive steps then generate a saturated fatty acid. This process repeats itself until the fatty acid is fully elaborated.

1.4.2 Polyketides[31]

Polyketides have a very diverse range of structures that are based on linear β-polyketone chains. These chains can be assembled from the condensation of C_2 units $(-CH_2CO)_n-$) or C_3 propionate units $(-CHMeCO)_n-$) in a rather analogous manner to the classical fatty acid biosynthesis. However, unlike the fatty acid backbone, the corresponding polyketide skeleton may contain double bonds, ketone or OH functional groups. [Fig. 1.3, Route 1]. The various types of polyketide metabolites that may be formed are illustrated in Fig. 1.3. Route 2 occurs mainly in bacteria and marine organisms where the incorporation of propionate and butyrate units lead to pendant methyl and ethyl groups, respectively. One such example is the macrolide antibiotic aglycone, 6-deoxyerythronolide-B[30] **(34)**. Route 3 provides an example of a polyketide chain with continuous β-keto groups which give rise to aromatic phenols. It may be of interest to note that the marine environment is pre-eminent in elaborating various polyketide metabolites. Maitotoxin,[32] for instance, is the largest secondary metabolite known and is isolated from the marine organism, *G. toxicus.*

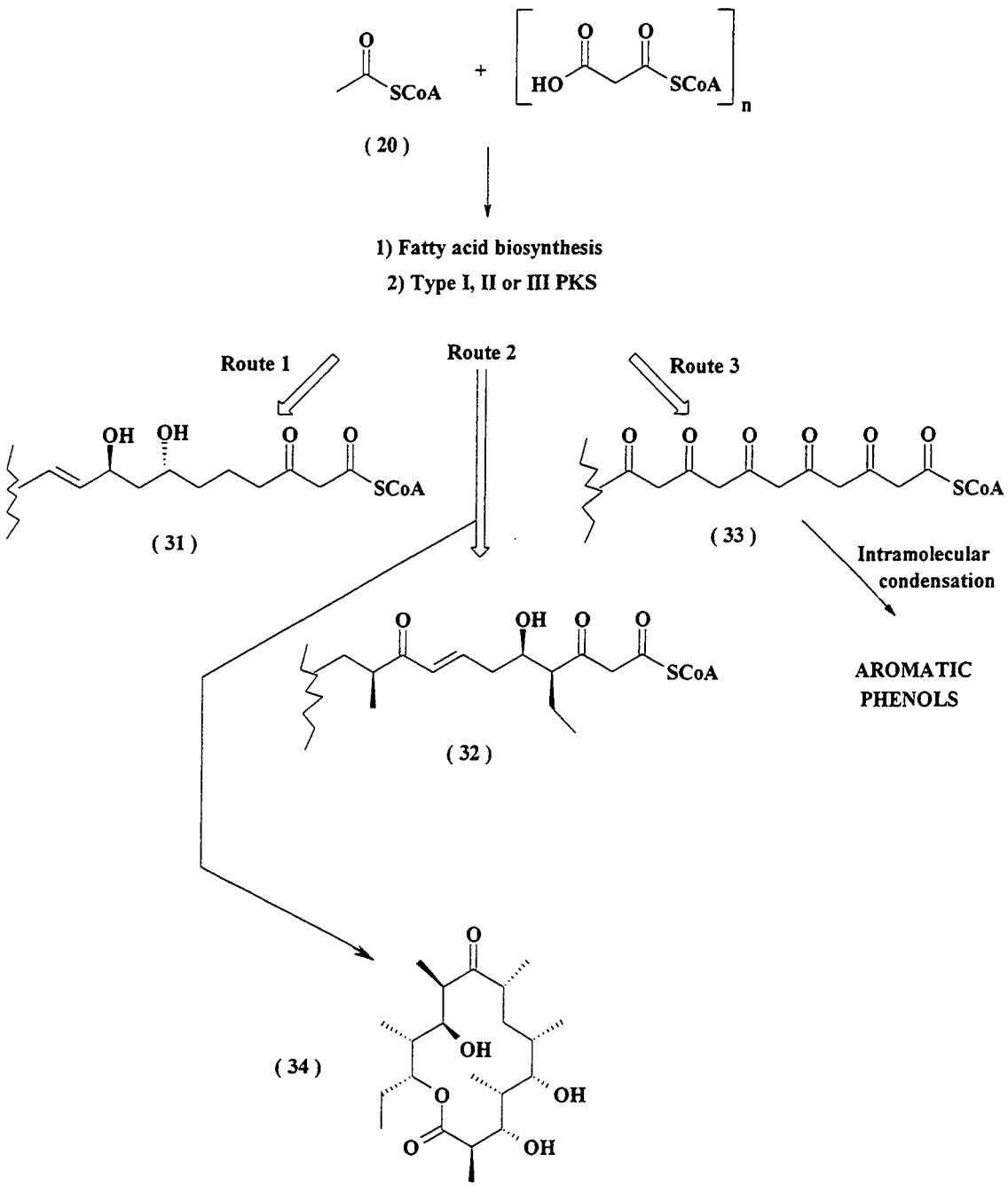

Fig. 1.3

1.4.3 Terpenes and Steroids [33,34]

Terpenes and steroids are based on the repeating isoprene (2-methylbutadiene) unit which is ultimately derived from acetyl-CoA *via* mevalonic acid. Terpenes and steroids appear to be widespread in plants, animals and micro-organisms and include compounds

such as menthol **(39)** and cholesterol **(40)**. The mechanism of the formation of the isoprene unit is outlined in Fig. 1.4.

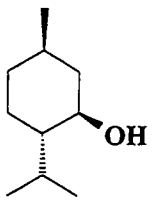

(39)

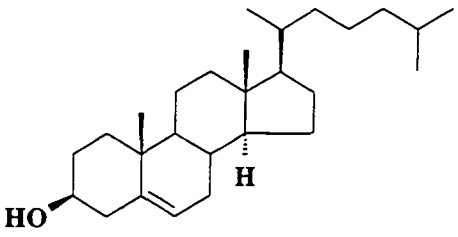

(40)

The Claisen ester condensation, catalysed by thiolase, between two molecules of acetyl-CoA is followed by an aldol type reaction to generate **(35)** which undergoes reduction to produce mevalonic acid (MVA) **(36)**.

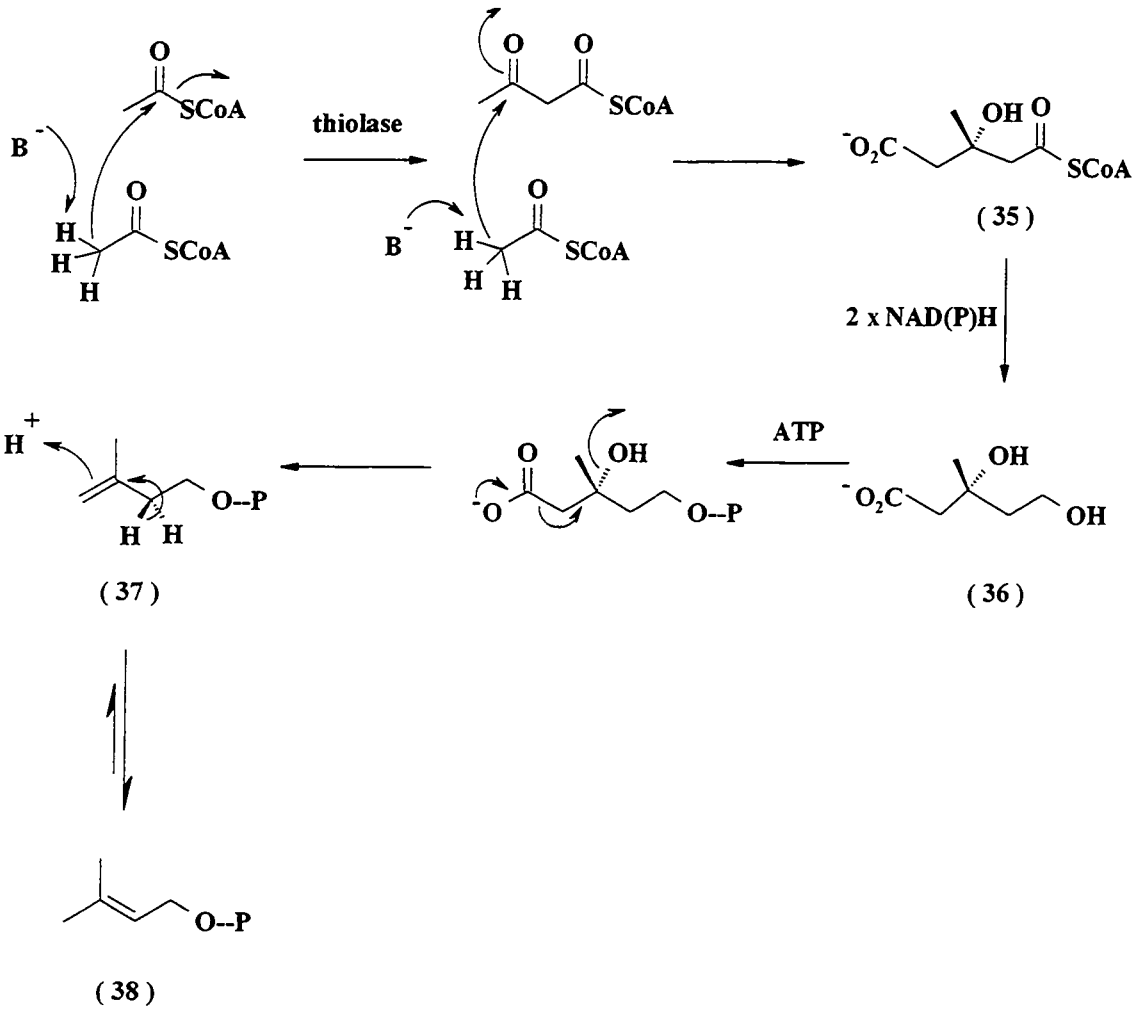

(35)

(37)

(36)

(38)

Fig. 1.4

This key intermediate is phosphorylated to MVA-5-pyro-phosphate which is then decarboxylated and dehydrated to produce the C_5 isoprene units isopentyl pyrophosphate (IPP) **(37)** and dimethylallyl pyrophosphate **(38)**. Organisms condense C_5 units to produce a vast array of isoprenoids such as monoterpenes[35,36] (C_{10}), diterpenes[37] (C_{20}), sesterterpenes[38,39] (C_{25}), steroids[40] and triterpenes[41] (C_{30}).

1.4.4 Shikimate pathway [42]

The shikimate pathway generates L-phenylalanine, L-tyrosine and L-tryptophan which are important progenitors of numerous secondary metabolites. The pathway which starts from erythrose-4-phosphate and phosphoenol pyruvate is shown in Fig. 1.5.

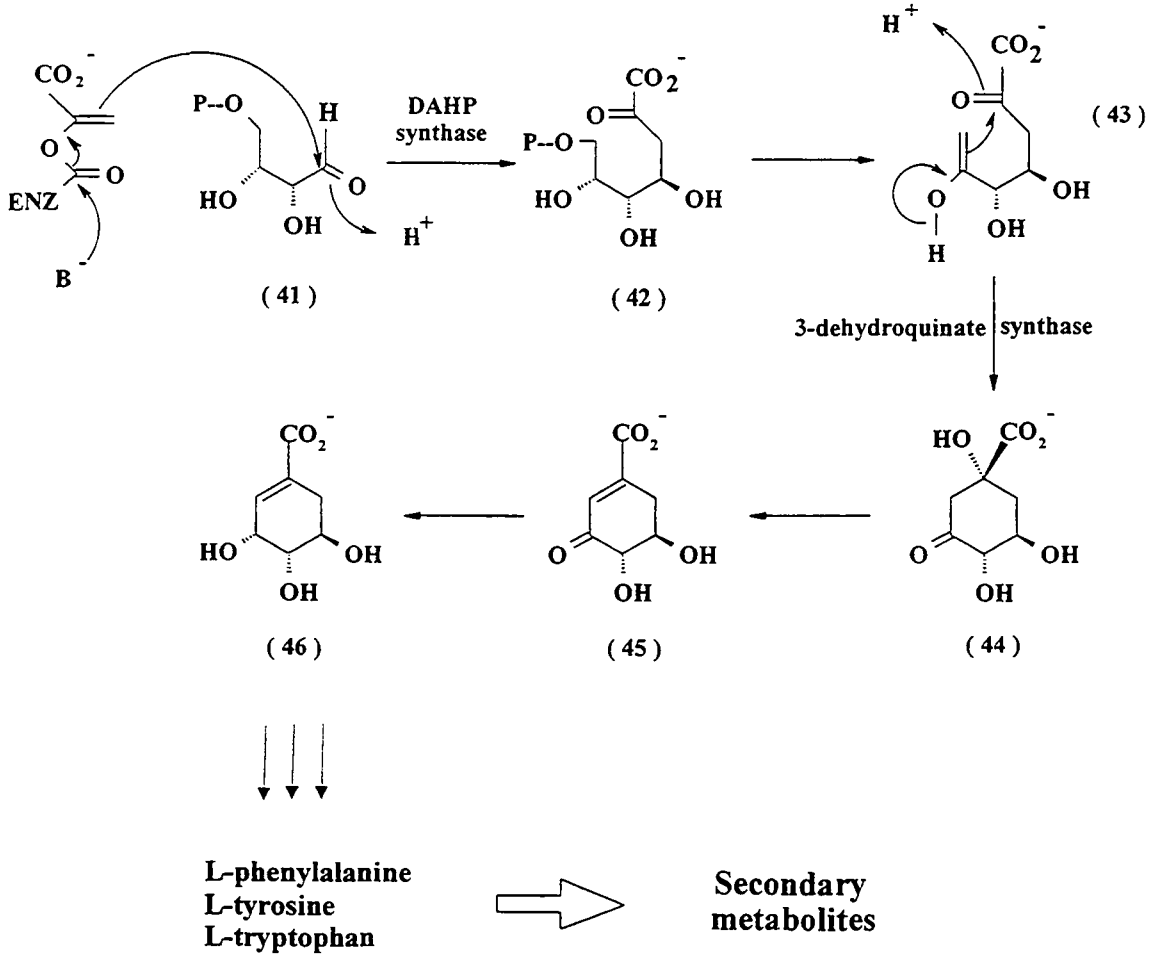

Fig. 1.5

Shikimate derives from an aldol reaction between phosphoenol pyruvate and the sugar, erythrose-4-phosphate **(41)** to produce 3-deoxy-D-arabino-heptulosonate-7-phosphate (DAHP) **(42)**. This key intermediate loses phosphate and cyclises to 5-dehydroquinic acid **(44)** which is subsequently transformed to 5-dehydroshikimate **(45)** and shikimate **(46)**. Secondary metabolites which derive from shikimic acid tend to be largely distributed in plants and micro-organisms since animals cannot carry out the *de novo* synthesis of shikimic acid using this pathway. Thus L-phenylalanine and L-tyrosine are essential amino acids that must be obtained in the diet of the animal.

1.4.5 Alkaloids [43]

The alkaloids which are essentially non-peptidic, non-nucleosidic nitrogenous compounds, are a diverse and complex class of secondary metabolites.[7] The large majority of the alkaloids isolated to date are plant based but a rapidly growing number have been identified in arthropods, marine organisms, fungi, micro-organisms and amphibians.[44] They may be classified according to their ring systems, *i.e.* pyridine, pyrrolizidine, tropane, indole and purine alkaloids are but a few examples of the types of ring systems found in alkaloid structures. The majority of alkaloids are derived from amino acids or closely related compounds. For instance L-ornithine and L-lysine give rise to pyrrolizidine[45,46] and piperidine alkaloids respectively, L-phenylalanine and L-tyrosine are the progenitors of opium alkaloids and L-tryptophan is used for the biosynthesis of the indole alkaloids.[47]

In general, most alkaloids are toxic but some are known to act as antifeedants or as anti-microbial products. For example,[48] the Tiger moth which feeds on the plant Senecio, accumulates the pyrrolizidine alkaloid **(47)** which is highly toxic and the venom secreted by the Red-fire ant is known to possess insecticidal and antibiotic properties.

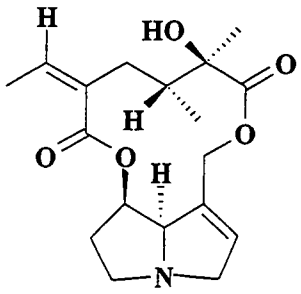

(47) senecionine

1.5 Techniques used to Delineate Secondary Metabolic Pathways

Generally, biosynthetic pathways are elucidated by experimental methods which lead to the establishment of precursor-product relationships. Once the structure of the metabolite has been rationalised it is possible to hypothesise a biosynthetic pathway from a particular precursor species. In the search for the origins and mechanism of formation of secondary metabolites a variety of techniques have developed.

1.5.1 Radioisotopic Labelling

The most important radioisotopes used in biosynthetic studies of secondary metabolites are the β emitters ^{14}C ($t^1/_2$=5640years) and ^{3}H ($t^1/_2$=12.1years).[49] The phosphorus isotope ^{32}P serves an important role in the field of molecular biology but has found few applications in secondary metabolite studies.[50] Using ^{14}C and ^{3}H, the fates of individual C or H atoms of a precursor can be traced to the metabolite and so a measure of the incorporation rates of the putative precursors is possible. Despite the high sensitivity, the drawback of deploying radioactive isotopes as tracers is that site-specific data or a complete labelling pattern is provided only through time consuming chemical degradation of the resultant labelled material. It is also difficult to assess whether certain portions of universally labelled substrates are incorporated intact or undergo scrambling and then recombination. However with the emergence of stable isotopes and sophisticated nuclear magnetic resonance (NMR) techniques, radioisotopic

investigations are now chiefly used to gain an insight into the nature of the carbon precursor involved in the biosynthetic pathway.

Tritium labelling combined with ^{3}H-NMR spectroscopy is proving to be a useful probe.[49] ^{3}H-NMR spectra give sharp signals that are easily interpreted by virtue of the similarity of chemical shifts with proton resonances. Nonetheless, handling, storage, and cross contamination of radioactive materials continues to be a handicap.

1.5.2 Stable Labelled Isotopes [51]

The incorporation of NMR active stable isotopes into a secondary metabolite has the advantage of revealing important regiochemical data, *i.e.* the enriched atoms can be located quickly by a comparison of the resultant NMR spectrum with that of the natural abundance spectrum. The stable isotopes available for NMR spectroscopic analysis include ^{13}C (I=$^{1}/_{2}$), ^{2}H (I=1) [52], ^{15}N (I=$^{1}/_{2}$) [53] and ^{18}O (I=0).

^{2}H-NMR is a valuable analytical tool with the advantage that assignments are straightforward because the chemical shift values in ^{2}H-NMR are similar to those in the corresponding ^{1}H-NMR. In addition the low natural abundance (0.016%) makes it detectable at low incorporation levels. The main application of deuterium in this project is in conjunction with ^{13}C and ^{19}F nuclei (see Chapter 3)

1.5.2.1 Intact Bond Incorporation

α-shift

The incorporation of ^{13}C (natural abundance 1.1%) atoms from enriched precursors into secondary metabolites can be followed to specific carbons by analysis of the enrichments in the ^{13}C-NMR spectrum of the resultant metabolite. One effective

strategy is the incorporation of contiguous labelled (^{13}C-^{13}C) substrates which provide invaluable data about intact C-C bonds, *e.g.* the use of [1,2-$^{13}C_2$]-acetate as a tracer species has been valuable particularly in polyketide biosynthesis. The presence or absence of a residual ^{13}C-^{13}C coupling in the ^{13}C-NMR spectrum of the metabolite will discriminate whether the C-C bond has been transferred intact from the precursor to the metabolite.

In appropriate cases, atoms adjacent to ^{13}C may be substituted for other NMR active nuclei such as ^{2}H or ^{15}N. For instance when a single deuterium atom is directly bonded to a carbon-13, it couples to the carbon, changing its multiplicity to a triplet (^{2}H, I=1) and shifts its resonance to a lower frequency by $\Delta\delta$ = 0.25-0.3ppm (α-effect/ shift). The multiplicity and magnitude of the shift correlates directly to the number of deuterium atoms attached to the carbon atom. Similarly ^{13}C-^{15}N intact bond incorporations display isotopic induced shifts and couplings.[54]

Oxygen-18 is not NMR active, however, its presence can be determined by ^{13}C-NMR where an isotope induced shift in the signal reveals the presence of one ($\Delta\delta$ = 0.01-0.03ppm) or two ($\Delta\delta$ = 0.03-0.05ppm) ^{18}O atoms, directly bonded to the reporter carbon.

<u>β-shift</u>

An alternative approach to determining the incorporation of intact bonds is to make use of a precursor molecule in which the NMR active nucleus is two bonds away from ^{13}C. A combination of ^{13}C-$^{12}C_{\alpha}$-$^{13}C_{\beta}$, if incorporated intact, can be detected by a β-shifted resonance in the ^{13}C-NMR spectrum. This β-effect is smaller in magnitude than the α-shift, but is readily observable. Deuterium atoms located in a β position to the ^{13}C nucleus (^{13}C-$^{12}C_{\alpha}$-$^{2}H_{\beta}$) cause the ^{13}C-NMR resonance to shift to a lower frequency ($\Delta\delta$ = 0.05-0.08ppm per deuterium atom). ^{15}N in a molecule containing the sequence ^{13}C-$^{12}C_{\alpha}$-$^{15}N_{\beta}$ [54] also gives rise to a characteristic shift in the ^{13}C-NMR

spectrum. These strategies have proven effective at detecting two adjacent bonds that have remained intact during a biosynthetic process.

The single natural isotope of fluorine has an atomic mass of 19, and like hydrogen it has a spin quantum number $I=^{1}/_{2}$.[55] The coupling constants and chemical shifts of fluorine are an order of magnitude higher than those for hydrogen. In the context of this thesis ^{19}F-NMR spectroscopy emerges as a powerful analytical tool used to assess the incorporation of putative precursors into the fluorinated natural products, fluoroacetate and 4-fluorothreonine. A detailed discussion of the effect of deuterium β (^{19}F-$^{12}C_{\alpha}$-$^{2}H_{\beta}$) and γ (^{19}F-$^{12}C_{\alpha}$-$^{12}C_{\beta}$-$^{2}H_{\gamma}$) on ^{19}F-NMR resonances is deferred to Chapter 3 (section 3.1.1), but suffice to say at this stage a ^{19}F-^{12}C-^{2}H combination induces an observable β-shift in the ^{19} F-NMR spectra relative to ^{19}F-^{12}C-^{1}H. Similarly, an observable but smaller γ-shift is seen for ^{19}F-^{12}C-^{12}C-^{2}H.

1.5.3 Cell-free Extracts and Mutants [56]

Incorporation rates from tracer experiments are often low since administered substrates can suffer metabolic degradation within the cell. Enzyme preparations/ cell-free extracts offer the possibility of obtaining detailed information about each step of a secondary metabolic pathway. However, enzymatic work can only be initiated after enzyme-substrate relationships have been developed on the particular pathway in question.

For a particular biosynthetic sequence, a primary metabolite **(PM)** may be converted by a series of enzymatic transformations (*e.g.* $\mathbf{E_1}$ to $\mathbf{E_4}$) to an end product **(Z)**, *via* intermediates (**W**, **X**, **Y**).

$$\mathbf{PM} \xrightarrow{\mathbf{E_1}} \mathbf{W} \xrightarrow{\mathbf{E_2}} \mathbf{X} \xrightarrow{\mathbf{E_3}} \mathbf{Y} \xrightarrow{\mathbf{E_4}} \mathbf{Z}$$

The sequence may be blocked at different stages by disrupting the expression of the relevant enzymes ($\mathbf{E_1}$ to $\mathbf{E_4}$). This can be achieved by inducing (chemically or by UV

radiation) a mutation in the wild type organism which damages the expression of a given enzyme. If, for example, $\mathbf{E_3}$ is no longer functional (in mutant strain 1) then **X** may accumulate in this mutant and its structure can then be determined. If the expression of $\mathbf{E_4}$ is blocked in another mutant (strain 2), this may result in the accumulation of **Y**. Clearly if **Y** is incubated with strain 1 in a co-synthesis study then **Z** should be produced if it is a true intermediate in the pathway. Similarly if **X** is introduced to strain 2 then **Y** should be produced. By such co-synthesis studies, the biosynthetic pathway may be elucidated.[57]

1.6 Organofluorine Compounds

Henri Moissan, in 1886, was the first to isolate fluorine by electrolysing anhydrous hydrofluoric acid in a platinum electrochemical cell containing dissolved potassium fluoride.[58] However, it was not until the late 1930's that fluorine was generated at any significant level and in this case for the preparation of fluorocarbons as refridgerants. Since then organofluorine compounds have attracted much attention from the chemical industry and they now play an increasingly significant role in the agrochemical and pharmaceutical industries. The widespread use of fluorine in organic chemistry is governed by its unique properties. The relatively high strength of the C-F bond (110 Kcal/ mol) compared with that for the C-H (99 Kcal/ mol) and C-Cl bond (85 Kcal/ mol) confers considerable chemical and thermal stability to organofluorine compounds. Insertion of fluorine into a compound induces minor steric, but significant electronic effects which can influence the chemical properties of that compound, *e.g.* monofluorination and trifluoromethylation of saturated aliphatic groups decrease lipophilicity,[59] a property which is an important consideration in the design of biologically active compounds. However introduction of a trifluoromethyl group into aromatic systems tends to increase the lipophilicity of the organic molecule. Fluorine has been used as both a -H and an -OH mimic in bio-organic chemistry and the CF_2 group has been used in certain cases to mimic -O.[60-62]

1.6.1 Uses of Organofluorine Compounds

Fluorine containing substances can be divided into two categories on the basis of their preparation and use. The first category is comprised of compounds which are :

(i) multiply fluorinated, and these include ;

fluorine containing anaesthetics, in particular halothane **(48)** which is extensively used in medicine.

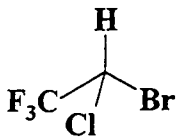

(48)

Bromine containing fluoroalkanes are the principal ingredient of fire extinguishers, *e.g.* CF_3Br, CF_2ClBr.[63] The major use of fluorine in organic compounds has been in the form of chlorofluorocarbons (CFC's) such as CCl_3F, CCl_2F_2 which were commonly employed as aerosol propellants, refridgerants and cleaning fluids prior to the Montreal Protocol. The production of HFC-134α (F_3C-CH_2F), having a considerably shorter stratospheric half-life is, however, on the increase. There is a growing market for fluorinated polymers, in particular PTFE (polytetrafluoroethylene) which owes its common usage to its outstanding chemical inertness and heat resistance. In addition, perfluorinated cycloalkanes are under development as potential blood substitutes[64] due to their low toxicity and ability to dissolve relatively high concentrations of oxygen.

(ii) Compounds with a low fluorine content (selectively fluorinated) have found applications as pharmacologically active substances, *e.g.* triamcinolone **(49)** which is used in the treatment of rheumatoid arthritis.[65]

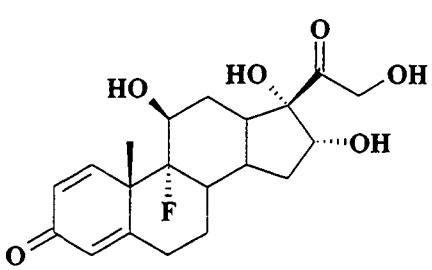

(49)

Fungicides **(50)**, insecticides and herbicides **(51)** dominate this category of organofluorine compounds and function mainly as agents for plant protection.[66] The properties of certain azo dyes can be changed by the introduction of a fluorine substituent into the molecule. *e.g.* its colour can be tuned depending upon the type and position of the fluorine containing substituent.

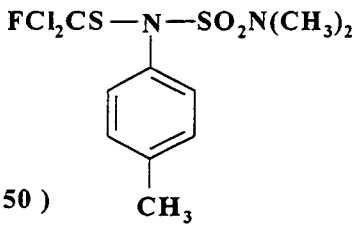

(50)

Euparen

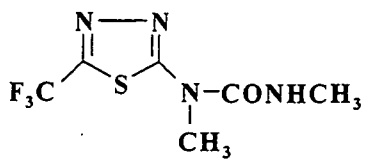

(51)

Thiazafluron

None-the-less by industrial standards, fluorine technology is still in its infancy. This is exemplified by the relatively crude and often unspecific methods of inserting fluorine into organic molecules. The current techniques for introducing fluorine into organic compounds require the use of catalysts such as the antimony halides, plus reagents such as hydrogen fluoride, metal fluorides, halogen fluorides and SF_4 which are difficult to handle on an industrial scale. Only recently has the direct fluorination (F_2) to selectively fluorinated compounds been explored in its application to fine chemicals. Biological fluorination, on the other hand, emerges as an attractive alternative but this is an arena which remains totally unexplored.

1.7 Fluorinated Secondary Metabolites in Nature

Of all of the elements, fluorine ranks 13th in natural abundance and is the most common halogen found in the Earth's crust.[67] Most of this fluorine is present as insoluble fluoride salts and therefore chlorine, due to its comparatively higher availability, is the most readily available halogen to living organisms. The fluoride content in soils is ultimately derived from minerals such as fluorospar (CaF_2), fluorapatite ($Ca_5FP_3O_{12}$) and cryolite

(Na_3AlF_6) amongst others. In addition, investigations have shown that the concentration of fluoride increases with soil depth.[68]

In sea water, fluoride is present in minute quantities (1.3ppm) in contrast to about 19 000ppm for chloride.[69] Nonetheless, inorganic fluoride is present in notable concentrations in certain marine life, such as the sponge *Halichondria moorei* which is capable of accumulating 10% fluorine on a dry weight basis as potassium fluorosilicate.[70] Terrestrial plants, particularly those of the genus *Camellia* can build up fluoride from quite low soil concentrations.[71] Plant species growing in areas with fluoride rich bedrock or areas polluted with fluorospar mining waste can selectively concentrate up to 10 000$\mu g\ g^{-1}$ dry weight fluoride.[72]

Organically bound fluorine is however scarce in nature. Only ten (five, plus five homologous fatty acids) naturally occurring organofluorine compounds have been identified in a small number of tropical and subtropical plants, and in only two micro-organisms. The unique physico-chemical properties of fluorine may provide an answer to the infrequent occurrence of these fluorinated natural products when compared to other halogenated metabolites. For comparison, over 130 chlorinated natural products are known to exist in plants alone,[73] and many more have been isolated from marine organisms.

Fluorine has been referred to as a 'superhalogen'.[74] This description can be appreciated from the data in Table 1.1 which shows a comparison of the physico-chemical parameters of fluorine and its family of halogens.

X	Bond dissociation energy CH_3-X (kcal/ mol)	Bond length C-X (Å)	Van der Waals radius (Å)	Hydration energy, X^- (kcal/ mol)	Electronegativity (Pauling scale)	Standrad oxid/ red. potential E° for $2X^- \rightleftharpoons X_2 + 2e^-$
F	110	1.39	1.35	117	4.0	-3.06V
Cl	85	1.78	1.80	84	3.0	-1.36V
Br	71	1.93	1.95	78	2.8	-0.07V
I	57	2.14	2.15	68	2.5	-0.54V
H	99	1.09	1.20	—	2.2	—

Table 1.1

It has the highest electron withdrawing power of all the elements forming the strongest single bond to carbon. In fluoroacetate for instance the bond remains intact when boiled in concentrated sulphuric acid and even a few hours are required to decompose it in hot concentrated alkaline conditions.

The small size of the fluoride ion and its consequent high charge density account for its unique susceptibility to bind to water molecules. It is indeed capable of containing up to five water molecules in its hydration sphere which can be compared with three for chloride, two for bromide and three or four for iodide.[58] As a direct result of the ease of solvation (high enthalpy of hydration) the nucleophilicity of the fluoride anion is significantly compromised in water. The high heat of hydration is also responsible for the high redox potential (-3.06V) for the oxidation of fluoride and this clearly highlights the difficulty in generating both the fluorine radical and cation, reactive forms which are essentially inaccessible in biochemistry. Haloperoxidases, for example, cannot oxidise fluoride, as hydrogen peroxide is not a sufficiently strong oxidising agent (Fig. 1.6). These properties of fluorine coupled with the difficulty of releasing a heavily hydrated fluoride ion within the cell are probably the most important factors restricting fluorine from playing an active role in biochemical processes.

$$2F^- \rightleftharpoons F_2 + 2e \quad (E^0 = -3.06\ V)$$

$$H_2O_2 + 2H^+ + 2e \rightleftharpoons 2H_2O \quad (E^0 = +1.71\ V)$$

Fig. 1.6

1.7.1 Fluorinated Natural Products in Plants

Plants have been found to be the richest source of fluorine containing natural products with over 40 varieties producing fluoroacetate, and in one case *Dichapetalum toxicarium* which produces a range of ω-fluorinated lipids (see 1.7.1.2). Fluoroacetate tends to accumulate in high concentrations in certain plants originating from tropical and subtropical regions of the world.

1.7.1.1 Fluoroacetate

Of the ten naturally occurring organofluorine metabolites, the most ubiquitous is the toxin fluoroacetic acid. In 1943 Marais[75,76] identified it from the S. African plant *Dichapetalum cymosum*, which was responsible for a considerable loss of cattle in the Transvaal region.[77] This low growing shrub, named Gifblaar (poison leaf) by the natives, proved to be exceptionally difficult to eliminate because of its persistent and extensive underground stem and root system.[78] The young leaves of the plant can accumulate fluoroacetate up to 2500 μg g^{-1} dry weight.[79] Plants generally contain 0.1 to 10 μg fluoride.g dry $weight^{-1}$,[80] but a few can store greater amounts from comparatively low soil concentrations. Recently fluoroacetate concentrations of up to 8000 μg g^{-1} dry weight have been recorded in the young leaves and seeds of *D. braunii* from south-eastern Tanzania.[81] This is the highest recorded level of the compound reported in a plant to date.

In Australia alone fluoroacetate has been identified as the toxic principle of at least 35 plant species.[82] The most widely studied Australian plant, *Acacia georginae* found in Queensland, accumulates the toxin in its leaves and seeds and can contain up to 250 and 400 μg g^{-1} of fluoroacetate in dry weight respectively.[83] There has been a report of a Brazilian species, *Palicourea margravii*, with a capacity to biosynthesise up to 5000 μg g^{-1} dry weight.[84] These reports suggest that fluoroacetate producing plants appear to be distributed in all tropical and subtropical regions of the globe.

The concentration of this toxin varies significantly between different organs in the plant.[85] The levels may also depend on the climate, geographical location, time of year and age of the species in question, e.g. at springtime the young shoots and leaves have high levels of fluoroacetate but as it matures the levels subside becoming negligible within a few months.[86]

1.7.1.2 ω-Fluorofatty acids

ω-Fluorinated fatty acids constitute about 3% of the lipids in the seeds of *D. toxicarium* found in Sierra Leone.[87] The major fluorinated constituent is ω-fluoro-oleic acid **(52)** with traces of fluorocapric **(53)** ω-fluoromyristic **(54)** and ω-fluoropalmitic **(55)** acids.[88] Recent re-examination of such seeds using GC-MS revealed the presence of more ω-fluorinated lipid derivatives.[89]

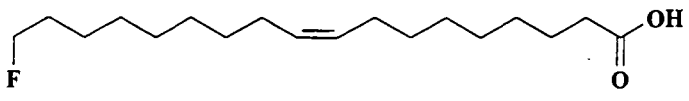

(52)

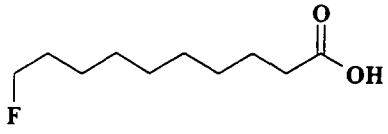

(53)

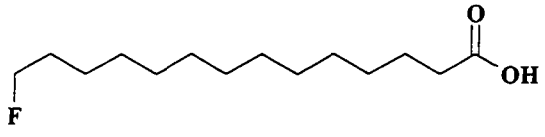

(54)

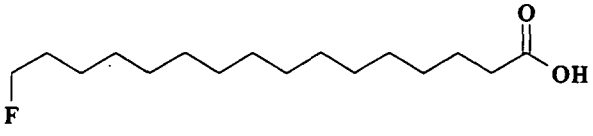

(55)

GC-MS investigations of the seed lipids of *D. toxicarium* revealed the low level presence of ω-fluoro derivatives of palmitoleic ($C_{16:1}$), stearic ($C_{18:0}$), linoleic ($C_{18:2}$), arachidic ($C_{20:0}$), eicosenoic ($C_{20:1}$) and docosanoic ($C_{22:0}$) acids. These ω-fluorofatty acids are extremely toxic waxes since they are readily absorbed through the skin and broken down to fluoroacetyl-CoA by β-oxidation processes.

In the fluorinated fatty acids identified from *D. toxicarium*, fluorine only occurs at the terminal carbon, and is consistent with fluoroacetyl-CoA replacing acetyl-CoA as the starter unit in fatty acid biosynthesis. A study conducted on the distribution of fluoroacetate within *D. toxicarium* suggested that fluoroacetate used in ω-fluorofatty

acid biosynthesis in the seed was not formed *in situ* but it is transported from the young leaves to the seeds.[86] This would explain why fluoroacetate was detectable in the young leaves and not the seeds.

1.7.1.3 Fluoroacetone

When Peters and Shorthouse [90] incubated homogenates of *A. georginae* and other plants with inorganic fluoride, they noticed a substantial loss of total fluorine from the solution. This loss could only be correlated in terms of its conversion into a volatile form. The volatile constituent in the homogenate was identified as fluoroacetone **(59)**.[91] Other volatile fluorinated compounds which were unidentified may have been produced, since fluoroacetone (hydrazone derivative) only accounted for 13% of the loss. The biosynthesis of fluoroacetone may be an early branching of fatty acid biosynthesis as depicted in Fig.1.7.

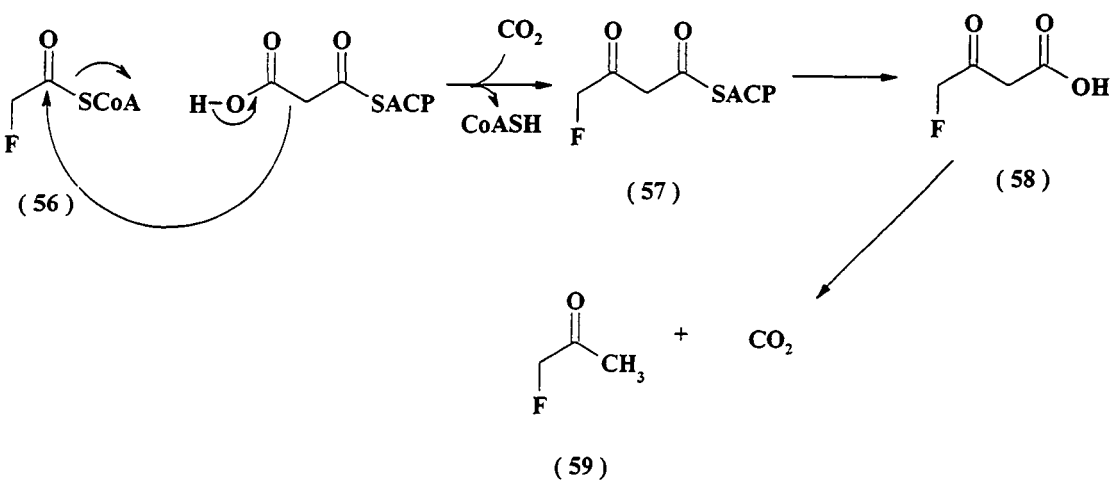

Fig. 1.7

If fluoroacetyl CoA replaced acetyl CoA in conventional fatty acid biosynthesis (section 1.4.1), a fluorinated β-ketothioester **(57)** would be formed. Hydrolysis would yield 4-fluoroacetoacetate **(58)** which could decarboxylate to give fluoroacetone **(59).** Since

the fluoroacetate concentration in plants, in particular *D. braunii,* drops dramatically from spring (7200 μg g $^{-1}$ dry weight) through to summer (200 μg g^{-1})[81], Peters speculated that here was a plausible detoxification strategy which could be induced whenever the requirement for the toxin diminished.

1.7.1.4 (2*R*,3*R*)-2-Fluorocitrate

The co-metabolite of fluoroacetate, (2*R*,3*R*)-2-fluorocitrate **(61)**, is produced *via* condensation of fluoroacetyl-CoA **(56)** with oxaloacetate **(60)**, a reaction mediated by citrate synthase. Fluorocitrate has been detected at various but low concentrations in forage plants such as soya bean and alfalfa,[92] and at low levels in oatmeal, while commercial tea [92] can contain up to 30μg g^{-1} dry weight. Stereochemical studies[93] on the citrate synthase reaction with fluoroacetyl-CoA have shown that the 2-*pro-S* hydrogen of the fluoroacetyl group is removed exclusively prior to condensation. Attack occurs with inversion of configuration at C-2 to liberate (2*R*,3*R*)-2-fluorocitrate as the single stereoisomer of four possibilities (Fig. 1.8).

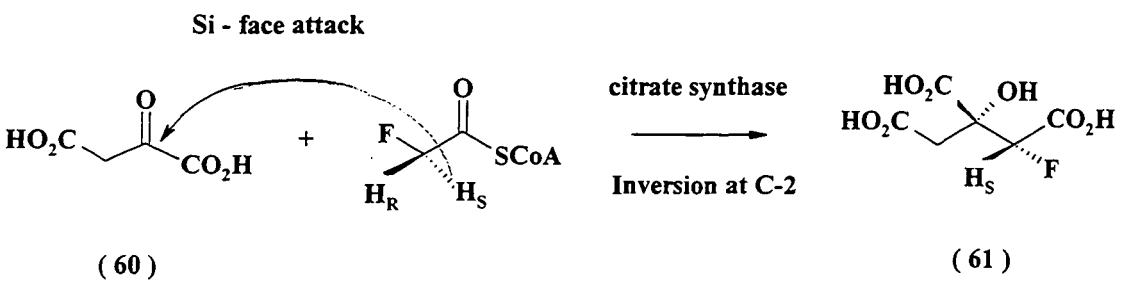

(60) (61)

Fig. 1.8

It is interesting to note that unlike malate synthase, citrate synthase is capable of distinguishing the difference between the prochiral protons of CH_2F.[94] Recent studies by O'Hagan *et al.* have proposed that this selectivity arises due to the intermediacy of a more stable E enol (over the Z enol) intermediate.[95]

Plants which accumulate high levels of fluoroacetate must clearly have mechanisms for preventing autotoxicity. Fluoroacetate, however, poses a problem to mammalian cells as it inhibits the central pathway responsible for generating metabolic energy - the citric acid cycle. Its toxicity has rendered it a rodenticide under the tradename 'Compound 1080'.[96] The oral lethal dose in humans is in the order of 6 mg kg^{-1} and 1080 has been responsible for accidental deaths and suicides.[97]

The toxicity arises when fluoroacetate **(62)** is converted to fluoroacetyl-CoA **(56)** which competes with acetyl-CoA **(20)** for the enzyme citrate synthase. The (2*R*,3*R*)-2-fluorocitrate stereoisomer (the other 3 isomers being non-toxic) is a potent mechanistic inhibitor of aconitase [E.C. 4.2.1.3.] (see Fig. 1.9).

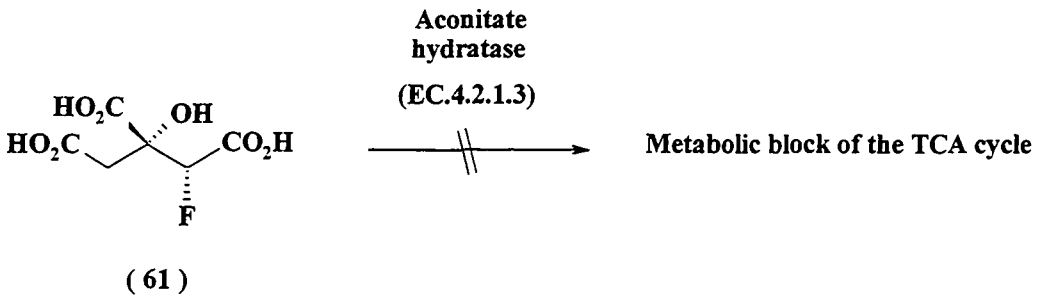

(61)

Fig. 1.9

More recently the studies of Kun and co-workers[98] have indicated that the inhibition of citrate transport was a more significant factor in fluoroacetate toxicosis. Their experiments suggested that a covalent bond is formed between ^{14}C radiolabelled fluorocitrate and inner mitochondrial membrane bound proteins leading to inhibition of citrate transport across the cell's mitochondrial membrane. Recently, Lauble *et al.*, showed that the crystal structure of the aconitase - (*2R,3R*)-2-fluorocitrate, enzyme-inhibitor complex, did indeed provide evidence of a strong interaction beween the enzyme and the inhibitor.[99]

1.7.2 Fluorinated Natural Products in Mammals and Insects

Organofluorine compounds are not restricted to the plant and microbial kingdoms. Animals such as the moth (*Nygmia pseudoconspersa*) feeding on a tea plant is capable of concentrating fluoride to a level of 5000μg g^{-1} dry weight in the wings and 1100μg g^{-1} in the cocoon.[100] Caterpillars of the moth *Sindris albimaculatus* feed on the young leaves and fruit of the fluoroacetate containing plant, *D. cymosum.* These caterpillars are highly toxic to predators and it has been postulated that fluoroacetate accumulates in vacuoles within the larvae.[101]

Human plasma has been reported to contain 1-4 μM of organic fluorine.[102] About 30% of this fluorine can be accounted for by perfluorofatty acids which are used in oil and water repellents for fabric treatment and in the formulation of waxes. The remaining 70% is probably anthropogenic in origin but this remains to be answered.

Marsupials, emus and bush rats of some regions of Australia have a remarkable tolerance to fluoroacetate poisoning compared with those from other parts of the continent.[103] Although no conclusive biochemical explanation has been given for this tolerance, one suggestion, bearing in mind that a glutathione-dependant defluorinating enzyme was found in the liver of the brush-tailed possum, is that glutathione may play a role in the resistance process. This may be achieved by either defluorination of fluoroacetate or fluorocitrate or possibly by affecting the enzyme aconitase, or citrate metabolism more generally.

1.7.3 Fluorinated Natural Products from Micro-organisms

1.7.3.1 Nucleocidin

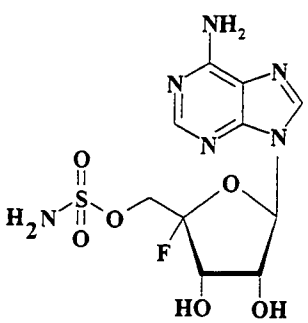

(64)

Streptomyces calvus, isolated from an Indian soil sample,[104] was shown to elaborate an adenine-containing antibiotic named nucleocidin **(64)**. This compound was the first fluorinated metabolite to be characterised from a microbial source, and it showed antibiotic activity against a broad spectrum of bacteria. It was particularly effective as an anti-trypanosomal agent.[105] However, its toxicity placed limitations on its clinical use. The total synthesis of this molecule confirmed the structure and absolute configuration as shown.[106] Fluoride was not an added component of the microbial culture media, however the medium contained trace levels in the mineral salts and tap water. Subsequent but unsuccessful attempts to re-isolate nucleocidin from *S. calvus* have prevented biochemical studies with this system. Nucleocidin is not obviously derived from fluoroacetate and may therefore involve a C-F bond-forming enzyme unique to *S. calvus.*

1.7.3.2 4-Fluorothreonine and Fluoroacetic Acid

Sanada *et al.*,[107] discovered that *S. cattleya,* when incubated in a culture medium containing inorganic fluoride, biosynthesised millimolar concentrations of the metabolites fluoroacetate and 4-fluorothreonine **(65)**. Evidence from ^{19}F-NMR studies showed that fluoroacetate accumulated in the culture medium to a concentration of 2-3mM.

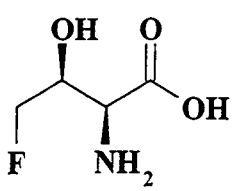

(65)

The compound is an optically active single stereoisomer proposed to be stereochemically analogous to L-threonine. Studies in this Thesis confirm this

stereochemistry. An acetylenic amino acid **(66)** was also isolated during purification of 4-fluorothreonine from the fermentation broth of *S. cattleya.*[108] The similarity in structure between this amino acid and 4-fluorothreonine may suggest a common biosynthetic origin however this is no experimental evidence in support of this. The identification of nucleocidin **(64)** and 4-fluorothreonine **(65)** are exciting and indicate that bacteria may emerge as an untapped source of novel fluorinated metabolites.

It is interesting to note that *Streptomyces sp. OH 5093* has recently been found to secrete the metabolite, 4-chlorothreonine[109] **(67)** which is probably stereochemically analogous to 4-fluorothreonine **(65)**. The biosynthesis of these two amino acids in *Streptomyces* could be similar.

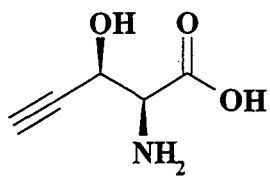

(66)

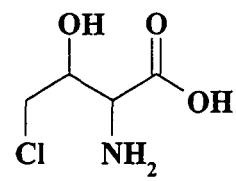

(67)

1.8 Fluoroacetate Dextoxification Strategies

Various explanations have been forwarded for the resistance of organisms to autotoxicity from fluoroacetate production. In plants it is thought that the toxin may be compartmentalised within cell vacuoles remote from the mitochondria, so avoiding conversion to fluorocitrate.[110] Plant aconitase may be less sensitive to fluorocitrate than animal aconitase, *i.e* it was reported that aconitase from sycamore (*Acer pseudoplatanus*) cells was 2000 times less sensitive to fluorocitrate than that from pig heart[111] and similarly it has been speculated that *D. cymosum* possesses a citrate synthase enzyme which has a low affinity for fluoroacetyl-CoA. Recently a hydrolase enzyme, capable of hydrolysing fluoroacetyl-CoA to fluoroacetate without affecting

acetyl-CoA, was discovered in cell free extracts of *D. cymosum.*[112] This enzyme would restrict the accumulation and processing of the metabolically active fluoroacetyl-CoA.

A number of micro-organisms namely *Pseudomonas spp., Penicillium spp.,* and *Fusarium oxysporium,* possess enzymes capable of cleaving the very stable C-F bond of fluoroacetate.[113] *Pseudomonas cepacia* (a symbiotic parasite of *D. cymosum*) has been found to defluorinate fluoroacetate[114] and it probably does this with the use of a halido hydrolase[115] (Fig. 1.10). The mechanism proposed involves attack of a thiol group (since the enzymes are quite sensitive to thiol blocking agents) to fluoroacetate displacing fluoride and generating a thioether which hydrolyses to glycolate **(63)**, the defluorinated product. The defluorinating activity of a variety of soil inhabiting micro-organisms, found in Western Australia, is well documented in the literature.[116]

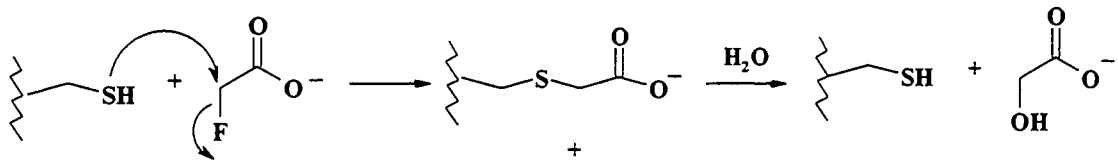

Fig. 1.10

Some mammals and birds in the same region appear to have an increased fluoroacetate tolerance compared with animals in other areas of Australia and concomitantly have increased glutathione levels.[117] Interestingly, the moth *Sindris albimaculatus* is capable of degrading fluoroacetate to inorganic fluoride and CO_2.[101]

1.9 Proposed Mechanisms to Organofluorine Metabolites

1.9.1 Pyridoxal Phosphate - Catalysed Incorporation of Fluoride

Plants contain a multitude of β-substituted alanines[118] which are believed to be formed by nucleophilic attack at C-3 of a pyridoxal phosphate enamine adduct.

A. georginae elaborates at least seven β-substituted alanines suggesting that the process is mediated by a non-specific synthase which catalyses the incorporation of a range of nucleophiles to generate the various structures (Fig. 1.11).

In the light of these findings, Mead and Segal[119] postulated that the biosynthesis of fluoroacetate could involve a pyridoxal phosphate enamine with fluoride as the nucleophile (Fig. 1.12). The hypothesis essentially involves the attack of a pyridoxal phosphate enamine intermediate **(68)** by a fluoride ion to produce pyridoxamine phosphate-bound fluoropyruvate **(72).** This intermediate **(74)** may undergo hydrolysis to fluoropyruvate **(74)** which can then decarboxylate to form fluoroacetic acid **(62)**. The hypothesis was tested by investigating the effect of cyanide and fluoride ions on the conversion of L-cysteine to pyruvate in cell-free extracts of *A. georginae.* Cyanide inhibited this conversion and β-cyanoalanine was isolated, which indicated that the enamine adduct underwent nucleophilic attack by CN^-. However, there was no evidence of fluoropyruvate **(74)** formation and no detectable traces of β-fluoroalanine **(73)**.

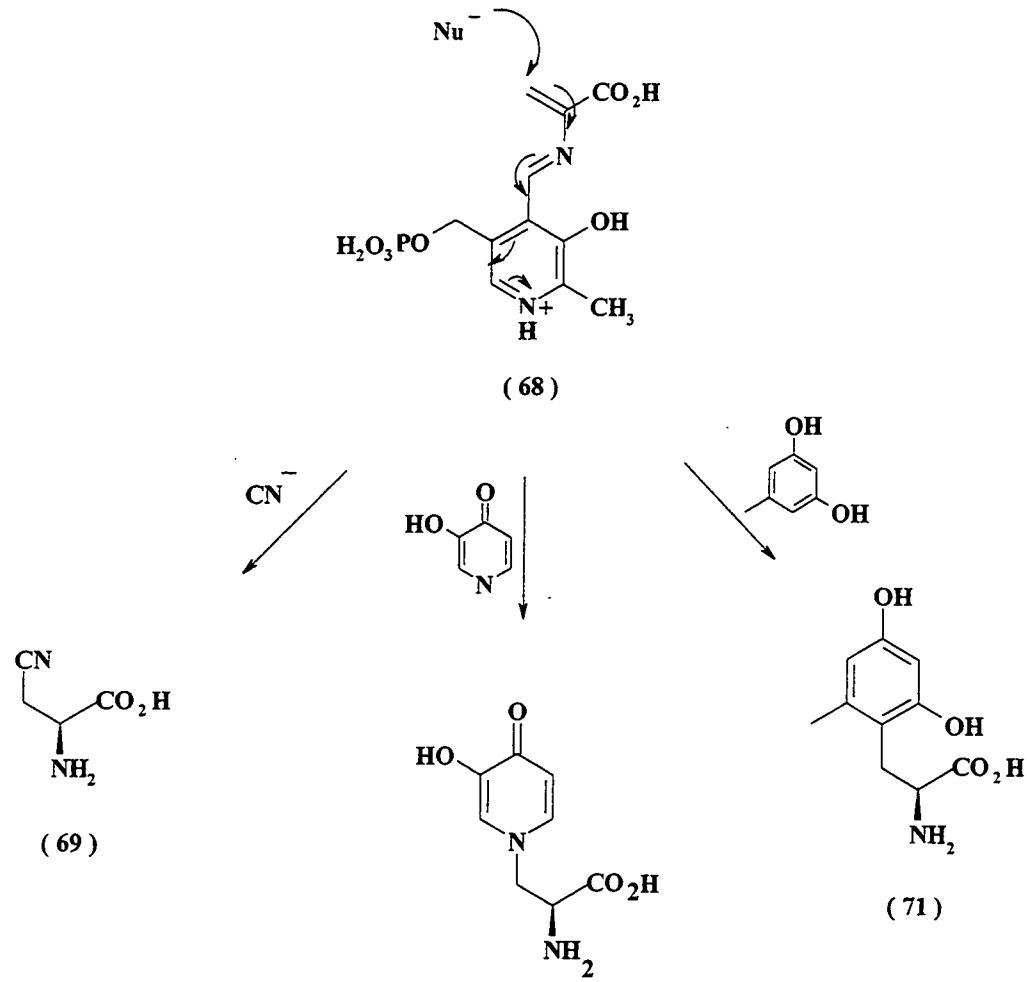

Fig. 1.11

These results tend to suggest that this pathway for fluoride incorporation is not operating in *A. georginae*. Studies conducted by Meyer and O'Hagan have shown that fluoropyruvate **(74)** is readily 'biotransformed' to fluoroacetate **(62)** in *D. cymosum* tissue cultures.[120]

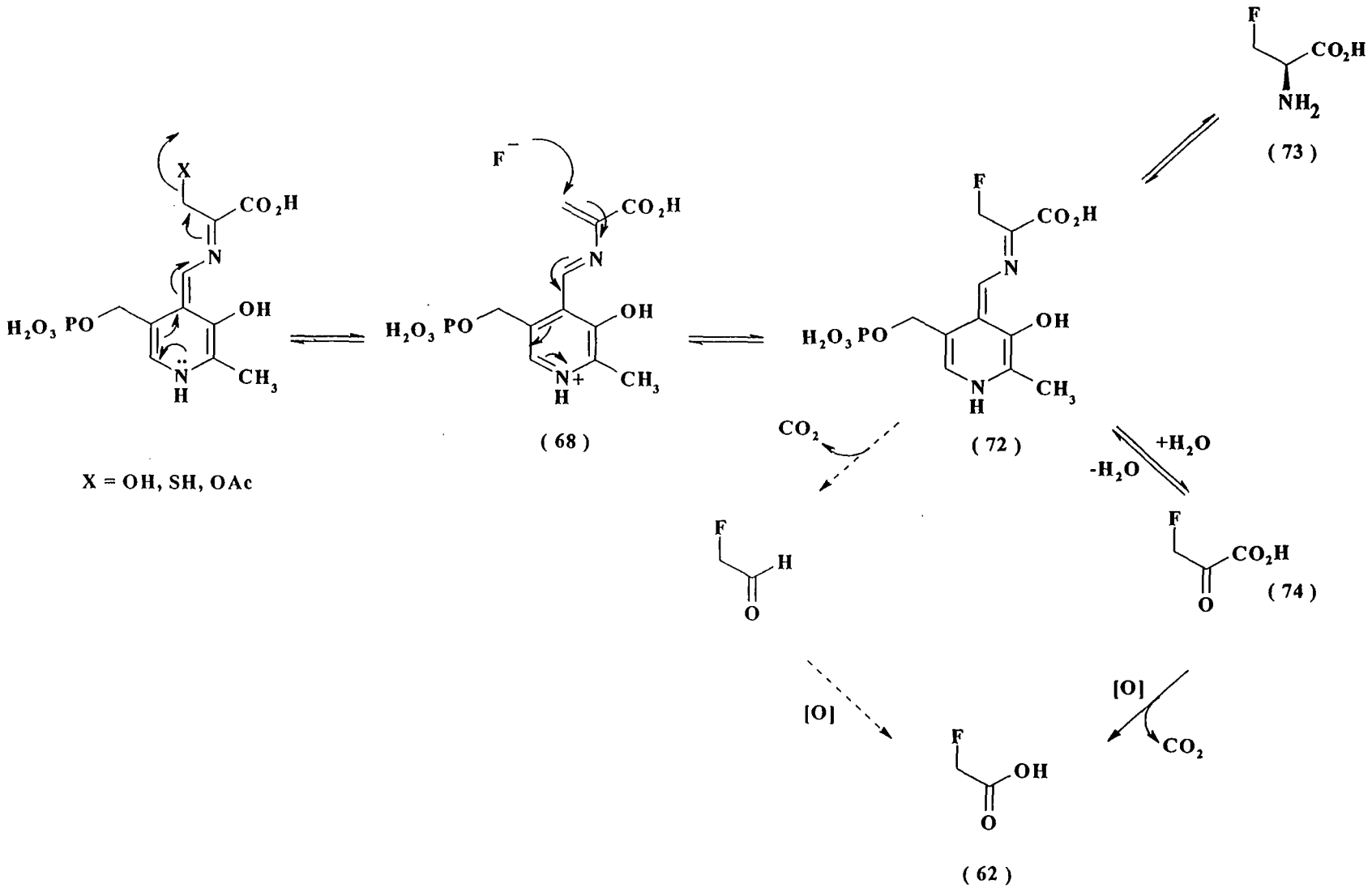

Fig. 1.12

1.9.2 Acetate, Ethylene and Halometabolites as Precursors to Fluoroacetate

Acetate is unlikely to be a direct precursor to fluoroacetate as its methyl group is not activated for fluoride attack. Some support, albeit negative, is provided from experiments demonstrating the failure of *D. cymosum* leaves to label fluoroacetate when incubated with [2-^{14}C]-acetate.[121] In the course of their studies, Peters and Shorthouse found that the plant hormone ethylene was also a by-product of the biosynthesis of fluoroacetone.[122] On the basis of this finding, Peters speculated that fluoroacetate could be derived from ethylene *via* vinyl fluoride **(75)** or fluoroethane **(76)** as depicted in Fig. 1.13.

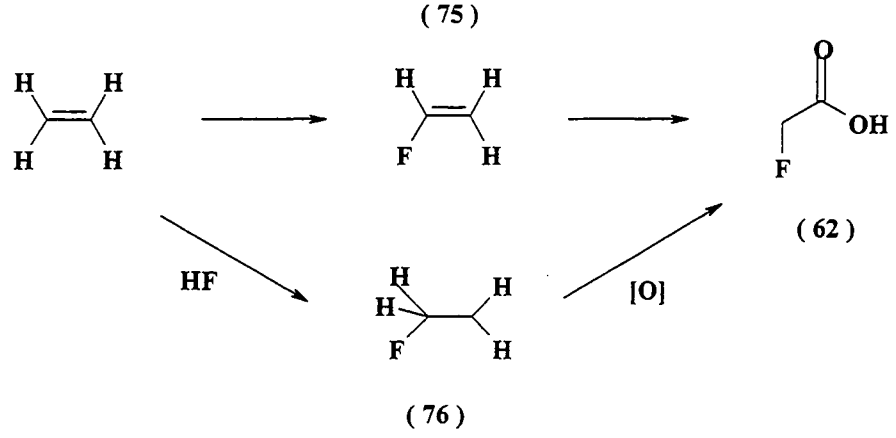

Fig. 1.13

An alternative pathway shown in Fig. 1.14 involves ethylene oxide **(77)**,[123] however there is no experimental evidence to suggest that either of the two pathways are operating in *A. georginae* or indeed any other plant system.

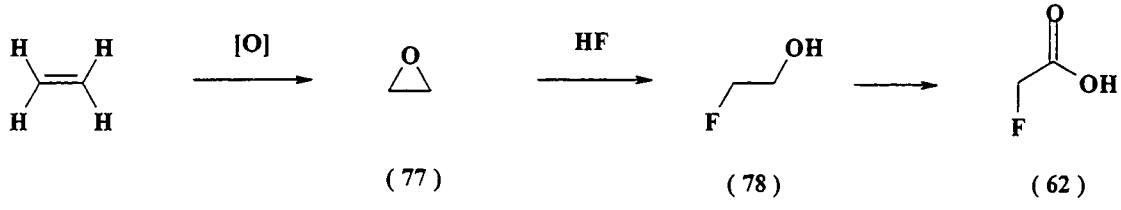

Fig. 1.14

Peters also investigated the possibility of chloroacetate as an intermediate in the biosynthesis of fluoroacetate in *A. georginae*.[124] Despite observing a relatively high uptake of chloride ions by the plant homogenates, no chlorinated organic compounds were detected. Vickery *et al.*,[125] observed chloroacetate as a major product of the reaction between malonic acid and sodium hypochlorite at 25°C. The addition of fluoride to the mixture resulted in the detection of trace amounts of fluoroacetate which appeared to be formed by attack of a fluoride ion on the C-Cl bond of 2-chloromalonic acid which decarboxylates to generate fluoroacetate.[125]

1.10 *Streptomyces cattleya*

The vast majority of *Streptomyces*, the largest genus of *Actinomycetes*, are soil inhabiting bacteria. They may constitute as much as one fifth of the total culturable soil population.[126] The odour of moist earth is largely due to the *Streptomyces* releasing volatiles such as geosmin **(79)**. These bacteria are perhaps best known for their elaboration of a multitudinous array of antibiotics which have found application in medical clinics. Examples include chloramphenicol **(80)**, erythromycin and tetracycline **(17)** (see also section 1.3).

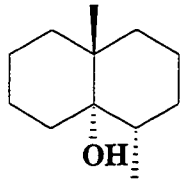

(79)

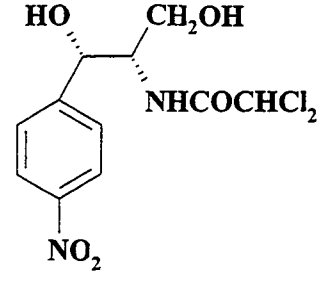

(80)

Kahan *et al.*,[127] was responsible for isolating *Streptomyces cattleya* from a soil sample in New Jersey, USA. Solid media cultures of the micro-organism give rise to

aerial mycelia with a characteristic orchid pigmentation,[127] and appropriately, the name '*cattleya*' originates from the botanical orchid genus.

Streptomyces cattleya NRRL 8057 has been known to elaborate a range of β-lactam antibiotics including thienamycin, cephamycin C, penicillin N. Thienamycin **(81)** is a broad spectrum antibiotic that possesses a carbapenem ring system and is highly active against both Gram positive and Gram negative bacteria.[59] Thienamycin is resistant to a multitude of β-lactamases which normally hydrolyse penicillins and cephalosporins. Biosynthetic studies on the antibiotic have shown that the pyrrolidine ring was derived from glutamate,[128] the cysteaminyl side chain from cysteine, and acetate formed C6 and C7 of the β-lactam ring while two methionines donate two methyl groups for the synthesis of the hydroxyethyl group.

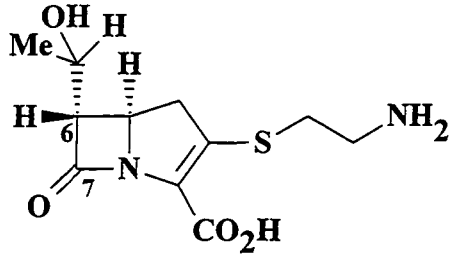

(81)

S. cattleya also produces 2-hydroxymethylcyclopent-4-ene-1,3-dione **(82)**, a cyclopentenedione antibiotic which is weakly active against Gram positive and Gram negative bacteria but inactive towards fungi.[129]

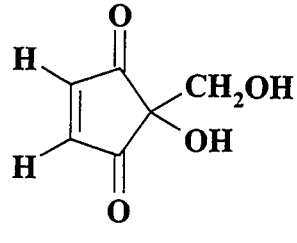

(82)

Sanada *et al.*, suggested a condensation reaction between fluoroacetaldehyde and glycine as the process for the biosynthesis of 4-fluorothreonine (Fig. 1.15). [107]

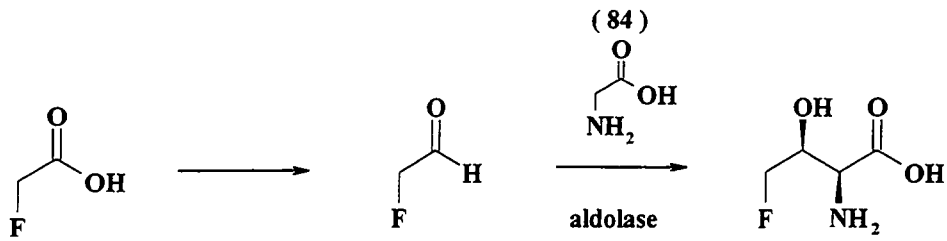

Fig. 1.15

During the course of this work, Tamura *et al.*,[130] in Japan reported the only other biosynthetic study of fluoroacetate in *S. cattleya* (*S. cattleya NTG 29*). They showed that [U-^{14}C]-glucose, [U-^{14}C]-glycerol, [^{14}C]-serine and [U-^{14}C]-β-hydroxypyruvate were all incorporated (0.2% - 0.4%) more efficiently than [3-^{14}C]-pyruvate, [2,3-^{14}C]-succinate and [U-^{14}C]-aspartate (0.04% - 0.08%). Furthermore, incubation of [2-^{13}C]-glycerol resulted in a clear enrichment at C-1 (40%) of fluoroacetate (Fig.1.16, 1.17). These authors concluded that the fluoroacetate backbone was derived from C-1 and C-2 of glycerol through β-hydroxypyruvate and proposed that the hydroxyl group of β-hydroxypyruvate was ultimately replaced by fluoride.

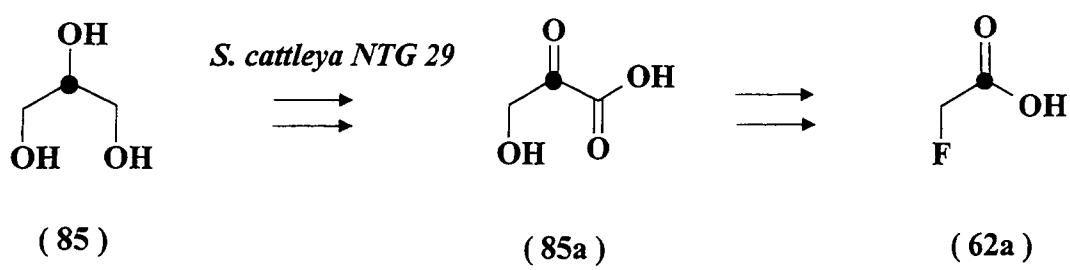

Fig. 1.16

Fig. 1.17 ^{19}F-NMR of [1-^{13}C]-fluoroacetate and non-labelled fluoroacetate from culture suspensions incubated with [2-^{13}C]-glycerol, Tamura *et al.*[130]

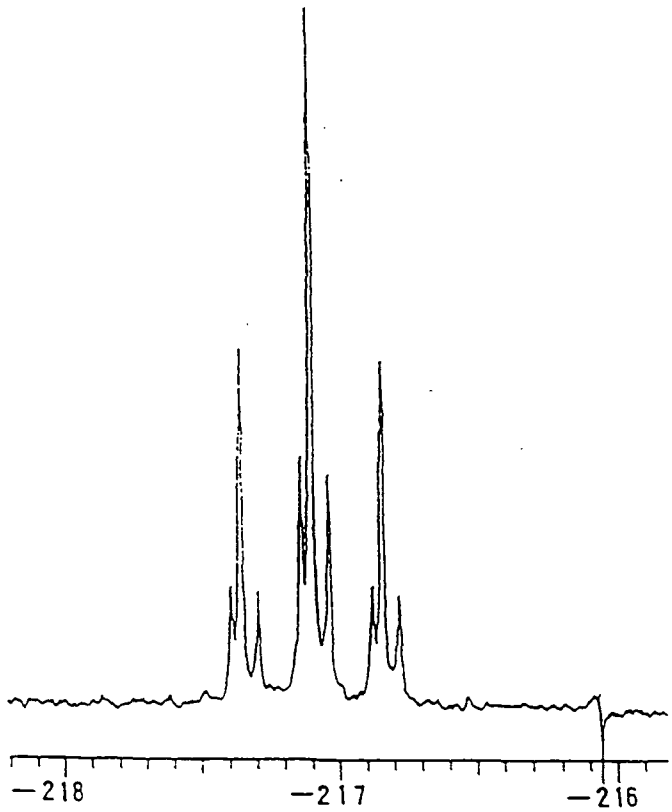

CHAPTER 2

Exploratory experiments on fluorometabolite biosynthesis in *S. cattleya*

CHAPTER 2

Exploratory experiments on fluorometabolite biosynthesis in *S. cattleya*

2.1 Background

A clear reason for the limited literature on the biochemistry and enzymology of biological fluorination is that plant tissue cultures of the fluoroacetate producing plants have proved difficult to generate and culture. Only two bacterial strains, Actinomycete soil bacteria of the genus *Streptomyces*, have been shown to secrete fluorinated metabolites. One of these, *S. calvus*, appears to biosynthesise nucleocidin (64)[131] however only *S. cattleya* is a candidate organism for biosynthetic studies as it is capable of producing fluoroacetate and 4-fluorothreonine in appreciable concentrations and is therefore an extremely attractive system to investigate. The discovery of these two micro-organisms suggests that bacteria may be a more common source of fluorinated metabolites. At the moment however, details of possible substrates and mechanism of fluorination remain ill-defined and speculative. Thus the current studies represent the first substantial investigation on the biosynthesis of organofluorine compounds.

2.1.1 Growth of *S. cattleya* [132]

The growth of *S. cattleya NRRL 8057* was first established on solid agar medium at 28°C. After a suitable incubation period (24-48h), the surface of the agar was examined visually for the presence of individual cell colonies. Smooth white spores were apparent after 96h and the petri-dishes were left for a further 4 days [Fig. 2.1(a), (b)]. The spores were then transferred by loop from solid agar medium to liquid culture media.

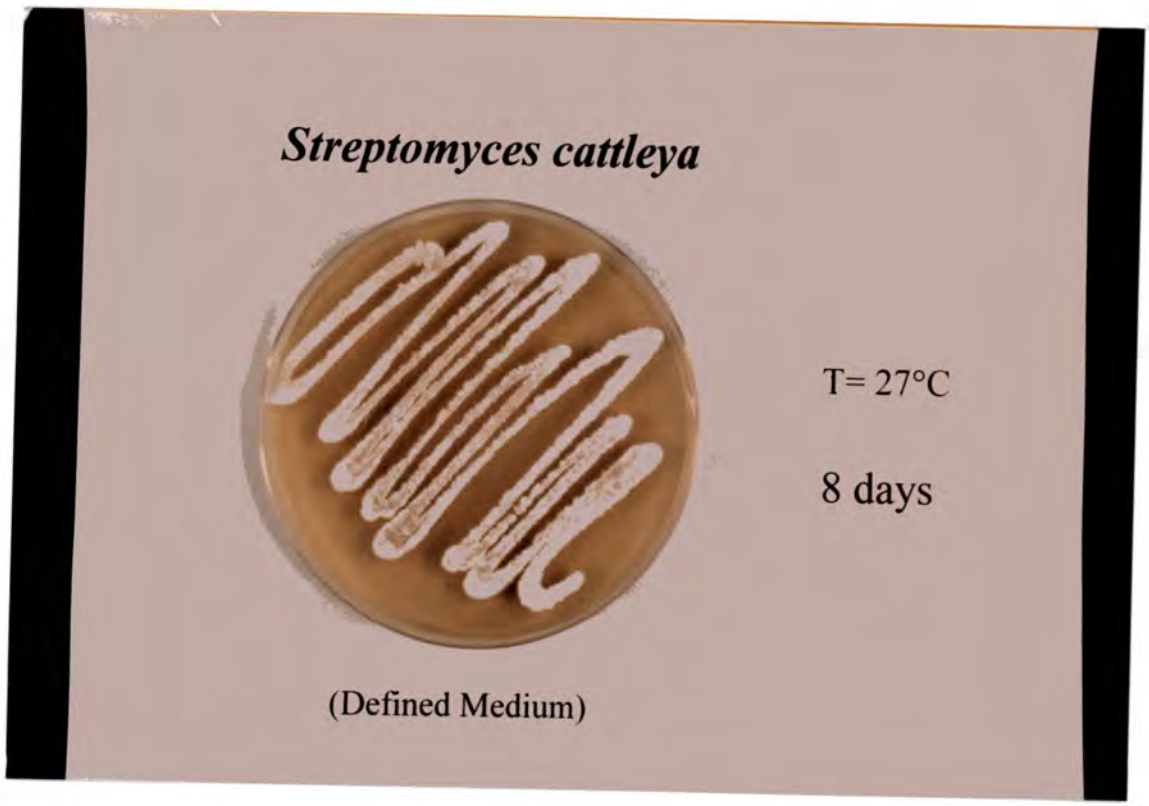

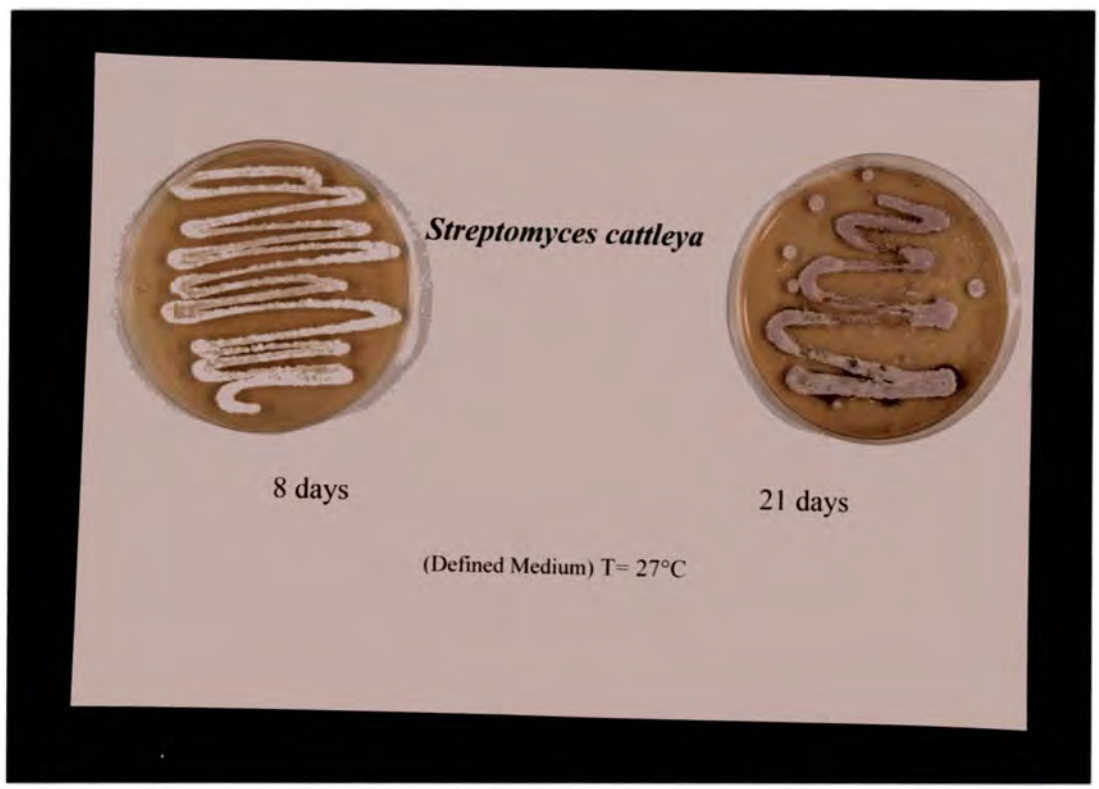

Fig. 2.1(a), (b) Photographs showing spores of *S. cattleya* grown on solid agar medium

2.1.2 Preparation of suspension cultures of *S. cattleya*

In general suspension (batch) cultures were prepared by inoculating several Erlenmeyer flasks (500ml) containing sterilised defined medium (100ml) by loop transfer from agar slants. The flasks containing the media were subsequently incubated for 28 days in an orbital shaker (28°C and 200 rpm).

Colonies of *S. cattleya* developed after 1-2 days and continued to grow until approximately 4 days at which stage the culture acquired a pink coloration corresponding to the end of the growth phase (trophophase). The culture subsequently entered the static phase (idiophase) where the mycelial network disintegrated and the supernatant appeared golden brown in colour. Aliquots of culture supernatant from batch suspensions of *S. cattleya* cells of different ages were collected and analysed by ^{19}F-NMR to assess fluorometabolite production. The fluorinated metabolites were not generally detectable by ^{19}F-NMR until after 10 days had elapsed and the production of fluoroacetate and 4-fluorothreonine continued for a further 14 days. It is interesting to note that the production of geosmin[24] **(76)** by *S. cattleya* appears to be concomitant with the biosynthesis of the two fluorometabolites. The odour of this compound serves as an indicator of the presence of fluoroacetate and 4-fluorothreonine in the culture medium.

Incubation experiments with putative isotopically labelled precursors involved pulse feeding batch cell suspensions of *S. cattleya* on the 6th, 8th and 10th days. After an additional 14 days the cells were separated by centrifugation and the supernatants were stored at 4°C pending analysis of incorporation into fluoroacetate and 4-fluorothreonine.

2.1.3 Fluoride uptake and fluorometabolite production in batch culture by *S. cattleya* [132]

The production of the fluorometabolites by *S. cattleya* has been monitored several years ago by the Belfast Group. It is apparent that in the absence of fluoride, batch cells reached their growth maximum after 2 days, however the presence of 2mM fluoride inhibits growth, taking a further 2 days to reach the end of the trophophase. Fluoride uptake by the cells commenced after 4 days until complete consumption after 28 days (Fig. 2.2).

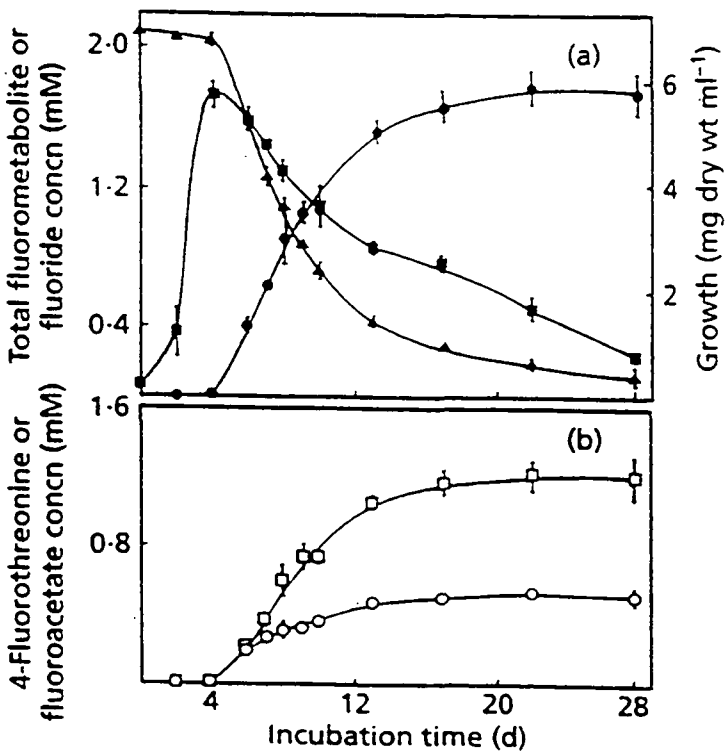

Growth of *S. cattleya* on defined medium supplemented with 2 mM NaF. Growth ■ ; fluoride ▲ ; total fluorometabolites ● ; fluoroacetate □ ; 4-fluorothreonine ○.

Fig. 2.2 [132]

The fluoride ion concentration began to fall after six days and was concomitant with total fluorometabolite (fluoroacetate and 4-fluorothreonine) production. Accumulation of the fluorometabolites was approximately linear with respect to time between 4 and 10 days and reached a plateau after 12 days. It is noteworthy that the initial concentrations of fluoroacetate and 4-fluorothreonine are approximately equal after 6 days but with time the concentration of fluoroacetate exceeded that of 4-fluorothreonine reaching a ratio of 70:30 after 28 days and a final concentration of 1.2mM.

2.1.4 Preparation of resting cell cultures of *S. cattleya*

The term resting cells is applied to those cells whose growth has ceased and have subsequently entered a secondary stage of metabolism (idiophase). Resting cells suspended in buffer offer a substantially cleaner medium than the batch cultures for feeding experiments. This has the advantage of washing away any extraneous organic material often improving precursor incorporations.

Typically five Erlenmeyer flasks of *S. cattleya* cells were grown in batch culture on a defined medium for six days, and harvested cells (usually 10-15g) were washed with MES buffer (pH 6.5). The resultant cell mass was usually between 10-15g wet weight per flask. Thereafter washed cells were resuspended in the buffer at a concentration of 0.15g wet wt ml^{-1}. For feeding experiments washed cells were incubated with 10mM precursor and 2mM NaF at 28°C on an orbital shaker at 200 rpm for 96h. Cells were then separated by centrifugation and the supernatant analysed for incorporation of putative precursors into the fluorometabolites using GC-MS and ^{19}F-NMR. (see sections 2.3)

2.1.5 Fluorometabolite production by resting cultures of *S. cattleya* [132]

The effect of time on fluorometabolite biosynthesis was studied by Reid *et al.*,[132] by preparing resting cell cultures harvested from batch cells aged between 4 and 16 days and incubating them in the presence of fluoride for 96h. No significant fluorometabolite production was detected using 4 day old cells, but cells aged 6 days had the capacity to biosynthesise low concentrations of both fluorometabolites. Fig. 2.3 illustrates the level of production of the fluorometabolites by resting cells of *S. cattleya* (harvested from 6 day old batch culture) monitored over a period of 96h.

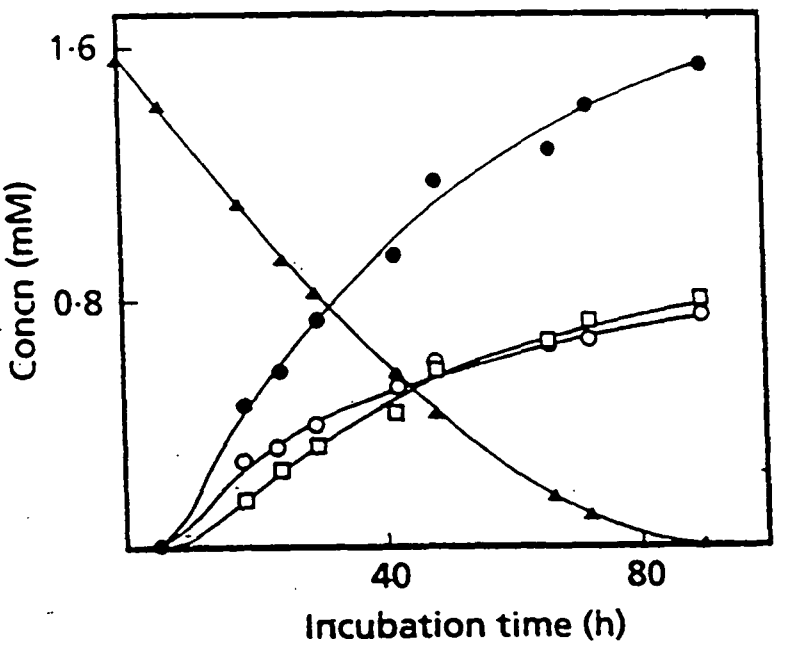

Biosynthesis of fluorometabolites by resting cell suspensions of *S. cattleya* prepared from 6-d old batch cultures, incubated with 1.55mM NaF in 50mM MES buffer at pH 6.5. ; fluoride △ ; total fluorometabolites ● ; fluoroacetate □ ; 4-fluorothreonine ○ .

Fig. 2.3 [132]

The profile clearly indicates complete conversion of fluoride to the fluorometabolites within 96h and an almost equal concentration of fluoroacetate and 4-fluorothreonine by 50h. Resting cells prepared from 10, 12 and 16 day old cells displayed a progressively lower fluoride uptake and a declining rate of fluorometabolite biosynthesis. These results indicate that the optimum harvesting age of cells from batch cultures is 6 days and thus this preparation was used throughout the feeding experiments.

2.1.6 Parameters affecting fluorometabolite production by resting cells of *S. cattleya* [132]

Fluorometabolite production is strongly dependent on the pH of the culture medium. The optimum pH is 6.0 and production declines markedly at higher pH values, particularly in the case of fluoroacetate. It was speculated by Sanada *et al.*,[107] that 4-fluorothreonine was derived from fluoroacetate but studies carried out by Reid *et al.*,[132] contradicted this and suggested that the rate of interconversion of both fluorometabolites was too low to account for the normal resting cell concentrations of fluoroacetate and 4-fluorothreonine indicating that neither fluorometabolite was derived by metabolism of the other. The low-level interconversion observed was judged to be due to the ability of the resting cells of *S. cattleya* to defluorinate the fluorometabolites. The fluorinating system would then recycle the released fluoride for *de novo* fluorometabolite biosynthesis. Further incubation experiments with a variety of putative organofluorine precursors showed a similar result, i.e. elimination and subsequent reincorporation of fluoride to produce the fluorometabolites. Similar cases of fluoride release from organofluorine compounds have previously been documented.[133,134] Further, albeit

negative, evidence for this conclusion was provided after incubation experiments with [$^{2}H_2$]-fluoroacetate which was not incorporated into 4-fluorothreonine

In contrast to Sanada *et al.*'s[107] suggestion that fluorocitrate was inert to metabolism by *S. cattleya*, Reid *et al.*,[132] have shown that resting cells were capable of producing low concentrations of fluoroacetate and 4-fluorothreonine when incubated with DL-fluorocitrate. It would appear therefore that *S. cattleya* aconitase is not inhibited by fluorocitrate but rather the latter is metabolised and defluorinated. These authors also assessed the effect of possible precursors on fluorometabolite production through incubation studies with various TCA cycle intermediates and α-amino acids. However, no significant change in the overall ratios of the fluorometabolites was observed during such studies.

2.2 Incorporation of ^{14}C-radiolabelled substrates into fluoroacetate by resting cell cultures

This investigation was designed to provide an insight into the metabolic source of the carbon substrate for the fluorinating enzyme. Resting cell cultures were prepared as described in section 2.1.4 and incubated in the presence of 2mM NaF, 40 μmoles of unlabelled fluoroacetate and a selection of ^{14}C-labelled putative precursors ranging from the amino acids, L-threonine, glycine, L-serine, L-aspartate and L-glutamate; glucose and glycerol representatives of the glycolytic pathway; glycolate from the glyoxylate cycle plus acetate, citrate and succinate, intermediates of the TCA cycle. After the 96h incubation period, an aliquot of supernatant was retained for fluoride and fluorometabolite determination in Belfast while the remaining portion was derivatised (see section 2.3.1) and analysed using radiochemical scintillation counting in Durham.

2.3 Analytical methods

Three different procedures were adopted to determine the incorporation of putative precursors into the fluorometabolites. In the case of radiolabelled substrates, a chemical derivatisation of fluoroacetate was used to generate a crystalline compound. Recrystallisation allowed a given sample to be purified to constant radioactivity. For stable isotopes, GC-MS and ^{19}F-NMR were employed to determine the incorporation of ^{13}C and ^{2}H labelled substrates.

2.3.1 Investigation of the incorporation of ^{14}C- radiolabelled compounds into fluoroacetate

A number of analytical techniques have been reported for the analysis of fluoroacetate particularly in small quantities from organic materials. Colourimetric procedures have been used for the analysis of fluoroacetic acid in *D. cymosum*.[135] A fluoride ion-selective electrode has also been used to detect fluoride ion release after pretreatment of a fluoroacetate containing sample.[136,137] In 1972 Hall[138] suggested ^{19}F-NMR as an alternative assay method, and more recently Baron *et al.*,[139] reported that the limit of detection of fluoroacetate by NMR was ~4μg/g. In comparison to gas-chromatographic (0.1μg/g)[140,141] and liquid chromatographic methods,[142] ^{19}F-NMR is significantly less sensitive but technically easier since derivatisation of the fluoroacetate is unnecessary. The GC-MS method described by Vertainen and Kauranen[143] is apparently the most sensitive technique for fluoroacetate determination to date, capable of detecting down to 0.005μg/g of fluoroacetate. Recently however Burke *et al.*,[144]

reported a novel derivatisation method for the quantitative determination of fluoroacetate by converting it to its dodecyl ester. The advantage of this technique over other chromatographic procedures is the low volatility of the fluoroacetate derivative enabling a high recovery of the analyte.

The method developed in Durham, several years ago, involves a simple derivatisation of fluoroacetate with p-phenylphenacyl bromide which can be analysed either by GC-MS or radiochemical scintillation counting depending upon the nature of the isotopes under investigation. After a given feeding experiment, cold sodium fluoroacetate is added to a freeze dried sample of the supernatant and the mixture treated with 4-phenylphenacyl bromide in the presence of a phase transfer catalyst, 18-crown-6 (Scheme 1). Following filtration and solvent removal the solid residue is purified by preparative tlc using toluene as the eluant. The silica band containing the ester derivative (87) (UV identification) is scraped off and extracted into dichloromethane. Subsequent removal of the solvent and recrystallisation of the crystalline derivative from ethyl acetate allows an accurately weighed sample of the derivative to be prepared. The recystallised material is dissolved in Ecoscint scintillation fluid and the sample is then ready for radiochemical counting.

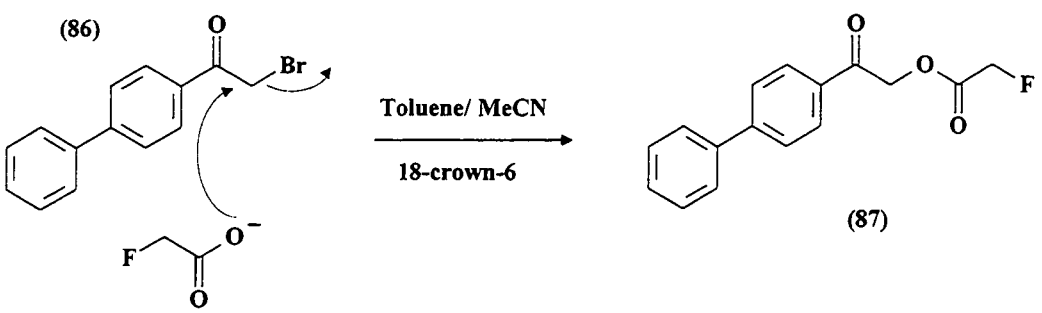

Scheme 1

2.3.2 Quantification of fluoroacetate and 4-fluorothreonine by GC-MS

The production of fluoroacetate and 4-fluorothreonine by *S. cattleya* was assayed by ^{19}F-NMR or alternatively by GC-MS and HPLC techniques. The GC-MS procedure, used to assay fluoroacetate, is based on the derivatisation of fluoroacetate with *p*-phenylphenacyl bromide. For quantification, the peak area is compared to an internal standard (sodium propionate) response curve. The limit of detection using this procedure is 0.01mM in a given supernatant aliquot.

Determination of 4-fluorothreonine is carried out by a fluorometric HPLC procedure commonly employed for amino acid analysis.[145] For quantification the peak area for 4-fluorothreonine is compared to an internal standard (tyrosine) response curve. The limit of detection is again 0.01mM in a given supernatant aliquot.

2.3.3 Determination of % incorporation into fluoroacetate by GC-MS

Isotope incorporations into the carbon skeleton of fluoroacetate can be determined by monitoring the increase in mass of the 4-phenylphenacyl derivative (*m/z* 272; molecular ion, M) of fluoroacetate. Fig. 2.4 shows the mass spectrum, obtained under EI (electron ionisation) conditions, illustrating the fragmentation pattern of this derivative. Detection of ions 273 (M+1) and 274 (M+2) indicates incorporation of single and double label respectively. Prior to calculations of % incorporations, corrections were made to each of the ion peak areas for natural isotope abundances. The level of incorporation into fluoroacetate is calculated by dividing the corrected peak area for each ion by the sum of total corrected peak areas for ions 272, 273 and 274. The natural abundances of ions 273 and 274 were determined experimentally using control samples.

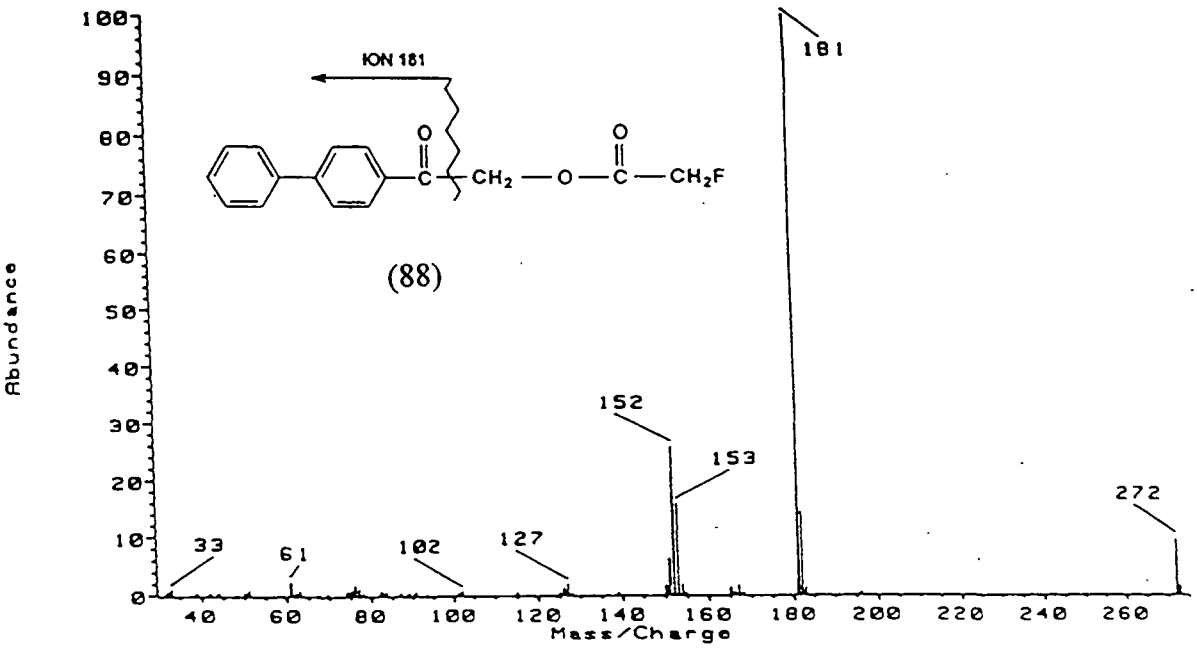

Fig. 2.4

2.3.4 Determination of % incorporation into 4-fluorothreonine [146]

Isotope incorporations into the various carbon atoms of 4-fluorothreonine were determined by monitoring the mass of selected fragments from a silylated derivative 4-fluorothreonine. This derivative of 4-fluorothreonine was prepared by reacting a sample of the freeze dried culture supernatant with N-methyl-N-(trimethylsilyl)-trifluoroacetamide (MSTFA). From the fragmentation pattern (depicted in Fig. 2.5) of the MSTFA derivative, detected under EI conditions, it is evident that two main fragments are present (m/z 236, m/z 218).

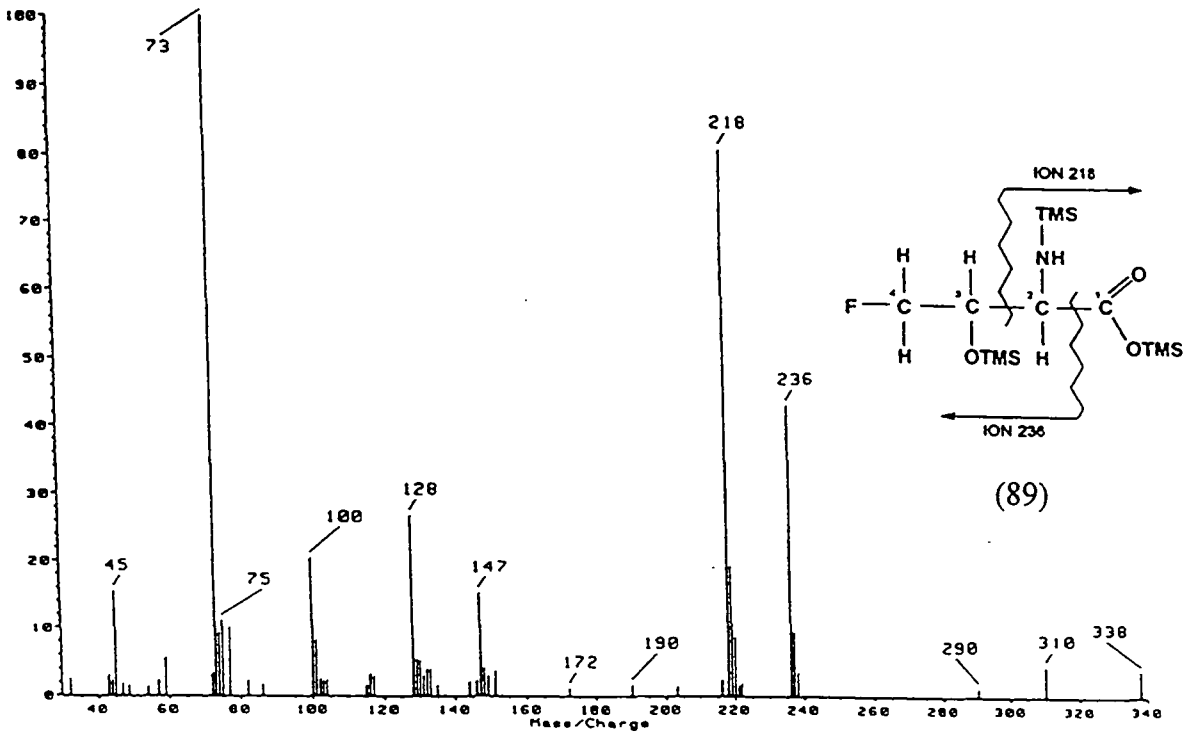

(89)

Fig. 2.5 [146]

Since the silylated derivative of 4-fluorothreonine yielded no significant molecular ion for monitoring the molecule as a whole, it is only possible to evaluate fragments of the molecule. Ions 218, 219, 220, and 221 permit an assessment of the incorporation into positions 1 and 2 of 4-fluorothreonine and ions 236, 237, 238 and 239 allow incorporations into positions 2, 3 and 4 to be determined. The natural abundance of the various ions was determined experimentally using control samples.

2.3.5 ^{19}F-NMR Spectroscopy

Cell supernatants may of course be analysed directly by ^{19}F-NMR without recourse to extraction and derivatisation. The clear advantage with ^{19}F-NMR is that it permits easy identification and quantification of the fluorometabolites produced by *S. cattleya*. The sensitivity of ^{19}F-NMR is not a problem since fluorine-19 possesses a large magnetic moment and has a natural abundance of 100%.[55] The majority of C-F resonances occur within a 300ppm sweep width, and the region of interest to this programme (CH_2F) is between -100ppm and -250ppm. Since $I = {}^1/_2$ for fluorine-19, coupling patterns to other nuclei (e.g. ^{13}C, ^{1}H, ^{2}H) are relatively easily evaluated. Fluorine-19 coupling is influenced by the nature of the atoms attached, and the number of intervening bonds between the fluorine atom and the active nucleus. The value of the coupling constants are typically $^2J_{F\text{-}H} = 47$Hz for a geminal interaction to hydrogen and $^3J_{F\text{-}H} = 25$Hz for a vicinal coupling to hydrogen. However solvent and temperature effects are considerably greater in ^{19}F-NMR than in ^{1}H-NMR and consequently can give rise to significant changes in ^{19}F-NMR chemical shift.

2.3.5.1 ^{19}F-NMR Analysis of *S. cattleya* supernatants

Proton decoupled ^{19}F{^{1}H}-NMR spectra proved to be advantageous in simplifying complex peak multiplicities and the coupling patterns arising from each fluorinated metabolite. In general the decoupling strategy involved irradiation of protons with a separate radiofrequency (500.13MHz in this case) to that already applied (operating frequency 471.54MHz). This has the effect of saturating all of the proton resonance transitions such that signal splittings caused by fluorine-hydrogen couplings are

removed. In consequence the signals from the undecoupled ^{19}F-NMR spectrum, collapse to singlets as illustrated in $^{19}F\{^{1}H\}$-NMR spectrum (Fig.2.7).

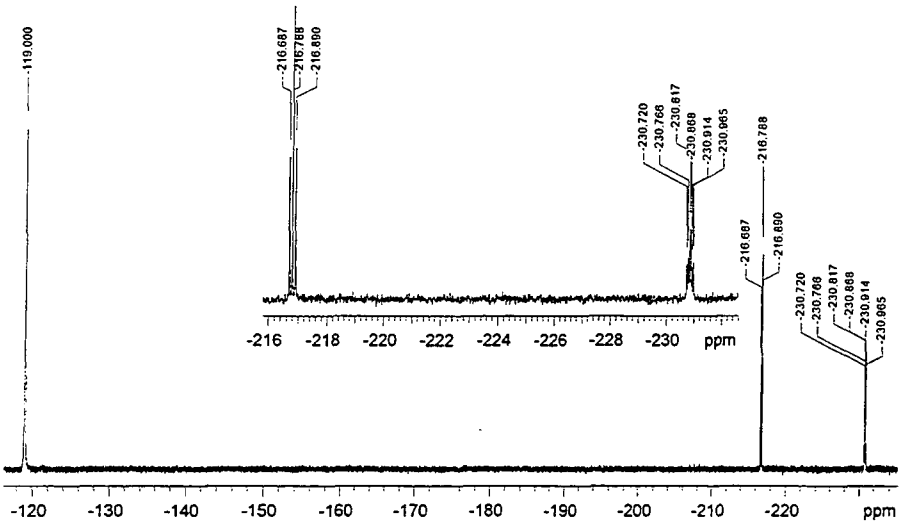

Fig. 2.6 ^{19}F-NMR spectrum of a suspension culture supernatant from *S. cattleya* cells aged 28days

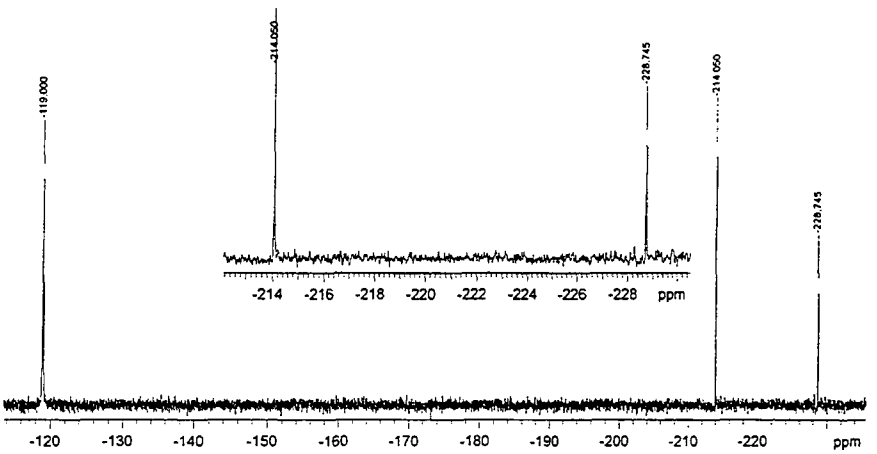

Fig. 2.7 $^{19}F\{^{1}H\}$NMR spectrum of a suspension culture supernatant from *S. cattleya* cells aged 28days

The fluoride signal (F^-) was used as an internal chemical shift reference. Despite the potential fluctuation of the F^- signal it was given a chemical shift value of -119ppm in

all of the spectra that were recorded. The triplet ($^2J_{F\text{-}H}$ = 47Hz) at -216.78ppm is a typical pattern that arises due to the fluoromethyl group of fluoroacetate. Also present in the culture supernatant is 4-fluorothreonine which appears a further 10-15ppm to lower frequency, as a doublet of triplets ($^2J_{F\text{-}H}$ = 47Hz, $^3J_{F\text{-}H}$ = 25Hz). The additional splitting of the fluoromethyl triplet is due to the vicinal C-3 proton of 4-fluorothreonine.

Close inspection of the ^{19}F-NMR spectra (Figs. 2.6 and 2.7) clearly demonstrate that ^{19}F{^{1}H}-NMR is the more sensitive technique facilitating analysis of spectra (see Chapter 3).The slight fluctuations in the chemical shift values of fluoroacetate, and 4-fluorothreonine are probably due to temperature, concentration and pH effects. Although the sample is run in a fairly constant ambient temperature, long aquisition times under continuous decoupling conditions causes sample heating, usually by 1-2 °C. In addition, individual samples may contain different concentrations of fluoride and fluorometabolites possibly due to small changes in the physiological age and state of cells.

2.3.5.2 The consequence of introducing ^{2}H and ^{13}C nuclei adjacent to fluorine in ^{19}F-NMR

^{19}F-^{2}H coupling interactions

Deuterium atoms adjacent to fluorine induce an additive shift to lower frequency in the ^{19}F-NMR spectrum. A model study investigating the exchange of the C-3 protons for deuterium in 3-fluoropyruvic acid elegantly illustrates that a single geminal deuterium adjacent to fluorine, alters the multiplicity of the signal and shifts it to lower frequency (β shift = 0.60ppm), Fig. 2.8. The number of energy states allowed for a nucleus where I =1, is three. Consequently one deuterium geminal to fluorine generates a triplet, while

two deuterium atoms geminal to fluorine produces a shifted (2 x β shift = 1.2ppm) pentet.

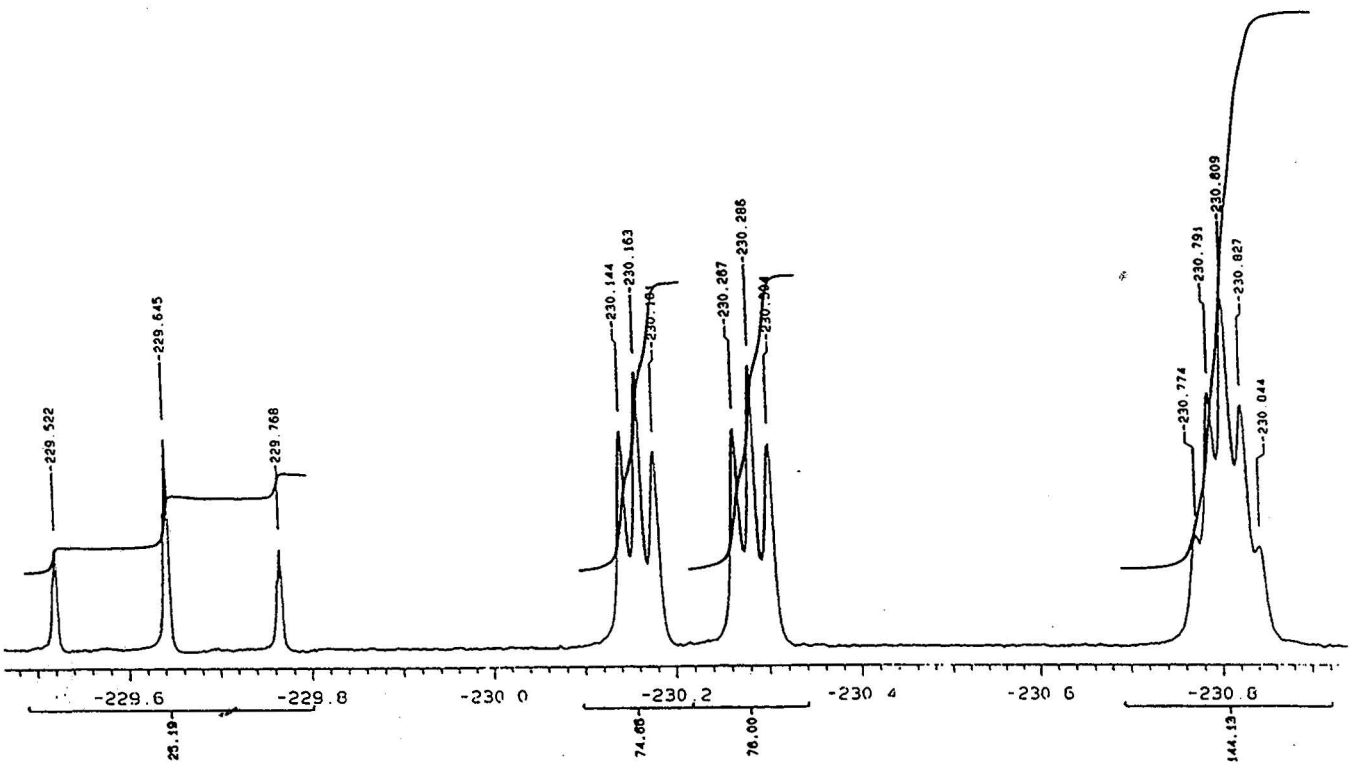

Fig. 2.8 ^{19}F-NMR spectrum of 3-fluoropyruvate, [3-^{2}H]- and [3-^{2}H$_2$]- fluoropyruvate

The sensitivity of the method can be increased by applying $^{19}F\{^{1}H\}$ decoupling which removes proton coupling, thus deuterium incorporation into the fluorometabolites is readily observed.

Retey *et al.*,[93] has demonstrated this β-effect in a ^{19}F-NMR spectrum of (*2R,3R*)-2-[2-^{2}H]-fluorocitric acid which was prepared from the condensation of (*2R*)-[2-^{2}H]-fluoroacetyl CoA and oxaloacetate catalysed by citrate synthase. Fig. 2.9 illustrates the doublet at δ = -198.6ppm ($^{2}J_{H-F}$ = 47Hz) generated by 2-fluorocitric acid and the triplet at δ = -199.2ppm ($^{2}J_{D-F}$ = 6.5Hz) resulting from the substitution of ^{1}H-^{12}C-^{19}F by ^{2}H-^{12}C-^{19}F in (*2R,3R*)-2-[2-^{2}H]-fluorocitric acid .

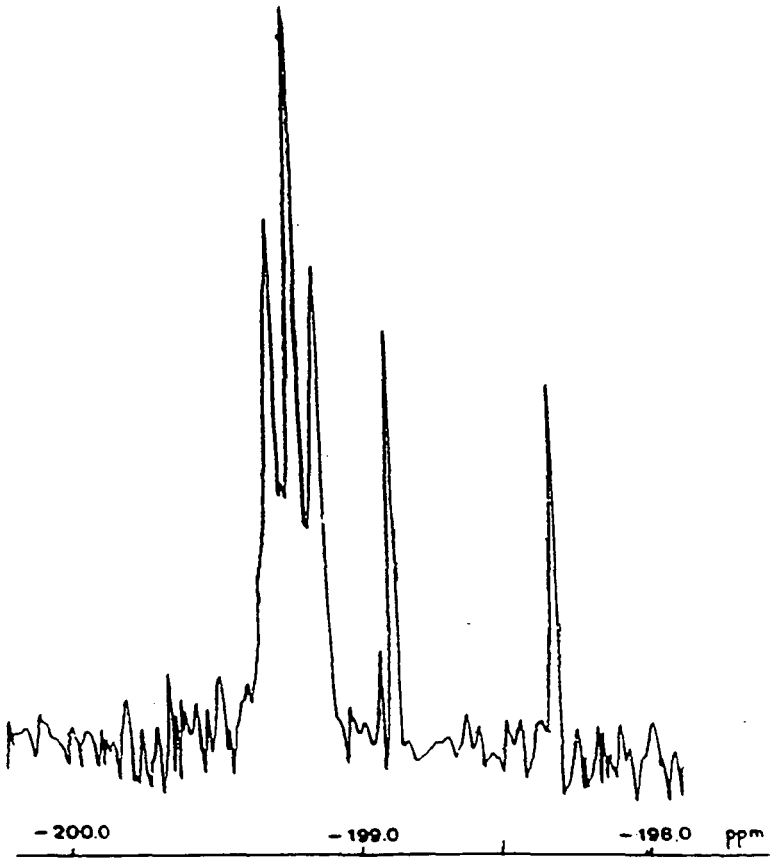

Fig. 2.9 ^{19}F-NMR spectrum of *(2R,3R)*-2-[2-^{2}H]-fluorocitric acid [93]

^{19}F-^{13}C coupling interactions

For carbon-13 $I = {}^{1}/_{2}$ and a given nucleus can occupy one of two energy levels. An intact ^{19}F-^{13}C coupling pattern gives rise to a doublet ($^{1}J_{C\text{-}F}$ = 165Hz) in the ^{19}F{^{1}H} NMR.

System	Type	Typical *J* value/ Hz
^{13}C-F	$^{1}J_{CF}$	160-370
^{13}C-C-F	$^{2}J_{CF}$	15-45
^{13}C-C-C-F	$^{3}J_{CF}$	5-15
^{13}C-C-C-C-F	$^{4}J_{CF}$	1-5

Table 2.1 Table listing some typical ^{13}C-^{19}F coupling constants, *J* (Hz). [146]

Combinations of ^{19}F-^{12}C-^{13}C and ^{19}F-^{13}C-^{13}C coupling patterns result in a doublet ($^2J_{C\text{-}F}$ = 18Hz) and a doublet of doublets ($^1J_{C\text{-}F}$ = 165Hz, $^2J_{C\text{-}F}$ = 18Hz) respectively.

Fig. 2.10 $^{19}F\{^1H\}$ NMR of fluoroacetate and [1,2-$^{13}C_2$]-fluoroacetate

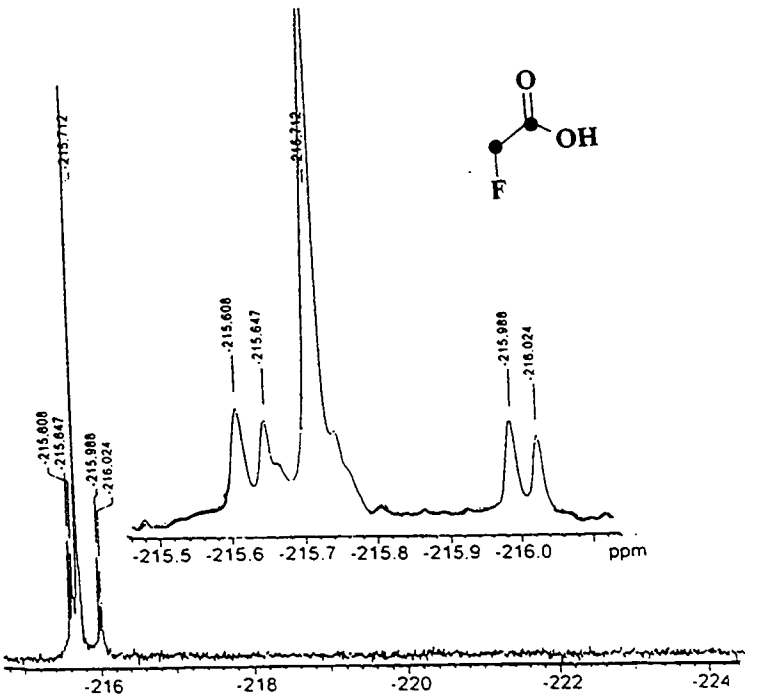

Fig. 2.10 Shows a high field $^{19}F\{^1H\}$ NMR of fluoroacetate acid containing a population of molecules with contiguous ^{13}C atoms both coupling to the ^{19}F nucleus to generate the shifted (α + β shift = 0.12ppm) doublet of doublets. This spectrum is for illustration only at this stage and will be discussed in detail later (see section 3.3).

2.4 Results and discussion

2.4.1 General calculation of levels of incorporation

Levels of incorporation of a given precursor can be calculated in a number of ways. The common terms applied are Absolute Incorporation, Specific Incorporation and Enrichment.

% Absolute incorporation (in the case radiochemical precursors) is defined by the following equation ;

$$\%\ Absolute\ incorporation = \frac{Total\ activity\ (dpm)\ in\ the\ isolated\ natural\ product}{Total\ activity\ (dpm)\ in\ the\ administered\ precursor} \times \frac{100}{1}$$

In the case of stable labelled precursors;

$$\%\ Absolute\ incorporation = \frac{Total\ excess\ isotope\ in\ the\ isolated\ natural\ product}{Total\ excess\ isotope\ in\ the\ administered\ precursor} \times \frac{100}{1}$$

Absolute incorporation gives a correlation between the amount of administered precursor and the amount incorporated into the metabolite. Its value can vary greatly because it depends on determining the total amount of metabolite biosynthesised during the experiment, which can be difficult.[10] A more reliable method is specific incorporation which is defined by the following equation;

$$\%\ Specific\ incorporation = \frac{Specific\ activity\ of\ the\ isolated\ natural\ product\ (dpm/mM\ or\ \%\ excess\ isotope)}{Specific\ activity\ of\ the\ administered\ precursor\ (dpm/mM\ or\ \%\ excess\ isotope)} \times \frac{100}{1}$$

The inverse of the value of % specific incorporation is known as Dilution. This particular method gives a measure of the amount of product formed from the administered labelled precursor relative to that formed from the pool of endogenous unlabelled precursor.[10] Determination of the Specific Activity of the product is generally more straightforward than the Absolute Incorporation since only a portion of the product requires isolation.

2.4.2 Calculation of incorporation rates of potential precursors into fluoroacetate and 4-fluorothreonine

% Incorporation rate was calculated using the following equation;

$$\frac{\textit{Specific activity of fluoroacetic acid}}{\textit{Specific activity of precursor}} \times 100 = \%\ \textit{Specific incorporation}$$

The potential precursor (20 μCi) was administered to resting cells of *S. cattleya,* thus for each experiment 4.44 x 10^7 dpm in all was added (1 μCi = 2.22 x 10^6 dpm) with a few milligrams of cold carrier. This equates to total 'counts in' and the results are calculated as a percentage;

$$\frac{\textit{(total 'counts out') in fluoroacetic acid}}{\textit{(total 'counts in')}} \times 100 = \%\ \textit{incorporation}$$

By adding 30mg of fluoroacetate to the resultant fluoroacetate containing supernatants from feeding experiments, the total 'counts out' in fluoroacetate may be determined, 30mg = 0.3mmoles. The endogenous mass was considered to be zero. The fluoroacetate was derivatised to give a maximum of 0.3mmoles of *p*-phenylphenacyl derivative (Mwt = 272) and therefore a maximum weight of 81.6mg. The compound was recrystallised to constant radioactivity and a value of dpm/mg (subtracting background radiation) for each sample was obtained.

Precursor

threonine 1164 dpm/ mg

glycolate 1917 dpm/ mg

For L-[U-^{14}C]-threonine; 1164 x 81.6mg = 94982.4 dpm = Total 'counts out' in fluoroacetic acid, therefore % incorporation = [94982.4/ 4.44 x 10^7] x 100 = 0.21%

Likewise for [U-^{14}C]-glycolate; 1917 x 81.6mg = 156427.2 dpm = Total counts out in fluoroacetic acid, therefore % incorporation = [156427.2/ 4.44 x 10^7] x 100 = 0.35%

Precursor	**Incorporation (%)**		
	a	b	c
[U-^{14}C]-glycolate	3.25	4.05	1.73
D-[U-^{14}C]-glucose	1.42	1.92	-----
[U-^{14}C]-glycerol	1.08	1.12	-----
L-[U-^{14}C]-threonine	0.80	0.82	0.88
[U-^{14}C]-glycine	0.71	0.84	-----
L-[U-^{14}C]-serine	0.60	0.84	-----
[2,3-^{14}C]-succinate	0.64	0.37	-----
L-[U-^{14}C]-aspartate	0.50	-----	-----
L-[U-^{14}C]-glutamate	0.43	-----	-----
[U-^{14}C]-acetate	0.15	0.17	-----
[1,5-^{14}C]-citrate	0.015	0.028	-----

Table 2.2 [132] % Incorporation of ^{14}C-labelled precursors into fluoroacetate. Columns a, b, and c denote repeat experiments.

2.5 Discussion

Generally higher levels of incorporation were recorded from feeding [U-^{14}C]-glycolate although the variability of incorporation is noted. On average the level was about twice that from D-[U-^{14}C]-glucose and three fold that from [U-^{14}C]-glycerol. The biochemically related amino acids; L-[U-^{14}C]-threonine, [U-^{14}C]-glycine and L-[U-^{14}C]-serine all exhibited comparatively lower but similar levels of incorporation. The TCA cycle intermediate [2,3-^{14}C]-succinate showed levels of incorporation similar to that of L-[U-^{14}C]-aspartate and L-[U-^{14}C]-glutamate which feed into the TCA cycle. Finally, there is a very poor transfer of carbon atoms from acetate and citrate to fluoroacetate.

The comparatively low incorporation levels of L-[U-^{14}C]-aspartate (0.50%) and L-[U-^{14}C]-glutamate (0.43%) suggest that they are not direct intermediates in the biosynthesis of fluoroacetate. Aspartate is produced by transamination of oxaloacetate and can be further converted to asparagine (Fig. 2.11), reconverted to oxaloacetate or even converted to alanine by the action of aspartate-β-decaboxylase.[147] Alanine thus formed may enter the glycolytic or TCA pool *via* pyruvate

Like aspartate, glutamate can derive from a minor branch point of the TCA cycle. It may be converted to proline or glutamine but can further be processed into the TCA cycle *via* α-ketoglutarate as shown in Fig. 2.11. Thus glutamate can enter the TCA pool and experience a similar fate to that of the carbon atoms of aspartate. This may explain the similar levels of incorporation observed between these two amino acids. A route to fluoroacetate *via* proline is unlikely as this would imply that the substrate for fluorination is metabolically related to glutamate and one would anticipate an appreciable level of incorporation here.

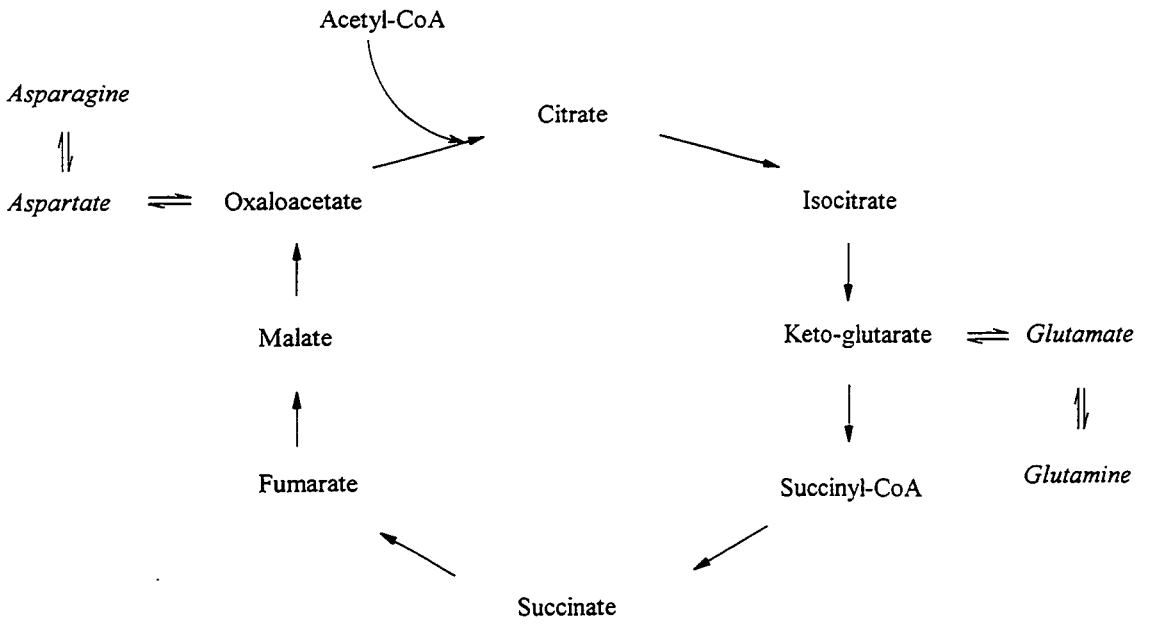

Fig. 2.11 A schematic of the TCA cycle

Succinate, an intermediate in the TCA cycle, is converted to fumarate by the action of succinate dehydrogenase and one of the routes for further metabolism of succinate is *via* the final stages of the TCA cycle. Its level of incorporation, given that only two of its four carbon atoms were labelled, is higher than aspartate and glutamate which were both universally labelled with ^{14}C atoms. This raised the possibility that succinate may be a closer intermediate to the fluorination event than the aforementioned amino acids. It also implies that carbons 2 and 3 of glutamate and aspartate are solely processed, probably *via* succinate, while the other carbons suffer a certain degree of scrambling. In spite of these deductions, succinate appears less close to the substrate for fluorination than for example [U-^{14}C]-glycerol which is incorporated at a substantially higher level than [2,3-^{14}C]-succinate. It is not clear why citrate shows poor levels of incorporation as it is expected to have a similar profile to glutamate, aspartate and

succinate. However this may be due in no small part to the complexity of citrate transport across the mitochondrial membrane.

Acetate was also poorly incorporated into fluoroacetate, one reason for this could be the heavy dilution it experiences in the metabolic pool. It is of interest to note that Eloff and Grobelaar[121] observed no incorporation of label from [2-^{14}C]-acetate into fluoroacetate produced in leaves of the *D. cymosum* plant.

The metabolically related amino acids threonine, glycine and serine all exhibited similar levels of incorporation with threonine showing the highest incorporation of the three and was judged to warrant further investigation as a potential precursor. Threonine can be degraded to glycine and acetyl-CoA by the action of threonine dehydrogenase and α-amino-β-ketobutyrate lyase.[148] The glycine thus produced can be further metabolised to serine. The similar incorporation values of glycine (0.71%, 0.84%) and serine (0.60%, 0.84%) suggests that they undergo very similar metabolic processing. Serine and glycine interconvert by the action of serine hydroxymethyl transferase and their close metabolic relationship in *S. cattleya* is discussed in detail in the Chapter 3, where stable isotope incorporations are explored.

The high incorporation of carbon atoms from glucose is perhaps not surprising as it is readily utilised as a carbon source in cell metabolism. None-the-less an intimate role in fluorometabolite production cannot be dismissed. Glycerol also appears to label fluoroacetate very efficiently and this may implicate the glycolytic pool as the source of the direct precursor. However, again the high incorporation may be due to glycerol acting as the major carbon source, used in the defined culture medium, on which the organism was grown. It is relevant however that during the course of this work Tamura *et al.*,[130] have demonstrated the efficient incorporation of [2-^{13}C]-glycerol into

fluoroacetate produced by a mutant strain of *S. cattleya*, and this has been further confirmed by our studies with [2-^{13}C]-glycerol.

Glycolate incorporations were surprisingly high in these early ^{14}C experiments, particularly with respect to subsequent stable isotope incorporations using [2-^{13}C]-glycolate. However in later ^{13}C/ ^{2}H labelled glycolate studies (Chapter 3), incorporations were very low but this was found to be due to changes in the resting cell density and precursor concentration (refer to Chapter 3, section 3.2.2, p79)

2.6 Conclusions

It is difficult to draw definitive conclusions from these preliminary radiolabelling results. The radiochemical results can be summarised as illustrated in Fig. 2.12 with glycolysis as a central pathway. It became necessary to prepare the corresponding stable labelled compounds and assess them as potential precursors of fluoroacetate and 4-fluorothreonine as it was judged at this stage that stable isotope investigations would provide much required regiospecific data and would test the radiochemical results.

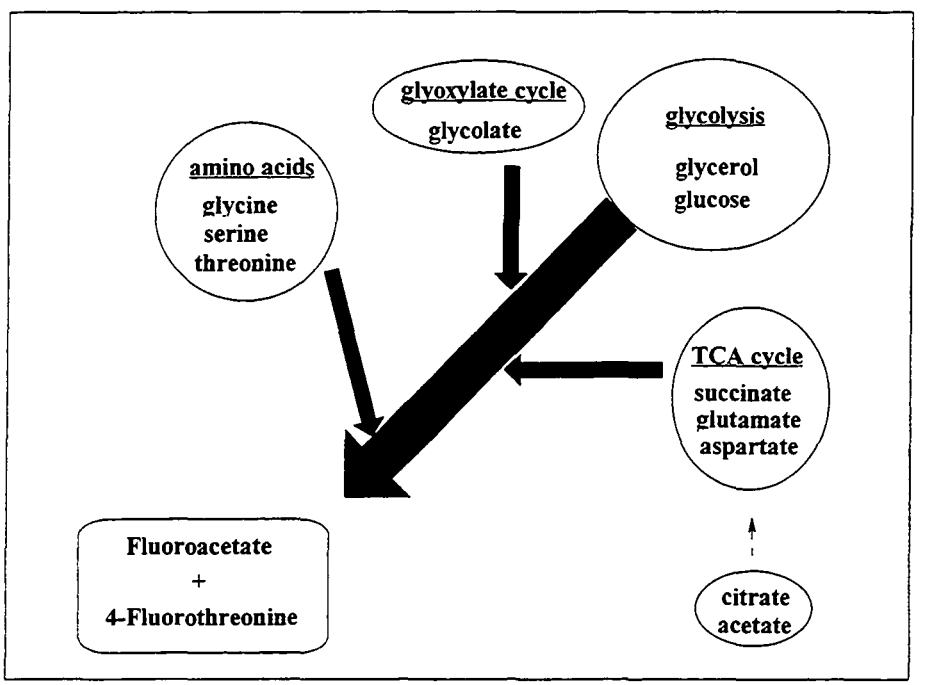

Fig. 2.12 A schematic representation of metabolite relationships in fluorometabolite biosynthesis in *S. cattleya*

CHAPTER 3

$^{13}C/^{2}H$ labelling studies on fluorometabolite biosynthesis in *S. cattleya*

Chapter 3

3. Stable isotopic labelling studies on the biosynthesis of fluoroacetate and 4-fluorothreonine in *S. cattleya*

On the basis of the radiochemical results discussed in Chapter 2, it was judged appropriate to carry out incorporation experiments with stable isotope labelled compounds, such that incorporations could be analysed directly by ^{19}F-NMR. Analysis of deuterium incorporation into fluoroacetate and 4-fluorothreonine was explored initially to assess the level of labelling in certain positions of the fluorometabolites. The presence of carbon-13, one and two bonds away from the fluorine-19 nucleus is readily identified by the magnitude of the $J^{13}_{C\text{-}F}$ coupling constant. Examples are explored in this thesis. The focus of the following stable isotope studies was to identify the relevant pathway (TCA pool, glycolytic pool etc.,) accommodating the fluorination event. Suspension culture feeding experiments were all conducted at Durham University and resting cell feeding studies were carried out at Queen's University in Belfast.

3.1 Investigation of *S. cattleya* cells supplemented with ^2H_2O

The objective of this experiment was to determine if protons derived from ^2H_2O are readily exchanged into fluoroacetate and 4-fluorothreonine during their biosynthesis. The experiment was conducted in batch and in resting cell suspensions of *S. cattleya*. Batch cells were incubated with ^2H_2O administered at a level of 10%. Three volumes of ^2H_2O were pulse fed to the cells on the 6th, 8th and 10th days and the cells were harvested after 28 days. Resting cells were incubated with ^2H_2O/ H_2O (50:50) at 28°C for 10, 24, 48, and 96h, and the supernatant from each experiment was centrifuged, freeze-dried and analysed by GC-MS.

3.1.1 Isotope incorporations after supplementing suspension cultures with 10% ^2H_2O

High field $^{19}F\{^1H\}$-NMR analysis of the fluorometabolites after growing *S. cattleya* cells in ^2H_2O (10%) clearly indicated the incorporation of one and two deuterium atoms into the fluoromethyl carbons of both fluorometabolites (Fig. 3.1). Fig. 3.1 highlights the β and 2β shifted signals (-218.7ppm and -219.3ppm) corresponding to [2-^{2}H]-fluoroacetate and [2,2-$^2H_2$]-fluoroacetate respectively.

The four signals, shifted progressively to lower frequency from the parent 4-fluorothreonine signal, can be assigned to the labelled species shown as a result of γ, β, β+γ and 2β shifts. The closest upfield shifted signal to that for unlabelled 4-fluorothreonine is assigned to **(93)** where deuterium is located 3 bonds away from fluorine atom and is assigned as a γ-shift (~0.30ppm). It is perhaps interesting to note that the observed γ-shift (~0.30ppm) is half the value of a β-shift (0.60ppm). Unfortunately the peak multiplicities cannot be clearly assigned due to the decoupling conditions under which the NMR spectrum was acquired. The second peak (expected triplet) at δ = -233.3ppm is attributed to a β-shift (0.6ppm) corresponding to single deuterium label at C-4 **(94)**. Similarly two deuterium atoms geminal to the fluorine atom of 4-fluorothreonine generate a peak (pentet) shifted by ~1.2ppm. The results appear to suggest that under batch cell conditions, protons from water are assimilated into fluoroacetate and sites C-3 and C-4 of 4-fluorothreonine. This experiment did not allow the detection of deuterium incorporation at C-2 of 4-fluorothreonine as the value of the δ-shift is too small. The results from GC-MS analysis (in Belfast), did however reveal significant incorporation into this site (see Table 3.2).

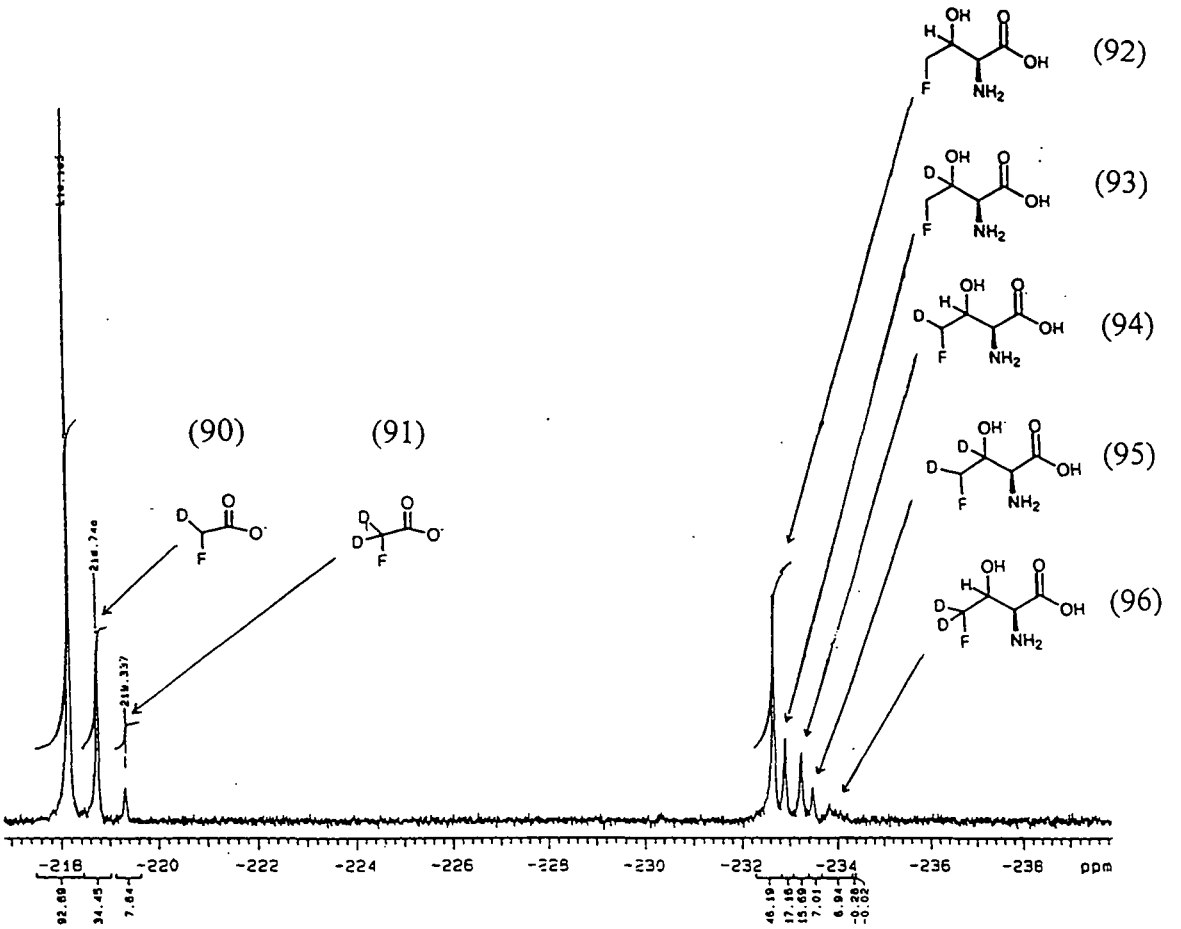

Fig. 3.1 $^{19}F\{^{1}H\}$-NMR spectrum of the supernatant from resting cells of *S. cattleya* incubated with 10% $^{2}H_2O$ after 28 days

3.1.2 Results of the incubation experiment with resting cells of *S. cattleya* supplemented with $^{2}H_2O$

The GC-MS data in Tables 3.1 and 3.2 clearly demonstrate that deuterium atoms are incorporated into both fluoroacetate and 4-fluorothreonine at all incubation times studied. After 10h, the incorporation of both one (22.9%) and two (6.0%) deuterium atoms into fluoroacetate were detected. The level of deuterium exchange at the

fluoromethyl carbon of fluoroacetate appears to increase with incubation time reaching a maximum of 36% single label after 96h.

Table 3.1 GC-MS incorporation data of ^2H into fluoroacetate by resting cells of *S. cattleya* supplemented with ^2H_2O/ H_2O (50/ 50)

Treatment	Incubation time (hrs)	% label		
		None	Single	Double
^2H_2O	10	71.1	22.9	6.0
^2H_2O	24	63.1	28.0	8.9
^2H_2O	48	55.7	32.8	11.5
^2H_2O	96	50.8	35.5	13.8

(as determined in Belfast)

A high level of exchange is clearly evident for 4-fluorothreonine with over 50% being labelled after 96h. Significant amounts of single (29.5%), double (12.0%) and triple (3.0%) labelled 4-fluorothreonine are apparent only after 10hrs (Table 3.2). The labelling pattern observed for positions 1 and 2 of fluoroacetate is very similar to that for positions 3 and 4 of 4-fluorothreonine. ^{19}F-NMR results of the resting cell experiments are consistent with those obtained under batch culture conditions. It is satisfying that the proportions of single and double label ($^{19}F\{^1H\}$-NMR, Fig. 3.1) into positions 2, 3 and 4 from the batch cell experiment closely parallel those obtained by GC-MS. It is obvious from Fig. 3.1 and Table 3.2 that the proportion of single label [(93) + (94)] in ion 236 is twice that for double label. Populations of triple labelled 4-fluorothreonine (~4.0%) can be detected by GC-MS but are not evident in the $^{19}F\{^1H\}$-NMR highlighting this limitation. A significant amount of single label (~8.0%) in ion 218 (positions 1 and 2 of 4-fluorothreonine) is also observed indicating that the

deuterium label predominates in position 2 of 4-fluorothreonine since no exchangeable protons are present on the neighbouring carboxylate carbon.

Table 3.2 GC-MS incorporation data of ^2H label into selected positions of 4-fluorothreonine by resting cells of *S. cattleya* supplemented with ^2H_2O/ H_2O (50/ 50)

Treatment	Incubation time	% label in ion 218 (Positions 1 and 2)		% label in ion 236 (Positions 2,3 and 4)			
	(hrs)	None	Single	None	Single	Double	Triple
^2H_2O	10	92.0	8.0	55.6	29.5	12.0	3.0
^2H_2O	24	91.6	8.4	48.2	32.7	15.1	4.0
^2H_2O	48	91.6	8.4	44.5	35.2	16.0	4.2
^2H_2O	96	90.5	9.5	42.3	34.9	18.1	4.7
Control incubation of 4-FT with ^2H_2O	168	100	0	99.4	0.6	<0.5	<0.5

(as determined in Belfast)

3.1.3 Conclusion

Deuterium is exchanged into the fluoromethyl position of fluoroacetate and three different sites of 4-fluorothreonine from ^2H_2O, although the process of exchange into the various positions can only be speculated. One plausible explanation for the presence of deuterium in position C-3 of 4-fluorothreonine **(93)** (χ to the fluorine moiety) is the reduction of a 3-keto analogue of 4-fluorothreonine by NAD^{2}H. Accumulation of a labelled pool of such a co-factor is not unlikely (Fig. 3.2). NAD(P)$^+$/ NAD(P)H are cofactors for a large number of biological redox reactions. When a substrate is oxidised, hydride is transferred from the substrate to C-4 of the nicotinamide ring of NAD(P)$^+$ (97) thus producing NADP(H) (Fig. 3.2).

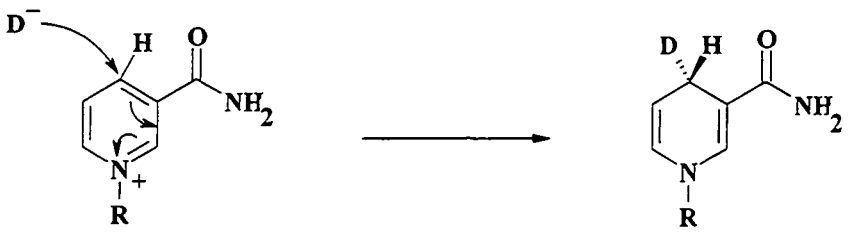

(97) (98)

R = H, NAD^+

R = 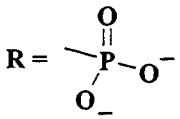 , $NADP^+$

Fig. 3.2 Formation of NAD^2H

[3-^{2}H]-4-Fluorothreonine **(93)** may then be generated as a result of NAD^2H acting on the β-carbonyl group, reducing it to the alcohol (Fig. 3.3).

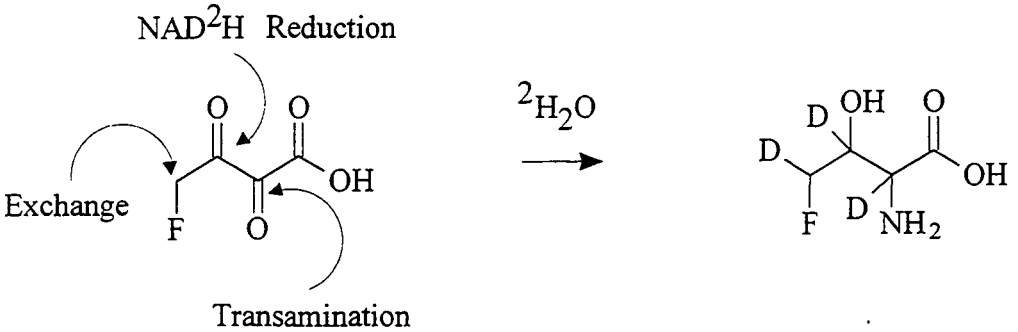

(99) (100)

Fig. 3.3

The C-2 of 4-fluorothreonine is most probably labelled with deuterium arising from the transamination of the α-carbonyl group (Fig. 3.3). Thus transamination at C-2, NAD^2H reduction at C-3 and deuterium exchange at C-4 of **(99)** may account for the observed labelling pattern.

3.2 Experiments to determine the relative efficacy of glycine and glycolate as precursors to fluoroacetate and 4-fluorothreonine in *S. cattleya*

Radiolabelled glycolate exhibited the highest incorporation of carbon-14 into fluoroacetate. However, this finding is not consistent with the recent work carried out by Tamura *et al.*,[130] who demonstrated a relatively low incorporation of [2-^{14}C]-glycolate and [1,2-$^{13}C_2$]-glycolate into fluoroacetate. It became important at the time of this publication to determine whether the disparity is due to differences in cell density and precursor concentration. Accordingly [2-^{13}C]-glycolate was incubated at two different concentrations under two different conditions of resting cell density. Controls using [2-^{13}C]-glycine were employed in these experiments.

3.2.1 Synthesis of [2-^{13}C]-Glycolate and [1,2-$^{13}C_2$]-Glycolate[130]

Glycolate was prepared from 2-bromoacetic acid by treatment with aq KOH. The reaction was heated at 120°C in a sealed tube for 3h. The resulting acidified mixture was loaded onto an Extrelute column and glycolic acid was eluted using diethylether as the eluant. The free glycolic acid was neutralised and freeze dried to give sodium glycolate in 75% yield. An identical protocol was followed for the preparation of [2-^{13}C]-glycolate **(102)** and [1,2-$^{13}C_2$]-glycolate **(104)** using [2-^{13}C]-bromoacetic acid **(101)** and [1,2-$^{13}C_2$]-bromoacetic acid **(103)** respectively (Scheme 2 and 3). However the yields of [2-^{13}C]-glycolate and [1,2-$^{13}C_2$]-glycolate were comparatively poor, 40% and 27% respectively. The presence of carbon-13 isotopes were obvious by ^{1}H-NMR analysis. For example, in the ^{1}H-NMR spectrum for [1,2-$^{13}C_2$]-glycolate, the methylene

signal appears as a doublet of doublets ($^{1}J_{H\text{-}}{}^{13}{}_{C}$ = 143.24Hz; $^{2}J_{H\text{-}}{}^{13}{}_{C\text{-}}{}^{13}{}_{C}$ = 4.02Hz, Fig. 3.4).

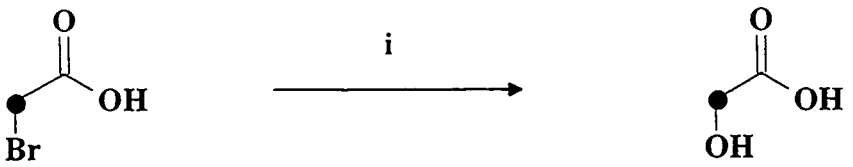

(101) (102)

Scheme 2 (i) aq. KOH, sealed tube/ 120°C/ 3h

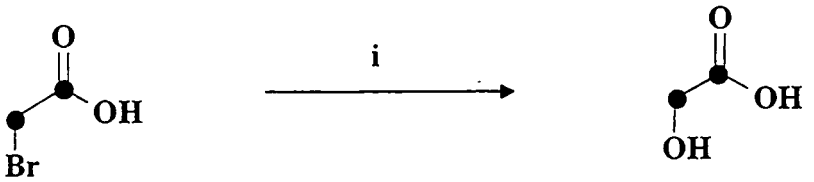

(103) (104)

Scheme 3 (i) aq. KOH, sealed tube/ 120°C/ 3h

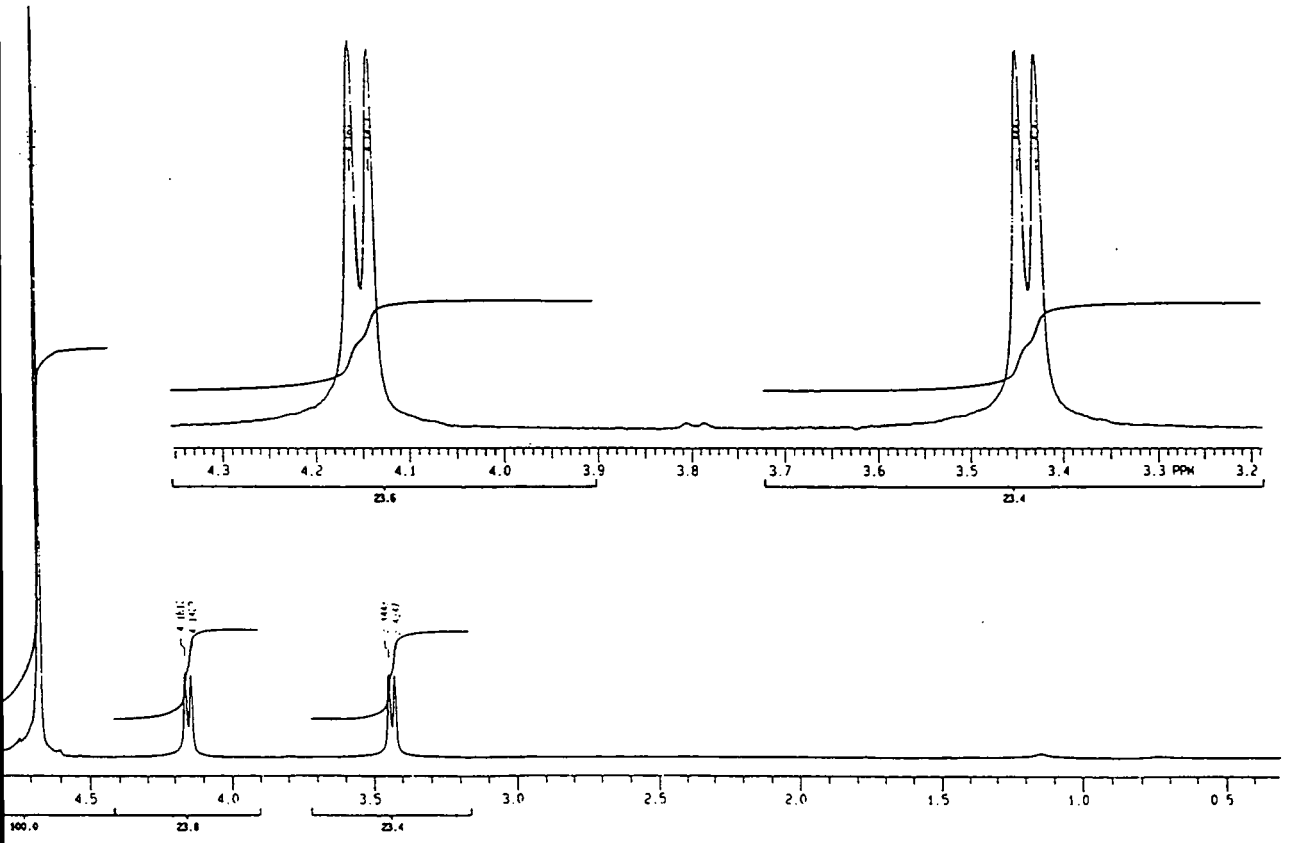

Fig. 3.4 ^{1}H-NMR spectrum of [1,2-$^{13}C_2$]-glycolate

3.2.2 Results of the incorporation of varying concentrations of [2-^{13}C]-glycolate and [2-^{13}C]-glycine at differing resting cell densities

The synthesised materials were sent to Belfast for feeding studies and GC-MS analysis. It is apparent from Tables 3.3 and 3.4 that at a cell density of 3g/ 18ml and 2mM precursor, [2-^{13}C]-glycolate gives rise to both single (5.4%) and double (8.0%) labelled fluoroacetate whereas ^{13}C atoms from [2-^{13}C]-glycine produced lower levels of single (2.8%) and double (1.1%) labelled fluoroacetate. It is noteworthy that similar cell density (3g) and precursor concentration (2mM) ratios, used in the radiochemical investigations, resulted in a relatively high incorporation of label from [U-^{14}C]-glycolate into fluoroacetate (1.75% - 4.05%), a level which was approximately 2- 5 times greater than that from [U-^{14}C]-glycine (0.71% - 0.84%) (refer to Chapter 2). However [2-^{13}C]-glycine (10mM) incubated at a cell density of 0.75g/ 20ml shows a significantly higher level of incorporation (approx. 50%) of ^{13}C into both fluorometabolites compared with [2-^{13}C]-glycolate (approx. 12%). A parallel situation was found for 4-fluorothreonine.

The graph (Graph 3.1) shows the relationship between precursor concentration (glycine and glycolate) and cell mass versus % incorporation of ^{13}C into fluoroacetate. It can be seen that, by increasing the precursor concentration per unit mass of cells, there is a linear increase in the % incorporation of [2-^{13}C]-glycine whereas the incorporation of [2-^{13}C]-glycolate appears to be independent of such precursor concentration and cell mass variations. It is interesting to note that below a value of 3 mM/ g cells, the incorporation of [2-^{13}C]-glycolate and indeed [U-^{14}C]-glycolate is higher than the corresponding labelled glycines, however incubation at values above 3 mM/g cells results in a greater incorporation of [2-^{13}C]-glycine.

Table 3.3 GC-MS incorporation data of ^{13}C into fluoroacetate after 48h incubation of resting cells [2-^{13}C]-glycine and [2-^{13}C]-glycolate

(as determined in Belfast)

Treatment	% label			
	None	Double	Single	
			Position 1	Position 2
0.75g cells/ 10mM [2-^{13}C]-glycine	50.5	38.2	8.5	2.8
0.75g cells/ 10mM [2-^{13}C]-glycolate	88.3	9.2	2.5	<0.5
0.75g cells/ 2mM [2-^{13}C]-glycine	85.7	8.9	5.4	<0.5
0.75g cells/ 2mM [2-^{13}C]-glycolate	82.5	13.1	3.8	0.6
3g cells/ 10mM [2-^{13}C]-glycine	81.2	8.6	8.5	1.6
3g cells/ 10mM [2-^{13}C]-glycolate	87.5	8.4	3.2	0.8
3g cells/ 2mM [2-^{13}C]-glycine	96.2	1.0	1.9	0.9
3g cells/ 2mM [2-^{13}C]-glycolate	86.6	8.0	4.5	0.9

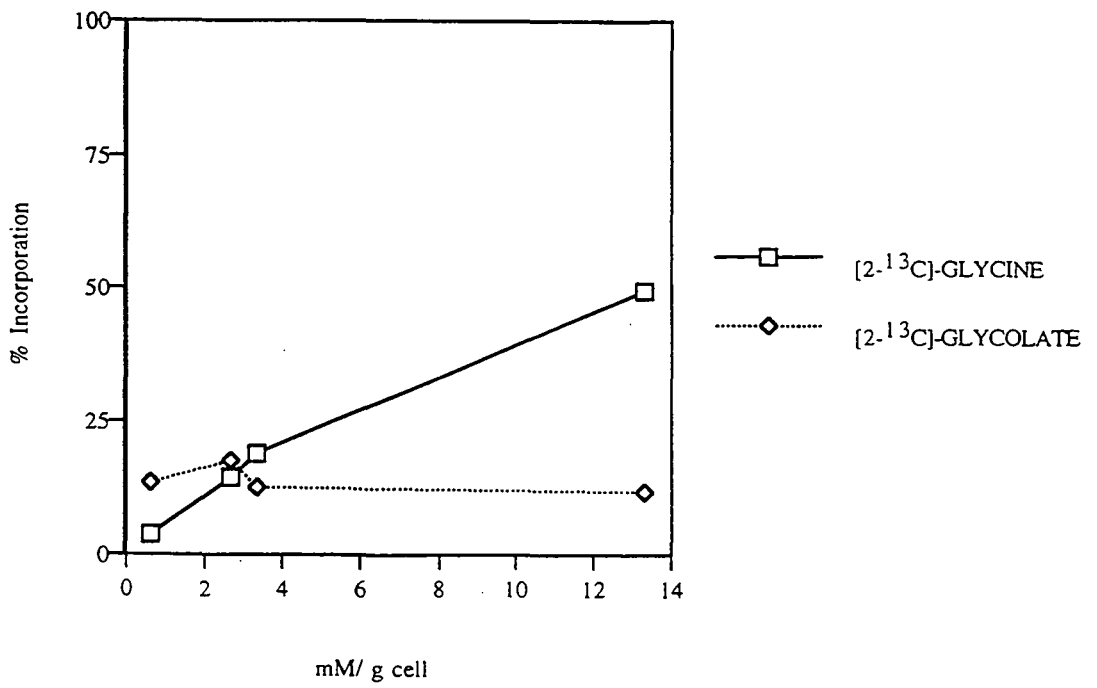

Graph 3.1

Table 3.4 GC-MS incorporation data of ^{13}C into positions 2,3 and 4 of 4-fluorothreonine after 48h incubation of resting cells with [2-^{13}C]-glycine and [2-^{13}C]-glycolate

Treatment	% Incorporation into positions 2,3 and 4 (Ion 236)			
	None	Single	Double	Triple
0.75g cells/ 10mM [2-^{13}C]-glycine	50.0	14.7	29.5	5.8
0.75g cells/ 10mM [2-^{13}C]-glycolate	89.3	2.8	7.9	<0.5
0.75g cells/ 2mM [2-^{13}C]-glycine	86.8	6.1	7.1	<0.5
0.75g cells/ 2mM [2-^{13}C]-glycolate	85.5	3.3	11.2	<0.5
3g cells/ 10mM [2-^{13}C]-glycine	85.4	6.6	8.0	<0.5
3g cells/ 10mM [2-^{13}C]-glycolate	90.1	2.5	7.3	<0.5
3g cells/ 2mM [2-^{13}C]-glycine	96.3	2.1	1.6	<0.5
3g cells/ 2mM [2-^{13}C]-glycolate	90.9	2.5	6.7	<0.5

(as determined in Belfast)

Unlike glycolate, glycine incorporations are particularly sensitive to cell density, possibly due to the rapid utilisation of glycine as a carbon source by the resting cells. A low precursor (glycine) concentration and high resting cell mass is consistent with the rapid metabolism of glycine such that the availability of glycine for incorporation into the fluorometabolites is short-lived.

3.2.3 Study to investigate the fate of label from [1,2-$^{13}C_2$]-glycolate, [2-^{2}H]-glycolate and [2,2-$^{2}H_2$]-glycolate

3.2.3.1 Synthesis of [2-^{2}H]-glycolate and [2,2-$^{2}H_2$]-glycolate

The incorporation of a single deuterium atom from [2-^{2}H]- and [2,2-$^{2}H_2$]-glycolate into the fluorometabolites produced by *S. cattleya* cells was investigated. [2-^{2}H]-Glycolate was synthesised by sodium borodeuteride ($NaBD_4$) reduction of glyoxylic acid. Glyoxylic acid was found to be partially stable to reduction with $NaBD_4$ generating [^{2}H]-glycolate with incomplete conversion (~50%). The resulting basic mixture did not favour complete reduction to the alcohol and it was rationalised that this may be due to the formation of a stable hydrate of glyoxylic acid. Consistent with this, acidification (pH 2) of the partially reduced mixture reconverted the base stable hydrate of glyoxylic acid to the aldehyde, which was then reduced with $NaBD_4$ resulting in its complete reduction to the alcohol, thus achieving up to 100% conversion. (Scheme 4). The deuterium labelled glycolate is readily identified by ^{13}C-NMR. The signal corresponding to C-2, of the hydrate of glyoxylic acid, appears as a singlet at δ = 89.5ppm, but after reduction, it becomes a triplet due to ^{2}H-^{13}C coupling at δ = 63.8ppm.

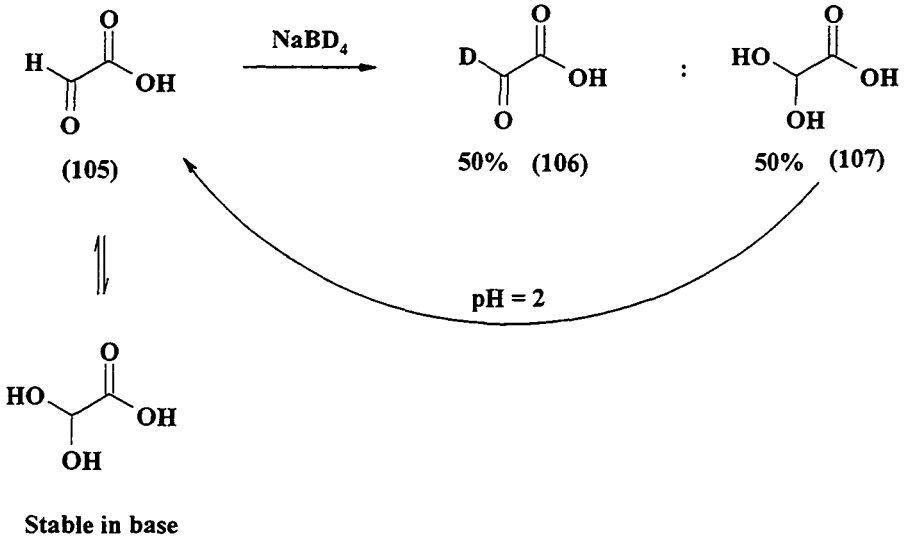

Scheme 4

Glycolate was synthesised using an alternative route by treatment of bromoacetic acid, with a sat. aqueous suspension of calcium carbonate. The filtered mixture was stored at -10°C for 24h to yield the calcium salt of glycolic acid.[149] In order to introduce both deuterium atoms, [2,2-$^2H_2$]-bromoacetic acid **(109)** was prepared from [$^2H_3$]-acetic acid **(108)**. Treatment of **(109)** with calcium carbonate afforded a white calcium salt of [2,2-$^2H_2$]-glycolic acid **(110)** (Scheme 5).

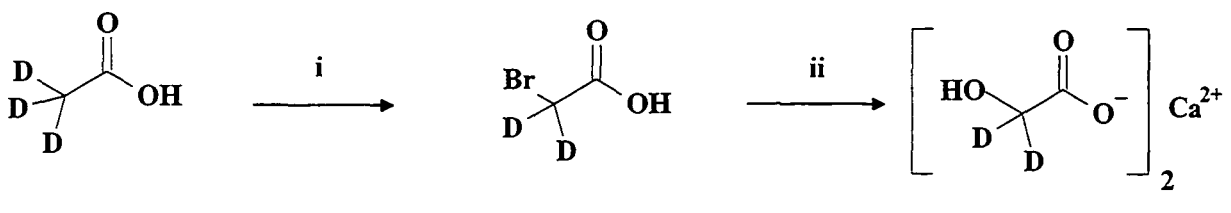

(108) **(109)** **(110)**

Scheme 5 (i) Trifluoroacetic anhydride, phosphorus, Br_2/ 60°C/ 4h

(ii) sat. $CaCO_3$/ 90°C/ 60h

3.2.3.2 Incorporation of [2-^{2}H]-glycolate, [2,2-$^{2}H_2$]-glycolate and [1,2-$^{13}C_2$]-glycolate into the fluorometabolites

[2-^{2}H]- And [2,2-$^{2}H_2$]-glycolate were incubated with suspension cultures of *S. cattleya* at a final concentration of 1.29mM in each case. ^{19}F-NMR spectra of lyophilised batch cell extracts of these feeding experiments showed the presence of a shifted signal (*dt*) at the base of the fluoroacetate peak indicating that one deuterium was incorporated into fluoroacetate at a low level (approx. <2%) (Fig. 3.5(a)).

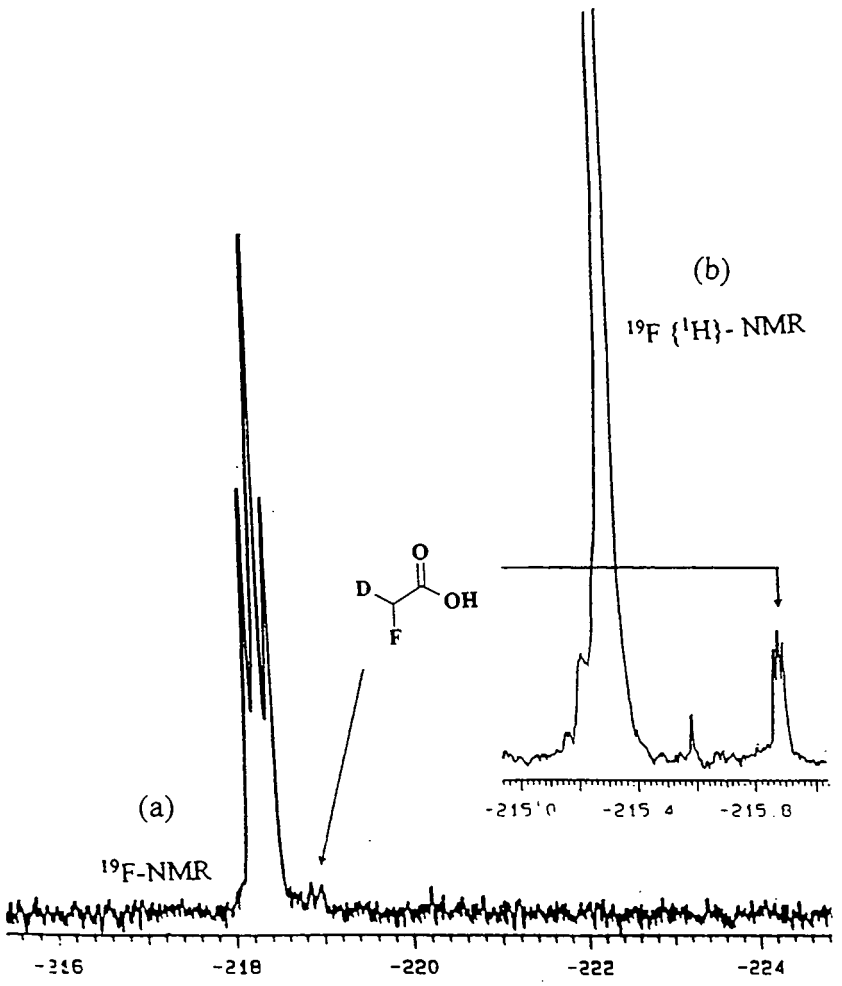

Fig. 3.5 (a) 200MHz ^{19}F-NMR spectrum and (b) 500 MHz ^{19}F{^{1}H}-NMR spectrum of *S. cattleya* resting cell supernatants from [2,2-$^{2}H_2$]-glycolate feeding experiment.

The triplet in the corresponding $^{19}F\{^{1}H\}$-NMR (Fig. 3.5(b)) unambiguously demonstrates the presence of a single deuterium, albeit with a low incorporation, into fluoroacetate. The GC-MS analysis of this sample further reinforced this conclusion (Table 3.5). A similar incorporation level of deuterium atoms into 4-fluorothreonine is also observed. In general however the resting cell experiments showed a very low level of incorporation of isotopes from both [2-$^{2}H_2$]-glycolate and [2,2-$^{2}H_2$]-glycolate. Furthermore the incorporation of label was not significantly affected by the length of the incubation time. Single and double label were present to an extent of <2.0% and <0.5% (Table 3.5 and 3.6).

Table 3.5 GC-MS incorporation data of [2-^{2}H]-glycolate, [2,2-$^{2}H_2$]-glycolate and [1,2-$^{13}C_2$]-glycolate into fluoroacetate

	Incubation time	% label			
Precursor	(hrs)	None	Double	Single	
				Position 1	Position 2
[1,2-$^{13}C_2$]-glycine	24	48.3	41.0	6.6	4.1
(control)	48	52.1	33.7	8.1	6.1
[2-^{2}H]-glycolate	24	100	<0.5	-	<0.2
	48	100	<0.5	-	<0.2
[2,2-$^{2}H_2$]-glycolate	24	100	<0.5	-	<0.2
	48	98.9	<0.5	-	1.1
[1,2-$^{13}C_2$]-glycolate	24	94.1	2.5	<0.5	3.4
	48	86.2	8.3	2.7	2.7

(as determined in Belfast)

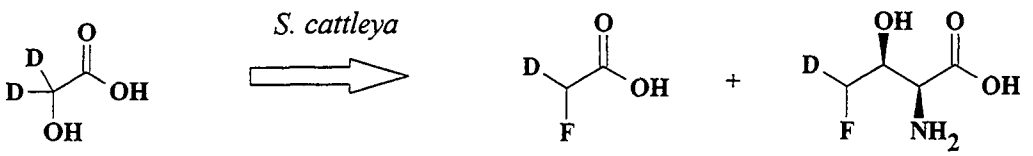

(110) **(90)** **(94)**

Scheme 6

Table 3.6 GC-MS incorporation data of [2-^{2}H]-glycolate, [2,2-$^{2}H_2$]-glycolate and [1,2-$^{13}C_2$]-glycolate into selected positions of 4-fluorothreonine

Precursor	Incubation time	% label in ion 218 (Positions 1 and 2)			% label in ion 236 (Positions 2,3 and 4)			
	(hrs)	None	Single	Double	None	Single	Double	Triple
[1,2-$^{13}C_2$]-glycine	24	74.3	7.4	18.3	43.8	17.6	29.4	9.2
(control)	48	78.8	5.8	15.4	46.4	19.0	29.6	7.0
[2-^{2}H]-glycolate	24	100	<1.0	<1.0	100	<1.0	<1.0	<1.0
	48	100	<1.0	<1.0	100	<1.0	<1.0	<1.0
[2,2-$^{2}H_2$]-glycolate	24	100	<1.0	<1.0	100	<1.0	<1.0	<1.0
	48	100	<1.0	<1.0	98.7	1.3	<1.0	<1.0
[1,2-$^{13}C_2$]-glycolate	24	100	<0.5	<0.5	91.4	3.6	5.0	<0.5
	48	100	<0.5	<0.5	87.5	5.1	7.4	<0.5

(as determined in Belfast)

The results indicate comparatively low levels of incorporation of label into fluoroacetate from [1,2-$^{13}C_2$]-glycolate after both 24 and 48h incubation periods (Tables 3.5 and 3.6) where labelled fluoroacetate was present at levels of 5.9% and 13.8%. The proportion of single label (2.7%) into positions 1 and 2 of fluoroacetate was very similar after 48h and it is perhaps interesting to note that the amount of double labelled fluoroacetate increases from 2.5% after 24h to 8.3% after 48h. However no significant incorporation was observed in positions 1 and 2 of 4-fluorothreonine demonstrating that the carbon atoms of glycolate are not direct precursors to C-1 and C-2 of 4-fluorothreonine. These results are illustrated in the $^{19}F\{^{1}H\}$-NMR spectrum (Fig. 3.6) of the corresponding feeding experiments which clearly show the incorporation of a single ^{13}C label into the terminal carbon atoms of both fluorometabolites. The observed labelling patterns can be rationalised if [1,2-$^{13}C_2$]-glycolate undergoes cleavage followed by incorporation of one of the carbon fragments. Furthermore it is evident that

the incorporation of label from [1,2-$^{13}C_2$]-glycolate into both flurometabolites proved to be significantly lower than that for [1,2-$^{13}C_2$]-glycine.

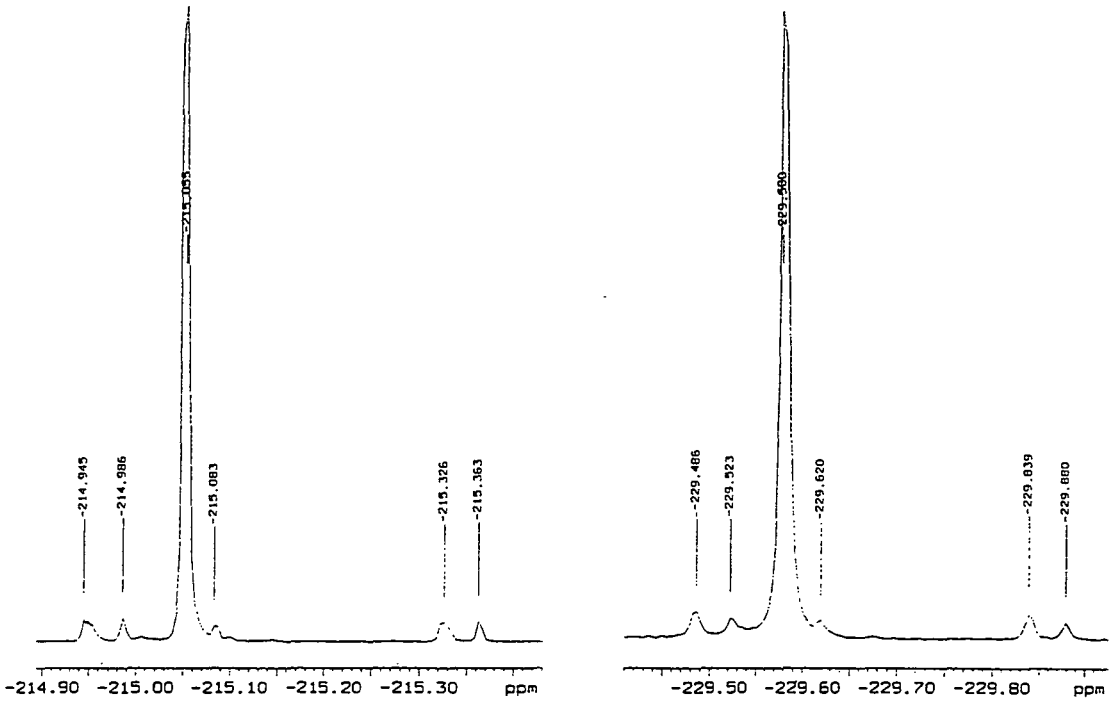

Fig. 3.6 $^{19}F\{^1H\}$-NMR spectrum of the supernatant from resting cells of *S. cattleya* incubated with [1,2-$^{13}C_2$]-glycolate

3.2.4 Conclusion

Due to the low levels of incorporation of label from stable isotope labelled glycolates it is concluded that glycolate is not a direct precursor to fluoroacetate or 4-fluorothreonine. The low level incorporation of a single deuterium atom from [2,2-$^{2}H_{2}$]-glycolate may have been a direct incorporation, however the experiment does not rule out the reintroduction of label from an enriched pool of NAD(P)^{2}H co-factor. Differences in the % incorporation from radio (^{14}C) and stable (^{13}C) labelled glycolate relative to glycine are in fact due to changes in the ratio of resting cell density and precursor concentration. Furthermore it is important to note that investigations carried out in Belfast have shown that a substantial amount of exogenous glycolate is present in the supernatant after incubation of resting cells with isotopically labelled glycolate for 48 hours indicating either a low rate of uptake or slow metabolism of glycolate. Indeed Tamura *et al.*,[130] did not consider intact cells to be permeable to glycolate and used benzyl alcohol to mediate permeability of *S. cattleya* cells prior to the addition of glycolate.

3.3 Metabolism of glycine during the biosynthesis of fluoroacetate and 4-fluorothreonine

The high incorporation of label from [1,2$^{13}C_2$]-glycine into the component carbon atoms of both fluorometabolites warranted a more detailed investigation of its role in the biosynthetic pathway. The objective of this investigation was to determine the % incorporation of label from various stable labelled glycines incubated at a final concentration of 10mM with resting cells of *S. cattleya*. The incorporation of the ^{13}C and ^{2}H atoms into the fluorometabolites was examined using GC-MS after 24h and 48h, and ^{19}F-NMR after 48h.

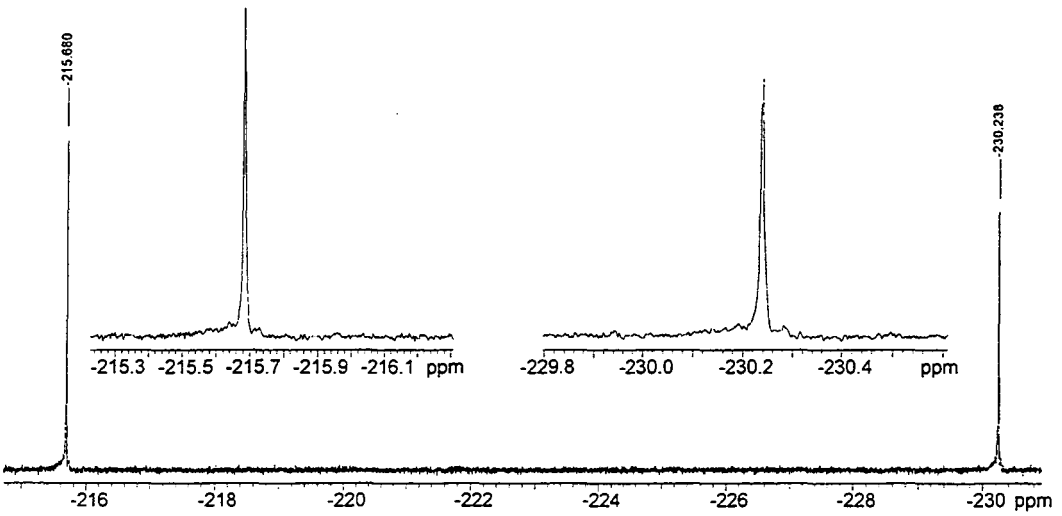

Fig. 3.7 $^{19}F\{^{1}H\}$-NMR spectrum of the supernatant from resting cells of *S. cattleya* incubated with [1-^{13}C]-glycine

From the GC-MS data presented in Tables 3.7 and 3.8 it would appear that cells of *S. cattleya* supplemented with [1-^{13}C]-glycine showed no appreciable incorporation of label into either positions of fluoroacetate or position 3 and 4 of 4- fluorothreonine. This is reinforced by the $^{19}F\{^{1}H\}$-NMR of the supernatant after the [1-^{13}C]-glycine incubation experiment as no ^{13}C satellites are associated with the

fluoroacetate and 4-fluorothreonine peaks (Fig. 3.7). However a low but significant incorporation (~2%) of single label from [1-^{13}C]-glycine was evident in positions 1 and 2 of 4-fluorothreonine by GC-MS analysis.

In contrast to [1-^{13}C]-glycine, incubation of [1,2-$^{13}C_2$]-glycine with the resting cells of *S. cattleya* showed significantly higher levels of incorporation into fluoroacetate (>50%) and positions 2, 3 and 4 of 4-fluorothreonine (>50%). Again, a very similar labelling pattern is observed for both fluorometabolites, particularly positions 1 and 2 of fluoroacetate and positions 3 and 4 of 4-fluorothreonine (Tables 3.7 and 3.8).

Table 3.7 GC-MS incorporation data of ^{13}C and ^{2}H labelled glycines into fluoroacetate

Precursor	Incubation time (hrs)	% label			
		None	Double	Single	
				Position 1	Position 2
[1,2-$^{13}C_2$]-glycine	24	48.3	41.0	6.6	4.1
	48	52.1	33.7	8.1	6.1
[1-^{13}C]-glycine	24	97.7	<0.5	2.0	<2.0
	48	96.0	<0.5	1.3	2.4
[2-^{13}C]-glycine	24	49.2	39.2	5.8	4.4
	48	54.7	31.9	8.3	5.1
[$^{2}H_2$]-glycine	24	93.9	0.6	-	6.0
	48	95.8	<0.5	-	3.8

(as determined in Belfast)

Table 3.8 GC-MS incorporation data of ^{13}C and ^{2}H labelled glycines into selected positions of 4-fluorothreonine

Precursor	Incubation time	% label in ion 218 (Positions 1 and 2)			% label in ion 236 (Positions 2,3 and 4)			
	(hrs)	None	Single	Double	None	Single	Double	Triple
[1,2-$^{13}C_2$]-glycine	24	74.3	7.4	18.3	43.8	17.6	29.4	9.2
	48	74.8	5.8	15.4	46.4	19.0	29.6	7.0
[1-^{13}C]-glycine	24	92.1	7.9	<1.0	96.4	3.0	<1.0	<1.0
	48	94.0	6.0	<1.0	95.9	3.5	<1.0	<1.0
[2-^{13}C]-glycine	24	75.1	13.2	11.7	44.7	17.7	28.4	9.2
	48	79.6	10.7	9.7	48.2	18.8	26.3	6.7
[$^{2}H_2$]-glycine	24	100	<1.0	<1.0	92.9	6.0	1.1	<1.0
	48	100	<1.0	<1.0	93.8	5.2	1.0	<1.0

(as determined in Belfast)

One striking feature to emerge was that cells supplemented with [1,2-$^{13}C_2$]-glycine generated labelling patterns, in both fluorometabolites, that were almost identical to that observed for [2-^{13}C]-glycine. This indicated that only C-2 of glycine is contributing any label. $^{19}F\{^{1}H\}$-NMR Analysis of the supernatants from resting cell experiments incubated with [1,2-$^{13}C_2$]-glycine (Scheme 7 and Fig. 3.7) and [2-^{13}C]-glycine (Scheme 8 and Fig. 3.8) allowed an immediate assessment of the incorporation of ^{13}C label into positions 1 and 2 of fluoroacetate and positions 3 and 4 of 4-fluorothreonine which complemented the GC-MS data. It is noteworthy that both one and two ^{13}C atoms are incorporated from [1,2-$^{13}C_2$]-glycine and [2-^{13}C]-glycine into positions 1 and 2 of 4-fluorothreonine whereas only a single label is detected in these positions from [1-^{13}C]-glycine.

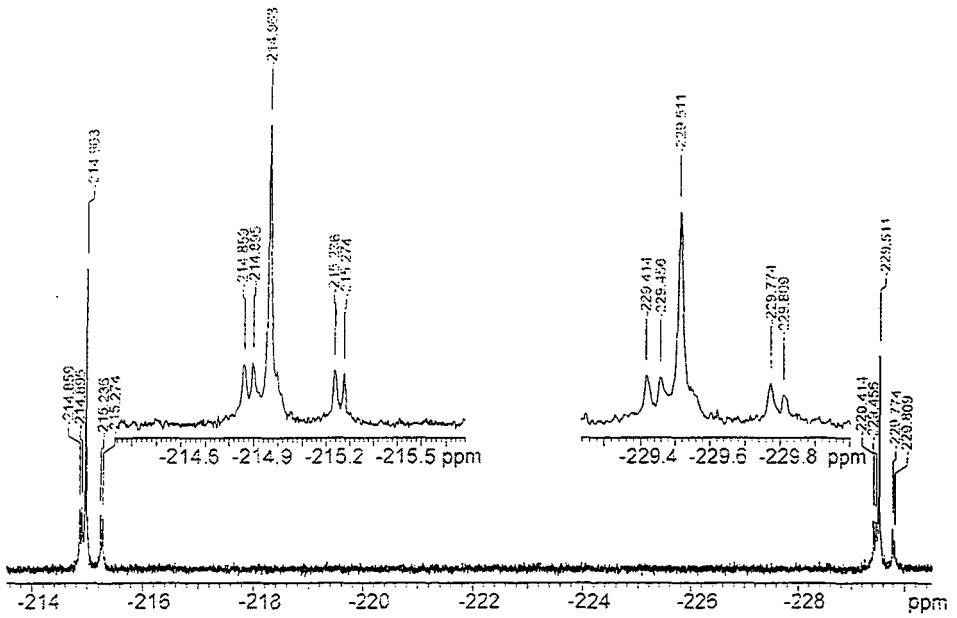

Fig. 3.8 $^{19}F\{^{1}H\}$-NMR spectrum of the supernatant from resting cells of *S. cattleya* incubated with [1,2-$^{13}C_2$]-glycine

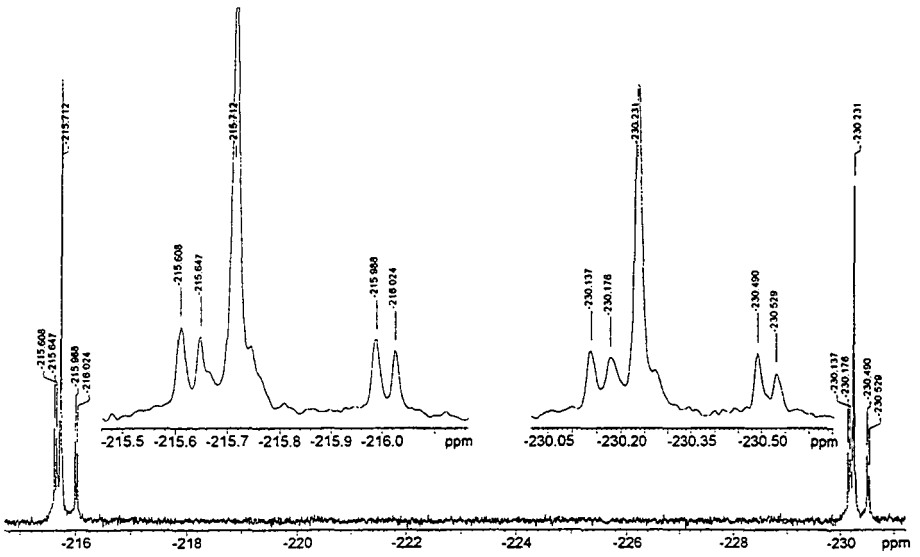

Fig. 3.9 $^{19}F\{^{1}H\}$-NMR spectrum of the supernatant from resting cells of *S. cattleya* incubated with [2-^{13}C]-glycine

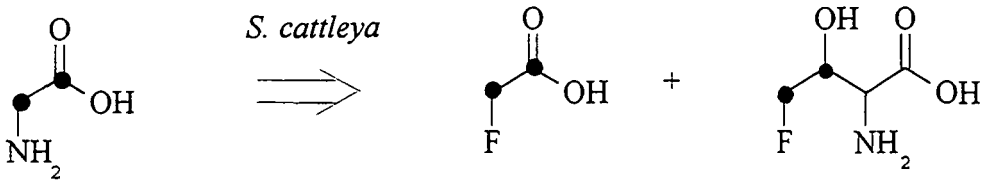

(111) **(112)** **(113)**

Scheme 7

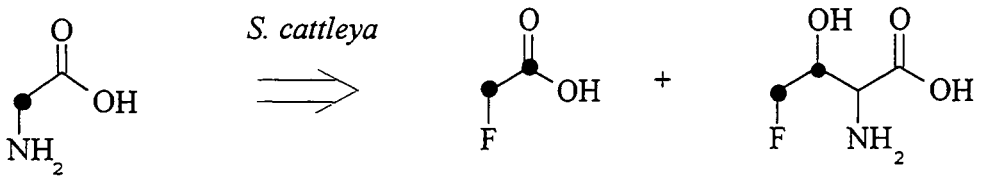

(114) **(112)** **(113)**

Scheme 8

The $^{19}F\{^{1}H\}$-NMR signals for each of the two fluorinated metabolites possess similar multiplicities indicating that the incorporations into fluoroacetate mirror those into C-3 and C-4 of 4-fluorothreonine. A closer inspection of the insets from Figures 3.8 and 3.9 show that in each case the parent (unlabelled) signal (singlet) has a predominant doublet of doublets (160 Hz, 18 Hz, α + β-shift = 0.09ppm) associated with it due to populations (~40%) of fluoroacetate and 4-fluorothreonine with an intact ^{19}F-^{13}C-^{13}C combination. The small increase in intensity of the left hand arms of the doublet of doublets (*dd*) in each case is due to populations (~5%) with a ^{19}F-^{13}C-^{12}C combination (α shift = 0.07ppm, 165Hz). The right hand arm of a doublet (18 Hz, β-shift= 0.02 ppm) at the base of the dominant parent peaks for fluoroacetate and 4-fluorothreonine is also apparent and are due to molecules (~7%) with a ^{19}F-^{12}C-^{13}C combination. Clearly then the GC-MS and ^{19}F-NMR data provide convincing evidence of the similarity of labelling patterns from [1,2-$^{13}C_2$]-glycine and [2-^{13}C]-glycine indicating that the high level double incorporation (~40%) in the [1,2-$^{13}C_2$]-glycine experiment is not due to the incorporation of glycine as an intact two carbon unit but rather that C-2 of glycine is recombining during the biosynthesis. The high level of recombination of C-2 atoms of [1,2-$^{13}C_2$]-glycine and the lack of retention of C-1 of glycine suggests an efficient conversion of glycine to serine.[150] An analogous pathway has been shown to operate in the bacterium *D. glycinophilus*.[151]

A mechanistic interpretation of the metabolic conversion of glycine to serine catalysed by serine hydroxymethyl transferase, is shown in Fig. 3.10 and Fig. 3.11. The former illustrates the transfer of a methylene group to the tetrahydrofolate cofactor generating 5,10-methylene tetrahydrofolate (THFA) **(119)**.[152]

Fig. 3.10

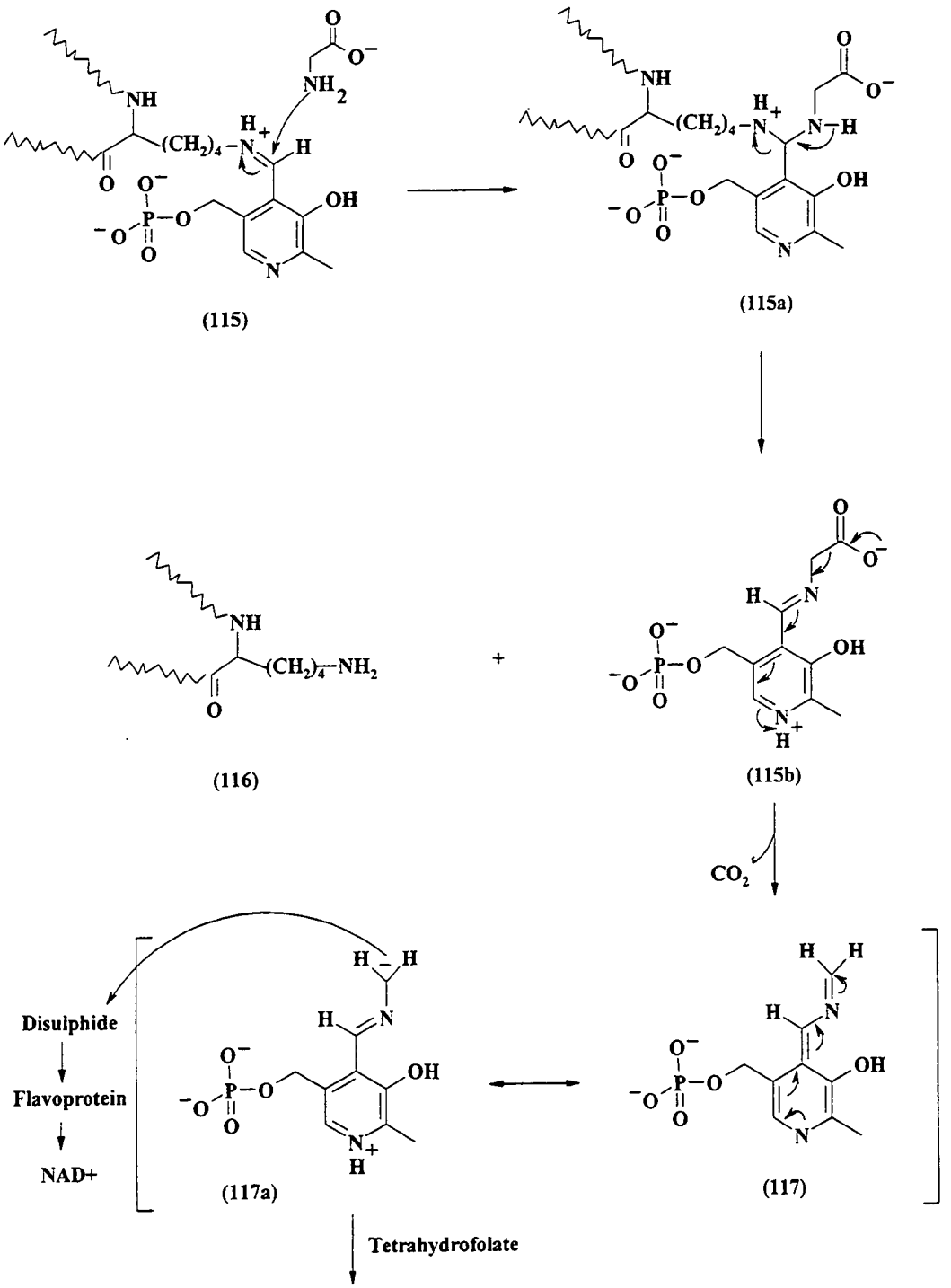

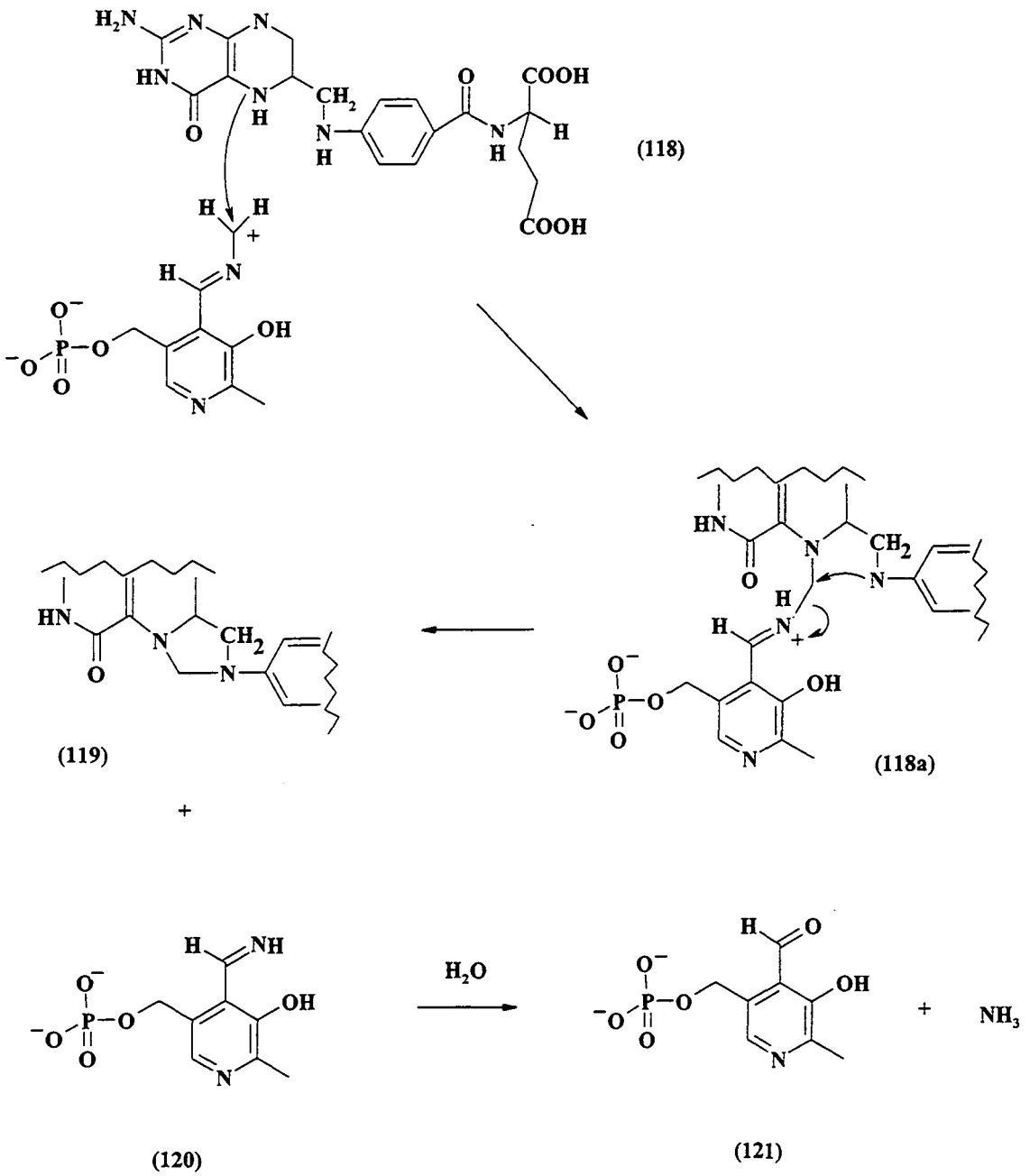

The metabolic conversion of glycine to serine essentially requires two molecules of glycine for every molecule of serine produced. Fig. 3.11 shows the transfer of the C-2 atom from a pyridoxal bound glycine molecule **(122a)** to the N-hydroxymethyl intermediate **(119b)** commonly derived from the reaction between a water molecule and the methylene group of methylene tetrahydrofolate **(119a)**. The Schiff base **(123)** is then

hydrolysed to produce serine **(124)** with the regeneration of pyridoxal-5-phosphate **(121)**

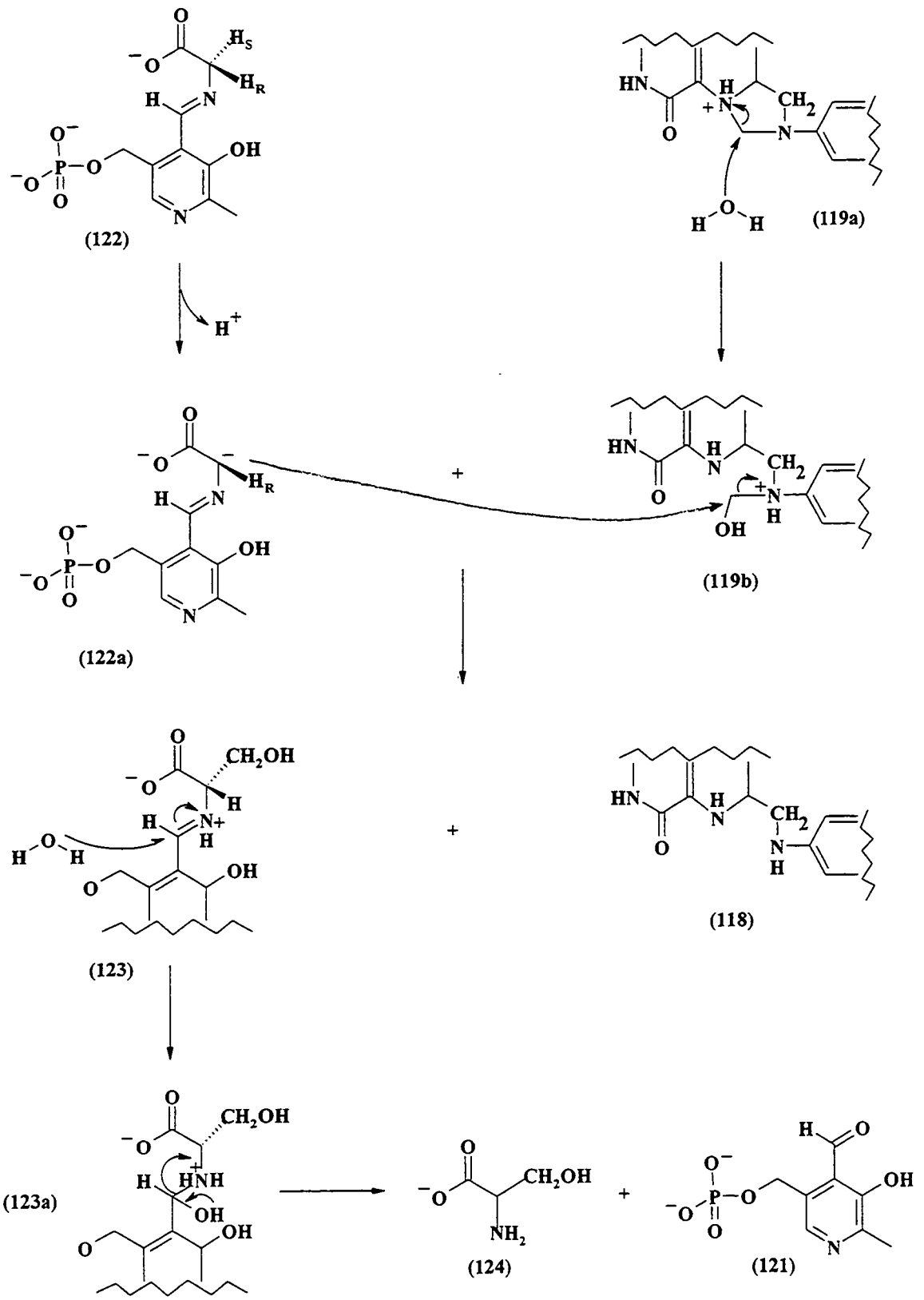

Fig. 3.11

The recombination process involves the attack of ^{13}C-labelled methylene tetrahydrofolate **(126)** to [2-^{13}C]-glycine **(101)** which is already bound to pyridoxal-5-phosphate **(125)** to produce a [2,3-^{13}C]-serine-pyridoxal-5-phosphate complex **(127)**. Hydrolysis of this complex gives [2,3-^{13}C]-serine **(128)** as depicted in Fig. 3.12. The ^{13}C-^{13}C bond of serine is then presumably incorporated intact into fluoroacetate and positions 3 and 4 of 4-fluorothreonine *via* an appropriate intermediate.

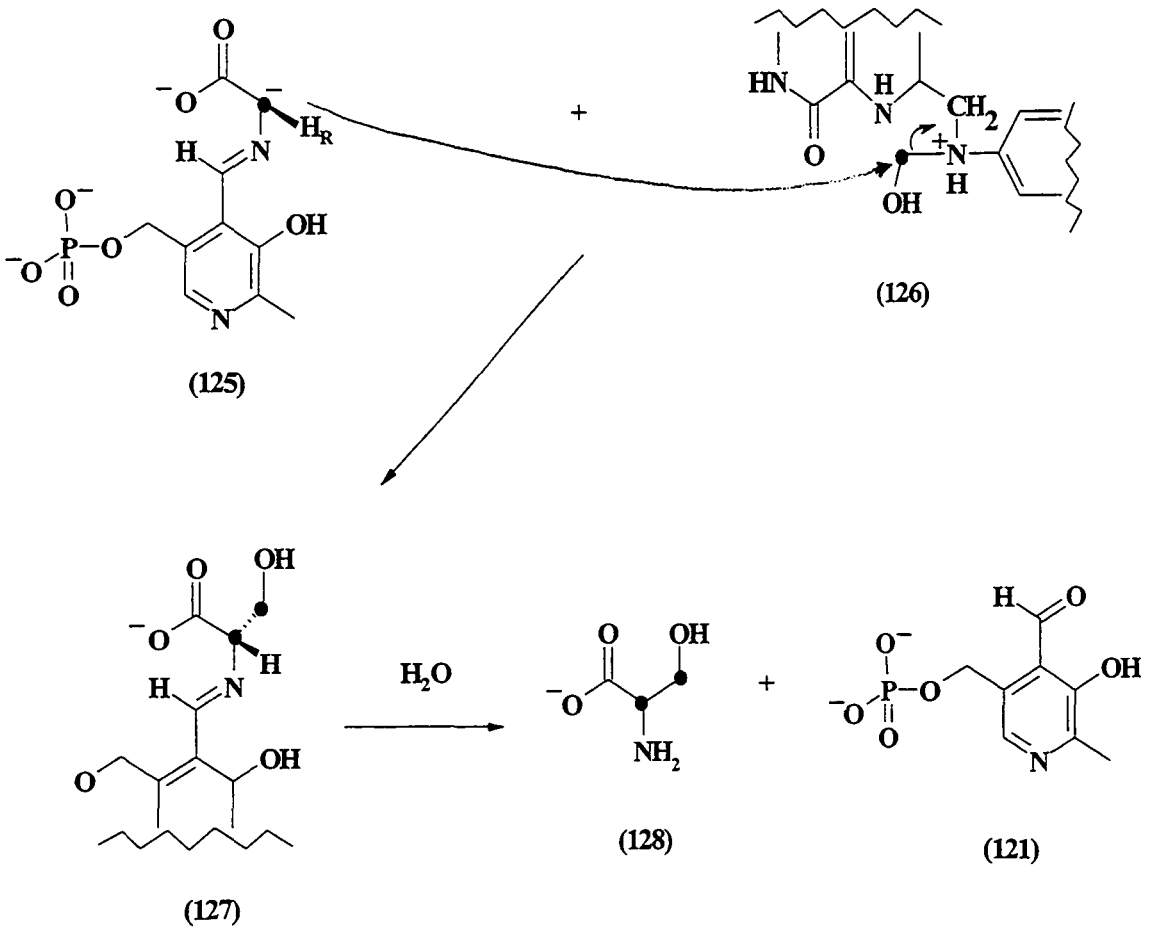

Fig 3.12 The recombination of ^{13}C atoms derived from [2-^{13}C]-glycine during the course of biosynthesis of fluoroacetate and 4-fluorothreonine in *S. cattleya*

It is interesting to note that the incubation of [2-$^{2}H_2$]-glycine **(129)** resulted in an appreciable level of single isotope incorporation into both fluorometabolites (Tables 3.7 and 3.8) accompanied by a small but measurable level of double label into fluoroacetate and 4-fluorothreonine. These incorporations are observed in the $^{19}F\{^{1}H\}$-NMR spectrum of the resultant supernatant (Fig. 3.13).

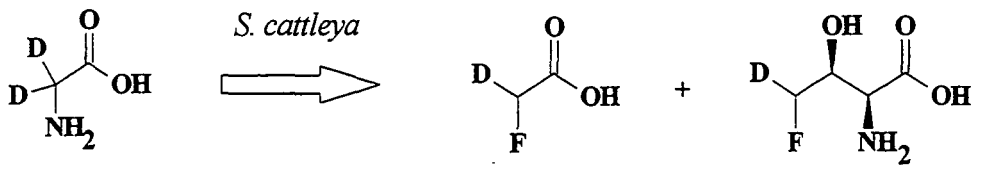

(129)

Scheme 9

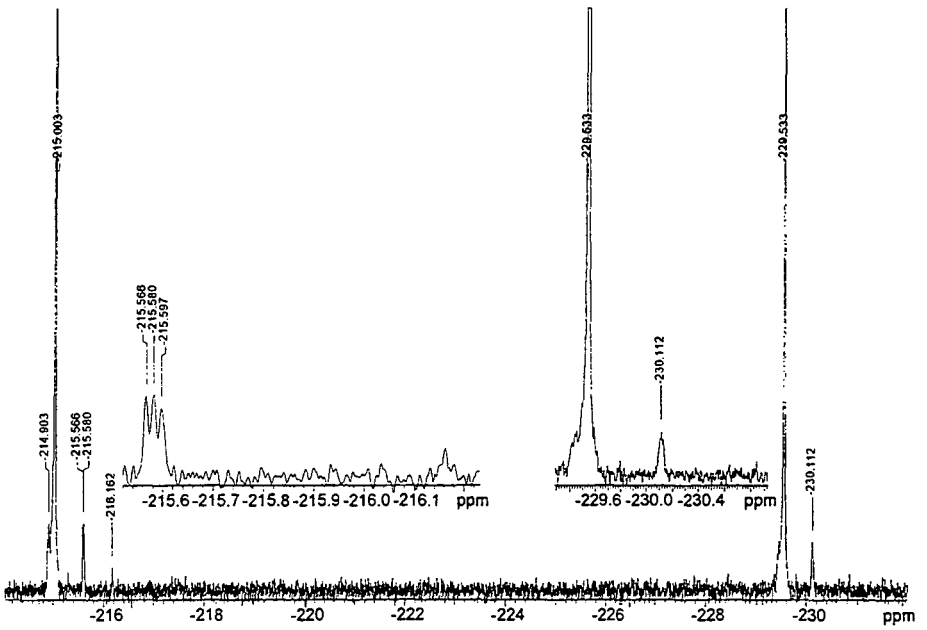

Fig. 3.13 $^{19}F\{^{1}H\}$-NMR spectrum of the supernatant from resting cells of *S. cattleya* incubated with [2-$^{2}H_2$]-glycine

The appreciably lower incorporation into the fluorometabolites from [2-$^{2}H_2$]-glycine compared to [2-^{13}C]-glycine (7% versus 50% respectively) suggests a significant level of hydrogen exchange during the biosynthesis of the fluorometabolites. This is consistent with the earlier complementary experiment using $^{2}H_2O$ which

demonstrated a high level of deuterium labelling into both of the fluorometabolites. The low incorporation of deuterium from [2-$^2H_2$]-glycine is consistent with its conversion to L-serine as discussed above. The fact that some molecules of fluoroacetate retain both α deuterium atoms from [2-$^2H_2$]-glycine indicates that there is no obligatory oxidation occurring at C-2, consistent with the mechanism outlined in Figures 3.11 and 3.12.

3.4 Incorporation of [3-^{13}C]-serine into the fluorometabolites

If glycine is converted to serine during fluorometabolite biosynthesis in *S. cattleya*, a comparatively high incorporation of serine into both fluoroacetate and 4-fluorothreonine is anticipated. With this in mind, resting cells of *S. cattleya* were incubated with [3-^{13}C]-serine at a final concentration of 10mM. The resultant levels of incorporation into fluoroacetate and 4-fluorothreonine are given in Tables 3.9 and 3.10. To allow a relative comparison of the labelling results from the feeding experiments, this study was carried out simultaneously with a [1,2-$^{13}C_2$]-glycine control feeding experiment.

Table 3.9 GC-MS incorporation data of [3-^{13}C]-serine into fluoroacetate produced by resting cells of *S. cattleya*

Precursor	Incubation time (hrs)	% label			
		None	Double	Single	
				Position 1	Position 2
[1,2-$^{13}C_2$]-glycine	24	52.9	35.2	7.3	4.6
	48	50.7	30.4	9.6	9.3
[3-^{13}C]-serine	24	71.5	2.7	6.3	19.4
	48	77.6	1.8	5.5	14.1

(as determined in Belfast)

Table 3.10 GC-MS incorporation data of [3-^{13}C]-serine into selected positions of 4-fluorothreonine produced by *S. cattleya*

Precursor	Incubation time (hrs)	% label in ion 218 (Positions 1 and 2)			% label in ion 236 (Positions 2,3 and 4)			
		None	Single	Double	None	Single	Double	Triple
[1,2-$^{13}C_2$]-glycine	24	88.6	4.0	7.4	56.5	13.0	27.9	2.6
	48	91.0	3.1	5.9	52.8	16.6	28.9	1.7
[3-^{13}C]-serine	24	82.7	14.9	2.4	62.5	31.9	5.6	<1.0
	48	86.4	12.0	1.6	71.0	25.3	3.7	<1.0

(as determined in Belfast)

The GC-MS data (Table 3.9/ 3.10) clearly show a significant incorporation from [3-^{13}C]-serine into the fluorometabolites, as anticipated. The incorporation of label from [3-^{13}C]-serine is mainly into position 2 of fluoroacetate (~19%) with an appreciable level in position 1 (~6%). A significant proportion of label is also apparent in positions 2,3 and 4 of 4-fluorothreonine (ion 236), positions which cannot be uniquely evaluated by GC-MS. However inspection of the ^{19}F{^{1}H}-NMR spectrum of the supernatant from the [3-^{13}C]-serine experiment reveals an identical labelling pattern for fluoroacetate and positions 3 and 4 of 4-fluorothreonine (Fig. 3.14).

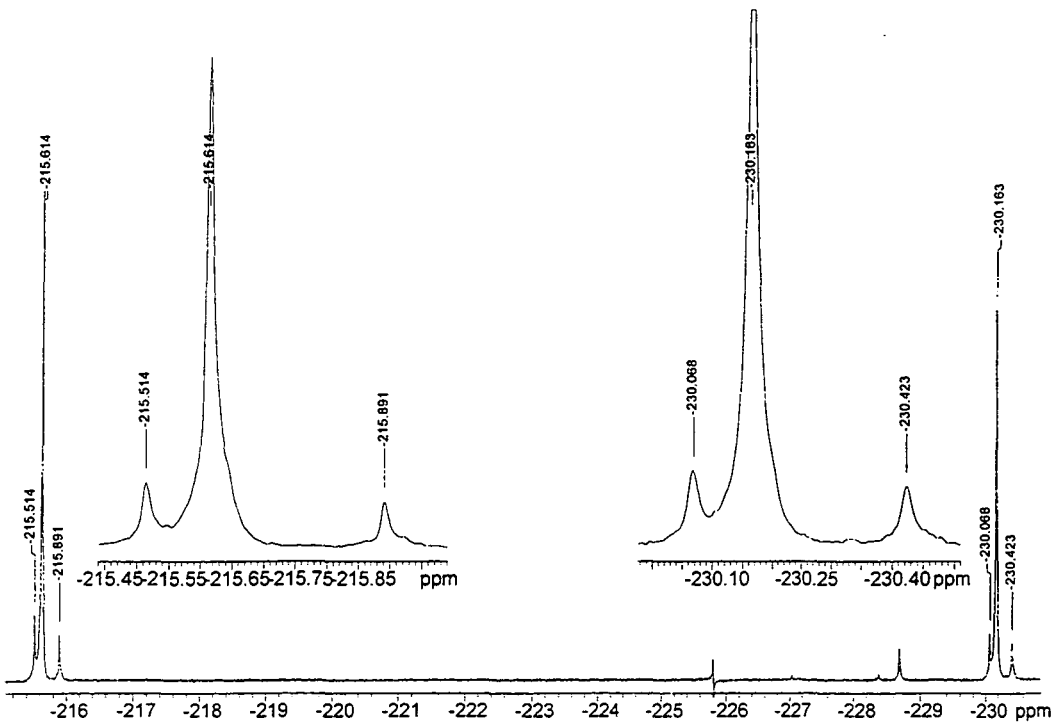

Fig. 3.14 ^{19}F-{^{1}H}-NMR spectrum of the *S. cattleya* supernatant from the [3-^{13}C]-serine incubation experiment

Fig. 3.15 illustrates the presence of doublets (165Hz, α-shift = 0.07ppm) associated with each parent peak (singlet) dominant for both fluoroacetate and 4-fluorothreonine, indicating populations of molecules with a ^{19}F-^{13}C-^{12}C combination. We deduce

therefore that most of the ^{13}C label in the ion 237 (M+1) exists in positions 3 and 4 of 4-fluorothreonine rather than in position 2. Again the striking feature about the spectrum (Fig. 3.15) is the similar labelling pattern for fluoroacetate and 4-fluorothreonine suggesting a single fluorinating enzyme operating in *S. cattleya.*

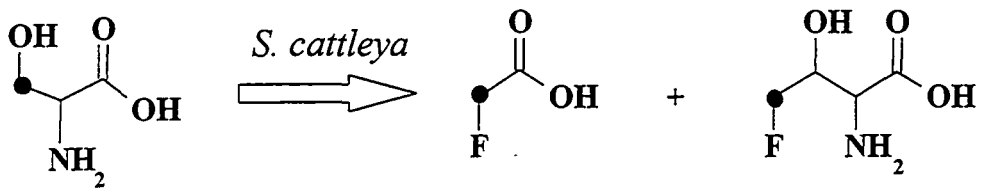

(130) **(131)** **(132)**

Scheme 10

There is an appreciable level of double labelled fluoroacetate (2.7%) and double label into positions 2,3 and 4 of 4-fluorothreonine (5.6%) from [3-^{13}C]-serine. This can be accounted for by the recombination *via* [2-^{13}C]-glycine to produce [2,3-$^{13}C_2$]-serine *in vivo.* The presence of single label in positions 1 and 2 of 4-fluorothreonine from incubation experiments with [3-^{13}C]-serine is consistent with the idea of a three carbon symmetrical intermediate as discussed in section 3.6. In view of the GC-MS incorporation and ^{19}F-NMR data, it is concluded that C-3 of serine contributes C-2 of fluoroacetate and C-4 of 4-fluorothreonine, results which reinforce the hypothesis that glycine is converted to serine prior to incorporation into the fluorometabolites.[150]

3.5 Incorporation of label from [1-^{13}C]-, [2-^{13}C]- and [3-^{13}C]-pyruvates.

Serine is closely related to pyruvate in metabolism. It is well known that the conversion of L-serine into pyruvate is catalysed by the pyridoxal phosphate-dependent enzyme, L-serine dehydratase (EC 4.2.1.13) and it was anticipated that the carbon atoms of pyruvate would become incorporated into the carbon skeletons of both fluorometabolites and furthermore show a similar labelling pattern to that of serine. [1-^{13}C]-, [2-^{13}C]- And [3-^{13}C]-pyruvates were separately incubated with resting cells of *S. cattleya* at a final concentration of 10mM in each case. Again to allow a relative comparison of the labelling results, the feeding experiments were carried out simultaneously with a [1,2-$^{13}C_2$]-glycine control feeding experiment.

In general, the GC-MS incorporation data in Tables 3.11 and 3.12 show a high incorporation of carbon-13 label from [2-^{13}C]-pyruvate and [3-^{13}C]-pyruvate into the fluorometabolites. However, it is noteworthy that [1-^{13}C]-pyruvate gives rise to a single label in position 2 of fluoroacetate (4.0%) and therefore position 4 of 4-fluorothreonine (4.3%), an observation which is clearly evident in the ^{19}F{^{1}H}-NMR spectrum (Fig. 3.15) of the supernatant from the [1-^{13}C]-pyruvate feeding experiment. The accompanying doublets with each dominant peak are due to populations of fluorometabolite molecules containing a ^{19}F-^{13}C-^{12}C combination. It is not clear how [1-^{13}C]-pyruvate is incorporated into the terminal carbon atoms of the fluorometabolites, but for this to occur, the carboxyl moiety of [1-^{13}C]-pyruvate must undergo reduction to a hydroxymethyl functionality which may then be activated for fluorination. Alternatively, decarboxylation of [1-^{13}C]-pyruvate would generate carbon dioxide which can be reincorporated *via* tetrahydrofolate.

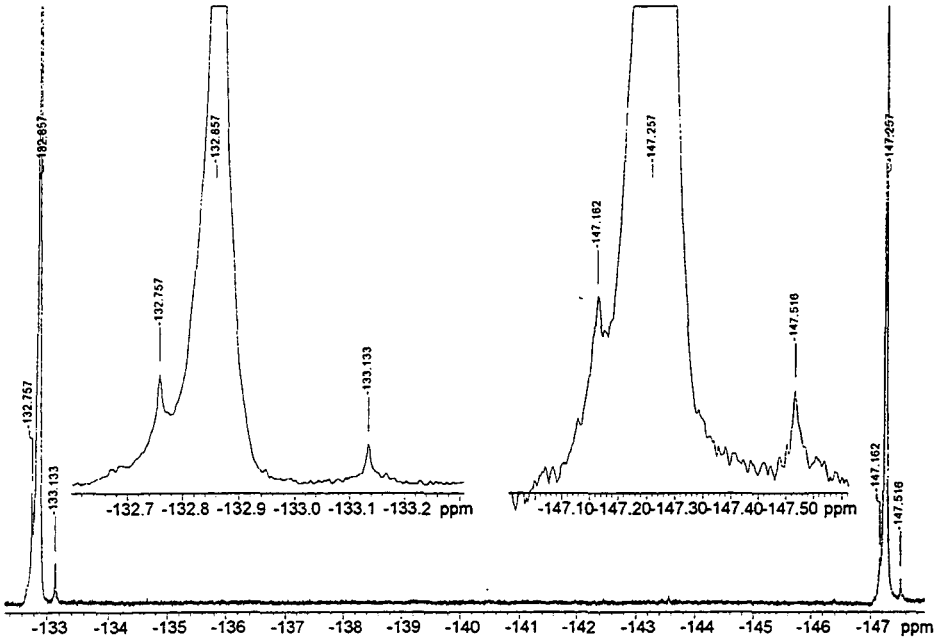

Fig. 3.15 ^{19}F-{^{1}H}-NMR spectrum of the *S. cattleya* supernatant from the [1-^{13}C]-pyruvate feeding experiment

Table 3.11 Incorporation of label into fluoroacetate from stable labelled (^{13}C) pyruvates

Precursor	Incubation time (hrs)	% label			
		None	Double	Single	
				Position 1	Position 2
[1,2-$^{13}C_2$]-glycine	24	47.6	38.8	9.1	4.5
	48	54.5	29.6	8.1	7.7
[1-^{13}C]-pyruvate	24	97.8	<1.0	1.2	1.0
	48	94.9	<1.0	1.1	4.0
[2-^{13}C]-pyruvate	24	54.7	<1.0	41.5	3.8
	48	57.5	<1.0	36.0	5.6
[3-^{13}C]-pyruvate	24	57.0	3.3	8.3	31.4
	48	70.2	2.3	6.8	20.7

(as determined in Belfast)

Table 3.12 Incorporation of label into selected positions of 4-fluorothreonine from stable labelled (^{13}C) pyruvates

Precursor	Incubation time	% label in ion 218 (Positions 1 and 2)			% label in ion 236 (Positions 2,3 and 4)			
	(hrs)	None	Single	Double	None	Single	Double	Triple
[1,2-$^{13}C_2$]-glycine	24	90.0	3.1	5.9	52.5	13.5	31.7	2.3
	48	93.2	2.6	4.2	58.0	17.4	24.6	<1.0
[1-^{13}C]-pyruvate	24	97.2	2.8	<1.0	100	<1.0	<1.0	<1.0
	48	95.4	4.6	<1.0	94.8	4.6	<1.0	<1.0
[2-^{13}C]-pyruvate	24	88.9	10.5	<1.0	54.9	43.7	1.4	<1.0
	48	88.4	11.6	<1.0	55.9	42.1	2.0	<1.0
[3-^{13}C]-pyruvate	24	93.1	6.6	<1.0	56.9	38.2	4.9	<1.0
	48	95.2	4.4	<1.0	69.2	27.8	3.0	<1.0

(as determined in Belfast)

Inspection of the GC-MS results of [2-^{13}C]-pyruvate and [3-^{13}C]-pyruvate indicate that the labelling pattern, for carbons 1 and 2 of fluoroacetate are virtually identical to that for carbons 2,3 and 4 of 4-fluorothreonine in each case. Poignantly the results indicate that the label from [2-^{13}C]-pyruvate is almost exclusively incorporated into position 1 (~40.5%) of fluoroacetate and those from [3-^{13}C]-pyruvate indicate incorporation primarily into the fluoromethyl group (~31.4%) of fluoroacetate. Thus these incorporations closely mirror those of [3-^{13}C]-serine, as anticipated.

$^{19}F\{^{1}H\}$-NMR Analysis of the supernatants from the [2-^{13}C]-pyruvate experiment (Fig. 3.17) shows the parent fluoroacetate and 4-fluorothreonine peaks (δ =- 214.6ppm and -229.0ppm) with an accompanying doublet (18.8Hz, β-shift = 0.02ppm) due to populations of fluoroacetate and 4-fluorothreonine molecules containing ^{19}F-^{12}C-^{13}C combinations. Since incorporation of label from [2-^{13}C]-pyruvate into the fluoromethyl carbon of fluoroacetate is low (~4%) the signal representing [2-^{13}C]-

fluoroacetate ($^{1}J^{13}_{C\text{-}F}$ = 165Hz) is visible in the baseline. From the Belfast GC-MS incorporation data of [2-^{13}C]-pyruvate (Table 3.12), it is difficult to assign the enriched site of 4-fluorothreonine (2,3 or 4), however this becomes obvious by ^{19}F{^{1}H}-NMR analysis as shown in Fig. 3.16.

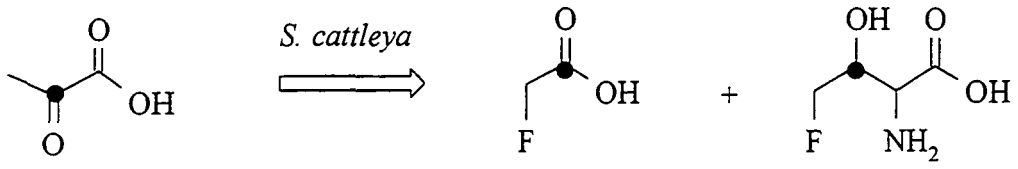

(133) **(134)** **(135)**

Scheme 11

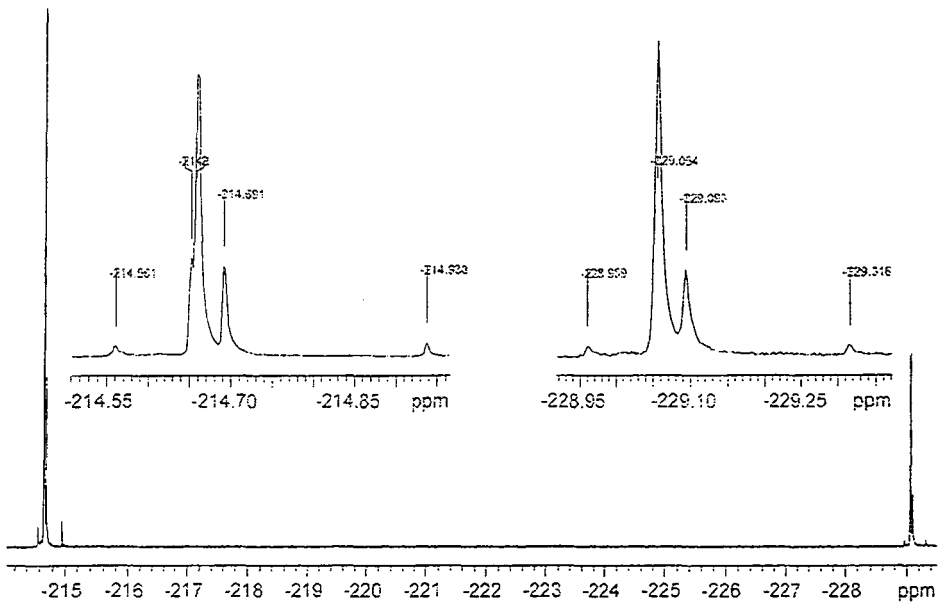

Fig. 3.16 ^{19}F-{^{1}H}-NMR spectrum of incorporation of label into fluoroacetate and 4-fluorothreonine by resting cells of *S. cattleya* incubated with [2-^{13}C]-pyruvate

The 4-fluorothreonine signal has an accompanying doublet (δ = -229.07ppm) with a coupling constant value of 18.3Hz indicative of carbon-13 in position 3 of

4-fluorothreonine. This analysis clearly demonstrates that the majority of the single label from [2-^{13}C]-pyruvate resides in the 3 position of 4-fluorothreonine as illustrated in Scheme 11. A similar analysis of the ^{19}F{^{1}H}-NMR spectrum of the supernatants from [3-^{13}C]-pyruvate (Fig. 3.17) shows that the ^{13}C primarily occupies the fluoromethyl carbons of both fluorometabolites, generating in each case a doublet (165Hz) due to a combination of ^{19}F-^{13}C-^{12}C (Scheme 12). These results show that C-2 and C-3 of pyruvate contribute to C-3 and C-4 of 4-fluorothreonine and carbons 1 and 2 of fluoroacetate as illustrated in scheme 13.[153]

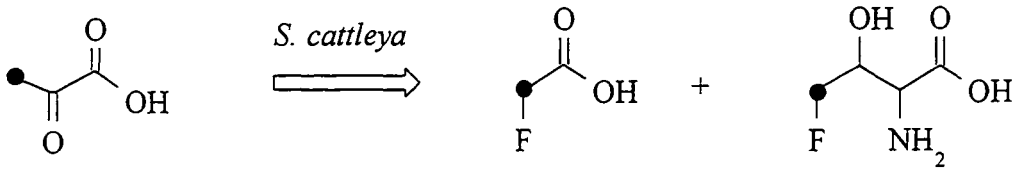

(136) **(131)** **(132)**

Scheme 12

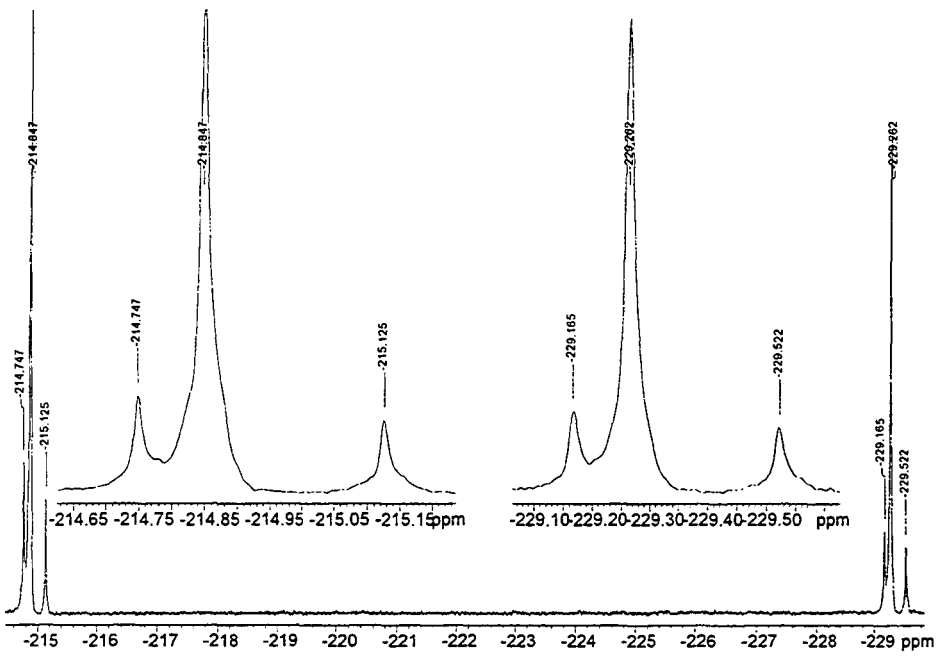

Fig. 3.17 ^{19}F-{^{1}H}-NMR spectrum of the incorporation of [3-^{13}C]-pyruvate into fluoroacetate and 4-fluorothreonine produced by resting cells of *S. cattleya*

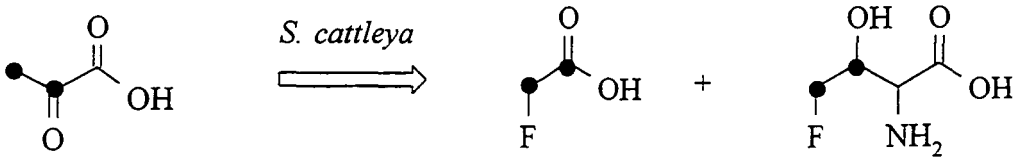

(137) **(112)** **(113)**

Scheme 13

3.6 Origin of the C-1 and C-2 fragment of 4-fluorothreonine

The GC-MS analysis (discussed in Chapter 2) of the incorporation of isotopes into 4-fluorothreonine produced by *S. cattleya* allows determination of label into C-1 and C-2 of 4-fluorothreonine. However it must be noted that it is not possible to uniquely discriminate the position of the label on the C-1 and C-2 fragment of 4-fluorothreonine. For the purpose of this investigation, reference will be made to the GC-MS incorporation data for the ^{13}C labelled pyruvates (Table 3.12). It can be seen from Table 3.12 that [2-^{13}C]-pyruvate is incorporated (single label) at a level (~11.6%) approximately twice that for either [1-^{13}C]-pyruvate (~4.6%) or [3-^{13}C]-pyruvate (4.4%) into positions 1 and 2 of 4-fluorothreonine. This suggests the possibility of scrambling of carbons 1 and 3 of pyruvate prior to its incorporation into the α-aminocarboxylate portion of 4-fluorothreonine. One hypothesis, which also accounts for the incorporation pattern of ^{13}C from [1-^{13}C]-glycine (compare Tables 3.8 and 3.10 for incorporation of [1-^{13}C]-glycine and [3-^{13}C]-serine respectively into ion 218) *via* [1-^{13}C]-serine envisages the formation of a symmetrical 3-carbon intermediate from serine, as depicted in Fig. 3.18.

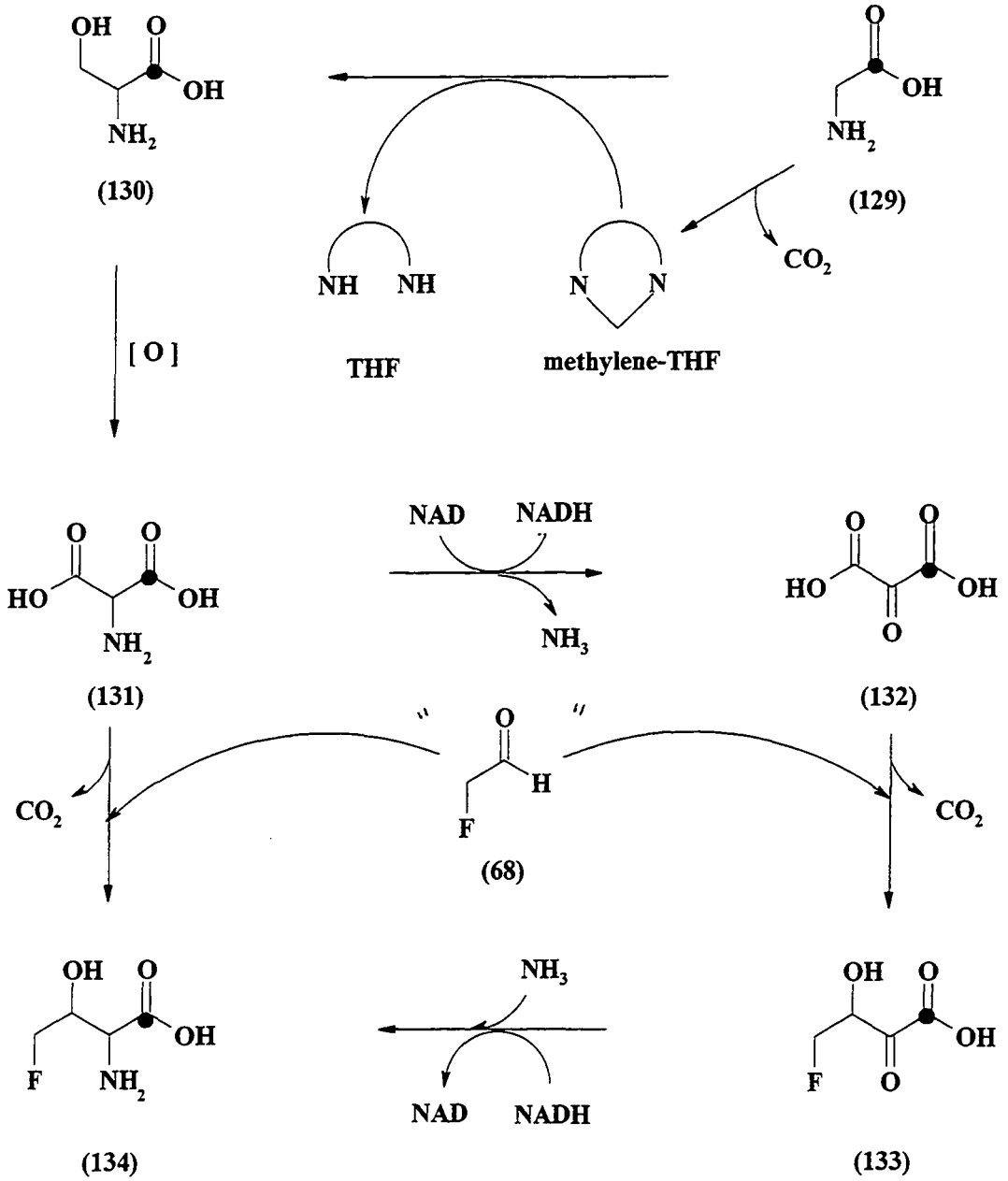

Fig. 3.18 A hypothetical route to positions 1 and 2 of 4-fluorothreonine by ^{13}C label from [1-^{13}C]-glycine

This hypothetical route suggests the conversion of serine to 2-aminopropanedioic acid **(140)** or 2-ketopropanedioic acid **(141)**, followed by decarboxylation and condensation with a fluoroacetaldehyde **(68)** equivalent. During the decarboxylation step there exists an equal likelihood that either C-1 or C-3 of the symmetrical 3-carbon intermediate is lost. Thus a ^{13}C-atom in position 1 or 3 of serine or C-2 of glycine would contribute to position 1 of 4-fluorothreonine.

3.7 The incorporation of isotopically labelled alanine into fluoroacetate and 4-fluorothreonine

L-Alanine is the transamination product of pyruvate. In view of the role of pyruvate as a precursor to the fluorometabolites, an investigation into the relative incorporation of stable isotope from DL-[3-^{13}C]-alanine, DL-[3,3,3-$^{2}H_3$]-alanine and DL-[3-^{13}C-3,3,3-$^{2}H_3$]-alanine was initiated. It proved easier to prepare deuterium labelled alanines than deuterium labelled pyruvates, and thus alanine was used here essentially as a pyruvate surrogate. The deuterium labelled alanines were synthesised using a modification of Seebach's imidazolidinone methodology[154] for the preparation of amino acids (refer to Chapter 4 for a detailed discussion of the methodology)

3.7.1 Synthesis of DL-alanine and [3,3,3-$^{2}H_3$]-alanine

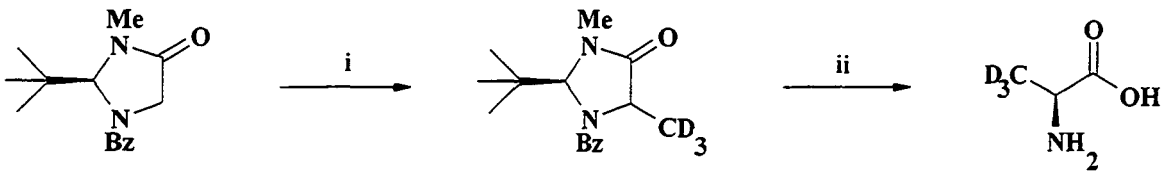

(±) (±) (±)

(144) **(145)** **(146)**

Scheme 14 (i) LDA/ CD_3I/ -100°C (ii) 6N HCl/ 180°C/ Carius tube/ 12h

DL-[3,3,3-$^{2}H_3$]-Alanine may be prepared in two steps by coupling the imidazolidinone **(144)** with [$^{2}H_3$]-methyliodide (Scheme 14). Accordingly the racemic auxiliary **(144)** was deprotonated with LDA and reacted with [$^{2}H_3$]-methyl iodide to give the [$^{2}H_3$]-adduct **(145)**. The desired DL-[3,3,3-$^{2}H_3$]-alanine **(146)** was obtained after acid hydrolysis of **(145)** and purification on acidic ion-exchange resin.

3.7.2 Results of the incorporation of isotopically labelled alanines

To allow a relative comparison of the labelling results, the feeding experiments were carried out simultaneously with a [1,2-$^{13}C_2$]-glycine control experiment.

Table 3.13 GC-MS incorporation data of (^{13}C/ ^{2}H) alanines into fluoroacetate

Precursor	Incubation time (hrs)	% label			
		None	Double	Single	
				Position 1	Position 2
[1,2-$^{13}C_2$]-glycine	24	47.2	39.4	8.3	5.1
	48	50.1	34.0	10,1	5.8
[3-^{13}C]-alanine	24	62.3	3.6	3.2	30.9
	48	72.0	2.6	6.7	18.7
[3,3,3-$^{2}H_3$]-alanine	24	86.6	6.4	-	7.0
	48	90.0	5.1	-	4.9

(as determined in Belfast)

Resting cells of *S. cattleya* supplemented with [3-^{13}C]-alanine showed an almost exclusive incorporation (30.9%) into position 2 of fluoroacetate. The labelling pattern for [3-^{13}C]-pyruvate is similar suggesting that alanine and pyruvate are equally effective precursors of fluoroacetate and 4-fluorothreonine as anticipated. Moreover a comparable proportion of single label (~37%) from [3-^{13}C]-alanine was observed in positions 2,3 and 4 of 4-fluorothreonine. From the resultant $^{19}F\{^{1}H\}$-NMR spectrum (Fig. 3.19), it is apparent that the label from [3-^{13}C]-alanine, like that from [3-^{13}C]-serine and [3-^{13}C]-pyruvate, predominates in the fluoromethyl carbons of each fluorinated metabolite. Inspection of the insets from Fig. 3.19 shows that the dominant unlabelled signal in each case has an associated doublet (168-177Hz, α-shift = 0.08-0.09ppm) due to populations of fluoroacetate and 4-fluorothreonine containing a ^{19}F-^{13}C-^{12}C combination. The small

increase in intensity of the right hand arms of each doublet is due to molecules of fluoroacetate and 4-fluorothreonine with a ^{19}F-^{13}C-^{13}C pattern. The right hand arm of a doublet (18Hz, β-shift = 0.02ppm) at the base of the parent peaks for fluoroacetate and 4-fluorothreonine is also apparent and is due to molecules with a ^{19}F-^{12}C-^{13}C combination.

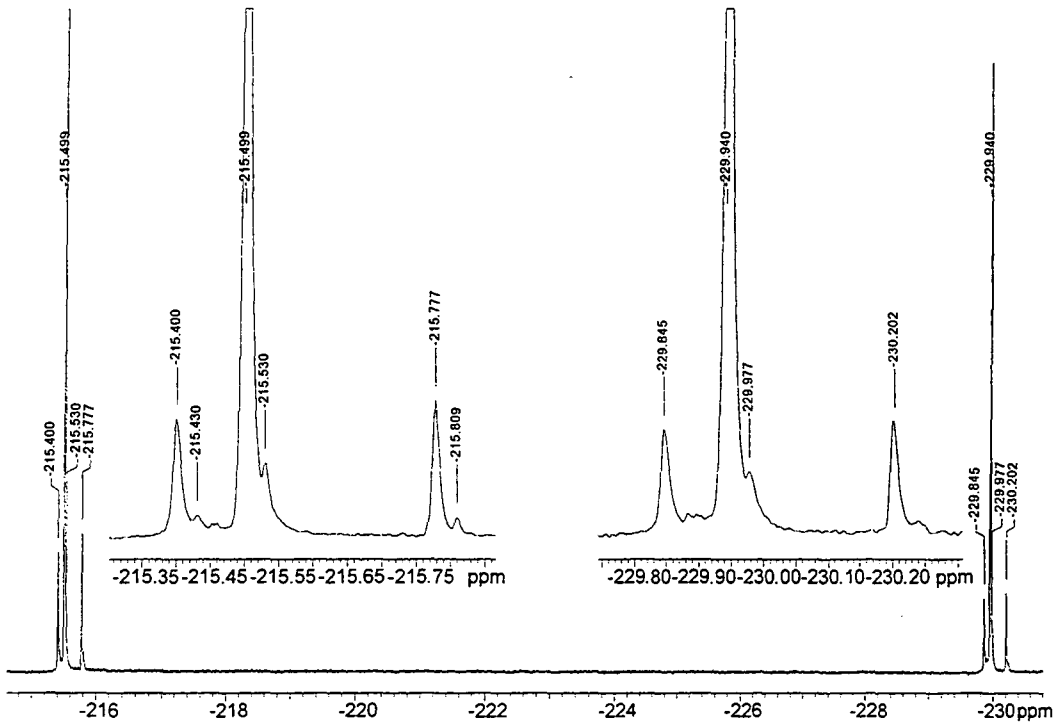

Fig. 3.19 $^{19}F\{^{1}H\}$-NMR spectrum of the supernatant from resting cells of *S. cattleya* incubated with [3-^{13}C]-alanine

Table 3.14 GC-MS incorporation data of [3,3,3-$^{2}H_3$-3-^{13}C]-alanine into fluoroacetate

Precursor	Incubation time (hrs)	% label			
		None	Double	Single	
				Pos. 1	Pos. 2
[1,2-$^{13}C_2$]-glycine	24	59.0	28.7	7.9	4.4
	48	39.2	45.6	9.7	5.5

Precursor	Incubation time (hrs)	% label in positions 1 and 2				% label in position 2			
		None	Single	Double	Triple	None	Single	Double	Triple
[3,3,3-$^{2}H_3$-3-^{13}C]-alanine*	24	64.7	17.5	8.1	9.7	71.5	13.3	6.0	9.2
	48	64.7	17.6	6.9	10.8	74.2	14.5	4.9	6.4

(as determined in Belfast)

Table 3. 15 GC-MS incorporation data of (^{13}C/ ^{2}H) alanines into selected positions of 4-fluorothreonine

	Incubation time	% label in ion 218 (Positions 1 and 2)			% label in ion 236 (Positions 2,3 and 4)			
	(hrs)	None	Single	Double	None	Single	Double	Triple
[1,2-$^{13}C_2$]-glycine	24	87.8	3.8	8.4	48.8	14.5	33.3	3.4
	48	89.3	3.5	7.2	51.3	17.5	28.6	2.6
[3-^{13}C]-alanine	24	79.2	18.0	2.8	51.6	37.0	10.6	<1.0
	48	82.6	15.2	2.2	60.3	32.7	6.7	<1.0
[3,3,3-$^{2}H_3$]-alanine	24	100	<1.0	<1.0	85.4	6.6	8.0	<1.0
	48	100	<1.0	<1.0	88.7	5.3	6.0	<1.0
[1,2-$^{13}C_2$]-glycine	24	89.5	3.6	6.9	59.4	14.6	24.3	1.7
	48	80.0	5.5	14.5	39.4	18.0	36.0	6.6
[3,3,3-$^{2}H_3$-3-^{13}C]-alanine *	24	73.9	21.2	4.9	51.7	26.1	12.1	10.1
	48	73.1	21.4	4.5	54.9	27.4	9.8	7.9

*(as determined in Belfast) * synthesised by Dr. N. Chesters, Durham*

It is perhaps interesting to note that the level of single label detected in positions 1 and 2 of 4-fluorothreonine after incubation with [3-^{13}C]-alanine is three fold higher than that observed for [3-^{13}C]-pyruvate (compare Tables 3.15 and 3.12). Furthermore incubation studies with [3,3,3-$^{2}H_3$]-alanine showed that one (~6%) and two (~7%) deuterium atoms were incorporated into the fluoromethyl moieties of each fluorinated metabolite.

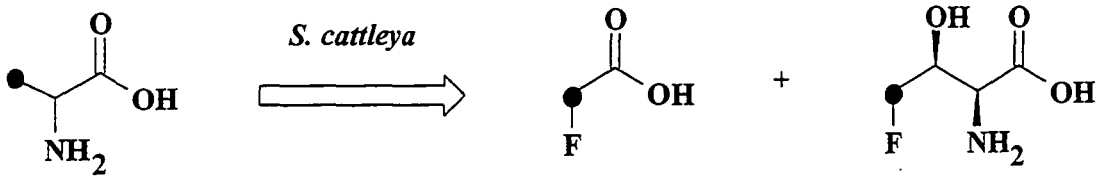

(147)

Scheme 15

The GC-MS data (Tables 3.14/ 3.15) indicate that the labelling pattern derived from [3-^{13}C,3,3,3-$^{2}H_3$]-alanine (synthesised by Dr. N. Chesters, Durham) closely resembles that for [3-$^{2}H_3$]- and [3-^{13}C]-alanine. However the GC-MS data for incorporations into ion 236 do not allow a definitive assignment of the number and type of label present at each position (2,3 or 4) of 4-fluorothreonine. Nevertheless a much clearer picture again emerges with ^{19}F{^{1}H}-NMR analysis allowing the presence of up to two deuterium atoms on the fluoromethyl group. The proton coupled ^{19}F-NMR [Fig. 3.20(a)] illustrates that each parent signal is associated with a pair of upfield shifted (1.24-1.28ppm) doublets (J=167Hz) corresponding to the presence of triple label consisting of two deuterium and one ^{13}C atom on the fluoromethyl positions of fluoroacetate and 4-fluorothreonine. Increasing the sensitivity of the ^{19}F-NMR experiment by applying proton decoupling unambiguously reveals, in each case, a set of

^{13}C satellites due to populations of fluorometabolite molecules with a ^{19}F-^{13}C-^{12}C sequence [Fig. 3.20(b)]. Fluorine signals due to ^{19}F-^{13}C-^{2}H populations of fluoroacetate and 4-fluorothreonine are also apparent (Scheme 16).

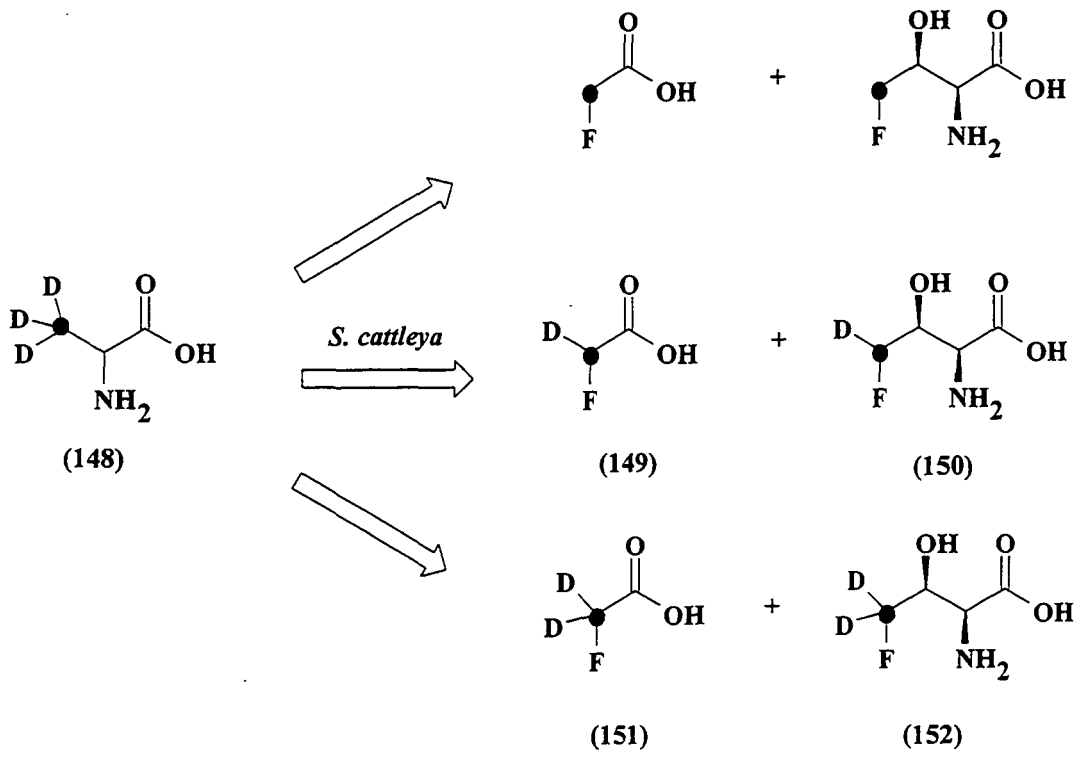

Scheme 16

The incorporation of two deuterium atoms from DL-[3-^{13}C,3,3,3-$^{2}H_3$]-alanine, albeit small, into the fluoromethyl group of both fluorometabolites suggests that oxidation of this group is not a necessary pre-requisite for fluorination. The similarities between the labelling patterns after incubations with DL-[3-^{13}C]-serine, DL-[3-^{13}C]-alanine and [3-^{13}C]-pyruvate suggests that these compounds interconvert and have a close metabolic relationship in *S. cattleya*. Of course it is well known that pyruvate can be derived from serine mediated by L-serine dehydratase and also from L-alanine through transamination during normal cell metabolism.

Fig. 3.20 (a) ^{19}F-NMR spectrum (b) ^{19}F{^{1}H}-NMR spectrum of the cell supernatant from the [3-^{13}C-3,3,3-$^{2}H_3$]-alanine feeding experiment.

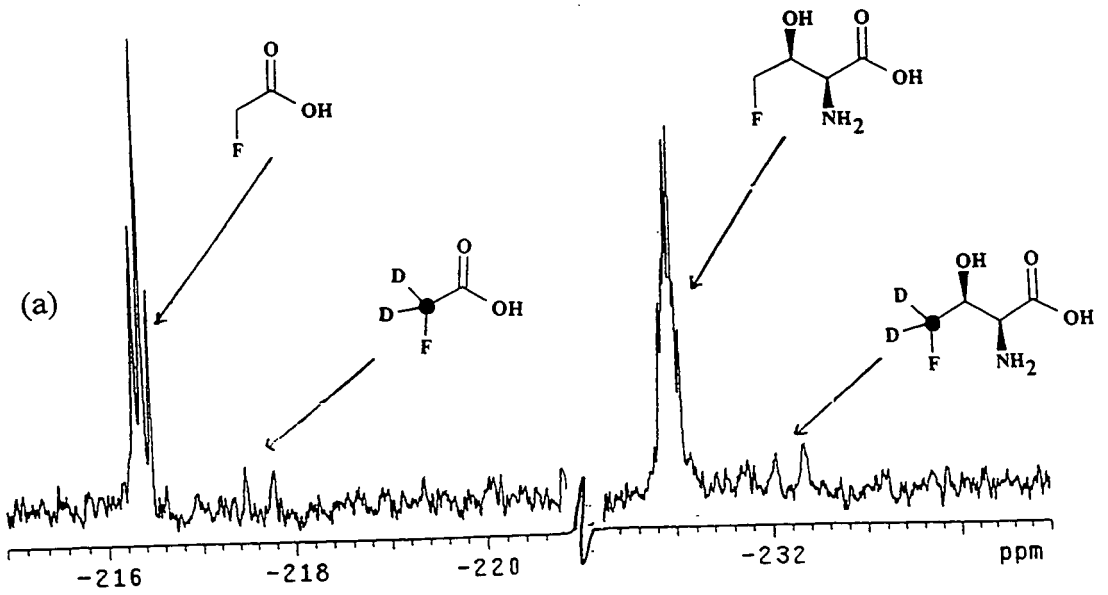

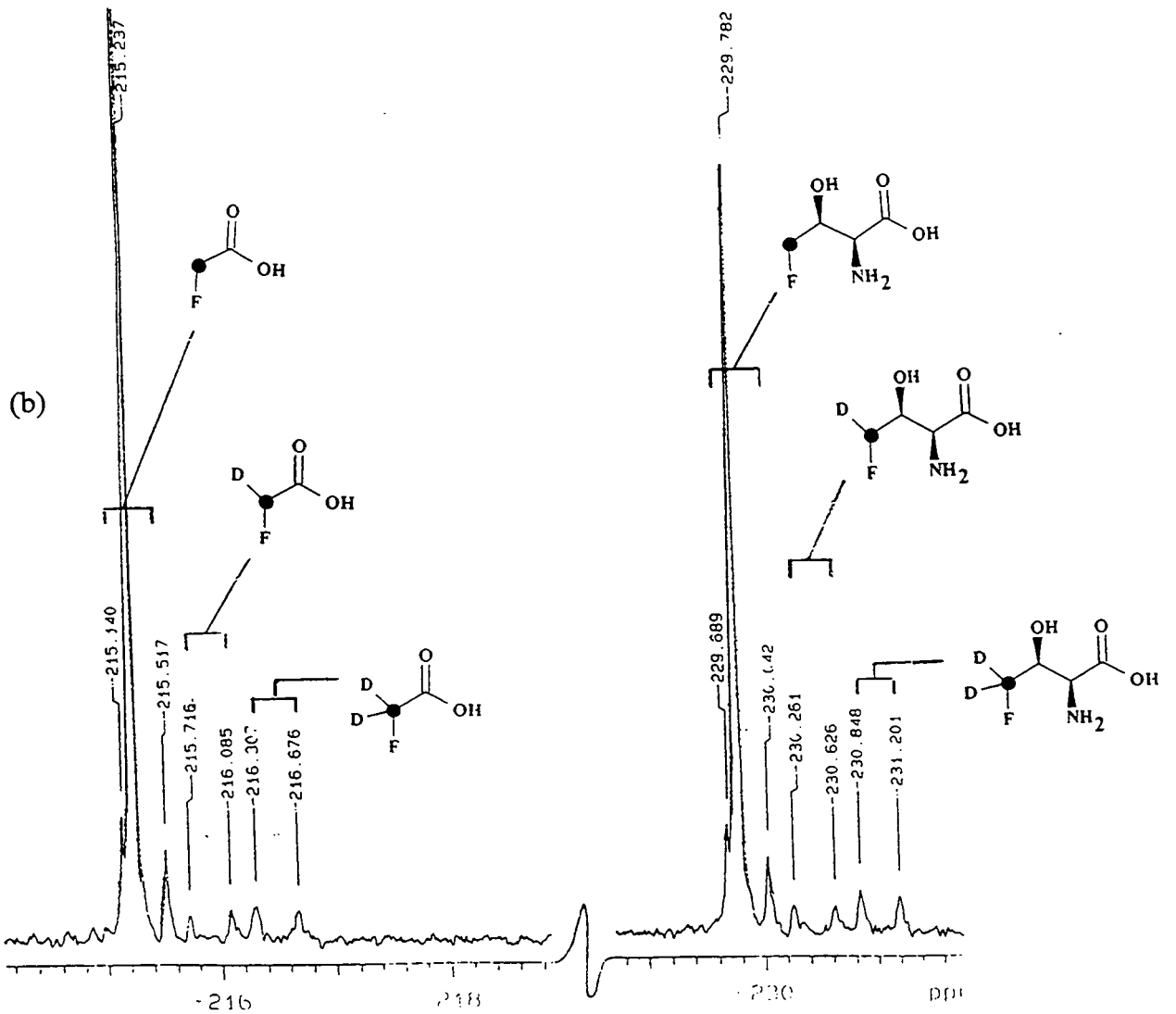

3. 8 Incorporation of deuterium from [2,2,3,3-$^2H_4$]-succinic and [2,3,3-$^2H_3$]-aspartic acids into fluoroacetate and 4-fluorothreonine.

The relatively high incorporation of ^{14}C-label from succinic and aspartic acids (see radiochemical results, Chapter 2) prompted us to investigate if the hydrogen atoms located at C-2 and C-3 of these metabolic acids could be incorporated intact into the appropriate carbon sites of fluoroacetate and 4-fluorothreonine (Schemes 17 and 18).

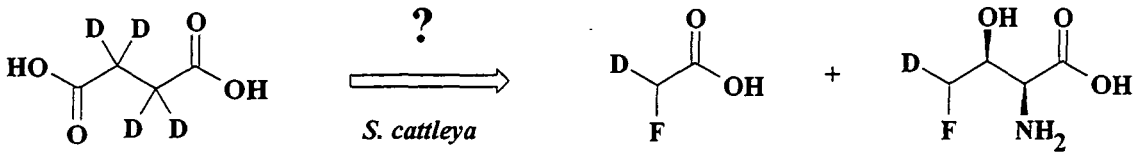

(153)

Scheme 17

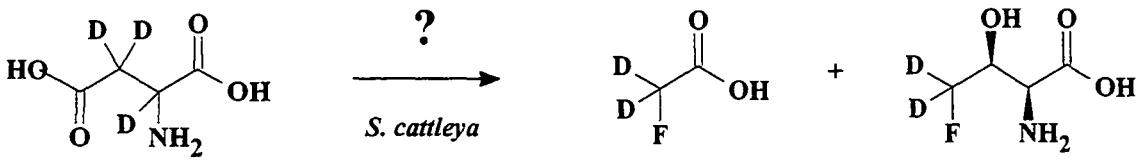

(154)

Scheme 18

It was anticipated that metabolism of the deuteriated succinic acid, through the TCA cycle, would generate [3-^2H]-oxaloacetate and furnish fluorometabolites bearing a single deuterium atom bonded to the fluoromethyl carbons. The processing of the deuterium atoms from [2,3,3-$^2H_3$]-aspartate was predicted to occur with retention of up to two deuterium atoms. Thus deuterium labelled succinate and aspartate were

administered to resting cells of *S. cattleya* at a final concentration of 10mM. The $^{19}F\{^{1}H\}$-NMR spectrum resulting from the incubation of [2,2,3,3-$^{2}H_4$]-succinate with resting cells of *S. cattleya* is shown in Fig. 3.21.

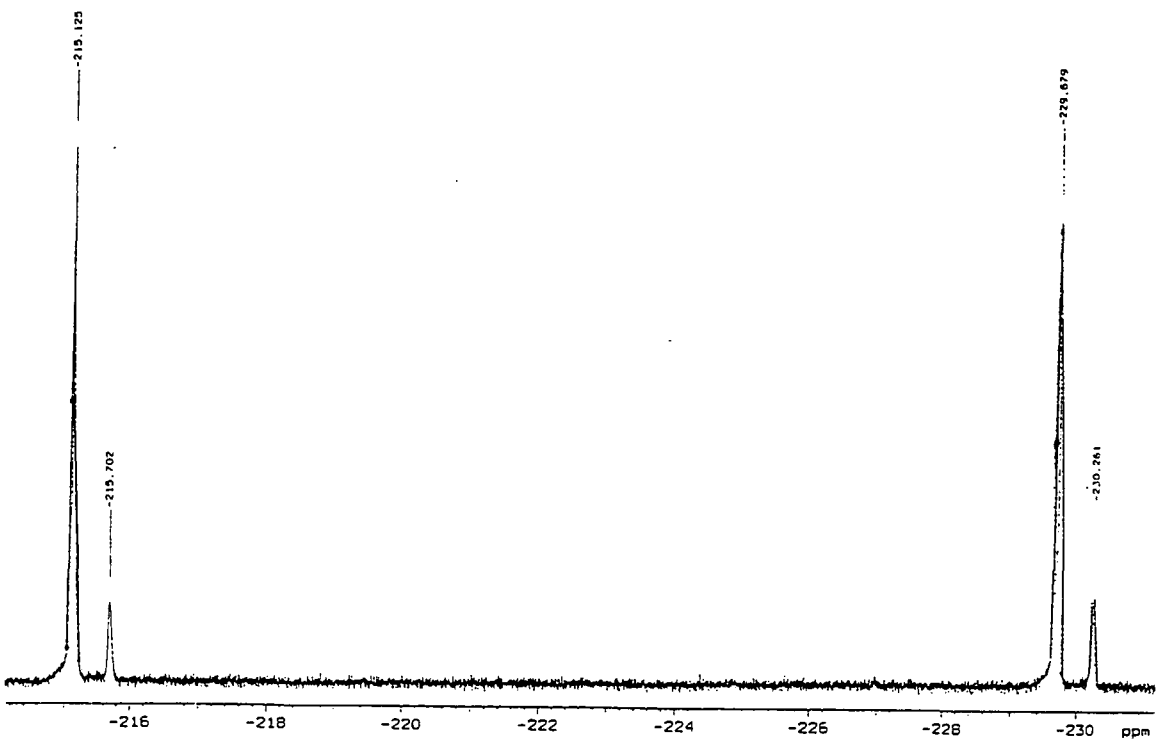

Fig. 3.21 $^{19}F\{^{1}H\}$-NMR of lyophilised cell extracts from the [2,2,3,3-$^{2}H_4$]-succinate feeding experiment

As predicted a single deuterium atom is retained in both fluoroacetate and 4-fluorothreonine as seen by the presence of an upfield shifted triplet (J=6 Hz, β-shift = 0.6ppm) associated with the parent (unlabelled) signals. The absence of the incorporation of two deuterium atoms is consistent with its *in vivo* conversion to oxaloacetate bearing one deuterium atom at C-3 **(157)** as outlined in Scheme 19. The deuterium atom retained in **(157)** is carried through to the fluoromethyl carbons of both fluorometabolites, presumably *via* the phosphoenolpyruvate intermediate **(158)**.

Table 3.16 GC-MS incorporation data of [2,2,3,3-$^2H_4$]-succinic and [2,3,3-$^2H_3$]-aspartic acids into fluoroacetate

Precursor	Incubation time	% label			
	(hrs)	None	Double	Single	
				Position 1	Position 2
[2,2,3,3-$^2H_4$]-succinate	24	82.3	1.2	-	16.5
	48	79.5	<0.5	-	20.0
[2,3,3-$^2H_3$]-aspartate	48	93.5	2.0	-	4.5

(as determined in Belfast)

Table 3.17 GC-MS incorporation data of [2,2,3,3-$^2H_4$]-succinic and [2,3,3-$^2H_3$]-aspartic acids into selected positions of 4-fluorothreonine.

Precursor	Incubation time	% label in ion 218 (Positions 1 and 2)			% label in ion 236 (Positions 2,3 and 4)		
	(hrs)	None	Single	Double	None	Single	Double
[2,2,3,3-$^2H_4$]-succinate	24	100	<0.5	<0.5	85.3	14.5	<0.5
	48	99.7	<0.5	<0.5	81.3	18.6	<0.5
[2,3,3-$^2H_3$]-aspartate	48	99.8	<0.5	<0.5	93.1	4.8	2.3

(as determined in Belfast)

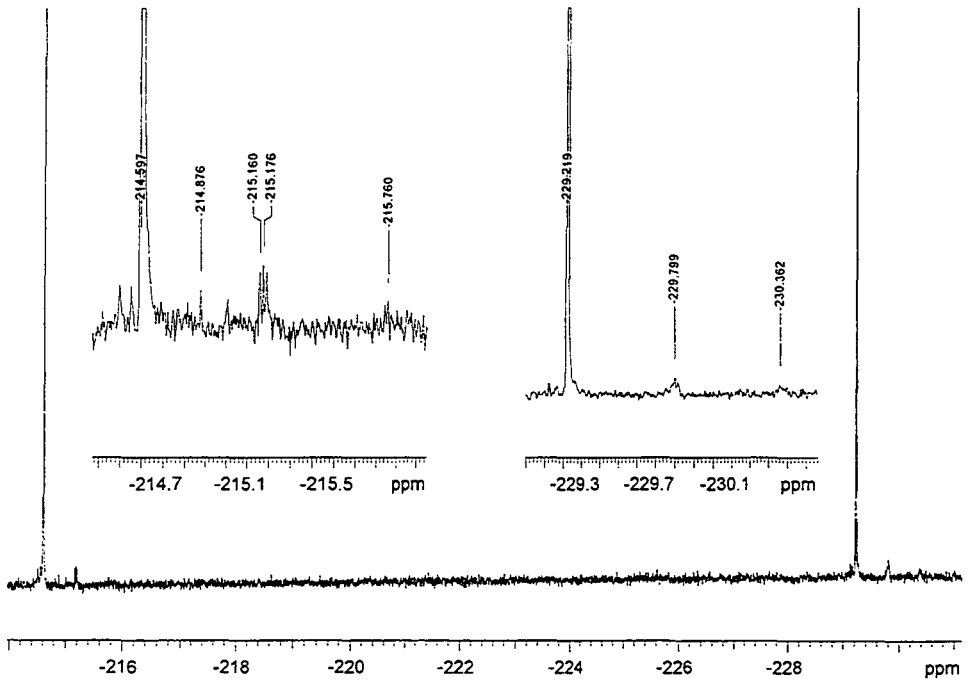

Fig. 3.22 $^{19}F\{^1H\}$-NMR spectrum of the supernatant from resting cells of *S. cattleya* incubated with [2,3,3-$^2H_3$]-aspartate

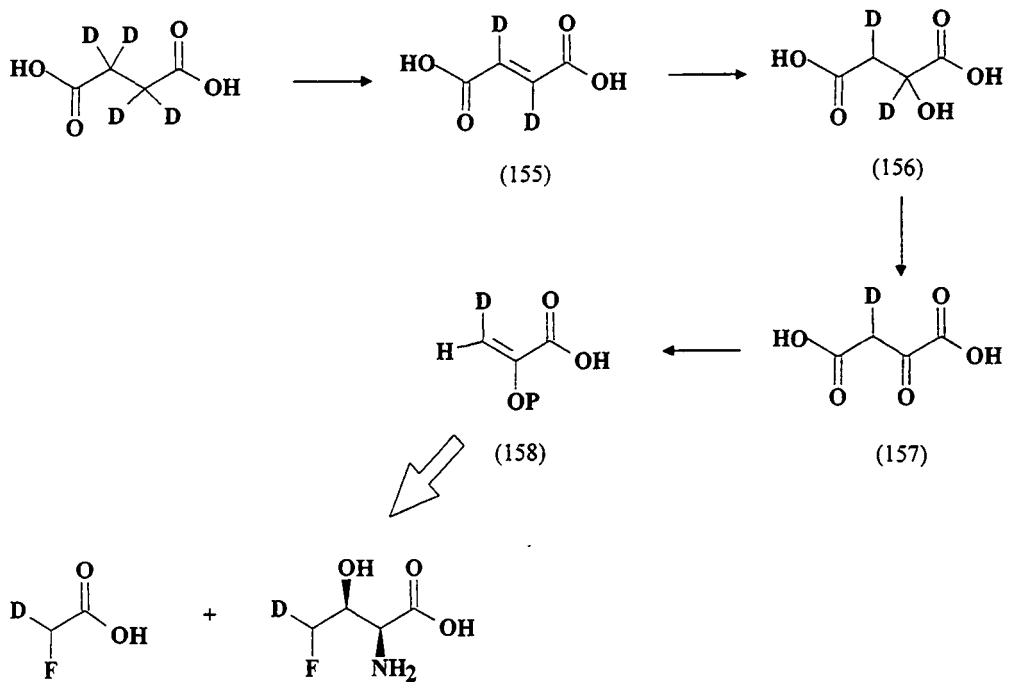

P = --PO_3^{2-}

Scheme 19

The incorporation of up to two deuterium atoms from [2,3,3-$^2H_3$]-aspartate can be rationalised if the latter is metabolised *via* transamination to oxaloacetate (Scheme 20). retaining a maximum of two deuterium atoms at C-3 **(157)**. Decarboxylation of **(159)** would generates **(160)** which predominantly transfers a single deuterium to the terminal carbon atoms of both fluorometabolites (Scheme 20). This result is apparent from the $^{19}F\{^1H\}$-NMR spectrum (Fig. 3.21) which shows that the dominant unlabelled signal for fluoroacetate and 4-fluorothreonine has an accompanying upfield shifted triplet

(β-shift = 0.6ppm). Importantly however, a low level of double labelled fluoroacetate and 4-fluorothreonine, is detectable by GC-MS and is also evident in the $^{19}F\{^1H\}$-NMR spectrum where a ^{19}F-^{12}C-($^2H_2$) combination is apparent as a small

upfield shifted multiplet (2β-shift = 1.2ppm) associated with each parent peak (Fig. 3.21).

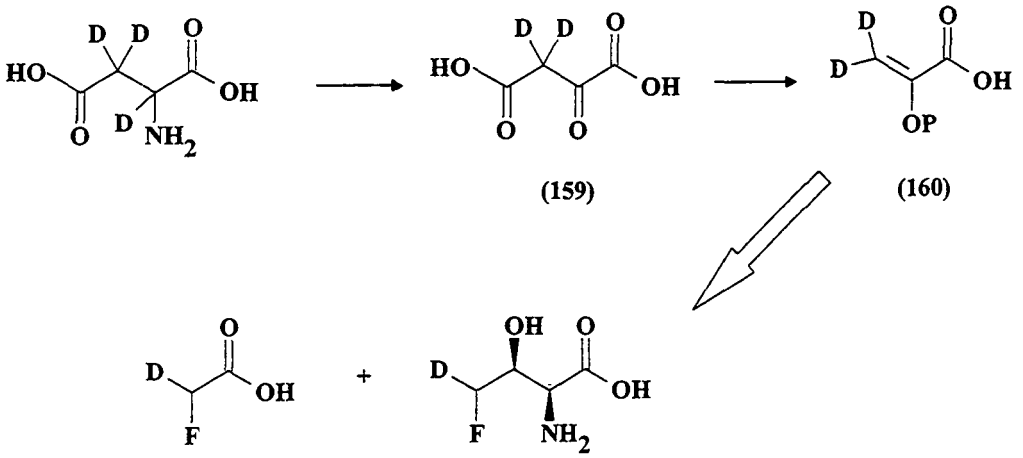

$P = --PO_3^{2-}$

Scheme 20

The transfer of deuterium label from [2,3,3-$^2H_3$]-aspartate and [2,2,3,3-$^2H_4$]-succinate provides strong evidence for the retention of hydrogen atoms of phosphoenolpyruvate and supports the hypothesis that phosphoenolpyruvate is an intermediate between the added precursors and the organofluorine metabolites produced in *S. cattleya.*

3.9 The incorporation of [2-^{13}C]-acetate into fluoroacetate and 4-fluorothreonine produced by resting cells of *S. cattleya*

As acetate serves as a central branch point linking many metabolic pools in most organisms, it was of particular interest to determine the incorporation of acetate into the fluorometabolites. Accordingly, [2-^{13}C]-acetate was administered to resting cells of *S. cattleya* at a final concentration of 10mM. To allow a relative comparison of the labelling results from feeding experiments, the feeding experiment with [2-^{13}]-acetate was carried out simultaneously with a [1,2-$^{13}C_2$]-glycine control feeding experiment.

Table 3.18 Incorporation of [2-^{13}C]-acetate into fluoroacetate

Precursor	(hrs)	None	Double	Single	
				Position 1	Position 2
[1,2-$^{13}C_2$]-glycine	24	47.2	39.4	8.3	5.1
(control)	48	50.1	34.0	10.1	5.8
[2-^{13}C]-acetate	24	64.5	18.1	7.8	9.6
	48	73.2	11.2	7.6	8.0

(as determined in Belfast)

Table 3.19 Incorporation of label into selected positions of 4-fluorothreonine from [2-^{13}C]-acetate

	Incubation time	% label in ion 218 (Positions 1 and 2)			% label in ion 236 (Positions 2,3 and 4)			
	(hrs)	None	Single	Double	None	Single	Double	Triple
[1,2-$^{13}C_2$]-glycine	24	87.8	3.8	8.4	48.8	14.5	33.3	3.4
(control)	48	89.3	3.5	7.2	51.3	17.5	28.6	2.6
[2-^{13}C]-acetate	24	92.3	5.8	1.9	58.6	20.1	20.3	1.0
	48	94.5	4.5	1.0	68.8	17.6	13.2	<0.5

(as determined in Belfast)

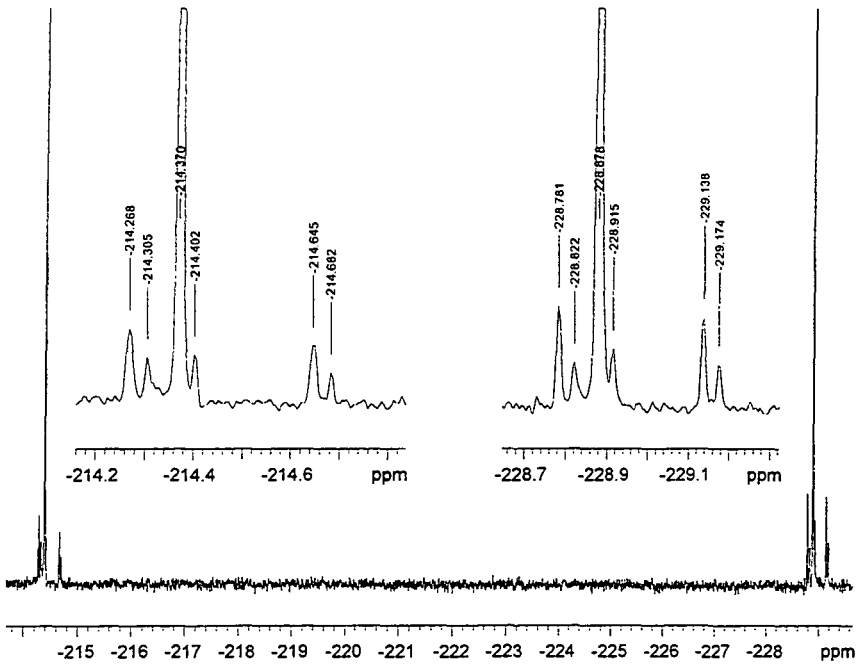

Fig. 3.23 $^{19}F\{^{1}H\}$-NMR spectrum of the supernatant from resting cells of *S. cattleya* incubated with [2-^{13}C]-acetate

Direct inspection of the $^{19}F\{^{1}H\}$-NMR spectrum (Fig. 3.23) of the [2-^{13}C]-acetate experiment reveals a similar multiplicity of the NMR signals for both fluorometabolites indicating that incorporations of [2-^{13}C]-acetate into fluoroacetate mirror those into C-3 and C-4 of 4-fluorothreonine. It is clear from the insets of the NMR signals for the fluoroacetate and 4-fluorothreonine that molecules containing the ^{19}F-^{13}C-^{12}C and ^{19}F-^{12}C-^{13}C combinations are present at a higher level than those containing a ^{19}F-^{13}C-^{13}C combination (doublet of doublets; 18Hz, 165Hz; α + β-shift = 0.09ppm). This is in good agreement with the GC-MS data for [2-^{13}C]-acetate (compare single and double incorporation after 48h, Tables 3.18 and 3.19).

The equal distribution of label in positions 1 and 2 of fluoroacetate (~8%, Table 3.16) can be rationalised by the pathway depicted in scheme 21 illustrating the conversion of labelled acetate **(161)** to labelled acetyl-CoA **(162)** to [2-^{13}C]-citrate **(163)** by condensation with oxaloacetate. The ^{13}C label would then be transferred *via*

intermediates of the TCA cycle to C-2 of fumarate **(164)**, a symmetrical intermediate, which gives rise to equivalent levels of [2-^{13}C]- **(165)** and [3-^{13}C]-oxaloacetate **(166)**. Such labelled oxaloacetates are converted to [2-^{13}C]-pyruvate and [3-^{13}C]-pyruvate which are respective precursors to [1-^{13}C]-fluoroacetate and [2-^{13}C]-fluoroacetate.

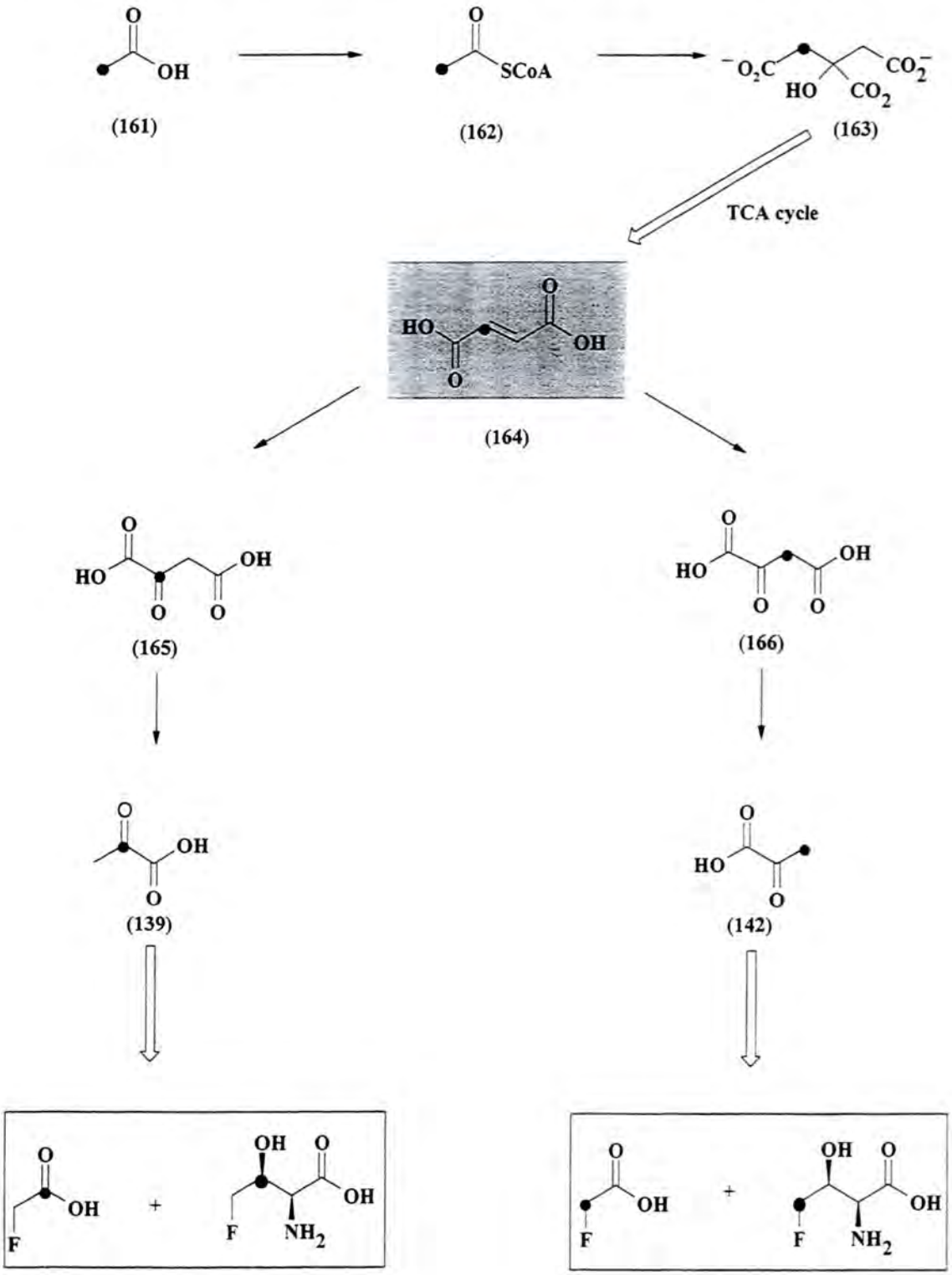

Scheme 21. Production of labelled fluorometabolites from [2-^{13}C]-acetate

A significant level of recombination of isotope (~18%) in fluoroacetate from [2-^{13}C]-acetate is also apparent and is clearly illustrated by the characteristic doublet of doublets at δ = -214.48ppm due to populations of [1,2-$^{13}C_2$]-fluoroacetate (Fig. 3.23). The rationale presented in scheme 21 is consistent with this observation if [2-^{13}C]-oxaloacetate **(165)** is condensed with [2-^{13}C]-acetyl-CoA and progressed around the TCA cycle to generate [2,3-$^{13}C_2$]-pyruvate.

3.10 Summary

The results of the ^{13}C and ^{2}H labelled studies on fluorometabolite biosynthesis in *S. cattleya* clearly indicate that glycine and pyruvate are efficiently incorporated into both fluoroacetate and 4-fluorothreonine. It is also interesting to note the mirroring of $^{19}F\{^{1}H\}$-NMR peak multiplicities for fluoroacetate and C-3 and C-4 of 4-fluorothreonine in all incubation experiments to date which suggests that fluoroacetate and C-3 and C-4 of 4-fluorothreonine have a common origin. The ^{19}F-NMR data is consistent with the conversion of glycine to pyruvate *via* serine as depicted in Fig. 3.24. The relatively high incorporations of [2-^{13}C]- and [3-^{13}C]-pyruvate provides evidence that the α and β carbon atoms of pyruvate are incorporated as a unit into fluoroacetate and C-3 and C-4 of 4-fluorothreonine. Phosphoenolpyruvate is derived from the TCA cycle intermediate oxaloacetate and consistent with this the citrate related metabolites succinate, aspartate and acetate also labelled the fluorometabolites. The results reinforce the conclusion that phosphoenolpyruvate is involved. Phosphoenolpyruvate can enter the glycolytic pool and recently Tamura *et al.*,[130] have shown that [2-^{13}C]-glycerol is exclusively incorporated into C-1 of fluoroacetate. Extending this study, the Durham

group (Dr. J. Nieschalk) have recently demonstrated the incorporation of the *pro-R* hydroxymethyl group of glycerol into the fluoromethyl groups of fluoroacetate and 4-fluorothreonine.[155]

Fig. 3.24 Summary of the results from stable labelled studies with succinate, aspartate and acetate

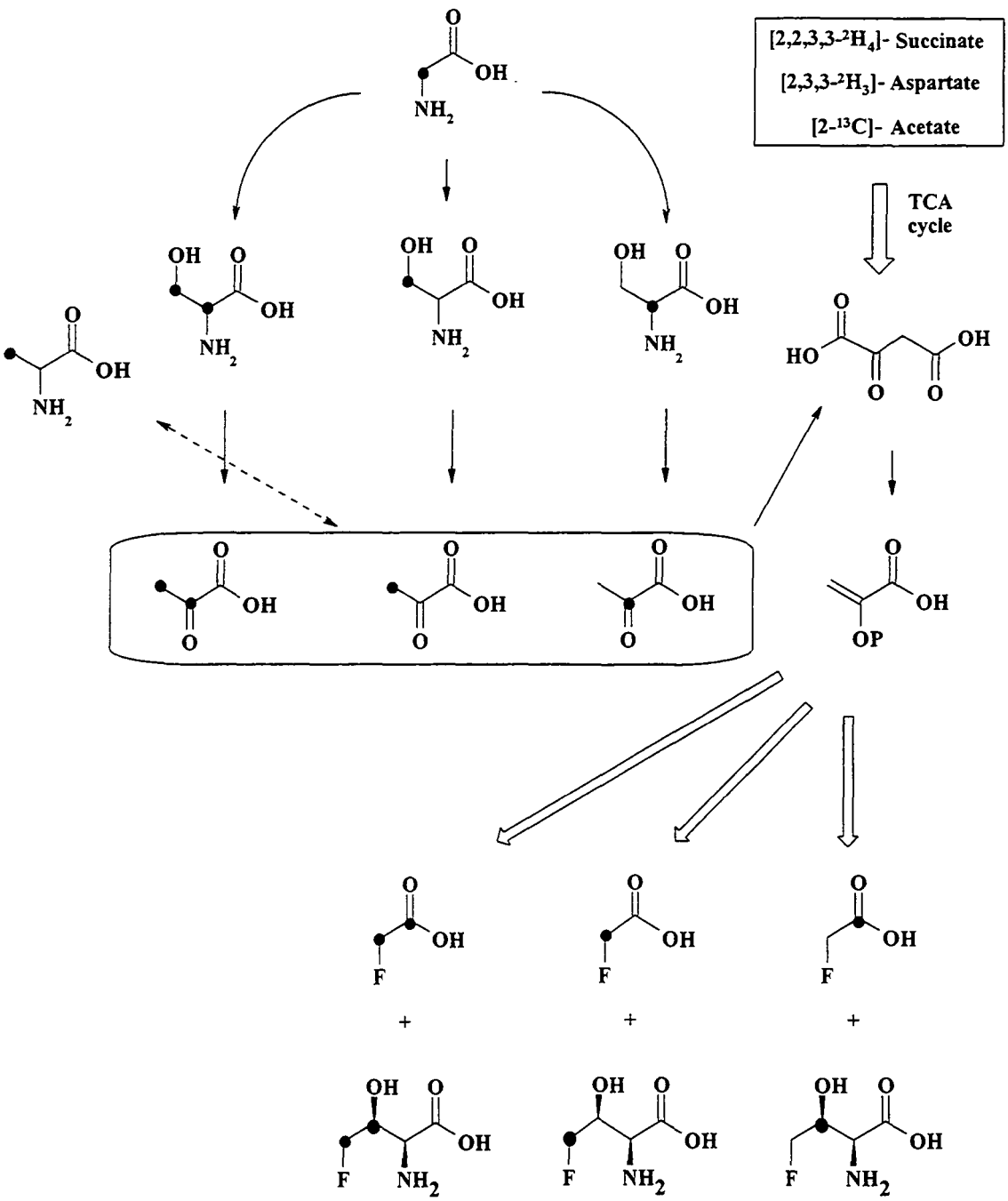

3.11 The incorporation of [2-^{13}C]-glycerol into fluoroacetate and 4-fluorothreonine produced by resting cells of *S. cattleya*

This particular investigation was designed to test the hypothesis that an intermediate of glycolysis was intimate with the fluorination event. In the only other biosynthetic study reported on these fluorometabolites, Tamura *et al,*[130] have shown that [U-^{14}C]-glycerol was very efficiently incorporated into fluoroacetate by suspension cells of *S. cattleya.* Moreover they demonstrated that the label from [2-^{13}C]-glycerol is incorporated (~40%) into the C-1 of fluoroacetate. These workers also noted a significant incorporation of C-2 and C-3 from β-hydroxypyruvate and accordingly concluded that fluoroacetate derives from C-1 and C-2 of glycerol *via* β-hydroxypyruvate. Thus the incorporation of label from [2-^{13}C]-glycerol into the fluorometabolites was re-evaluated in resting cells of *S. cattleya* at varying concentrations of [2-^{13}C]-glycerol over a 24h and 48h time period (Results shown in Tables 3.20/ 3.21). To allow a relative comparison of the labelling results from feeding experiments, this study was carried out simultaneously with a [1,2-$^{13}C_2$]-glycine control feeding experiment.

Although Reid *et al.*,[132] demonstrated a lower incorporation of [U-^{14}C]-glycerol into fluoroacetate compared with [U-^{14}C]-glycolate, the results from Tables 3.20 and 3.21 appear to indicate a higher level of incorporation of label from [2-^{13}C]-glycerol into both fluorometabolites. The isotope from [2-^{13}C]-glycerol appears to be incorporated particularly in position 1 of fluoroacetate (~56%, compared to ~40% reported by Tamura *et al.*) and positions 2,3 and 4 of 4-fluorothreonine (~60%) after 24h incubation with 7.5mM [2-^{13}C]-glycerol. Such high incorporation levels from a stable labelled precursor have not previously been observed in this study and suggest that glycerol is metabolically closer to the substrate for fluorination.

Table 3.20 GC-MS data of isotope incorporation from varying concentrations of [2-^{13}C]-glycerol into fluoroacetate

Precursor	Incubation time (hrs)	% label			
		None	Double	Single	
				Position 1	Position 2
[1,2-$^{13}C_2$]-glycine (10mM)	48	43.2	43.5	9.9	3.5
[2-^{13}C]-glycerol (2.5mM)	24	52.6	8.5	38.9	<0.5
	48	64.3	6.7	29.0	<0.5
[2-^{13}C]-glycerol (5.0mM)	24	39.2	10.4	50.4	<0.5
	48	51.0	8.5	40.6	<0.5
[2-^{13}C]-glycerol (7.5mM)	24	31.3	12.1	56.5	<0.5
	48	43.4	9.5	47.2	<0.5

(as determined in Belfast)

Table 3.21 GC-MS data of isotope incorporation into selected positions of 4-fluorothreonine from [2-^{13}C]-glycerol

Precursor	Incubation time (hrs)	% label in ion 218 (Positions 1 and 2)			% label in ion 236 (Positions 2,3 and 4)			
		None	Single	Double	None	Single	Double	Triple
[1,2-$^{13}C_2$]glycine (10mM)	48	87.2	3.5	9.3	45.8	15.2	33.9	5.2
[2-^{13}C]-glycerol (2.5mM)	24	95.9	2.1	2.0	60.2	39.4	<0.5	<0.5
	48	98.2	1.8	<0.5	70.3	29.4	<0.5	<0.5
[2-^{13}C]-glycerol (5.0mM)	24	92.8	5.0	2.2	46.4	52.0	1.6	<0.5
	48	96.1	3.9	<0.5	57.2	41.8	1.0	<0.5
[2-^{13}C]-glycerol (7.5mM)	24	89.4	7.2	3.4	39.6	57.7	2.7	<0.5
	48	92.6	7.4	<0.5	49.5	48.8	1.8	1.8

(as determined in Belfast)

$^{19}F\{^1H\}$-NMR data also show that the label from [2-^{13}C]-glycerol is located principally on the carboxylate carbon of fluoroacetate (Fig. 3.25(a)) and demonstrate that label in position 3 constitutes most of the label in positions 2,3 and 4 of 4-fluorothreonine (Fig. 3.25(b)).

Fig. 3.25 $^{19}F\{^{1}H\}$-NMR spectrum of the incorporation of [2-^{13}C]-glycerol into (a) fluoroacetate and (b) 4-fluorothreonine produced by resting cells of *S. cattleya*.

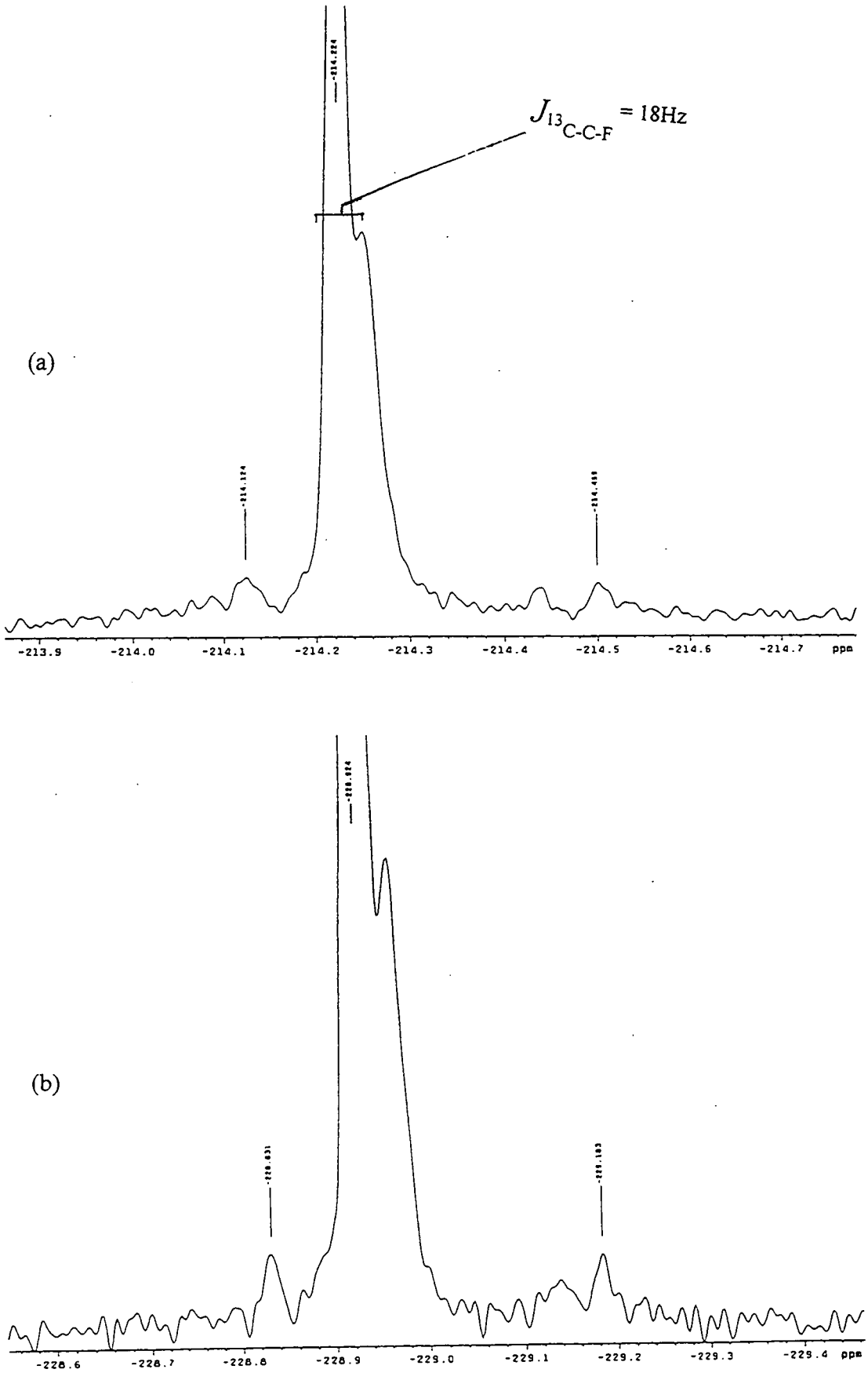

This observation is highlighted by the presence of a shifted signal (doublet, J=18Hz) associated with each dominant parent peak, corresponding to fluorometabolites with a ^{19}F-^{12}C-^{13}C combination.

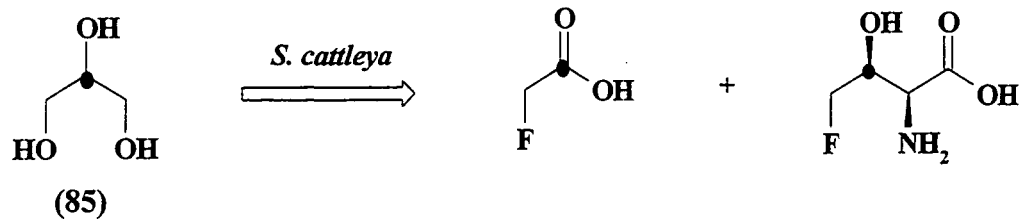

(85)

Scheme 22

Additional evidence for the role of glycerol in the biosynthesis is provided by incorporation experiments with (2*S*)- and (2*R*)-[1,1-$^{2}H_2$]-glycerol that have demonstrated the incorporation of deuterium label from only the (2*R*) enantiomer whilst the *pro-S* hydroxymethyl group is oxidatively cleaved during the biosynthesis.[155] This shows that the *pro-R* hydroxymethyl group of glycerol is eventually fluorinated and is consistent with the phosphorylation of this hydroxymethyl group by glycerol kinase. Indeed the predominant retention of both deuterium atoms from (2*R*)- [1,1-$^{2}H_2$]-glycerol provides unambiguous evidence that this carbon is not oxidised prior to fluorination.

It is therefore possible to envisage the metabolism of pyruvate and glycerol to fluoroacetate and 4-fluorothreonine proceeding *via* an intermediate of the glycolytic pathway as depicted in Fig. 3.26. This Figure summarises the overall link between the various precursors involved in the biosynthesis of fluoroacetate and 4-fluorothreonine and moreover introduces glycolytic intermediates as potential candidates for the substrate of the fluorinating enzyme.

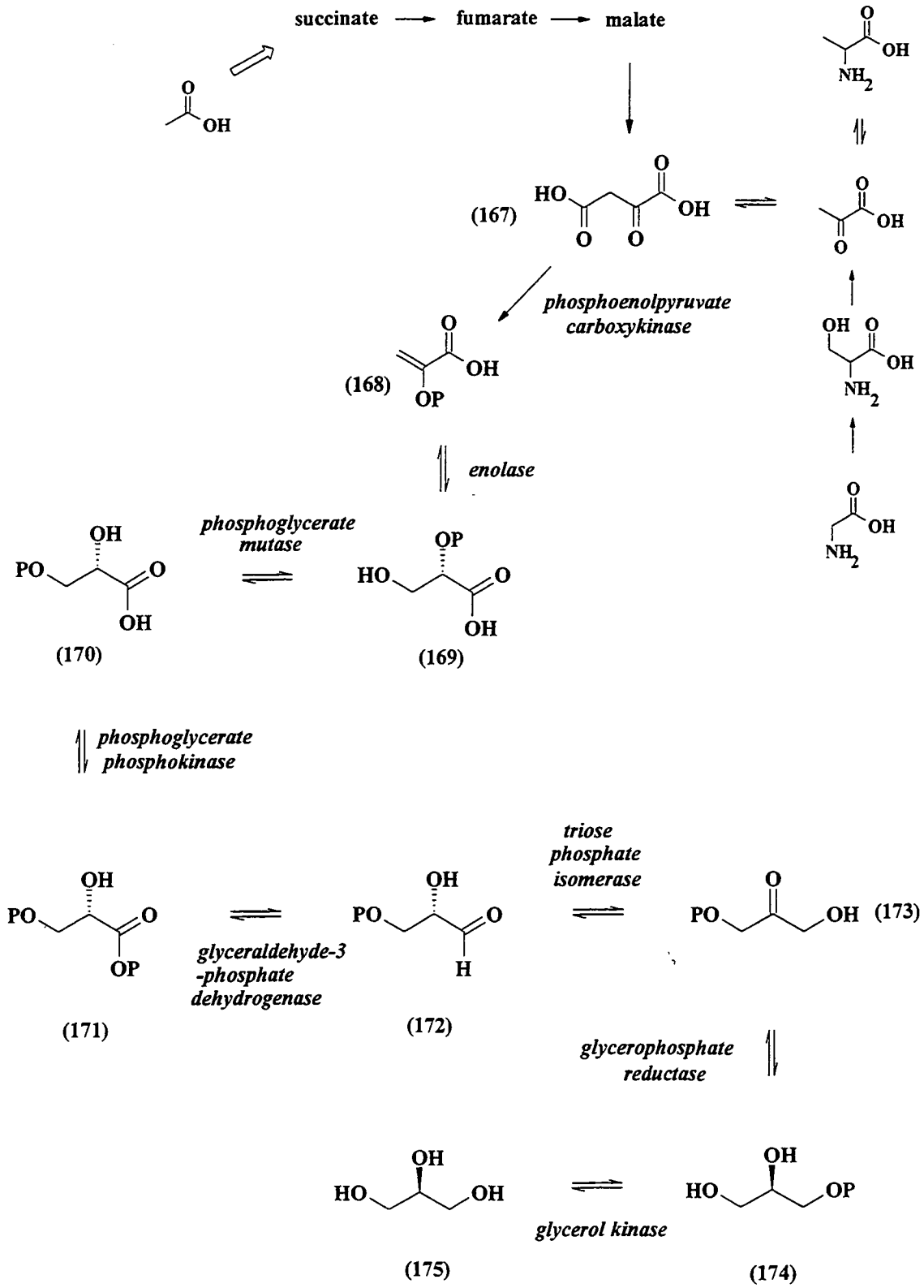

$P = -PO_3^{2-}$

Fig. 3.26 Summary of the incorporation results showing the relationship between isotopically labelled putative precursors in the biosynthesis of fluoroacetate and 4-fluorothreonine in *S. cattleya*

3.12 [3-$^{2}H_{x}$]-fluoropyruvate, [3-$^{2}H_{x}$]-3-fluorolactate and [3-$^{2}H_{x}$]-3-fluoropropane-1,2-diol as putative precursors of fluoroacetate and 4-fluorothreonine

In an effort to determine the nature of the initial product of fluorination on the biosynthetic pathway to fluoroacetate and 4-fluorothreonine, the incorporations of [3-$^{2}H_{x}$]-fluoropyruvate, [3-$^{2}H_{x}$]-3-fluorolactate and [3-$^{2}H_{x}$]-3-fluoropropane-1,2-diol. were investigated as putative post-fluorinated substrates. Each compound was synthesised carrying at least one deuterium label and their incorporations into fluoroacetate and 4-fluorothreonine were assessed in resting cells of *S. cattleya*. It is perhaps interesting to note that callus cultures of *D. cymosum* are capable of converting 3-fluoropyruvate to fluoroacetate[120] suggesting a role for 3-fluoropyruvate as a possible intermediate in fluoroacetate biosynthesis in plants.

3.12.1 Synthesis of isotopically enriched 3-fluoropyruvate and 3-fluorolactate.

3.12.1.1 Synthesis of [3-$^{2}H_{X}$]-fluoropyruvic acid

In order to prepare a sample of [3-$^{2}H_{x}$]-fluoropyruvate an investigation of deuterium exchange into unlabelled fluoropyruvate was undertaken. The presence of the fluorine atom, facilitates the enolisation process and has the added advantage that the course of the reaction can be monitored directly by ^{19}F-NMR. 3-Fluoropyruvic acid gives a triplet in the ^{19}F-NMR spectrum at -229.5ppm. When one geminal hydrogen is replaced by deuterium, the signal shifts to lower frequency by 0.6ppm (β-shift) and collapses to a doublet of triplets (*dt*) (Fig. 3.25(a)). Two deuterium atoms geminal to the fluorine shift the signal (now a pentet by virtue of the fluorine coupling to the two

deuterium atoms) to a lower frequency by 1.2ppm. Thus, by determining the splitting pattern and isotopic chemical shift value, the course of the deuterium exchange can be followed.

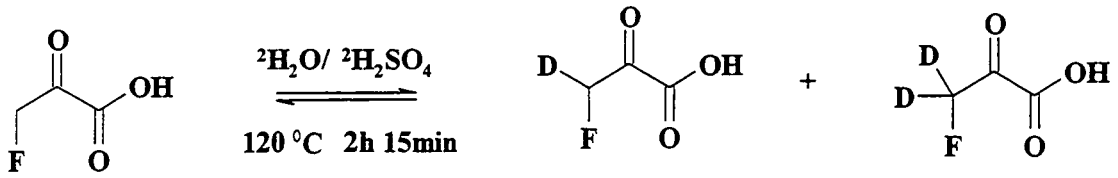

(176) (177) (178)

Scheme 23

The sodium salt of 3-fluoropyruvic acid was dissolved in ^2H_2O with a minimum amount of $^2H_2SO_4$ and heated in a sealed Carius tube at 120°C for 8h (Scheme 23). During the initial experiments, the ^{19}F-NMR spectrum of the resultant mixture showed an array of signals which could not be interpreted. However a pentet with the correct chemical shift for [$^2H_2$]-fluoropyruvate was observable in the mixture indicating that the protons had exchanged fully but decomposition products dominated. This gave problems with isolation and purification. Nevertheless, a time course study to investigate the rate of exchange of hydrogen for deuterium in 3-fluoropyruvic acid was carried out and the results are presented in Table 3.22. After 5min no exchange is observed, but after 15min, a low concentration of mono-labelled material becomes apparent (Fig. 3.27 (a)) as indicated by the 0.6ppm upfield shifted *dt* in the ^{19}F-NMR spectrum.

Fig. 3.27

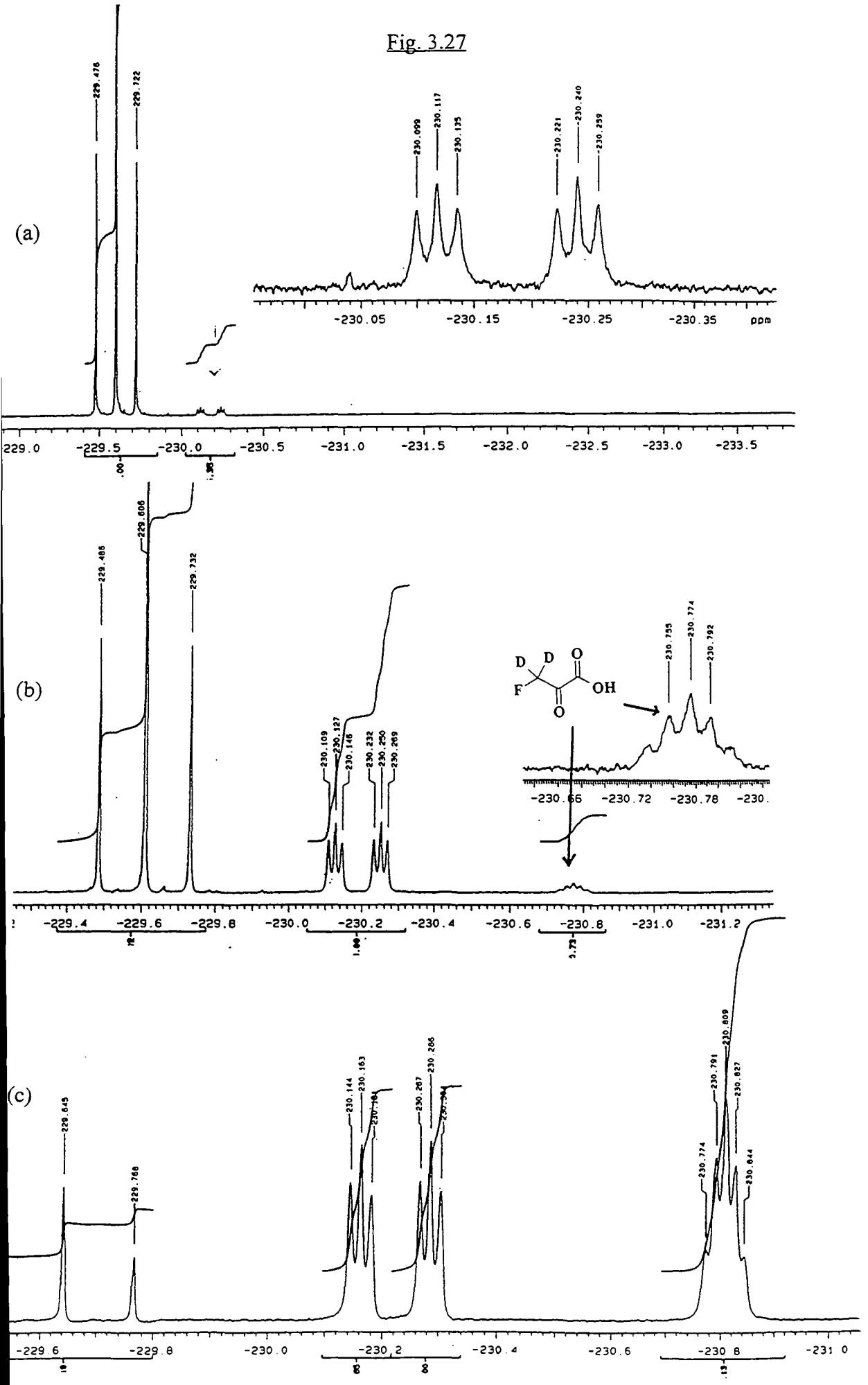
(a)
229.478
229.722
230.099
230.117
230.135
230.221
230.240
230.259
-230.05
-230.15
-230.25
-230.35
ppm
229.0
-229.5
-230.0
-230.5
-231.0
-231.5
-232.0
-232.5
-233.0
-233.5
(b)
229.486
229.606
229.732
230.109
230.127
230.146
230.232
230.250
230.269
D
D
O
F
O
OH
230.755
230.774
230.792
-230.66
-230.72
-230.78
-230.
-229.4
-229.6
-229.8
-230.0
-230.2
-230.4
-230.6
-230.8
-231.0
-231.2
(c)
229.645
229.768
230.144
230.163
230.267
230.286
230.774
230.791
230.809
230.827
230.844
-229.6
-229.8
-230.0
-230.2
-230.4
-230.6
-230.8
-231.0

Table 3.22 Time course study for the exchange of fluoropyruvate in D_2O/ D_2SO_2 at 120°C in Carius tube.

Reaction time	Concentration of starting material, 3-fluoropyruvic acid (%)	Concentration of mono-deuteriated product (%)	Concentration of di-deuteriated product (%)
5 min	100	0	0
15min	93	7	0
30 min	60	36	4
1.5h	7	44	49
2h 15min	1	29	70
3h	0	0	32

The double labelled material **(178)** becomes evident after only 30 min at 120°C (Fig. 3.27(b)), however a significant amount of unlabelled starting material persists after 1.5h (Fig. 3.27(c)). Nonetheless the optimum reaction time was found to be 2h 15min at which point the reaction mixture became pale yellow indicative of the onset of side products and decomposition. The optimal ratio of mono- to di- labelled sample, without the formation of side products, is 2.6 : 1, after 2h 15mins.

Continuous extraction of the acidic aqueous ^2H_2O layer into ethyl acetate allowed the recovery of 3-fluoropyruvic acid which was dissolved in water, neutralised and freeze dried to give the corresponding sodium salt (49%). It is important to note that this sample contained a mixture of the mono and di deuteriated forms of 3-fluoropyruvate therefore x = 1 or 2 in [3-^2H_x]-fluoropyruvate.

3.12.1.2 Synthesis of [3-$^{2}H_x$]-3-fluorolactate

A mixture of the mono- and di- deuteriated [3-$^{2}H_x$]-fluoropyruvic acid prepared above was dissolved in methanol and treated with sodium borohydride to give [$^{2}H_x$]-fluorolactate (Scheme 24). The reduction is readily followed by ^{19}F-NMR as the multiplicities of the fluorine signals (a triplet and doublet of triplets shown in Fig. 3.27) become more complex by virtue of the coupling to the new C-2 hydrogen of 3-fluorolactate. The ^{19}F-NMR spectrum in Fig. 3.28 clearly illustrates that the *dt* (δ=-230.2ppm, Fig. 3.27(c)) has been converted to a multiplet and similarly the pentet has been transformed to a more complex signal (doublet of pentets, *dp*). For the isolation of deuteriated [3-$^{2}H_x$]-3-fluorolactate, the aqueous layer was continuously extracted into ethyl acetate for 24h and the free acid dissolved in water, neutralised with 1N NaOH and freeze dried to afford the sodium salt of [3-$^{2}H_x$]-3-fluorolactic acid (38%).

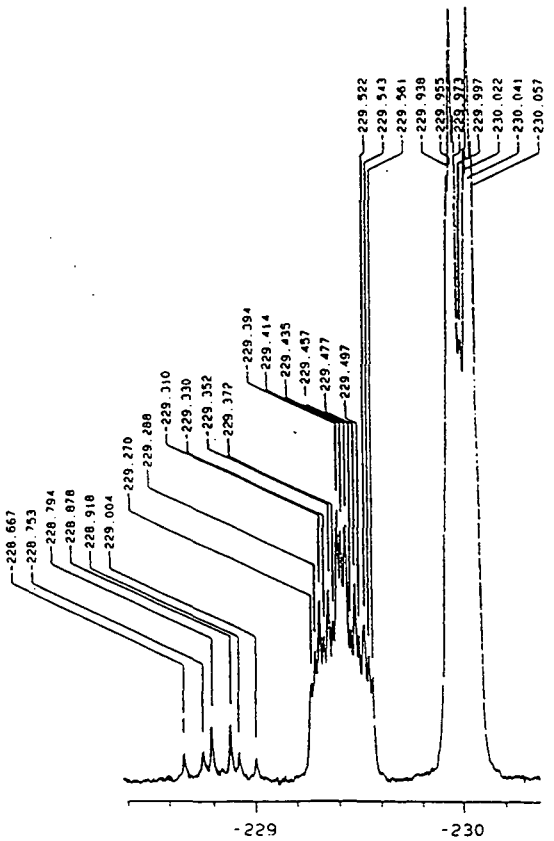

Fig. 3.28

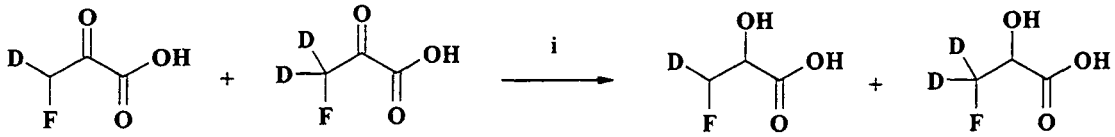

(177) (178) (179) (180)

Scheme 24

3.12.2 Incorporation of deuterium label from [3-^2H_x]-fluoropyruvate and [3-^2H_x]-3-fluorolactate into fluoroacetate and 4-fluorothreonine

Each of the candidate precursors were incubated with resting cells of *S. cattleya* at a final concentration 10mM. GC-MS analysis of the supernatants showed that 4-fluorothreonine was not significantly labelled with deuterium (Table 3.24) but a high level of (~23%) [2-^{2}H]-fluoroacetate was apparent (Table 3.23).

Table 3.23 GC-MS data of the incorporation of deuterium from [3-^2H_x]-fluoropyruvate and [3-^2H_x]-3-fluorolactate into fluoroacetate

(as determined in Belfast)

	Incubation time	% label		
Precursor	(hrs)	None	Double	Single (Position 2)
[3-^2H_x]-3-fluoropyruvate control (no cells) (10mM)	0	55.2	19.6	25.3
	24	56.0	19.2	24.9
	48	52.7	21.1	26.2
[3-^2H_x]-3-fluoropyruvate (10mM)	24	56.9	19.9	23.2
	48	75.5	11.6	13.0
[3-^2H_x]-3-fluorolactate (10mM)	24	97.6	<0.5	2.4
	48	94.5	3.8	1.7

x = 1 or 2

Table 3.24 GC-MS data for the incorporation of deuterium from [3-^2H_x]-fluoropyruvate and [3-^2H_x]-3-fluorolactate into positions 2,3 and 4 of 4-fluorothreonine

(as determined in Belfast)

Precursor	Incubation time (hrs)	% label in ion 236 (Positions 2,3 and 4)		
		None	Single	Double
[3-^2H_x]-3-fluoropyruvate (10mM)	24	96.5	2.5	1.0
	48	98.3	1.5	<0.5
[3-^2H_x]-3-fluorolactate (10mM)	24	100	<0.5	<0.5
	48	99.6	<0.5	<0.5

x = 1 or 2

However, comparable levels of single and double labelled fluoroacetate were detected in control samples (10mM [3-^2H_x]-fluoropyruvate, no cells, in MES buffer only) indicating that deuterium labelled fluoroacetate is not formed through biotransformation of [3-^2H_x]-fluoropyruvate but is rather produced from the oxidative decarboxylation of [3-^2H_x]-fluoropyruvate, thus accounting for the high concentrations of [2-^2H]- and [2,2-$^2H_2$]- fluoroacetate present in the supernatant. It is perhaps interesting to note that the ratio of label in the fluoroacetate (Table 3.23) from the 48h supernatant sample is different to that of the 48h control sample suggesting that [3-^2H_x]-fluoropyruvate is defluorinated and the fluoride is reincorporated for the *de novo* synthesis of fluoroacetate. Despite the anomalous fluoroacetate incorporation result, it has been suggested earlier in this thesis that the labelling pattern for the incorporation into C-1 and C-2 of fluoroacetate mirror those into positions 3 and 4 of 4-fluorothreonine. Hence GC-MS data for the incorporation into 4-fluorothreonine (Table 3.24) clearly show that single and double label in C-3 and C-4 are present at a low level and that this should also be reflected in fluoroacetate. These results are inconsistent with 3-fluoropyruvate or

3-fluorolactate as post fluorinated intermediates in fluorometabolite biosynthesis in *S. cattleya.*

3.12.3 Synthesis of [3-$^{2}H_{x}$]-3-fluoropropane-1,2-diol

It was judged appropriate to prepare [3-$^{2}H_{x}$]-3-fluoropropane-1,2-diol, to test the hypothesis that *sn*-glycerol-3-phosphate is the substrate for fluorination. If fluoride ion displaced the phosphate group then 3-fluoropropane-1,2-diol would be the post-fluorinated product and should become incorporated into the fluorometabolites. Accordingly [3-$^{2}H_{x}$]-3-fluoropropane-1,2-diol was prepared by treating [3-$^{2}H_{x}$]-fluoropyruvate with lithium aluminium hydride (Scheme 25) to produce a viscous mixture of [3-$^{2}H_{x}$]-3-fluoropropane-1,2-diol.

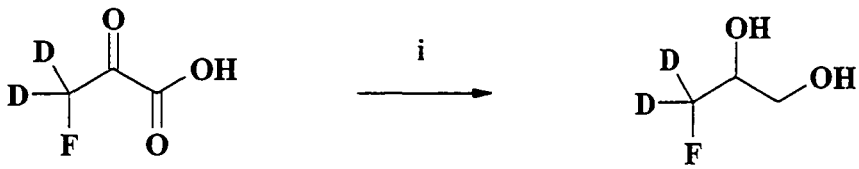

(178) **(181)**

Scheme 25

3.12.4 Incorporation of deuterium label from [3-$^{2}H_{x}$]-3-fluoropropane-1,2-diol into fluoroacetate and 4-fluorothreonine

[3-$^{2}H_{x}$]-3-Fluoropropane-1,2-diol was incubated with resting cells of *S. cattleya* at a final concentration of 10mM. It is clear from the GC-MS results shown in Tables 3.25 and 3.26 that there is a very low incorporation of deuterium label into both of the fluorometabolites. Approximately 95% of the 4-fluorothreonine molecules produced by

the resting cells remain unlabelled after a 48h incubation. A similar situation is apparent in fluoroacetate where the data indicate a very low level of label at its terminal carbon atom. These results are consistent with the $^{19}F\{^{1}H\}$-NMR (not shown) spectra of the fluorometabolites.

Table 3.25 GC-MS data for the incorporation of [3-$^{2}H_x$]-3-fluoropropane-1,2-diol into position 2 of fluoroacetate

Precursor	Incubation time	% label			
	(hrs)	None	Double	Single	
				Position 1	Position 2
[3-$^{2}H_x$]-3-fluoro-propane-1,2-diol	48	96.9	3.1	----	<0.5

(as determined in Belfast)

Table 3.26 GC-MS data for the incorporation of [3-$^{2}H_x$]-3-fluoropropane-1,2-diol into selected positions of 4-fluorothreonine

Precursor	Incubation time	% label in ion 218 (Positions 1 and 2)			% label in ion 236 (Positions 2,3 and 4)		
	(hrs)	None	Single	Double	None	Single	Double
[3,3-$^{2}H_x$]-3-fluoro-propane-1,2-diol	48	94.0	1.4	1.8	97.2	1.9	0.9

(as determined in Belfast)

A clear conclusion to emerge from this analysis is that the deuterium atoms from [3-$^{2}H_x$]-3-fluoropropane-1,2-diol are not incorporated into the fluorometabolites giving no support to the hypothesis that *sn*-glycerol-3-phosphate is the substrate for the fluorination enzyme.

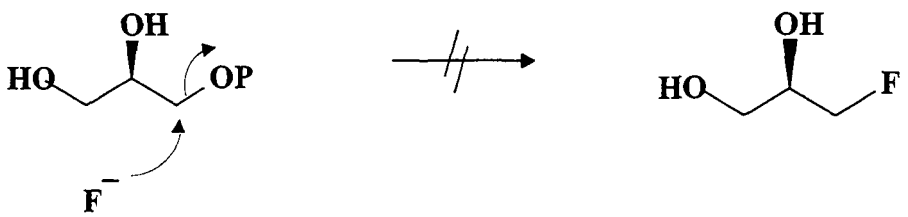

Fig. 3. 29

3.13 Discussion and Conclusion

It has been clearly established, from isotopic incorporations that the α-carbon atom of glycine, through an efficient recycling process, contributes to the construction of fluoroacetate and C-3 and C-4 of 4-fluorothreonine. However the carboxylate carbon of glycine is not retained to any significant extent in either fluorometabolite. GC-MS and $^{19}F\{^{1}H\}$-NMR data for the incorporation of labelled serine, alanine and pyruvate is consistent with the conversion of glycine to pyruvate *via* serine. Pyruvate then donates its α and β carbon atoms as an intact unit to form the carbon skeleton of fluoroacetate plus the corresponding C-3 and C-4 sites of 4-fluorothreonine. The incorporation of a single deuterium atom from [2,2,3,3-$^{2}H_4$]-succinate and up to two deuterium atoms from [2,3,3-$^{2}H_3$]-aspartate into the fluorometabolites can be rationalised *via* the intermediacy of oxaloacetate/ phosphoenol pyruvate.

The highest incorporation of label into fluoroacetate and positions 3 and 4 of 4-fluorothreonine was achieved using [2-^{13}C]-glycerol and the stereochemical labelling is consistent with glycerol entering the glycolytic pathway by the action of glycerol kinase. Tamura *et al.*,[130] after demonstrating the high incorporation of glycerol, concluded that C-1 and C-2 of fluoroacetate were derived from C-1 and C-2 of glycerol *via* β-hydroxypyruvate. They suggested that fluoroacetate could either be formed from the decarboxylation of β-hydroxypyruvate producing glycolate, the hydroxyl group of which, could be substituted by fluoride. Conversely, fluoroacetate could be formed by the initial displacement of the hydroxyl moiety of β-hydroxypyruvate by fluoride followed by decarboxylation. However, this investigation has demonstrated only a very poor incorporation of [U-^{14}C]- and [2--^{13}C]- glycolate into fluoroacetate. Furthermore the failure to detect incorporation of isotope from deuterium labelled β-fluoropyruvate

into the fluorometabolites does not support the intermediacy of β-fluoropyruvate. Our data force the conclusion that a presently unknown intermediate on the glycolytic pathway is the substrate for fluorination.

If *sn*-glycerol-3-phosphate was the substrate then deuterium atoms from [3-$^{2}H_{x}$]-3-fluoropropane-1,2-diol should have been incorporated into the fluorometabolites. However the very poor incorporation of deuterium label from [3-$^{2}H_{x}$]-3-fluoropropane-1,2-diol did not lend support to this notion. Similarly other isotopically labelled post-fluorinated substrates, namely [3-$^{2}H_{x}$]-3-fluoropyruvate and [3-$^{2}H_{x}$]-3-fluorolactate were poorly incorporated and these too are discounted as the initial products of the fluorination event. The other candidate glycolytic intermediates are dihydroxyacetone-phosphate and glyceraldehyde-3-phosphate, however the incorporation of the putative post-fluorinated metabolites of both of these compounds remains to be investigated.

The similarity in the labelling patterns observed for fluoroacetate and positions 3 and 4 of 4-fluorothreonine in all of the experiments indicate a single fluorinating enzyme and a common origin for these moieties.[150]

CHAPTER 4

Total Synthesis of 4-*(2S,3S)*-Fluorothreonine

Chapter 4

4. Total Synthesis of the natural product 4-fluorothreonine

4.1 Introduction

The primary objective of the synthetic chemistry was to establish the absolute stereochemistry of the natural product 4-fluorothreonine. An additional objective was to prepare a sample of deuterium labelled 4-fluorothreonine to investigate if 4-fluorothreonine is converted to fluoroacetate by resting cells of *S. cattleya*. An efficient route to isotopically labelled threonines was also developed during this work.

Optically active fluorinated threonines have attracted much interest due to their reported anti-tumour activities.[156] 4-(*2S,3S*)-Fluorothreonine has been prepared synthetically by Scolastico and co-workers in 1985 [157] before the natural product was identified. More recently Shimizu *et al.*, [158] prepared the same stereoisomer using a lipase enzyme in the key resolution step. For each case, the optical rotation value of the synthetic material was very close to that of the natural product ($[\alpha]_D$ = -18°) however the relative or absolute stereochemistry of the natural product has never been unambiguously established. In this investigation, the synthetic 4-fluorothreonine was co-analysed with the naturally produced 4-fluorothreonine, for the first time.

Seebach's imidazolidinone methodology emerged as an attractive and efficient route to α-amino-β-hydroxy acids.[154] The route involves the stereoselective alkylation of the enolate of 1-benzoyl-2-tert-butyl-3-methylimidazolidin-4-one (**144**, R=H) to generate products (**144a**) of electrophile approach *anti* to the tert-butyl moiety (Scheme 26). Subsequent hydrolysis of the alkylation product under acidic conditions affords the appropriate amino acid in enantiomerically pure form.

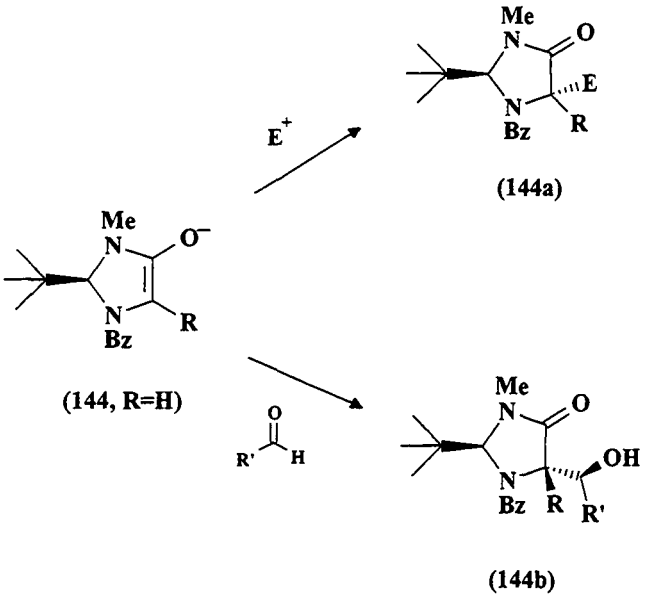

Scheme 26 *R' = CH_3, CF_3, CH_3CH_3*

Interestingly the condensation of (**144**, R=H) with aldehydes generates an additional stereocentre and moreover proceeds with high stereoselectivity affording a single major diastereoisomer (**144b**) (Scheme 26). Hydrolysis of this diastereoisomer produces the desired *threo* amino acid. In the case of using acetaldehyde, the condensation product (**186**) is generated which can be hydrolysed to give (2*S*,3*R*)-threonine (**187**) (Scheme 27).

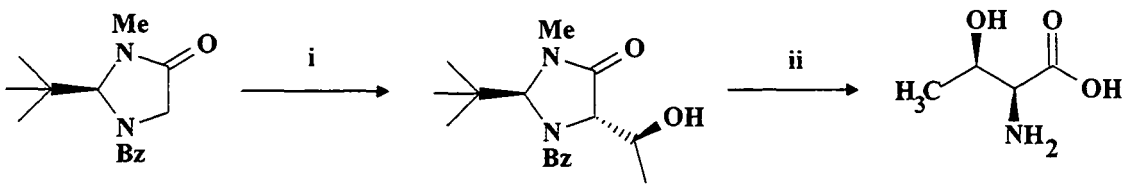

(144) **(186)** **(187)**

Scheme 27 **(I)** LDA/ CH_3CHO/ -100°C **(ii)** 10N HCl/ 100°C/ 72h

It is the *tert*-butyl group at the C-2 stereogenic centre that induces facial selectivity to the enolate carbon 5 during reactions with electrophiles to set the *anti-(S)* absolute stereochemistry at the α-carbon. Fig. 4.1 shows the three staggered approaches of acetaldehyde to the enolate. The addition is thought to occur *via* the transition state **(188)** as this is consistent with the observed stereocontrol at the β-centre generating the *threo* product. The transition state orientation in (**188**) is more favoured as the double bonds of the donor and the acceptor carbonyl are synclinal and not antiperiplanar as in **(190)**[159,160], preventing the separation of opposite developing charges and still allowing for the O-Li-----O chelation (twist-boat arrangement). Furthermore the methyl group is not over the face of the ring as in (**189**) plus there is maximum overlap of the donor and π-systems in (**188**).

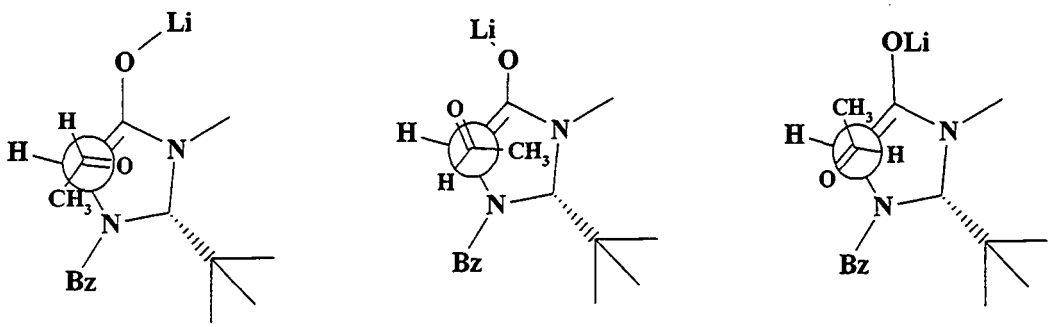

(188) **(189)** **(190)**

Fig. 4.1[154]

This methodology therefore offered potentially a more direct and convenient route for the preparation of 4-(2*S*,3*S*)-fluorothreonine.

4.2 Synthesis of (*2S,3R*)-threonine

4.2.1 Synthesis of DL-1-benzoyl-2-(*tert*-butyl)-3-methyl-imidazolidinone (144) [161]

The racemic form of the imidazolidinone **(185)** was prepared from glycine methyl ester hydrochloride by its initial conversion to the corresponding N-methylamide[161] **(183)**. The Schiff base **(184)** that is generated on reaction with pivalaldehyde was cyclised using methanolic HCl for 12h producing 2-(tert-butyl)-3-methyl-imidazolidinone **(185)** as outlined in Scheme 28.

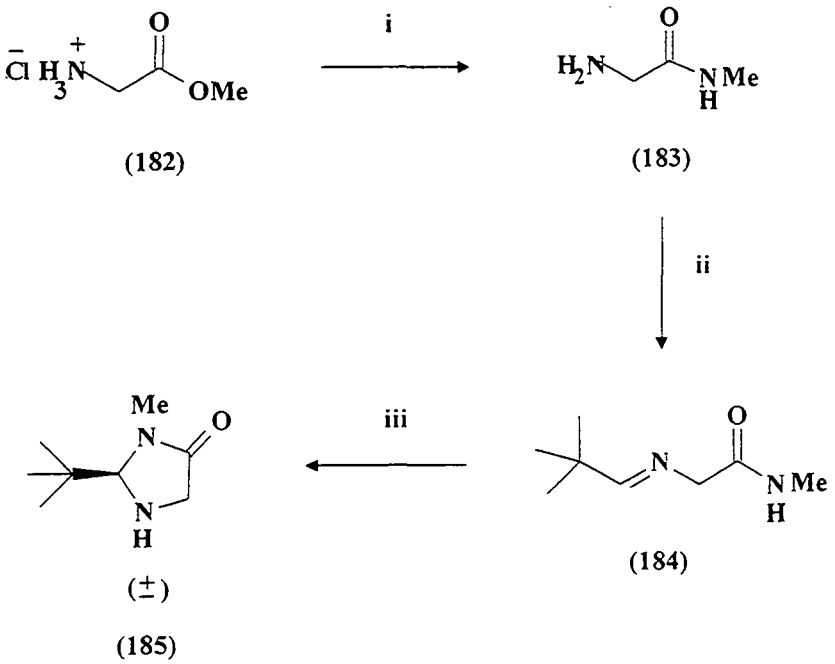

Scheme 28 (I) 8M CH_3NH_2 / DCM/ 25°C/ 15h (ii) Pivalaldehyde/ Et_3N/ reflux 10h (iii) acidic methanol/ 25°C/ 3h

The imidazolidinone **(185)** can at this point be resolved by crystallisation of the mandelate salts[161] and the desired imidazolidinone with (*R*) or (*S*) configuration may be

isolated. Subsequent treatment of **(185)** with benzoyl chloride generates 1-benzoyl-2-(tert-butyl)-3-methyl-imidazolidinone **(144)** (Scheme 29).

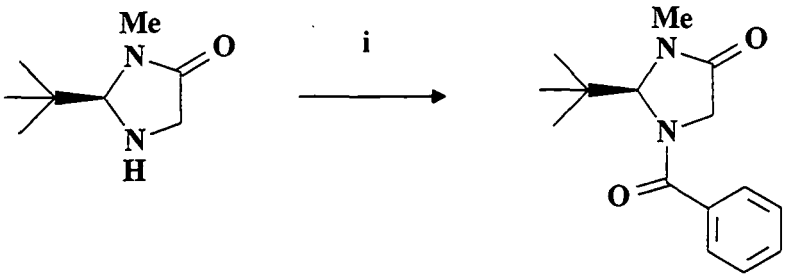

(185) **(144)**

Scheme 29 (I) Benzoyl chloride/ 1N NaOH/ 25°C/ 8h

Treatment of (*S*)-**(144)** with LDA/ THF at -78°C and then acetaldehyde at -100°C generated **(186a)**, one of the four possible diastereoisomers, usually to the extent of 85% d.e.

4.2.2. Hydrolysis of the alkylated imidazolidinone adduct

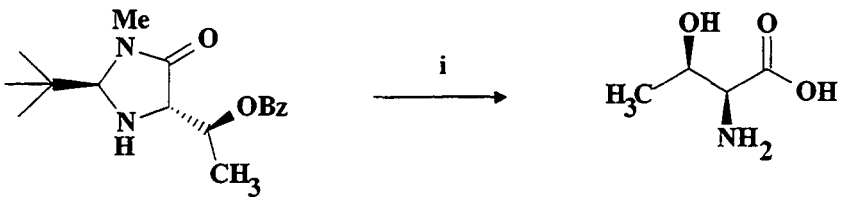

(186a) **(187)** (86% d.e.)

Scheme 30 (I) 10N HCl/ 100°C/ 72h

Although Seebach and co-workers have reported the hydrolysis of hydroxyalkylated imidazolidinones to be more facile than those derivatives geminally disubstituted in the C-5 position, in the event it proved difficult to drive the hydrolysis to completion using

the suggested conditions[160] (6N HCl/ 100°C/ 8h). Instead, such conditions generated the partially hydrolysed N-methyl amide. Hydrolysis was also attempted in a Carius tube under high pressure and temperature but these conditions were too vigorous yielding only decomposition products. However, heating the adduct continuously in 10N HCl/ 100°C for 72h allowed complete cleavage of the N,N acetal moiety generating (*2S,3R*)-threonine with no traces of the N-methylamide contaminant. The amino acid was purified by ion-exchange chromatography and recrystallised from ethanol to afford **(187)**.

A similar protocol was used for the preparation of [3,4,4,4-$^2H_4$]-threonine, employing [$^2H_4$]-acetaldehyde (Scheme 31). The singlet at 1.20 ppm and the singlet at 4.10 ppm in the ^{2}H-NMR spectrum of [3,4,4,4-$^2H_4$]-threonine **(192)** clearly illustrates the expected 3:1 ratio of the signals corresponding to the CD_3 and CD peaks respectively (Fig. 4.2). The minor *allo* diastereoisomer is evident at 4.2ppm, illustrating the moderate diastereoselectivity of the synthetic process.

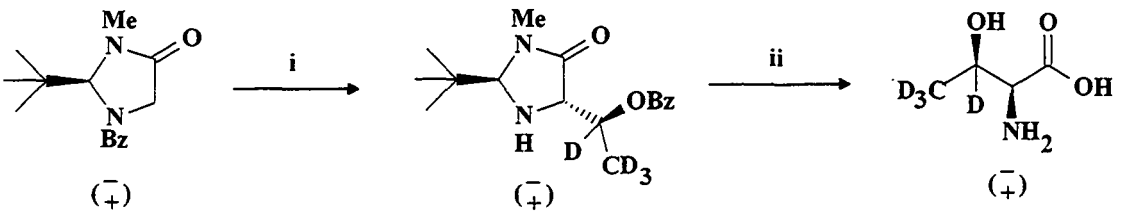

(144) **(191)** **(192)**

Scheme 31 (I) LDA/ CD_3CDO/ -100°C (ii) 10N HCl/ 100°C/ 72h

Resting cells of *S. cattleya* were incubated with DL-[3,4,4,4-$^2H_4$]-threonine to determine the incorporation of deuterium isotope into fluoroacetate and 4-fluorothreonine. In the

event the isotope was not incorporated into the fluoromethyl carbons of fluoroacetate or the terminal carbons of 4-fluorothreonine.

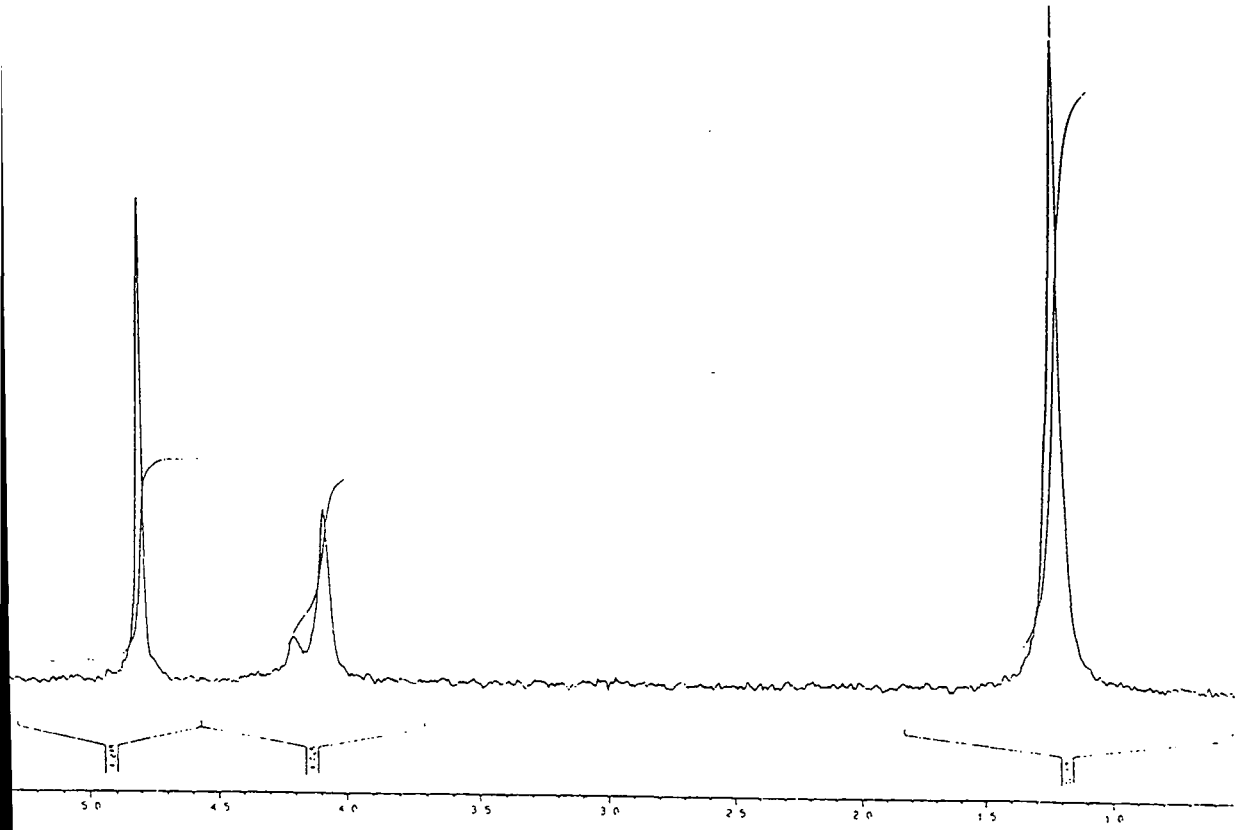

Fig. 4.2 ^{2}H-NMR spectrum of [3,4,4,4-$^{2}H_4$]-threonine **(192)**

4.3 Synthesis of 4-(*2S,3S*)-fluorothreonine

Previously cited[107, 157, 158] optical rotation data of synthetic 4-(*2S,3S*)-fluorothreonine appear to be consistent with that for the corresponding natural compound suggesting that the natural product also possesses a (*2S,3S*) *threo*-configuration. The Seebach methodology yields *threo* α-amino-β-hydroxy acids. However a straightforward

condensation of the imidazolidinone (**144**) and fluoroacetaldehyde is not possible due to the lack of availability of fluoroacetaldehyde in a non-aqueous form. We thus considered fluoroacetyl chloride as an alternative electrophilic substrate to explore the possibility of generating a β-ketone (**193**). The ketone may then be reduced and hydrolysed to give 4-(*2S,3S*)-fluorothreonine.

4. 3.1 Synthesis of the fluorinated 'β-ketone' (193)

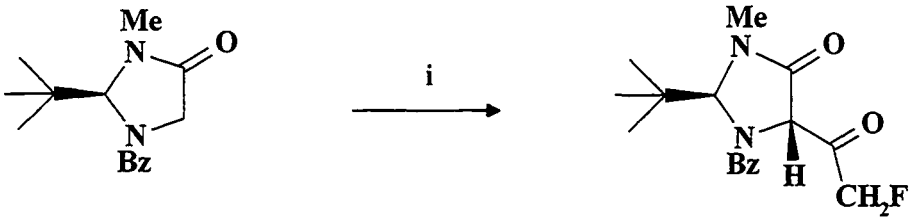

(144) **(193)**

Scheme 32 (I) LDA/ FCH_2COCl/ -100°C

Accordingly, the treatment of sodium fluoroacetate with phthaloyl chloride generated fluoroacetyl chloride in excellent yield.[162] The imidazolidinone adduct (**193**) which was generated after treatment of the enolate of (**144**) with fluoroacetyl chloride proved to be stable at room temperature. The yield of this condensation step was initially low (32%) due to the formation of (**196**), an adduct formed between diisopropylamine and fluoroacetyl chloride.

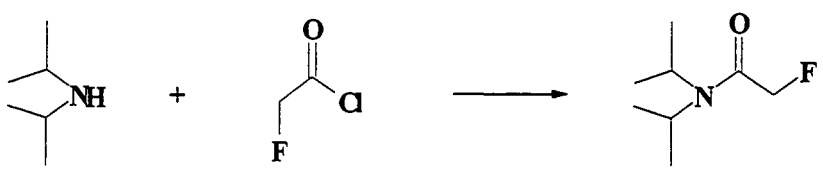

(194) **(195)** **(196)**

Scheme 33

In an attempt to increase the yield of this condensation step, various modifications were investigated, *i.e.* the reaction was quenched at -78°C, -50°C, -25°C, 0°C and 25°C but this did not improve the product profile. In an effort to suppress the side reaction (Scheme 33) experiments were conducted with n-butyllithium alone. However these conditions furnished many new unidentified side products which consequently led to poorer yields of **(193)** (See Table 4.1). Lithium hexamethyldisilazide (LHMDS) was then explored as an alternative base to LDA but only a minimal conversion to the product was achieved since the yield of the competing amide formation (Scheme 33) was even greater in this case.

Table 4.1

Reaction	**Yield of 'β-ketone' (193)**
LDA / fluoroacetyl chloride	32%
BuLi / fluoroacetyl chloride	14%
Hexamethyldisilazide / "	< 10%

Due to the high reactivity of fluoroacetyl chloride attention was focused on a milder electrophilic substrate, namely ethyl fluoroacetate. Deprotonation of the imidazolidinone (**144**) was achieved using LDA to generate the characteristic red coloured anion which was quenched with ethyl fluoroacetate. In the event, tlc results showed very little conversion of starting material **(144)** to product **(193)**. n-Butylilthium, LDA and hexamethyldisilazide were all explored as bases for reaction with ethyl fluoroacetate, but no notable increase in the yield of the product **(193)** (<10%) was observed (See Table 4.2).

Table 4.2

Reaction	Yield of 'β-ketone' (183)
LDA / Ethyl fluoroacetate	<10%
BuLi / Ethyl fluoroacetate	<10%
Hexamethyldisilazide / "	0%

Optimisation (1:1 ratio of LDA to starting imidazolidinone, stirred at -78°C for 30min followed by reaction with 10 equivalents of fluoroacetyl chloride at -100°C for 5min) of the LDA/ fluoroacetyl chloride mediated reaction increased the yield from 32% to 57%, after recrystallisation from ethanol, and ^{19}F, ^{13}C, ^{1}H NMR spectra all indicated the presence of a single diastereoisomer. A suitable crystal of (**195**) was submitted for X-ray analysis and the crystal structure is shown in Fig. 4.2. The most interesting feature of the structure is that the geometry of the stereogenic carbon centre at C-5 is tetrahedral indicating that the sterically bulky tert-butyl moiety occupies a position *anti* to the fluoroacetyl fragment. This is an important observation, as the tetrahedral geometry renders the β-ketone **(193)** resistant to epimerisation, and sets the desired stereogenic centre at C-5. It is interesting to note that the bond angles at C-5 of **(193)** are close to that of an ideal tetrahedral centre (Fig. 4.3). This tetrahedral character of the C-5 centre is further reinforced by the X-ray crystal structure of the acylated imidazolidinone derivative (**206**, see page 168, Appendix A4) derived from acetyl chloride rather than fluoroacetyl chloride.

* X-Ray crystallography performed by Dr. A. Batsanov and Miss J. Moloney.

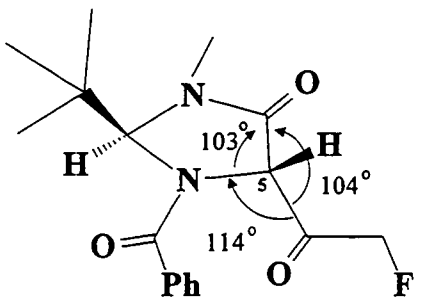

Fig. 4.3

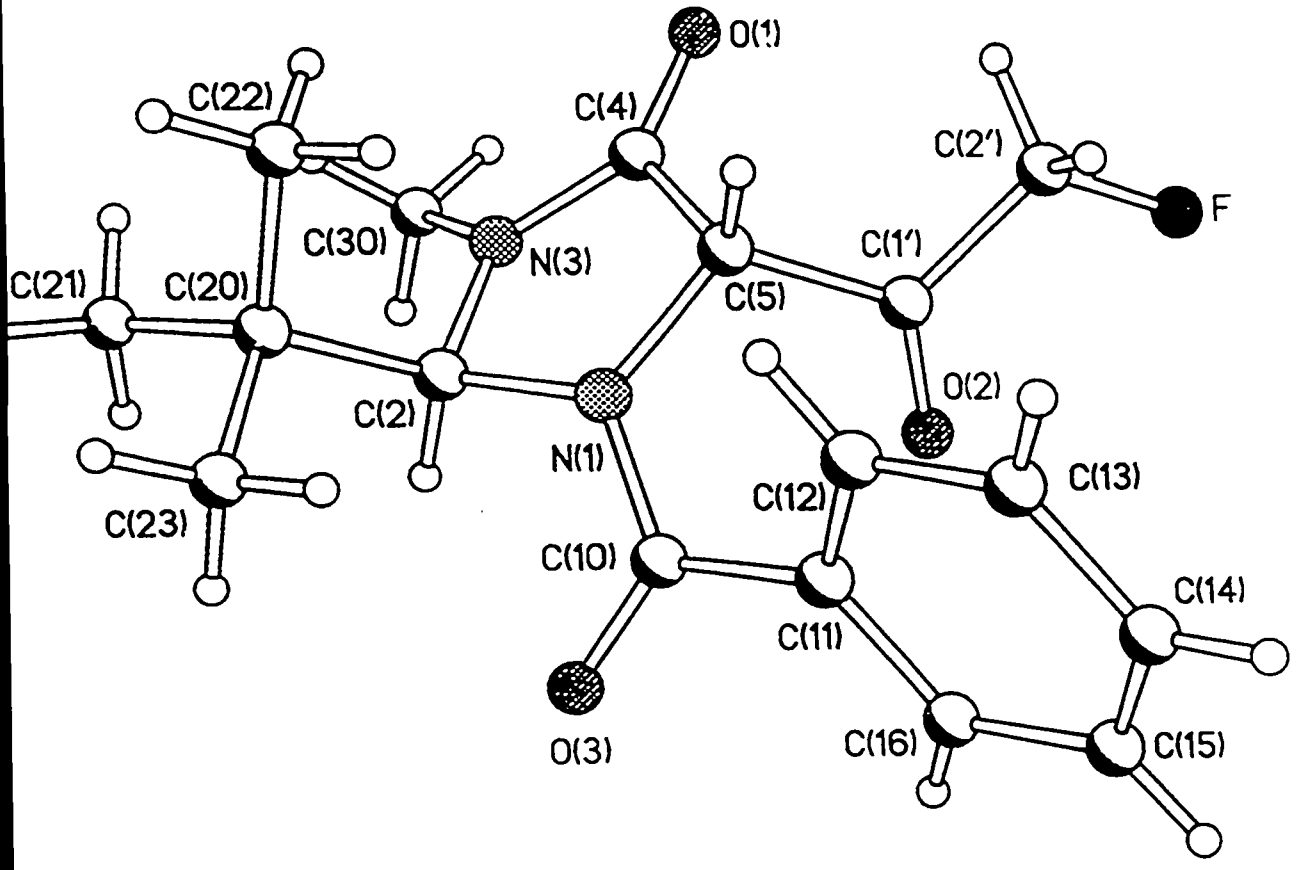

Fig. 4.4 *Crystal structure of* ***(193)*** *showing tetrahedral geometry at C(5).*

4.3.2 Reduction of the 'β-ketone' intermediate (193) to (197)

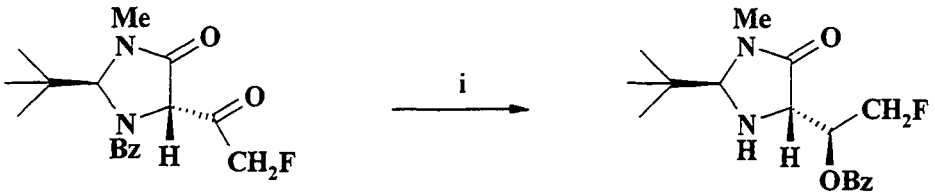

(193) **(197)**

Scheme 34 (I) $NaBH_4$/ MeOH/ 5min

The key issue now was whether the reduction of the β-ketone would be stereoselective and deliver the desired *threo* product, however in the event this proved to be the case. Reduction of **(193)** with sodium borohydride (excess) generated the ester **(197)** rather than the hydroxyamide **(197a)** due to a facile transesterification process. This phenomenon had previously been observed by Seebach.[154]

An optimum reaction time of 5min proved crucial in isolating the correct product and generated **(197)** as a single diastereoisomer, as determined by ^{19}F, ^{1}H, and ^{13}C NMR spectroscopy, clearly demonstrating the high stereoselectivity of the reduction step. Reaction times >5min for the reduction step resulted in the isolation of an additional product. This was obvious from mass spectroscopy data which showed a fragmentation pattern attributable to **(198)**. It was found that the aqueous extract from the sodium borohydride workup developed crystals which were identified as the sodium salt of benzoic acid **(199)**. The highly basic conditions of the reduction almost certainly promoted the hydrolysis of the ester group as depicted in scheme 35.

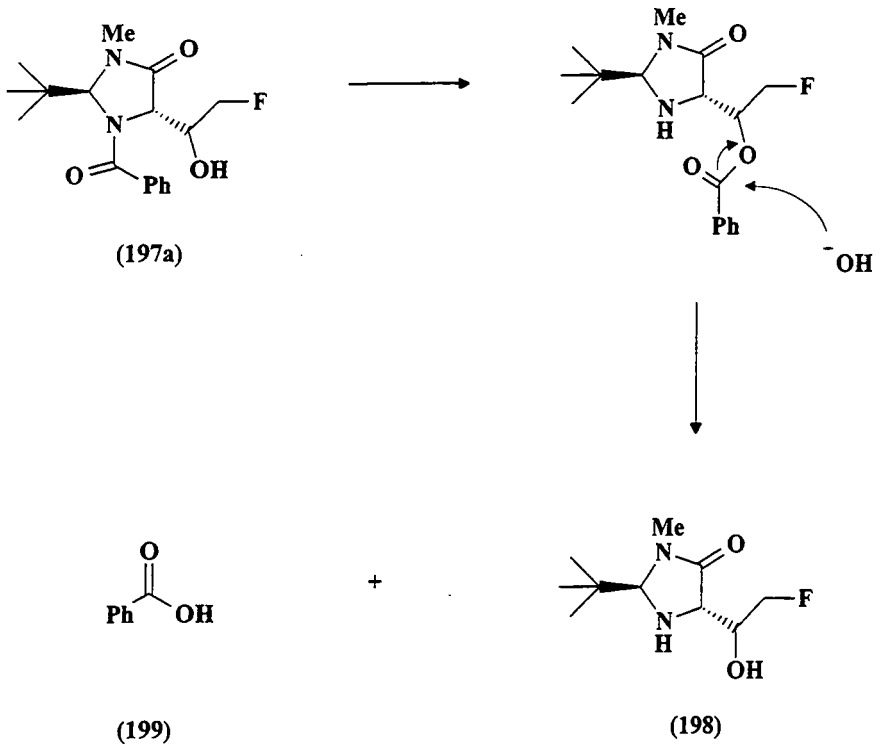

Scheme 35

This ester hydrolysis was arrested by neutralising the methanolic solution with 1N HCl. Tlc and ^{1}H-NMR analysis of the crude reaction mixture also revealed the presence of the starting imidazolidinone **(144)** (13%) if the reaction time is extended. This is presumably due to a 'retro-aldol' reaction occurring during the reduction process as outlined below (Fig. 4.5).

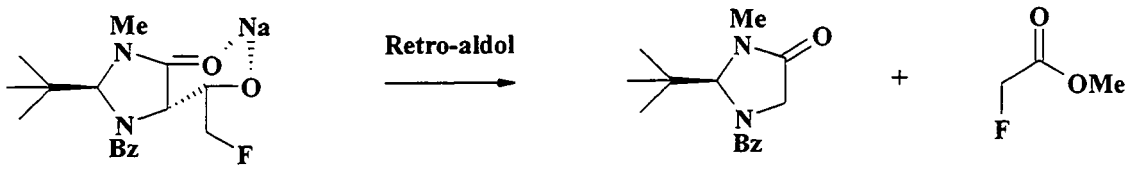

(200) **(144)** **(201)**

Fig. 4.5

It would appear that the hydride delivery is to the *re* face of the carbonyl group. This face is the more exposed of the two as the N-benzoyl aromatic ring hinders access to the *si* face. Additionally the imidazolidinone ring carbonyl may co-ordinate boron and direct hydride to the more open *re* face of (**193**) (Fig. 4.6). The crystal structure indicates that the *N*-benzoyl centre is relatively more planar than the other nitrogen centre of (**193**) and allows the phenyl group to occupy a position as depicted below. This attack of the hydride sets the desired (*S*) stereochemistry at the stereogenic centre C-1'.

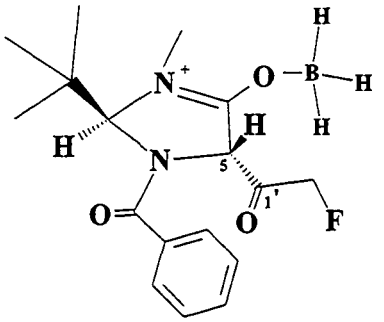

Fig. 4.6

4.3.3 Hydrolysis of (*2S,5S,1'R*)-5-(1'-benzoyloxy-2'-fluoroethyl)-2-(tert-butyl)-3-methylimidazolidin-4-one (197)

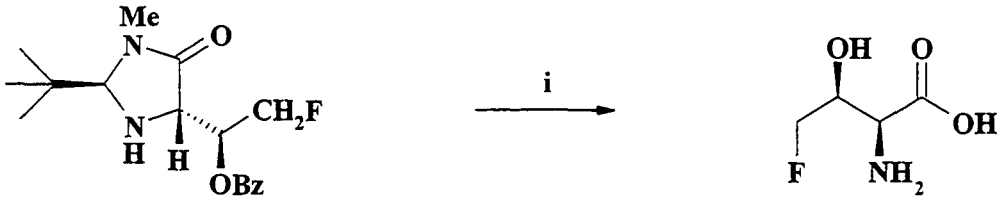

(197) **(202)**

Scheme 36 (I) 10N HCl/ 100°C/ 72h

Hydrolysis of **(197)** was achieved under vigorous acid conditions, 10N HCl / 100°C for 72h. The 4-*(2S,3S)*-fluorothreonine generated was recovered by ion-exchange chromatography and purified by recrystallisation from methanol/ water (9:1). The optical rotation of the synthetic material ($[\alpha]_D^{25}$ = -20°, c=5, H_2O) compared very well with that reported by the groups of Scolastico[157] ($[\alpha]_D^{25}$ = -18.4°, c=1, H_2O) and Shimizu[158] ($[\alpha]_D^{25}$=-20°, c=0.065, H_2O), clearly indicating that 4-*(2S,3S)*-fluorothreonine had been isolated. The relative stereochemistry of the fluorinated amino acid **(202)** was shown to be *threo* by X-ray analysis (Fig. 4.7, Appendix A2). Note that the CH_2F group is rotationally disordered over two positions due to the similar steric demands of fluorine and hydrogen which allows hydrogen to be replaced by fluorine in the solid state. The *(2S,3S)* absolute stereochemistry follows from the known absolute stereochemistry of the β-ketone **(194)**. Fig. A3 (Appendix A3) shows the 3-D network of hydrogen bonding interactions between molecules of 4-*(2S,3S)*-fluorothreonine in the crystal lattice. The shortest F-H interactions are typically 2.29 Å, 2.55 Å and will be weak interactions.

4.4 Comparison of natural and synthetic 4-fluorothreonine.

The natural 4-fluorothreonine was isolated from cultures of *S. cattleya* and supplied by Harper and co-workers at the Queen's University in Belfast. To determine if the synthetic (*2S,3S*) isomer was identical to the natural 4-fluorothreonine, an "add-mix" experiment was conducted. Addition of the synthetic 4-fluorothreonine (5mg/ml) to the natural material (2mg/ml) was carefully monitored by ^{19}F-NMR spectroscopy. No change was observed in the ^{19}F-NMR and furthermore the ^{1}H-NMR of the mixed sample revealed an identical set of signals signifying that the synthetic and the natural 4-fluorothreonine were in fact the same stereoisomer. It must be added that care was taken to ensure that no overdosing had occurred. The $[\alpha]_D$ of the natural product reported by Sanada *et al.*,[107] (-18°, c=1, H_2O) differs slightly from our value of -20° (c=5, H_2O). However this difference, in the optical readings, may be due to temperature and concentration effects. Moreover identical GC-MS, HPLC and ^{13}C-NMR data of the natural and synthetic forms of 4-fluorothreonine give reassurance that both compounds are identical (Fig. 4.8 and 4.9).

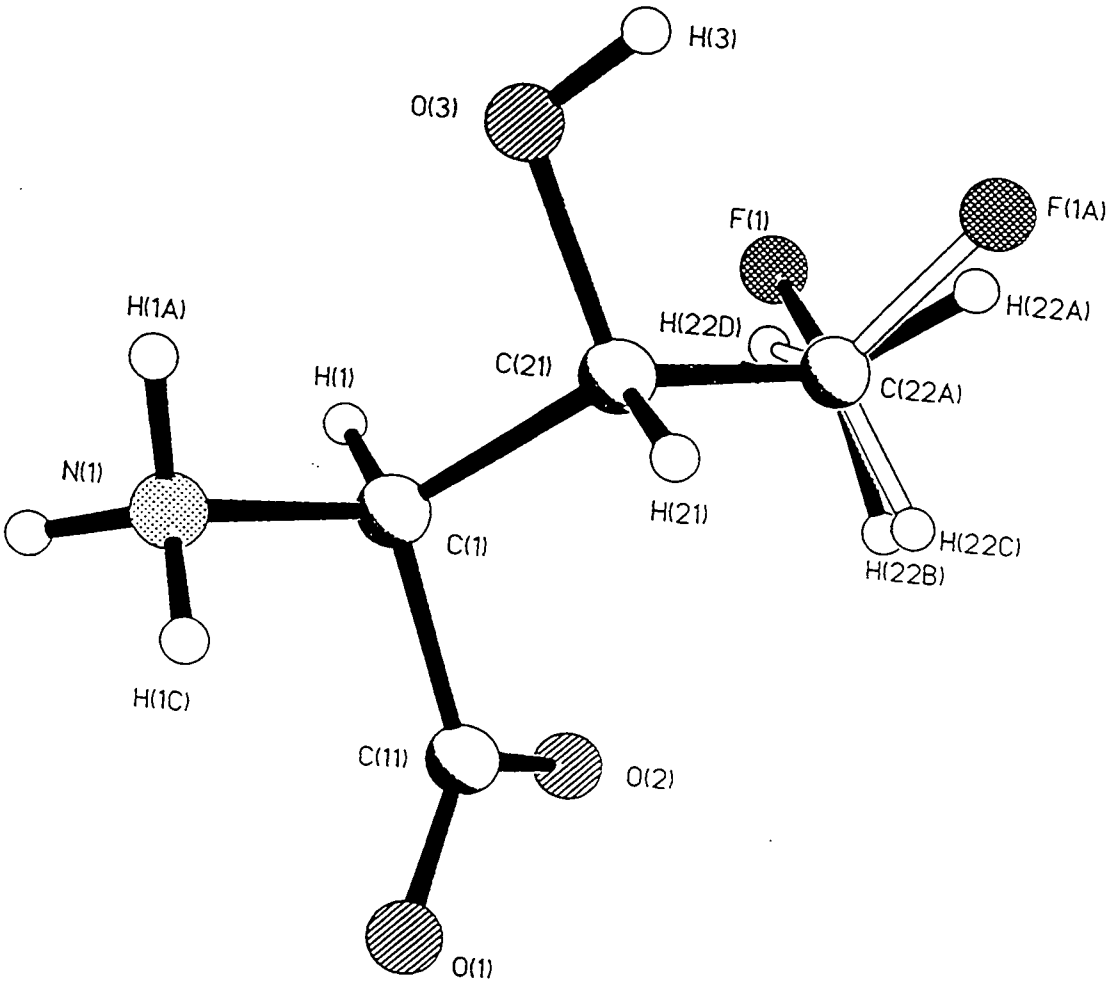

Fig. 4.7 *Crystal structure of 4-(2S,3S)-fluorothreonine* ***(202)***

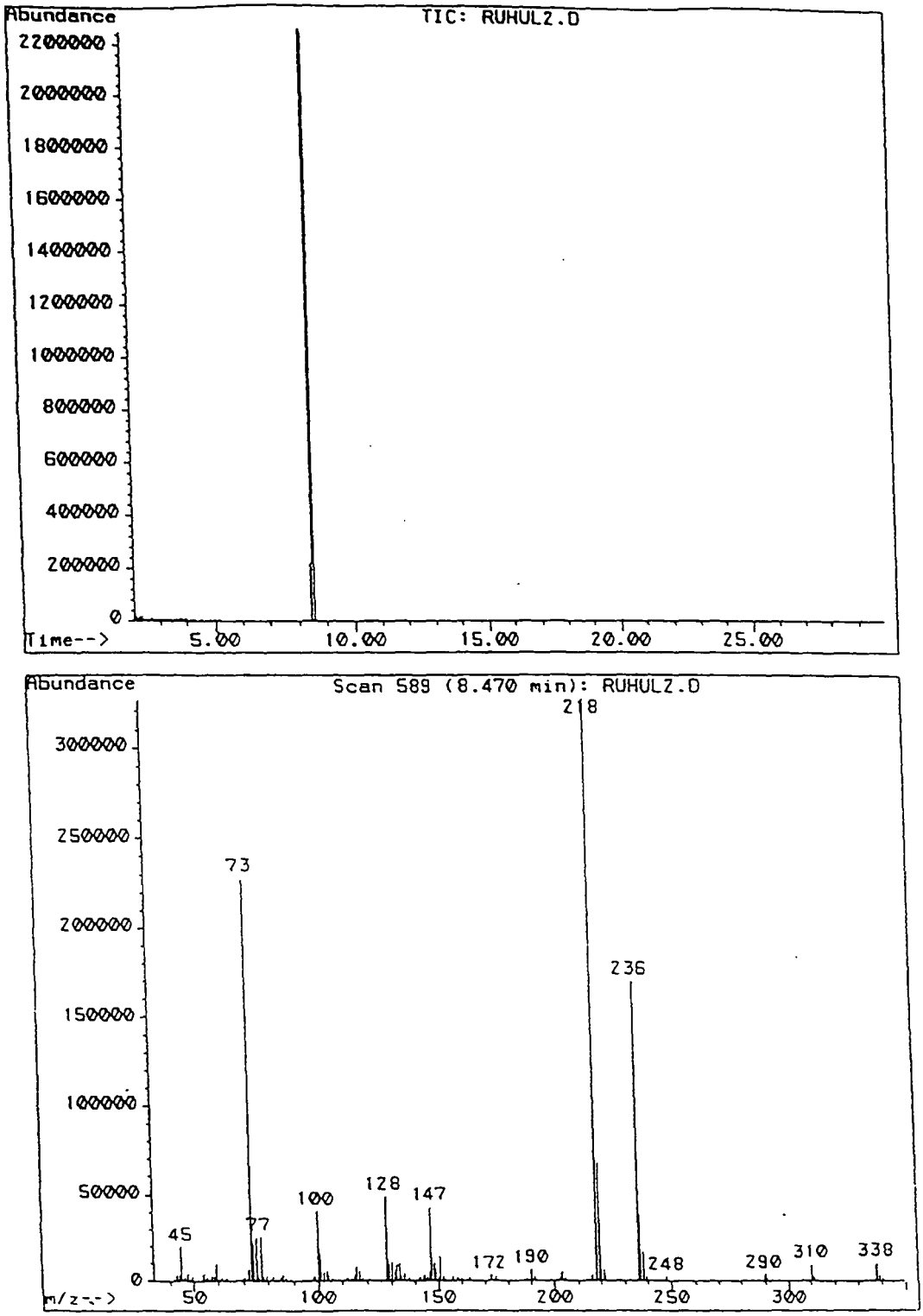

Fig. 4.8 *GC-MS trace of 4-fluorothreonine isolated from S. cattleya*

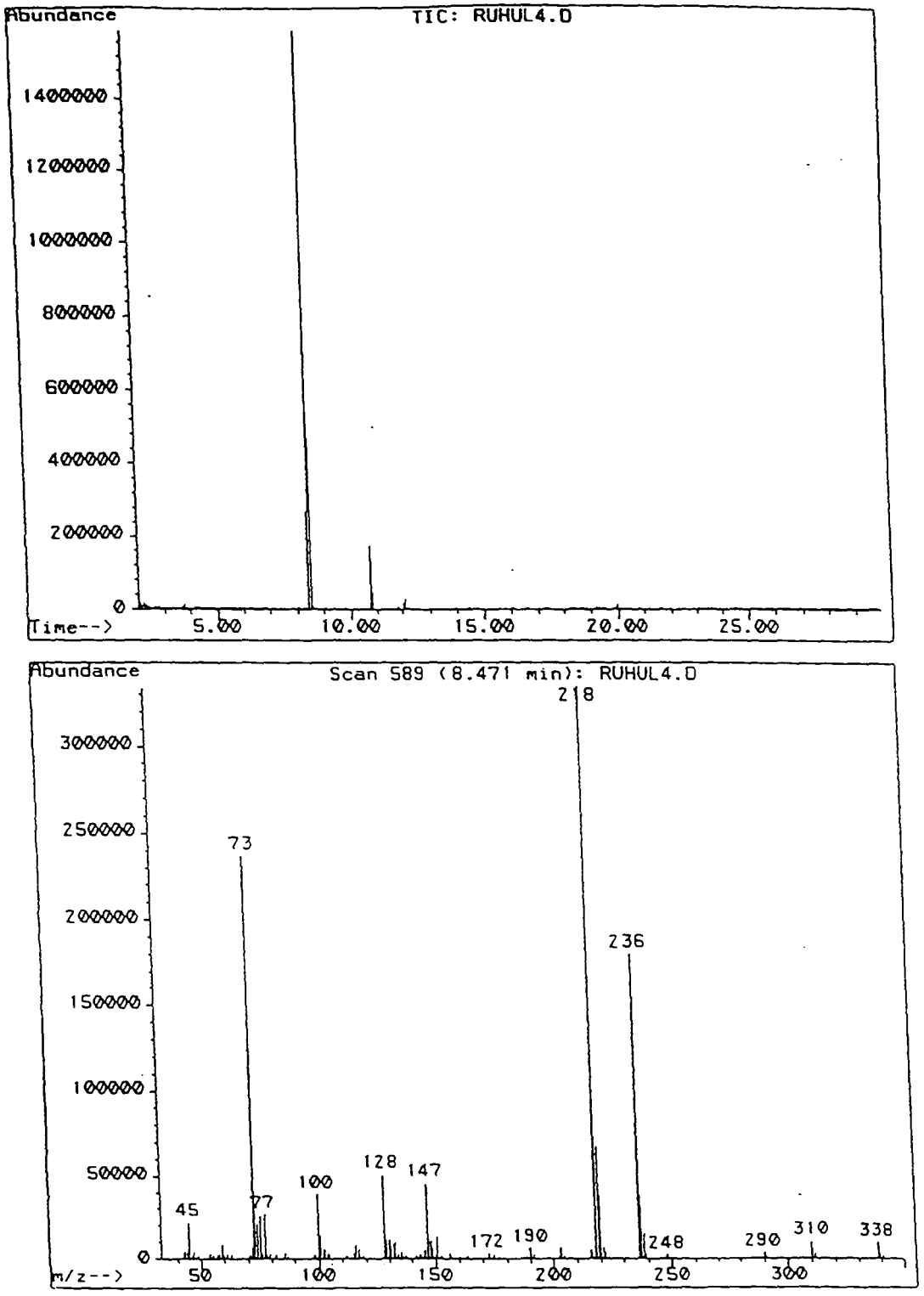

Fig. 4.9 *GC-MS trace of synthetic (2S,3S)-4-fluorothreonine* ***(202)***

Interestingly, Table 4.3 below shows the relationship of the optical rotation values between the various forms of threonine (*Ref. Aldrich Chemicals Cat.*)

Table 4.3

Threonine	**$[\alpha]_D$ (c=1, H_2O) at 25°C**
D- threonine	+ 27°
D-*allo*-threonine	- 8.8°
L-threonine	- 27.4°
L-*allo*-threonine	+ 9°

Note the marked difference in optical rotation values for *allo*-threonine and the L/ D forms. It is therefore anticipated that L-*allo*-4-fluorothreonine would give a significantly different optical rotation value from L-4-fluorothreonine. These data provide further, albeit circumstantial, evidence that the stereochemistry at positions C-2 and C-3 of the natural 4-fluorothreonine is *(2S,3S)*. Fig. 4.10 shows a 400MHz ^{19}F-NMR of the mixed sample of natural and synthetic 4-fluorothreonine indicating the presence of only a single diastereoisomer.

It is perhaps important to note that HPLC analysis of L-*allo*- and a synthesised sample of L-threonine showed different elution times whereas the natural and synthetic 4-fluorothreonines showed identical elution times [Fig. 4.11(a), (b)]. (N.B. the dominant peak at 11.3min on the chromatogram of the natural compound [4.11(b)] is due to tyrosine which was used as an internal standard).

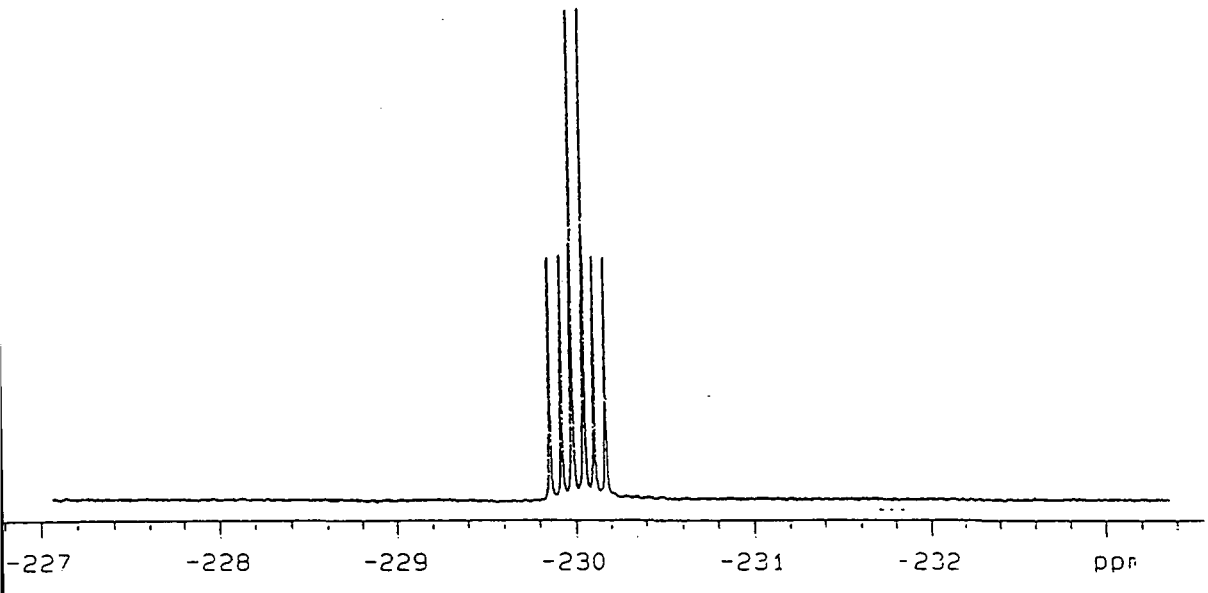

Fig. 4.10 400MHz ^{19}F-NMR spectrum of a mixed sample of natural and synthetic 4-fluorothreonine (2mg : 5mg)

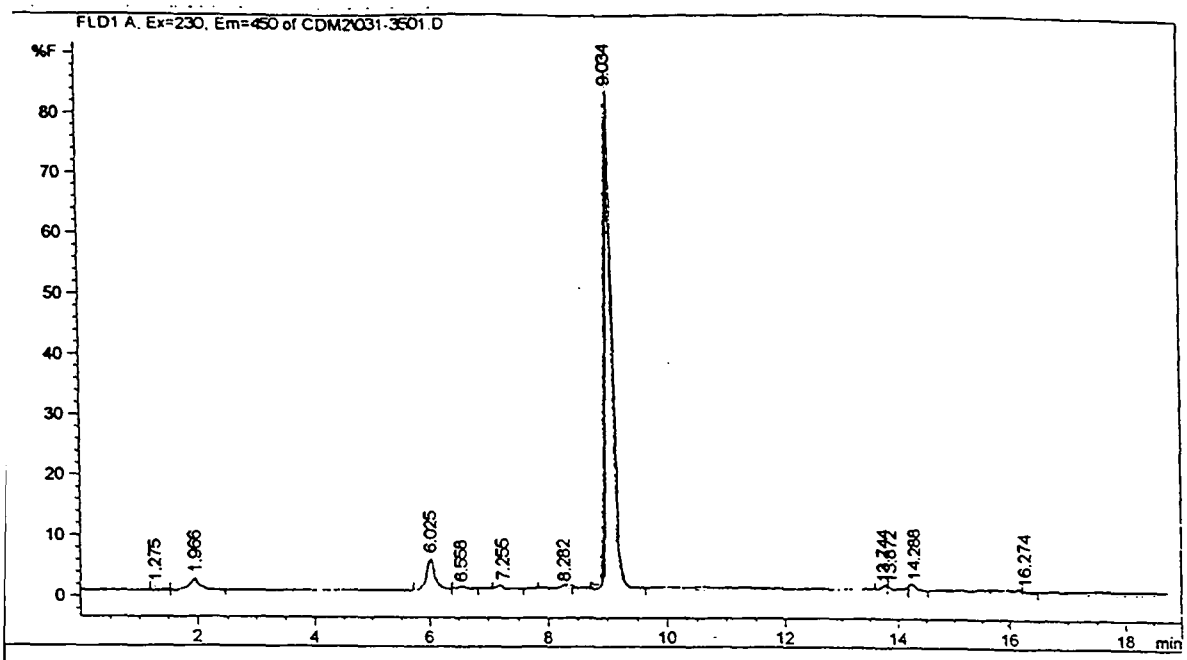

(a)

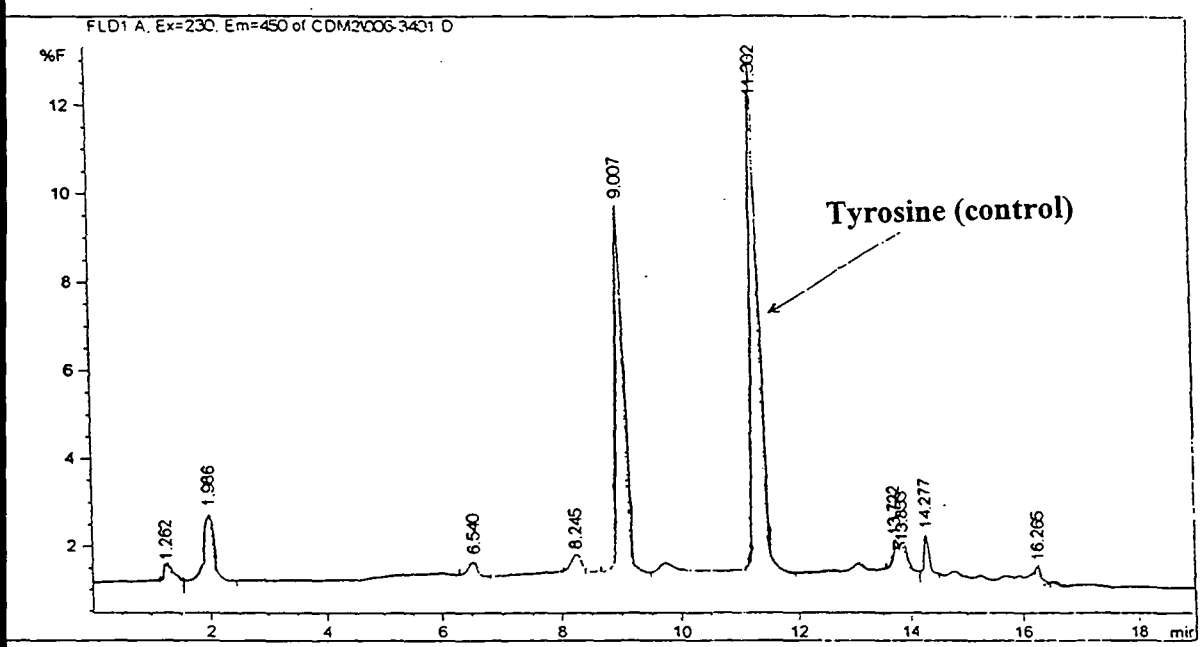

(b)

Fig. 4.11 Liquid chromatogram of (a) synthetic 4-*(2S,3S)*-fluorothreonine (b) natural 4-fluorothreonine

4.5 Synthesis of [3-^{2}H]-4-fluorothreonine (204)

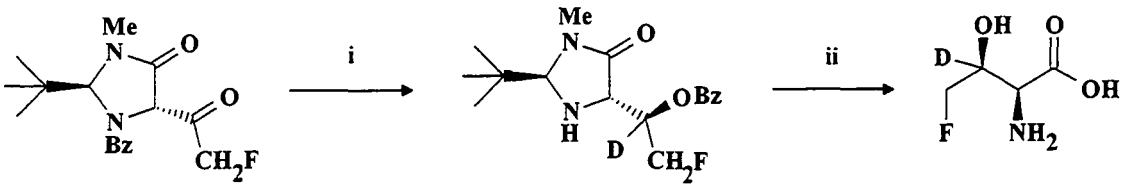

(193) **(203)** **(204)**

Scheme 37 (I) $NaBD_4$ (77%) (ii) 10N HCl/ 100°C/ 72h (67%)

The route to 4-(2S,3S)-fluorothreonine is amenable to isotope labelling and a deuterium label was introduced at C-3 of 4-fluorothreonine by treating **(193)** with $NaBD_4$ to generate **(203)**. Acid hydrolysis of **(203)** followed by isolation using ion-exchange chromatography allowed recovery of [3-^{2}H]-4-fluorothreonine **(204)** in satisfactory yield.

4.6 Synthesis of DL-[4,4,4-$^2H_3$]-threonine (208)

In the initial stages of the project, it was judged important to prepare DL-[4,4,4-$^2H_3$]-threonine to determine the incorporation of deuterium into fluoroacetate and 4-fluorothreonine. Thus acetyl chloride was investigated in place of acetaldehyde as the electrophile in Seebach's route to L-threonine.

4.6.1 Synthesis of (*2S,3R*)-threonine (**187**) using acetyl chloride as the electrophile

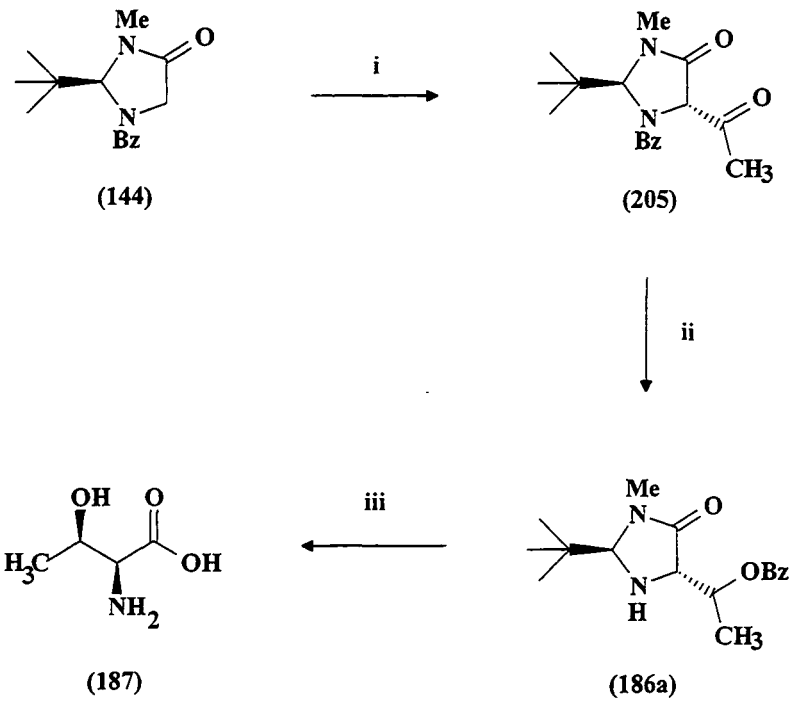

Scheme 38 (I) LDA/ CH_3COCl/ -100°C (40%) (ii) $NaBH_4$/ MeOH/ 5min (69%)

(iii) 10N HCl/ 100°C/ 72h (69%)

Coupling of the chiral imidazolidinone **(144)** with acetyl chloride generated the ketone **(205)** as a single diastereoisomer. X-ray analysis of a suitable crystal of the ketone **(205)** showed that the acetyl moiety occupies a site *anti* to the *tert*-butyl group (Fig. 4.12, for crystal data see Appendix A4). The tetrahedral geometry of the stereogenic centre at C-5 of **(206)** again indicates that this centre is resistant to epimerisation. Thus the structures of **(193)** and **(205)** show very similar characteristics.

Reduction of **(205)** generated the secondary alcohol which rearranged to the ester **(186a)** in an analogous manner to that of the fluorinated intermediate **(193,** see page 155).

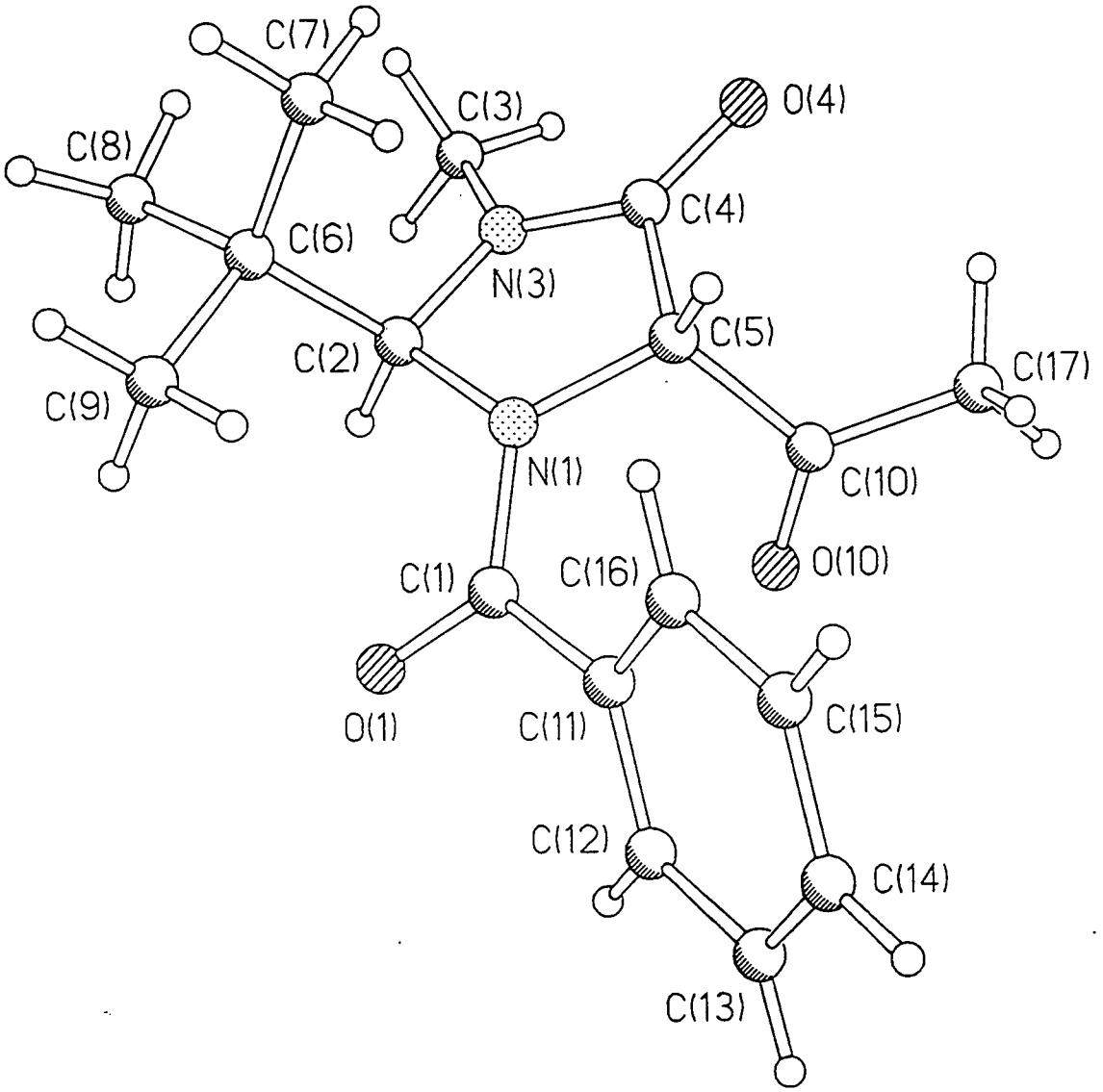

Fig. 4.12 *Crystal structure of 5 -(2S,5S) - (1' - carbonyl - 2' - methyl) - 2 - (tert - butyl) -3-methylimidazolidin-4-one* ***(205)***

The optical rotation value for (**186a**) ($[\alpha]_D$ = +90°) and of (**184a**) was similar to that ($[\alpha]_D$ = +85.7°)[154] reported for the aldehyde derived benzoyl ester (**186a**).

Hydrolysis under acidic conditions liberated (*2S,3R)*-threonine [(**187**), scheme 38] which was purified by ion-exchange chromatography. Comparison of the ^{1}H-NMR of the synthesised threonine and a reference sample of L-threonine and *allo*-threonine demonstrated that the route yielded the desired diastereoisomer. The ^{1}H-NMR spectra (Fig. 4.13(a), (b), (c)) clearly show that these two diastereoisomers are easily distinguished. The presence of only a single diastereoisomer, indicated again that the reduction takes place with a high level of stereoselectivity. Furthermore the optical rotation value of the prepared L-threonine ($[\alpha]_D$ = -24°, c=1, H_2O) was close to the literature value ($[\alpha]_D$ = -27.4°, c=1, H_2O).[154]

With the synthesis of threonine in place, the route was modified to prepare [4,4,4-$^2H_3$]-threonine. The coupling between [2,2,2-$^2H_3$]-acetyl chloride and the imidazolidinone enolate produced the corresponding deuteriated ketone (**206**) (Scheme 39). Reduction of this ketone with $NaBH_4$ followed by acid hydrolysis generated [4,4,4-$^2H_3$]-threonine (**208**) (24% overall yield) in a straightforward manner.

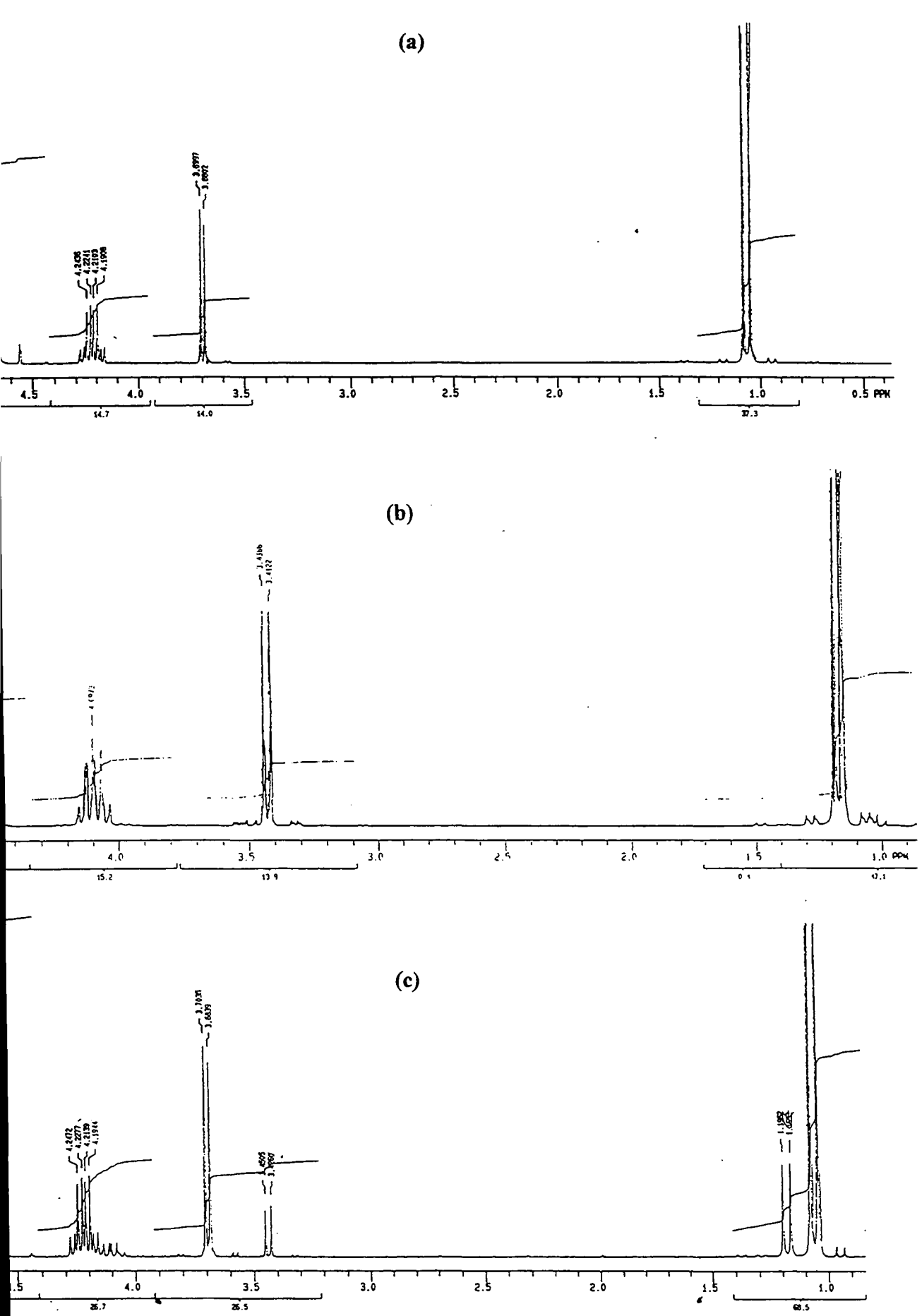

Fig. 4.13 ^{1}*H-NMR spectrum of (a) L-allo-threonine, (b) synthetic L-threonine, (c) L-allo-threonine and synthetic L-threonine mix*

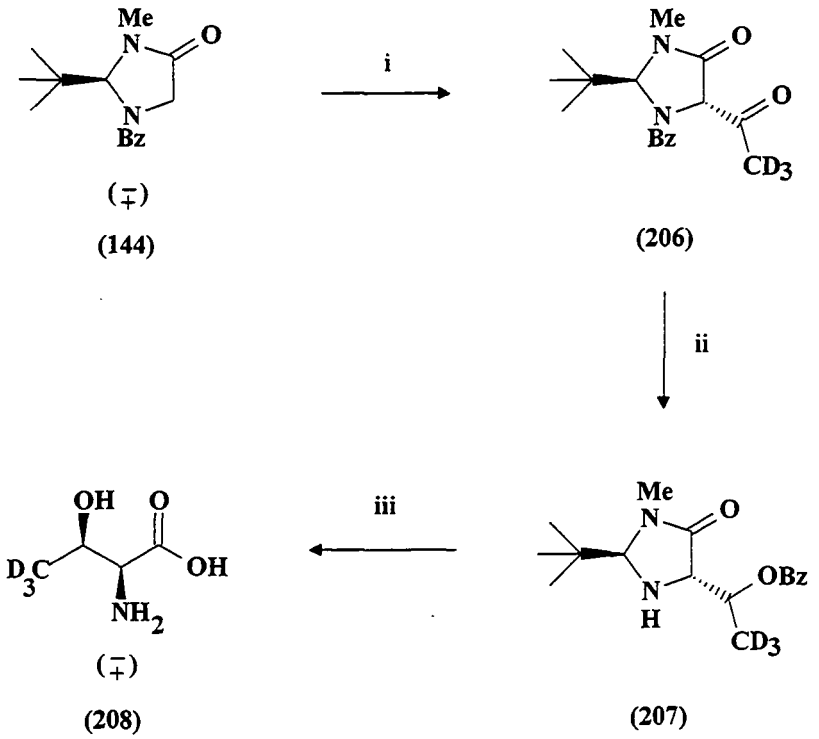

Scheme 39 (I) LDA/ CD_3COCl/ -100°C (ii) $NaBH_4$/ MeOH/ 5min

(iii) 10N HCl/ 100°C/ 72h

With the racemic [4,4,4-$^2H_3$]-threonine in hand, its incorporation into the fluorometabolites in resting cells of *S. cattleya* was studied. The GC-MS data indicated that the isotope is not significantly incorporated (~0.1%) into C-2 of fluoroacetate or C-3 and C-4 of 4-fluorothreonine (results not shown). From this study, it is evident that threonine is clearly not a precursor to the fluorometabolites. However, given the efficient serine hydroxymethyl transferase activity catalysing the interconversion of serine and glycine, it is possible to envisage this enzyme mediating the cleavage of threonine to acetaldehyde and glycine. The carbon atoms of glycine thus produced may be efficiently incorporated into the fluorometabolites, accounting for the relatively high incorporation level of [U-^{14}C]-threonine (see Chapter 2, Table 2.2, p 64).

4.7 Summary

A novel approach to the synthesis of threonines has been developed where acetyl chloride can be used as a good substitute for acetaldehyde in the diastereoselective acylation of a chiral imidazolidinone enolate, thus providing an alternative route to *threo*-amino acids such as L-threonine. This modification has the advantage of using acid chlorides in place of aldehydes when the requisite aldehyde is unavailable. The stereospecific synthesis of 4-(*2S,3S*)-fluorothreonine, using this modified procedure, has allowed the absolute stereochemistry of the natural product to be assigned.

4.8 Towards a synthesis of 4-chlorothreonine (67)

Yoshida *et al.*,[163] in 1994 have reported 4-chlorothreonine **(67)** as a microbial metabolite produced by *Streptomyces sp. OH-5093*. 4-Chlorothreonine is also a constituent of the naturally occurring syringostatins and syringomycin metabolites of *Pseudomonas syringae*.[164,165] The methodology developed in this thesis for the preparation of 4-fluorothreonine was explored towards the synthesis of 4-chlorothreonine.

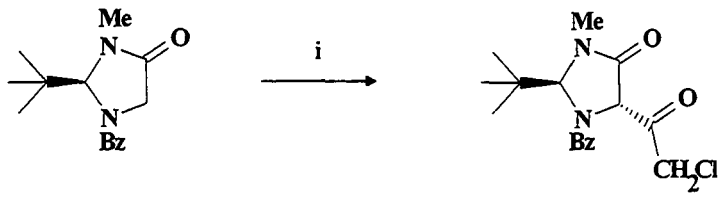

(144) **(209)**

Scheme 40 (i) LDA/ $ClCH_2COCl$/ -100°C

Deprotonation of the imidazolidinone was achieved with LDA. This was followed by acylation using chloroacetyl chloride which generated the chloroketone **(209)**. This compound proved difficult to purify by flash chromatography therefore the partially purified chloroketone was reduced directly with sodium borohydride.

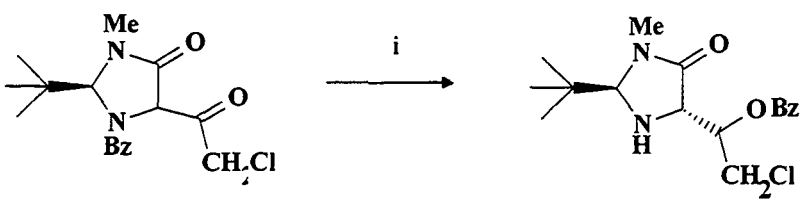

(∓) (∓)

(209) **(210)**

Scheme 41 (i) $NaBH_4$/ MeOH/ 5min (12%)

The reduction (Scheme 41) was neutralised after 5min and subsequent purification of the resultant product over silica afforded the chlorinated ester **(210)** which was isolated as a yellow oil (12% from **(144)**) and was fully characterised. Hydrolysis of **(210)** using 10N HCl at 100°C for 72h generated a complex mixture of products which could not be characterised. ^{1}H-NMR spectra of the hydrolysis products showed no obvious signals that could be attributed to 4-chlorothreonine. As a result of the labile C-Cl bond in (**210**), efforts to synthesise 4-chlorothreonine using this route were discontinued.

CHAPTER 5

EXPERIMENTAL

5. Experimental

(Part I)

General:

Flash column chromatography was performed with (FC) Fluka silica gel-60 (35-70μm) or Sorbsil-C60-M (40-60μm). Infra red spectra were recorded on a Perkin-Elmer F.T. 1600 or 1720X spectrometer ^{1}H-NMR spectra were recorded on a Varian Gemini 200MHz (199.977MHz), Varian XL-200 (200.057MHz), Varian VXR-400S (399.952) and Bruker AC-250 (250.133MHz) spectrometers. ^{13}C-NMR were obtained using Varian Gemini 200MHz (50.30MHz), Bruker AC-250 (62.257MHz) and Varian VXR-400S (100.577MHz) spectrometers. ^{2}H-NMR were recorded on a Bruker AMX-500MHz (76.775MHz) spectrometer. ^{19}F-NMR were recorded on a Bruker AC-250 (235.34MHz), Varian VXR-400S (376.289MHz) and a Bruker Spectrospin AMX-500MHz (471.54MHz) spectrometers. Chemical shifts (δ) are quoted in ppm relative to TMS for ^{1}H and ^{13}C-NMR and fluoride was used as a reference for ^{19}F{^{1}H}-NMR spectra. Coupling constants, J, are quoted in Hz. Radioactive analysis was performed on a Packard 200CA scintillation analyser in Ecoscint A fluid. Mass spectra were recorded on a VG analytical 7070E mass spectrometer. Melting points were performed on a Gallenkamp apparatus and are not corrected.

Note: Sodium fluoroacetate and fluoroacetyl chloride are both toxic compounds and must be handled with great caution.

5.1 Preparation of N-(2,2-Dimethylpropylidene)-glycine-(N-methylamide) (184) [161]

Glycine methyl ester hydrochloride **(182)** (12.56g, 0.10mol) was added slowly to cooled 8M ethanolic methylamine (37.5ml), with stirring at room temperature (~15h). After concentration of the suspension *in vacuo*, CH_2Cl_2 (20ml) was added to the resulting viscous material and the solution concentrated *in vacuo*. This residue, pivalaldehyde (23.5ml, 0.15mol) and triethylamine (20.9ml, 0.15mol) in CH_2Cl_2 (100ml) was heated under reflux for 10h. The cooled mixture was filtered and the filter cake washed with diethyl ether (50ml). The resulting white foamy filtrate was again filtered off and concentration of the filtrate gave N-(2,2-dimethylpropylidene)-glycine-(N-methylamide) **(184)** as a yellow oil (11.8g, 76%) B.p. 120°C / 0.1 Torr, lit. b.p. 119°C/ 0.1 Torr.[161] IR ($CHCl_3$): 3315m (br.), 2960s, 1660s, 1525s, 1405m. ^{1}H-NMR ($CDCl_3$): 7.60 (1H, s, H-C=N), 7.00 (1H, s, br, NH), 3.98 (2H, s, H_2-C(2)), 2.83 (3H, d, J=3.0, Me-N), 0.95 (9H, s, (t-Bu)). ^{13}C-NMR ($CDCl_3$): 172.5 (C-4), 115.0 (C-2), 46.1 (C-5), 39.4 (-$\underline{C}Me_3$), 27.0 (N-Me), 21.4 (t-Bu). MS: (EI); 157 (M^+ +1, 12%), 141 (2%), 113 (2%), 99 (86%), 73 (100%), 72 (23%), 41 (35%), 30 (48%).

5.2 Preparation of 2-(tert)-butyl-3-methyl-imidazolidin-4-one (185) [161]

A solution of **(184)** in methanol (30ml) was treated with a saturated solution of methanolic HCl at 0°C. After stirring (30min) at 0 °C the mixture was left to stir at room temperature for 3-4h. The resultant solution was concentrated to a syrup under reduced pressure, dissolved in CH_2Cl_2 (80ml), and washed with 3M aqueous NaOH (67ml). The

organic extract was dried ($MgSO_4$) and the solvent evaporated to afford the product **(185)** as a yellow oil. (10.7g; 69%). B.p. 128°C/ 0.05 Torr, lit. b.p. 130°C/ 0.05 Torr.[161] IR ($CHCl_3$): 3378m (br), 2963s, 1675s, 1400m, 1319m, 1110m. ^{1}H-NMR ($CDCl_3$): 4.13 (1H, s, H-C(2)). 3.43 (1H, s, H-C(5)), 2.92 (3H, s, Me-N), 2.36 (1H, s, br, NH), 0.97 (9H, s, $(Me)_3C$). ^{13}C-NMR ($CDCl_3$): 174.5 (C-4), 85.0 (C-2), 49.1 (C-5), 37.4 (-$\underline{C}Me_3$), 31.0 (N-Me), 25.4 (t-Bu). MS: (CI); 157 (M^+ +1, 2%), 141 (2%), 113 (2%), 99 (96%), 73 (100%), 42 (31%), 41 (32%), 30 (47%). Found 157.13392, $C_8H_{17}N_2O$ (M^++1) requires 157.13408.

5.3 Preparation of DL-1-benzoyl-2-(tert)-butyl-3-methylimidazolidin-4-one (144)[161]

Benzoyl chloride (0.89g, 0.73ml) and 1M NaOH (3.9ml) was added to a stirred solution of 2-(tert)-butyl-3-methylimidazolidin-4-one **(185)** (1.00g, 6.4mmol) in CH_2Cl_2 (10ml) with ice-cooling. The reaction was monitored by t.l.c. and when judged complete, the solvent was removed under reduced pressure to afford a yellow oil which was dissolved in diethyl ether (25ml) and washed with 1M NaOH. The organic layer was separarted and dried ($MgSO_4$). Removal of the solvent left an off-white solid which was recrystallised from a minimum amount of hot ethanol to give **(144)** in 85% yield. M.p. 142-143°C lit. 143-144°C.[161] IR (KBr): 3509m (br), 3390m (br), 2982s, 2879m, 1700s, 1646s, 1483m, 1378s, 1304s, 1253s, 1115m, 884m, 790m, 721m, 596m. ^{1}H-NMR ($CDCl_3$): 7.48 (5H, m, arom), 5.68 (1H, s, H-C(2)), 4.11 (2H, d, J_{gem} = 15.2, H_2-C(5)), 3.81 (2H, d, J_{gem} = 15.2, H_2-C(5)), 2.99 (3H, s, N-Me), 1.10 (9H, s, t-Bu). ^{13}C-NMR (D_2O): 171.5 (C-OPh), 164.2 (C-4), 134.2 (arom), 131.5 (arom), 128.5

(arom), 127.9 (arom), 80.7 (C-2), 66.9 (C-5), 39.7 (-$\underline{C}(Me)_3$), 31.5 (N-Me), 25.9 ($(Me)_3$). MS: (CI); 261 (M^++1, 100%).

5.4 Preparation of DL-1-benzoyl-2-(tert-butyl)-5-(1-hydroxy-ethyl)-3-methylimidazolidin-4-one (186) [154]

A solution of **(144)** (0.65g, 2.5mmol) in THF (15ml) was added slowly (*via cannula*) to a solution of diisopropylamine (0.35ml, 2.5mmol) and 1.6M butyllithium (1.87ml, 1.2equiv.) in THF (25ml) at -78 °C and left to stir at -78 °C for 15min. The temperature was lowered to -100 °C (liquid nitrogen/ diethylether) for 30 min and acetaldehyde (0.70ml, 12.5mmol) was added by syringe to the mixture which rapidly deolourized. After 1 min the reaction was quenched with saturated aqueous NH_4Cl (25ml) and Et_2O (25ml) and after warming to room temperature, the two phases were separated and the aqueous layer extracted into Et_2O (3 x 25ml). The combined organic extracts were washed with H_2O (20ml), dried ($MgSO_4$) and concentrated to afford a white solid. Crystallization from ethyl acetate/ petroleum ether (b.p. 60-80°C) (2:3) gave DL-1-benzoyl-2-(tert-butyl)-5-(1-hydroxy-ethyl)-3-methylimidazolidin-4-one **(186)** (0.23g, 30%). M.p. 165-166°C lit. 165.9-166.8°C.[154] IR ($CHCl_3$): 3420m (br), 2973s, 1681s, 1637s, 1377s, 1258m, 1126m, 1090s, 872m, 762m, 724s, 698s, 538m. ^{1}H-NMR ($CDCl_3$): 7.98-7.95 7.54-7.39 (5H, m, arom), 5.38 (1H, dq, J=6.5, 4.3, H-C(1')), 4.21 (1H, d, J=2.0, H-C(2)), 3.73 (1H, m, H-C(5)), 2.93 (3H, s, Me-N), 1.48 (3H, d, J=6.5, CH_3C(1')), 0.99 (9H, s, (t-Bu)). ^{13}C-NMR ($CDCl_3$): 172.3 (C-OPh), 162.8 (C-4), 136.2 (arom), 132.0 (arom), 128.5 (arom), 126.2 (arom), 81.7 (C-2), 65.7 (C-1'), 61.2 (C-5),

38.1 (-C(Me)$_3$), 31.5 (N-Me), 25.9 ((Me)$_3$), 19.3 (C-2'). MS (EI): 247 (M^+ -57, 25%), 203 (11%), 125 (49%), 105 (100%), 77 (36%).

5.5 Preparation of DL-threonine[154]

A mixture of **(186)** (0.304g, 1mmol) and 10N HCl (15ml) was heated under reflux at 100°C for 72h. The cooled solution was extracted into Et_2O (3x10ml) and the aqueous phase evaporated to leave a residue which was adsorbed onto *Dowex-50-W X8* ion-exchange resin (30g). The ion-exchange resin was primed by initially washing it until it was neutral, followed by acidification with dil. HCl and then the amino acid was eluted with 1.5M aqueous NH_4OH solution (250ml). Concentration of the aqueous ammonia solution under reduced pressure afforded DL-threonine as an amorphous white solid which was recrystallised from EtOH/ H_2O (0.085g, 71%). M.p. 241-244°C (dec.), lit. 242-245 °C (dec.).[154] IR (KBr): 3168s (br), 2975s (br), 2712m (br), 2049w, 1626s, 1456s, 1346s, 1112s, 1040s, 935s, 560s. ^{1}H-NMR (D_2O): 4.13 (1H, dq, J=6.3, 4.5, H-C(3), 3.45 (1H, d, J=4.5, H-C(2)), 1.23 (3H, d, J=6.2, Me-C(3). ^{13}C-NMR (D_2O): 181.4 (C-1), 70.1 (C-3), 62.7 (C-2), 20.0 (C-4). MS: (EI); 75 (M^+-44, 92%), 74 (23%), 57 (89%), 56 (29%), 45 (42%), 44 (100%), 42 (40%), 41 (16%).

5.6 Preparation of DL-[3,4,4,4-$^2H_4$]-threonine (192)

A solution of **(144)** (0.65g, 2.5mmol) in THF (15ml) was added slowly (*via cannula*) to a solution of diisopropylamine (0.35ml, 2.5mmol) and 1.6M butyllithium (1.87ml, 1.2equiv.) in THF (25ml) at -78 °C and left to stir at -78 °C for 15min. The temperature was then lowered to -100°C for 30min and [1,2,2,2-$^2H_4$]-acetaldehyde (0.70ml, 12.5mmol) was added by syringe to the mixture. After 1min the reaction was quenched with sat. aqueous NH_4Cl (25ml) and Et_2O (25ml). The aqueous layer was extracted into Et_2O (3 x 25ml) and the combined organic extracts were washed with H_2O (20ml), dried ($MgSO_4$) and concentrated to afford an off-white solid. This material was not characterised but directly dissolved in 10N HCl (10ml) and heated under reflux at 100° C for 72h. The cooled solution was extracted into Et_2O (3x10ml) and the aqueous phase evaporated to leave a residue which was adsorbed onto *Dowex-50-W X8* ion-exchange resin (30g). The product was eluted with 1.5M aqueous NH_4OH solution (250ml) and removal of the solvent *in vacuo* afforded DL-[3,4,4,4-$^2H_4$]-threonine (0.04g, 14% from starting material **(144)**). M.p. 235-239°C (dec.). IR (KBr): 3154s (br), 2971s (br), 2667m (br), 1619s, 1417s, 1040s, 701s, 563m. ^{1}H-NMR (D_2O): 3.45 (1H, d, J=4.5, H-C(2)). ^{2}H-NMR (H_2O): 4.20 (1D, s, minor diastereoisomer), 4.10 (1D, s, D-C(3)), 1.23 (3D, s, (CD_3)). MS: (CI); 137 ($M(NH_4)^+$ -2D, 7.9%), 105 (23.9%), 88 (41.6%), 78 (77.2%), 60 (20.7%), 49 (10.1%).

5.7 Preparation of 5-(*2S,5S*)-(1' - carbonyl - 2' - methyl) - 2 - (*tert* - butyl) -3-methylimidazolidin-4-one (205)

A solution of **(144)** (0.50g, 1.9mmol) in THF was added slowly (*via cannula*) to a solution of diisopropylamine (0.26ml, 1.9mmol) and 1.6M n-butyllithium (1.42ml, 1.2equiv.) in THF (15ml) at -78 °C and left to stir at -78 °C for 15min. The temperature was then lowered to -100 °C for 30 minutes and acetyl chloride (1.2ml, 15mmol) was added. After 3min the reaction was quenched with sat. aqueous NH_4Cl (25ml) and Et_2O (25ml) and left to warm to room temperature. The two phases were separated, the aqueous layer extracted into Et_2O (3 x 25ml) and the combined organic extracts were washed with H_2O (20ml), dried ($MgSO_4$) and evaporated to afford an off-white solid which was purified by recrystallisation from ethanol to afford **(205)** (200mg, 40%). M.p. 188-189°C (dec). $[\alpha]_D^{25}$= +120° (c=0.01, $CHCl_3$). IR (KBr): 2984s (br), 2940s (br), 22870s (br), 1732s, 1700s, 1397s, 1374m, 1152, 727s, 700m. ^{1}H-NMR ($CDCl_3$): 7.60-7.23 (5H, m, arom), 5.64 (1H, s, H-C(2)), 5.11 (1H, s, H-C(5)), 3.00 (3H, s, Me-N), 1.82 (3H, s, $\underline{C}H_3CO$), 0.99 (9H, s, t-Bu), ^{13}C-NMR ($CDCl_3$): 199.7 (C-1'), 171.3 (C-OPh), 165.3 (C-4), 136.3 (arom), 131.3 (arom), 128.6 (arom), 127.7 (arom), 79.9 (C-2), 70.5 (C-5), 40.3 (-$\underline{C}(Me)_3$), 32.1 (N-Me), 28.7 (-C-2'), 26.1 ($(Me)_3$). MS: (EI); 245 (M^+ -57, 37%), 204 (9%), 125 (51%), 105 (100%), 77 (36%) 43 (11%). CHN found C 56.18% H 72.73% N 9.21% $C_{17}H_{22}N_2O_3$ requires C 56.29% H 72.85% N 9.27%.

5.8 Preparation of 5 -(2S, 5S)- (1'- benzoyloxy) - 2'- methyl) - 2 - (tert -butyl) - 3 - methylimidazolidin - 4 - one (186a)

A solution of **(205)** (200mg, 0.65mmol) in methanol (60ml) was treated with sodium borohydride (24mg, 1 equiv.). After 5min the reaction was quenched to neutral pH by the addition of 1N HCl. The aqueous methanolic mixture was removed under reduced pressure to leave a dry white residue which was suspended in H_2O (15ml) and extracted into Et_2O (3x15ml). Removal of the solvent left a yellow gum (~300mg) which was purified by chromatography to afford **(186a)** as a white solid (136mg, 69%). M.p. 165-166°C, lit. 165.9-166.8°C.[154] $[\alpha]_D^{25}$= +82° (c=0.01, $CHCl_3$), lit. $[\alpha]_D$= +85.7° (c=1.03, $CHCl_3$).[154] IR ($CHCl_3$): 3420m (br), 2973s, 1681s, 1637s, 1377s, 1258m, 1126m, 1090s, 872m, 762m, 724s, 698s, 538m. ^{1}H-NMR ($CDCl_3$): 7.98-7.95 and 7.54-7.39 (5H, m, arom), 5.36 (1H, dq, J=6.5, 4.3, H-C(1')), 4.20 (1H, d, J=2.0, H-C(2)), 3.73 (1H, m, H-C(5)), 2.95 (3H, s, Me-N), 1.47 (3H, d, J=6.5, CH_3C(1')), 0.99 (9H, s, t-Bu). ^{13}C-NMR ($CDCl_3$): 173.3 (C-OPh), 164.2 (C-4), 133.2 (arom), 131.4 (arom), 128.1 (arom), 126.6 (arom), 82.4 (C-2), 67.3 (C-1'), 61.4 (C-5), 40.1 (-C(Me)$_3$), 33.7 (N-Me), 26.7 ((Me)$_3$), 21.3 (C-2'). MS: (EI); 245 (M^+ -57, 34%), 204 (19%), 125 (45%), 105 (100%), 77 (28%) 43 (9%). CHN found C 56.28% H 72.98% N 9.16% $C_{17}H_{24}N_2O_3$ requires C 56.29% H 72.85% N 9.27%.

5.9 Preparation of *(2S,3R)*-threonine (187)

A mixture of **(186a)** (0.300g, 1mmol) and 10N HCl (15ml) was heated under reflux at 100°C for 72h. The cooled solution was extracted into Et_2O (3x10ml) and the aqueous

phase evaporated to leave a residue which was adsorbed onto *Dowex-50-W X8* ion-exchange resin. The amino acid was eluted with 1.5M aqueous ammonia solution (250ml). Evaporation of the aqueous ammonia solution under reduced pressure afforded L-threonine which was recrystallised from EtOH/ H_2O (0.073g, 69.4%). M.p. 240-244° C (dec.), lit. 242-245 °C (dec.). $[\alpha]_D^{25}$= -25° (c=1, H_2O), lit. $[\alpha]_D^{25}$= -27.9° (c=1.02, H_2O).[154] IR (KBr): 3143s (br), 2971s (br), 2712m (br), 1635s, 1450s, 1246s, 1102s, 1040s, 915s. ^{1}H-NMR (D_2O): 4.11 (1H, dq, J=6.3, 4.5, H-C(3)), 3.48 (1H, d, J=4.5, H-C(2)), 1.20 (3H, d, J=6.2, Me-C(3)). ^{13}C-NMR (D_2O): 183.1 (C-1), 72.1 (C-3), 60.7 (C-2), 23.0 (C-4). MS: (EI); 75 (M^+-44, 92%), 74 (21%), 57 (75%), 56 (32%), 45 (45%), 44 (100%), 41 (16%). CHN found C 40.49% H 7.63% N 11.74% $C_4H_9NO_3$ requires C 40.34% H 7.56% N 11.76% %.

5.10 Preparation of DL-[4,4,4-$^2H_3$]-threonine (208)

DL-1-Methyl-2-tert-butyl-3-methyl-imidazolidinone **(144)** (0.65g, 2.5mmol) was slowly added (*via cannula*) to a solution of diisopropylamine (0.35ml, 2.5mmol) and 1.6M butyllithium (1.87ml,1.2equiv.) in THF (25ml) at -78 °C and left to stir at -78 °C for 15min. The reaction mixture went a deep red colour. The temperature was then lowered to -100 °C for 30 minutes and then [2,2,2-$^2H_3$]-acetyl chloride (1.4ml, 17.17mmol) was added. After 3min the reaction was quenched with saturated NH_4Cl (25ml) and ether (25ml) and left to warm to room temperature. The two phases were separated and the aqueous layer was extracted into Et_2O (3 x 25ml). The combined organic extracts were washed with H_2O (20ml), dried ($MgSO_4$) and evaporated to afford an off-white solid (~300mg) which was directly dissolved in methanol (60ml) and sodium borohydride

(0.20g, 1 equiv.) added. The mixture was left to stir for 1h and then the reaction was subsequently quenched with H_2O (10-15ml). The aqueous methanolic mixture was removed under reduced pressure to a leave a residue which was suspended in H_2O (10-15ml) and extracted into Et_2O (3x15ml). After removal of the solvent, the solid (~295mg) was dissolved in 10N HCl (10ml) and heated under reflux at 100°C for 72h, and then treated with acidic *Dowex* to afford DL-[4,4,4-$^2H_3$]-threonine (0.070g, 24% from starting material **(144)**). M.p. 238-241°C (dec). IR (KBr): 3023s (br), 2975s (br), 2515s (br), 1625s, 1417s, 1108s, 926s, 768m. ^{1}H-NMR (D_2O): 3.90 (1H, d, J=5.2 H-C(3)), 3.25 (1H, d, J=5.2 H-C(2)). ^{13}C-NMR (D_2O): 179.3 (C-1), 70.1 (C-3), 62.9 (C-2), 14.3 (septet, J=18.2, C-4). MS: (CI); 137 $(M(NH_4)^+$ -2D, 3.4%), 105 (15.1%), 89 (49.9%), 77 (11.3%), 42 (11.7%)

5.11 Preparation of ammonium [2-^{2}H]-glycolate (106)

Sodium borohydride (0.5g, 13.8mmol) was added to a solution of glyoxylic acid (1.0g, 10.8mmol) in methanol (30ml) and left to stir at room temperature for 2h. The reaction was acidified to pH 1 (1N HCl) and then another equiv. of sodium borohydride was again added and left to stir for another 2h at room temperature. The reaction was quenched with H_2O (2-3ml) and the solvent removed under reduced pressure to leave a residue which was dissolved in H_2O (30ml) washed with Et_2O (3x20ml) and then adsorbed onto basic *Dowex 1X8-50* ion-exchange resin (25g). The product was eluted with 1.5M aqueous ammonia solution which, after removal, afforded ammonium [2-^{2}H]-glycolate, as a white solid (880mg, 93%). M.p. 278-284°C (dec). IR (KBr): 3143s (br), 2780s (br), 2003m (br), 1740m, 1401s, 1101m (br). ^{1}H-NMR (D_2O): 3.9 (1H, s, H-

C(2)). ^{13}C-NMR (D_2O): 182.4 (C-1), 163.5 (t, J=21.5, C-2). MS: (FAB+); 223 ($M(glycerol)^+$ -63, 42%), 154 (0.84%), 131 (34.5%), 57 (27.5%).

5.12 Preparation of calcium glycolate (211)[149]

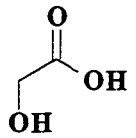

(211)

Trifluoroacetic anhydride (17.5g, 87.5mmol) was added to acetic acid (5g, 83mmol) at 0°C over 10min. After 25min of stirring, red phosphorus (75mg, 2.5mmol) was added. The mixture was heated to 60°C and stirred for 10min followed by addition of bromine (11.9g, 75mmol) with continuous stirring for 4h. The volatiles were removed directly by evaporation under reduced pressure, and on cooling bromoacetic acid solidified. The solid was broken up and dissolved in Et_2O (30ml) and filtered. The solvent was then removed under reduced pressure and then dried. A solution of the crude bromoacetic acid (1.39g, 10mmol) was then directly dissolved in water (20ml) and heated with calcium carbonate (4.5g, 45mmol) at 90°C for 60h. The reaction mixture was filtered hot and the filtrate (without the washings) was stored at -10°C for 24h. The crystalline calcium glycolate (412mg, 75%) was collected, washed with ethanol (30ml) and dried under vacuum. M.p. 293-297°C (dec). IR (KBr): 3226m (br), 2960s, 2873s, 2529s, 1731s, (br), 1462s, 1017m. ^{1}H-NMR (D_2O): 3.9 (2H, s, H_2-C(2)). ^{13}C-NMR (D_2O): 175.5 (C-1), 88.4 (C-1).

5.13 Preparation of calcium [2,2-$^2H_2$]-glycolate (110)

Trifluoroacetic anhydride (9.0g, 44mmol) was added to [2-$^2H_3$]-acetic acid **(108)** (2.5g, 41mmol) at 0°C over 10min. After 15min of stirring, red phosphorus (37.5mg, 1.25mmol) was added. The mixture was heated to 60°C and stirred for 10min after which bromine (6.0g, 38.5mmol) was added and stirring continued for 4h. The volatiles were removed by evaporation under reduced pressure, and on cooling a brown solid was evident. The solid was broken up and dissolved in methanol/ Et_2O (30ml) and filtered. The solvent was removed under reduced pressure to leave a [2-$^2H_2$]-bromoacetic acid **(109)** as a brown oil that solidified on cooling. A solution of this crude solid (0.70g) in water (20ml) was treated slowly with calcium carbonate (3.5g, 35mmol) and the mixture heated at 90°C for 60h. The reaction mixture was filtered while hot and the filtrate (without washings) kept at -10°C for 24h. The crystallised product was collected, washed with ethanol (30ml) and dried under vacuum to afford calcium [2,2-$^2H_2$]-glycolate as a soild (300mg, 76%). M.p. 290-294°C (dec). IR (KBr): 3224m (br), 2960s, 2865s, 1726s (br), 1471s, 998m. ^{13}C-NMR (D_2O): 182.7 (C-1), 63.5 (p, J=6.7, C-2). MS: (FAB-); 219 (M(glycerol)$^+$-67, 21.1%), 127 (100%), 129 (33.2%), 35 (50.8%).

5.14 Preparation of sodium [2-^{13}C]-glycolate (102)[130]

Trifluoroacetic anhydride (9.0g, 44mmol) was added to [2-^{13}C]-acetic acid (2.5g, 41mmol) at 0°C over 10min. After 15min of stirring, red phosphorus (37.5mg, 1.25mmol) was added. The mixture was heated to 60°C and stirred for 10min after which bromine (6.0g, 38.5mmol) was added and stirring continued for 4h. The volatiles were removed directly by evaporation under reduced pressure, and on cooling a brown

solid was evident. The solid was broken up and dissolved in methanol / Et_2O (30ml) and filtered. The solvent was removed under reduced pressure to leave a brown oil, [2-^{13}C]-bromoacetic acid **(101)** which solidified on cooling. A solution of the crude solid (1.0g) and potassium hydroxide (580mg, 14.5mmol) in water (10ml) was heated in a sealed Carius tube at 120°C for 3h. The solution was concentrated (3ml) and the pH adjusted to pH 2 (1N HCl) and loaded onto an Extrelute column. The product **(102)** was eluted with Et_2O (100ml) which was removed under reduced pressure affording [2-^{13}C]-glycolic acid. The solution was neutralised (1N NaOH) and then freeze dried to afford the sodium salt of [2-^{13}C]-glycolic acid as a white powder (224mg, 40%). M.p. 291-294°C (dec). IR (KBr): 3140s (br), 2710s (br), 1738m, 1391m, 1037m, 810m. ^{1}H-NMR (D_2O): 3.68 (2H, d, $J_{^{13}C\text{-}H}$=132.3). ^{13}C-NMR (D_2O): 173.8 (d, J=58.6, C-1), 62.0 (C-2). MS: 206 (M^+(MSTFA), 16.07%), 178 (14.3%), 162 (7.1%), 147 (85.7%), 73 (100%), 45 (17.3%).

5.15 Preparation of sodium [1,2-$^{13}C_2$]-glycolate (104)[130]

Trifluoroacetic anhydride (9.0g, 44mmol) was added to [1,2-$^{13}C_2$]-acetic acid (2.5g, 41mmol) at 0°C over 10min. After 15min of stirring, red phosphorus (37.5mg, 1.25mmol) was added. The mixture was heated to 60°C and stirred for 10min after which time elemental bromine (6.0g, 38.5mmol) was added and stirring was continued for 4h. The volatiles were removed directly by evaporation under reduced pressure, and on cooling a brown solid was evident. The solid was broken up and dissolved in methanol / Et_2O (30ml) and filtered. The solvent was removed under reduced pressure to afford [1,2-$^{13}C_2$]-bromoacetic acid **(103)** as a brown oil which solidified on cooling, A solution of the crude [1,2-$^{13}C_2$]-bromoacetic acid (1.0g, 7.1mmol) and potassium

hydroxide (580mg, 14.5mmol) in water (10ml) was heated in a sealed Carius tube at 120 °C for 3h. The solution was concentrated to 3ml and the pH adjusted to pH 2 (1N HCl) and then loaded onto an Extrelute column. [1,2-$^{13}C_2$]-Glycolic acid **(104)** was eluted with Et_2O (100ml) which was removed under reduced pressure. The solution was neutralised (1N NaOH) and then freeze dried to afford the sodium salt of [1,2-$^{13}C_2$]-glycolic acid as an amorphous white powder (201mg, 35%). M.p. 289-294°C. IR (KBr): 3130s (br), 2710s (br), 1748m, 1406m, 1011m, 810m. ^{1}H-NMR (D_2O): 3.68 (2H, d, $J_{^{13}C-H}$=134.3). ^{13}C-NMR (D_2O): 175.8 (d, J=58.3, C-1). 64.0 (d, J=58.3, C-2). MS: 206 (M (MSTFA)$^+$ - 1, 20.1%), 178 (11.1%), 148 (42.1%), 73 (100.0%), 45 (8.1%).

5.16 Preparation of DL-1-benzoyl-2-tert-butyl-3,5-dimethyl-imidazolidinone (212)[154]

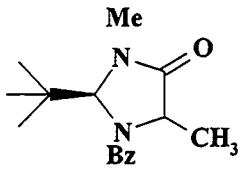

(212)

DL-1-Benzoyl-2-(tert)-butyl-3-methylimidazolidin-4-one **(144)** (1.3g, 5.0mmol) was slowly added (*via cannula*) to a solution of diisopropylamine (0.70ml, 5.0mmol) and 1.6M n-butyllithium (3.8ml, 5.0mmol) in THF (25ml) at -78°C and left to stir at -78°C for 45min. Methyliodide (0.31ml, 2.5mmol) was slowly added and after 1h at -78 °C, the temperature was allowed to rise to 0°C. The reaction was quenched with sat. NH_4Cl (25ml) and Et_2O (25ml) and after warming to room temperature, the aqueous phase was extracted into Et_2O (3x20ml). The combined organic extracts were washed with brine (30ml), water (30ml) and dried ($MgSO_4$) and the solution was filtered and the solvent

removed under reduced pressure to afford DL-1-benzoyl-2-tert-butyl-3,5-dimethyl-imidazolidinone **(212)** as an amorphous white solid (1.25g, 90%). M.p. 145-146°C lit. 145.5-146.5°C.[154] IR (KBr): 3342m (br), 2947s, 2865s, 1718s, 1615s, 1225m, 936m. ^{1}H-NMR ($CDCl_3$): 7.50-8.10 (5H, m, arom), 5.68 (1H, s, H-C(2)), 4.23 (1H, q, J=6.8, H-C(5)), 2.99 (3H, s, Me-N) 1.09 (9H, s, (t-Bu)), 0.97 (3H, d, J=6.8, H_3-C(1')). ^{13}C-NMR ($CDCl_3$): 172.3 (C-OPh), 169.2 (C-4), 136.2 (arom), 131.6 (arom), 128.7 (arom), 127.6 (arom), 80.4 (C-2), 57.3 (C-5), 40.1 (-C(Me)$_3$), 32.8 (N-Me), 26.3 ((Me)$_3$), 19.3 (C-1'). MS: (EI); 217 (M^+-57, 100), 106 (77). 105 (89), 85 (17), 77 (73). CHN found C 69.95% H 8.11% N 10.24% $C_{16}H_{22}N_2O_2$ requires C 70.07% H 8.02% N 10.22%.

5.17 Preparation of DL-1-benzoyl-2-(*tert*-butyl)-3-[5-^{2}H$_3$]-*methyl*]-imidazolidin-4-one (145)

DL-1-Benzoyl-2-(tert)-butyl-3-methylimidazolidin-4-one **(144)** (1.3g, 5.0mmol) was slowly added (*via cannula*) to a solution of diisopropylamine (0.70ml, 5.0mmol) and 1.6M n-butyllithium (3.8ml, 5.0mmol) in THF (25ml) at -78°C and left to stir at -78°C for 45min. [$^2H_3$]-Methyliodide (0.31ml, 2.5mmol) was slowly added with no immediate colour change, and after 1h at -78 °C, the temperature was allowed to rise to 0°C. The reaction was quenched with sat. NH_4Cl (25ml) and Et_2O (25ml) and after warming to room temperature, the product was extracted into Et_2O (3x20ml). The combined organic phases were washed with brine (30ml), water (30ml) and dried ($MgSO_4$), the solution was filtered and the solvent removed under reduced pressure to give an amorphous white solid (1.20g, 88%). M.p. 144-147°C. IR (KBr): 3004s, 2913s, 1710s, 1622s, 1375m, 1184s, 799m. ^{1}H-NMR ($CDCl_3$): 7.50-8.10 (m, arom), 5.68s (1H, s, H-C(2)),

3.82 (1H, s, H-C(5)), 3.05 (3H, s, Me-N) 1.09 (9H, s, (t-Bu)). ^{13}C-NMR ($CDCl_3$): 172.4 (C-OPh), 171.2 (C-4), 137.2 (arom), 131.9 (arom), 128.4 (arom), 127.4 (arom), 80.1 (C-2), 57.7 (C-5), 41.4 (-$\underline{C}(Me)_3$), 32.4 (N-Me), 26.1 ($(Me)_3$), 13.3 (septet, $J^{13}_{C-}{}^{2}_{H}$ = 19.0, -CD_3, (C-1'). MS: (EI); 220 (M^+-57, 100), 109 (57). 105 (95), 85 (19), 77 (92). CHN found C 69.51% H 9.19% N 10.13% $C_{16}H_{19}N_2O_2{}^2H_3$ requires C 69.31% H 9.13% N 10.11%.

5.18 Preparation of DL-alanine (213)[154]

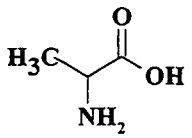

(213)

A mixture of DL-1-benzoyl-2-tert-butyl-3,5-dimethyl-imidazolidinone **(212)** (427mg, 1.54mmol) and 10N HCl (15ml) was heated in a sealed tube at 100°C for 24h. The cooled solution was extracted with Et_2O (3x20ml) and the aqueous phase evaporated to a residue which was adsorbed onto *Dowex-50-W X8* ion-exchange resin (50g). The ion-exchange resin was primed by initially washing till neutral, then acidifying with dil. HCl and then the product eluted with 1.5M ammonia solution (250ml). Evaporation of the solvent under reduced pressure afforded the free amino acid, DL-alanine **(213)** as an amorphous white solid. (95mg, 66%). M.p. 293-294°C (dec.), lit. 295-296°C (dec). IR (KBr): 3400s (br), 3101s (br), 2750s, 2299s, 2165s, 1586s, 1397s, 1335m, 1123m. ^{1}H-NMR (D_2O): 5.40 (1H, q, J=7.3, H-C(2)), 1.31 (3H, d, J=7.3, H_3-C(3)). ^{13}C-NMR (D_2O): 178.3 (C-1), 54.0 (C-2), 19.9 (C-3). MS: (CI); 90 (M^++1, 13.3%).

5.19 Preparation of DL-[3,3,3-$^2H_3$]-alanine (146)

A mixture of 1-benzoyl-2-tert-butyl-3-[5-$^2H_3$-methyl]-imidazolidin-4-one **(144)** (427mg, 1.54mmol) and 6N HCl (15ml) was heated in a sealed tube at 100°C for 24h. The cooled solution was extracted with Et_2O (3x20ml) and the aqueous phase evaporated to a residue which was adsorbed onto *Dowex-50-W X8* ion-exchange resin. The ion-exchange resin was primed by initially washing till neutral, then acidifying with dil. HCl and then the product was eluted with 1.5M ammonia solution (250ml). Evaporation of the solvent under reduced pressure afforded the free amino acid, [3,3,3-$^2H_3$]-alanine (303mg, 71%). M.p. 289-291°C (dec). IR (KBr): 3400s (br), 3119s (br), 2719s, 2310s, 2133s, 1545s, 1407s, 1315m. ^{1}H-NMR (D_2O): 4.92 (1H, s, H-C(2)). ^{13}C-NMR (D_2O): 178.3 (C-1), 53.5 (C-2), 17.9 (3D, septet, $J^{13}C\text{-}^2H$=17.0, D_3-C(3)). MS: (CI); 90 (M^+-1D, 23.9%). CHN found C 39.02% H 10.72% N 15.34% requires $C_3H_4NO_2{}^2H_3$ C 39.13% H 10.87% N 15.41%.

5.20 Preparation of [3-^2H_x]-fluoropyruvate (177,178)

A solution of the sodium salt of 3-fluoropyruvic acid **(176)** (1.0g, 7.8mmol) in D_2O (10ml) was acidified with a few drops of D_2SO_4. and heated in a Carius tube at 120°C for 2h 15min. The cooled reaction mixture was continuously extracted into ethyl acetate for 24h. The organic layer was collected, dried ($MgSO_4$) and the solvent removed under reduced pressure to afford a mixture of the mono-deutero and di-deutero forms of fluoropyruvic acid (1:2 respectively). The free acid was dissolved in water (5ml), neutralised with 1N NaOH and freeze dried to yield the corresponding sodium salt

(500mg, 50%) as a white amorphous solid. M.p. 287-293°C (dec). IR (KBr): 3427m (br), 3022s (br), 3022s (br), 2743m, 2656m, 2274m, 1615s, 1392s, 1140s. ^{1}H-NMR (D_2O): 4.15 (1H, d, J=46.3, H_2-C(3)). ^{13}C-NMR (D_2O): 215.7 (m, C-2), 163.5 (C-1), 115.2 (m, C-3). ^{19}F-NMR (D_2O): -230.75 (t, J=46.3, F-CHD), -231.31 (p, J=6.3, F-CD_2). MS: (CI); 126 ($M(NH_4)^+$, 3.73%), 88 (21.0%), 74 (9.1%), 52 (15.0%), 44 (8.3%).

5.21 Preparation of [3-$^{2}H_x$]-3-fluorolactate (179,180)

A solution of the mono-deutero and di-deutero (1:2 respectively) forms of 3-fluoropyruvic acid **(177,178)** (450mg, 4.2mmol) in methanol (30ml) was treated with sodium borohydride (I equiv.) and the reaction was left to stir at room temperature for 1h, when the volatiles were removed under reduced pressure. Water (20ml) was added to the residue and the aqueous layer extracted into ethyl acetate (3x25ml). The solvent was removed under reduced pressure to afford a residue which was further treated with water (5ml), neutralised with 1N NaOH and freeze dried to yield sodium [3-$^{2}H_x$]-3-fluorolactate as a white amorphous solid (390mg, 39%). M.p. 278-287°C (dec). IR (KBr): 3141m (br), 2929s (br), 2741s (br), 2645s (br), 1617s, 1317s. ^{1}H-NMR (D_2O): 4.43 (1H, d, J=25, H-C(2)). ^{13}C-NMR (D_2O): 161.1 (C-1), 110.5 (m, C-3, D_2CF), 64.8 (m, C-2). ^{19}F-NMR (D_2O): -228.3 (dt, J= 46.3, 31.5, H_2C-F), -229.41 (m, HDC-F), -229.99 (m, D_2C-F). MS: (CI); 127 ($M(NH_4)^+$, 0.5%), 83 (42.1%), 69 (50.0%), 57 (92.1%), 44 (100%).

5.22 Preparation of [3-$^{2}H_{x}$]-3-fluoro-propan-1,2-diol (181)

A solution of [3-$^{2}H_{x}$]-fluoropyruvic acid **(177,178)** (0.50g, 6.9mmol) in ether (15ml) was added dropwise to an ethereal solution of lithium aluminium hydride (0.79g, 21mmol) at a rate to maintain reflux. The reaction mixture was heated under reflux for a further 3h and then the contents allowed to cool. Quenching by dropwise addition of ethyl acetate (excess) and then addition of 10-15ml EtOH/ H_2O (50:50) generated a white residue. This residue was filtered and the volatiles were evaporated under reduced pressure to afford the title compound as a viscous oil (100mg, 20%). IR (KBr): 3110s (br), 2970s (br), 2721s (br), 1120m. ^{1}H-NMR (D_2O): 3.72 (1H, m, HC-2), 3.55-3.25 (2H, m, H_2-C-OH). ^{13}C-NMR (D_2O): 86.5 (m, C-3, F(D_2)-C), 64.8 (C-2), 58.3 (C-1). ^{19}F-NMR (D_2O): -233.41 (m, D-CH-F), -234.04 (m, D_2C-F). GC-MS: (CI); 96 (M^+ + 2D, 100%), 95 (M^++ D, 31.6%), 94 (M^+, 3.6%), 76 (1.5%), 61 (14.3%), 60 (10.4%).

5.23 Preparation of fluoroacetyl chloride (214)[169]

*** *Fluoroacetyl chloride is toxic and must be handled with great caution.*

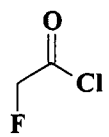

(214)

Sodium fluoroacetate (1.67g, 16.7mmol) and phthaloyl chloride (3.75g, 16.8mmol) were thoroughly mixed and gently heated to reflux. All the distillate of b.p. up to 90°C was collected and redistilled to yield fluoroacetyl chloride (1.38g, 95%) B.p. 70-71°C. IR ($CHCl_3$): 1830s. ^{1}H-NMR ($CDCl_3$): 5.1 (d, J=46.5). ^{13}C-NMR ($CDCl_3$): 169.4 (d, J=22.6, C-1), 82.6 (d, J=185.2, C-2). ^{19}F-NMR ($CDCl_3$): -210.32 (t, J=47.5).

5.24 Preparation of 5-(*2S,5S*)-(2'-fluoroacet-1'-one)-2-(tert-butyl)-3-methylimidazolidin-4-one (193)

A solution of **(144)** (1.3g, 5mmol) in THF (25ml) was slowly added (*via cannula*) to a solution of diisopropylamine (0.70ml, 5mmol) and 1.6M butyllithium (3.87ml, 5mmol) at -78°C and left to stir at -78°C for 15min. The reaction mixture immediately went red. The temperature was lowered to -100°C for 30min and then fluoroacetyl chloride (1.4ml, 25mmol) was syringed slowly into the mixture. After 5min the reaction was quenched sequentially with sat. NH_4Cl (25ml) and Et_2O (25ml). After warming to room temperature, the aqueous layer was extracted into Et_2O (3x25ml) and the combined organic extracts were washed with water (20ml), dried ($MgSO_4$) and evaporated to give the product as a white solid **(193)** (910mg, 57%). M.p. 197°C dec. $[\alpha]_D^{25}$ = +140° (c=1, $CHCl_3$). IR ($CHCl_3$): 3360m, 2960s, 1715s, 1695s, 1665m, 1415m, 1325m, 1119m, 1048s. ^{1}H-NMR ($CDCl_3$): 8.10-7.60 (5H, m, arom), 5.50 (2H, m, H_2C-F), 4.21 (1H, d, J=2.0, H-C(2)), 3.73 (1H, m, H-C(5)), 3.00 (3H, s, N-Me), 1.15 (9H, s, t-Bu). ^{13}C-NMR ($CDCl_3$): 197.7 (C-1', J=18.6), 170.6 (C-OPh), 165.0 (C-4), 135.8 (arom), 131.6 (arom), 128.8 (arom), 127.6 (arom), 83.8 (C-2', d, J=187), 80.4 (C-2), 66.2 (C-5), 40.3 (-$\underline{C}(Me)_3$), 32.2 (N-Me), 26.1 ($(Me)_3$), 19.3 (C-1'). ^{19}F-NMR ($CDCl_3$): -230.75 (t, J=46.7, CH_2-F). MS: (EI); 321 (M^++1, 22%), 320 (M^+, 100%), 302 (17%), 300 (14%), 180 (19%), 175 (12%), 121 (19%), 104 (39%), 100 (75%). CHN found C 63.52% H 6.63% N 8.63% $C_{17}H_{21}N_2O_3F$ requires C 63.68% H 6.55% N 8.74%.

5.25 Preparation of 5-(*2S,5S,1'R*)-(1'-benzoyloxy-2'-fluoroethyl)-2-(tert-butyl)-3-methylimidazolidin-4-one (197)

Sodium borohydride (50mg, 1.2mmol) was added to a solution of **(193)** (400mg, 1.2mmol) in methanol (60ml) and the reaction was left to stir at room temperature for 5min and was then neutralised with 1N HCl. The volatiles were removed under reduced pressure and the residue was suspended in H_2O (20-30ml) and extracted into Et_2O (3x25ml). Removal of the solvent left a yellow gum which was purified by flash chromatography to afford the product as a yellow oil (315mg, 67%). $[\alpha]_D^{20} = -13°$ (c=1, $CHCl_3$). IR ($CDCl_3$): 3360m (br), 2958s, 1675s, 1645m, 1398m, 1310m, 1095m. ^{1}H-NMR ($CDCl_3$): 8.10-7.60 (5H, m, arom), 5.62 (1H, m, H-C-OBz), 4.91 (2H, d m, H_2C-F), 4.31 (1H, d, J=2.1, H-C(2)), 4.15 (1H, m, H-C(5)), 3.02 (3H, s, N-Me), 1.15 (9H, s, (t-Bu)). ^{13}C-NMR ($CDCl_3$): 172.5 (C-OPh), 165.4 (C-4), 133.2 (arom), 129.6 (arom), 129.4 (arom), 128.3 (arom), 83.7 (C-2), 81.8 (C-2', d, J=172.4), 72.1 (C-1', d, J=19.4), 58.2(C-5), 37.2 (-C(Me)$_3$), 31.1 (N-Me), 25.3 ((Me)$_3$). ^{19}F-NMR ($CDCl_3$): -233.11, (dt, J=25, 47.4, F-CH_2). MS: Found (M^++H) 323.17628 $C_{17}H_{23}N_2O_3F$ (M^++H) requires 323.17709

5.26 Preparation of 4-*(2S,3S)*-fluorothreonine (202)

A solution of **(197)** (330mg, 1.02mmol) in 10N HCl (15ml) was heated under reflux for 72h. The cooled solution was extracted into Et_2O (3x10ml) and the aqueous phase evaporated to leave a residue which was adsorbed onto *Dowex-50-W X8* ion exchange resin. The resin was primed by initially washing with water till neutrality followed by

acidification with dil. HCl. The product was eluted with 1.5M ammonia solution (250ml) which was evaporated under reduced pressure to afford (*2S,3S*) 4-fluorothreonine. Recrystallisation of the crude material from ethanol : water /9:1 generated pure **(202)** (0.090g, 64%). Mp 182-183°C, lit. 181-182°C. $[\alpha]_D^{25}$ = -20° (c=5, H_2O), lit. $[\alpha]_D^{25}$ = -20° (c=0.060, H_2O). IR (KBr) 3500s, 3000s, 2800s, 1435m, 1130m. ^{1}H-NMR (D_2O): 4.52 (2H, ddd, J=46.5, 10.5, 3.9, H-C(4)), 4.22 (1H, dq, J=25, 4.6, H-C(3)), 3.72 (1H, d, J=4.8,H-C(2)). ^{13}C-NMR (D_2O): 175.5 (C-1), 87.8 (d, J=167.5, C-4), 70.8 (d, J=19.1, C-3), 59.2 (C-2). ^{19}F-NMR (D_2O): -229.73, (dt, J=47, 25). MS: 138 (M^+ +1, 100%), 118 (2%), 104 (5%), 92 (42%), 75 (67%), 59 (28%), 54 (11%), 46 (19%), 31 (11%). MS: Found ($M(H)^+$) 138.05664 $C_4H_8NO_3F$ requires 138.05682.

5.27 Preparation of 5-(*2S,5S*,1'R)-([1'-^{2}H]-1'-benzoyloxy-2'-fluoroethyl)-2-(tert-butyl)-3-methylimidazolidin-4-one (203)

Sodium borohydride was added to a stirred solution of **(193)** (400mg, 1.2mmol) in methanol (30ml) and the reaction left to stir at room temperature (5min) and then quenched to neutral pH with 1N HCl. The volatiles were removed under reduced pressure, H_2O (20-30ml) was added to the residue and the aqueous layer extracted into ethylacetate (3x25ml). The combined organic extracts were dried ($MgSO_4$) and evaporated to give the product as an oil (300mg, 77%). $[\alpha]_D^{25}$ =-17° (c=1, $CDCl_3$). IR ($CDCl_3$): 33691m (br), 2910s, 1677s, 1685m, 1265m, 1210m, 1015m. ^{1}H-NMR ($CDCl_3$): 8.11-7.58 (5H, m, arom), 5.5 (2H, m, H_2-CF), 4.25 (1H, d, J=2.0, H-C(2)), 4.19 (1H, d, J=2.0, H-C(5)), 2.97 (3H, s, N-Me), 1.10 (9H, s, (t-Bu)). ^{13}C-NMR

($CDCl_3$): 171.8 (C-OPh), 163.5 (C-4), 132.2 (arom), 129.8 (arom), 128.6 (arom), 128.1 (arom), 81.9 (C-2), 78.9 (C-2', d, J=175.0), 67.1 (C-1', m), 60.1 (C-5), 38.9 (-$\underline{C}(Me)_3$), 32.8 (N-Me), 26.3 ($(Me)_3$). ^{19}F-NMR ($CDCl_3$): -233.2 (t, J=46.8, F-CH_2). MS: (CI); 324 ($M(H)^+$, 6.78%), 263 (27.3%), 181 (3.7%), 143 (6.4%), 105 (3.3%), 86 (1.7%). CHN found C 63.22% H 7.69% N 8.65% $C_{17}H_{22}N_2O_3F^2H$ requires C 63.16% H 7.53% N 8.67%.

5.28 Preparation of [3-^{2}H]-4-(*2S,3S*)-fluorothreonine (204)

A solution of **(203)** (300mg, 0.9mmol) in 10N HCl (15ml) was heated under reflux for 72h. The resulting cooled solution was extracted into Et_2O (3x10ml) and the aqueous phase evaporated to leave a residue which was adsorbed onto *Dowex-50-W X8* ion exchange resin. The product was eluted with 1.5M ammonia solution (250ml). Evaporation of the solvent under reduced pressure afforded [3-^{2}H]-4-fluorothreonine which was recrystallised from methanol (0.050g, 67%). Mp 179-181°C. $[\alpha]_D^{25}$ = -14° (c=2, H_2O). IR (KBr) 3469s, 3100s, 2791s, 1423m, 1030m. ^{1}H-NMR (D_2O): 4.44 (2H, m, H_2C-F), 3.68 (1H, s, HC-2). ^{13}C-NMR (D_2O): 168.8 (C-1), 89.2 (d, J=177.3.2, C-4), 74.3 (m, C-3), 57.0 (C-2). ^{19}F-NMR (D_2O): -229.62 (t, J=46.3, F-CH_2). MS: (EI); 136 (M^+-D, 1.3%), 118 (2.2%), 104 (5.2%), 93 (19.1%), 75 (91.1%), 46 (5.2%), 31 (6.1%). CHN found C 34.61% H 6.39% N 10.12% $C_4H_7NO_3F^2H$ requires C 34.78% H 6.52% N 10.14%.

5.29 Preparation of DL-5-(1'-benzoyloxy-2'-chloroethyl)-2-(tert-butyl)-3-methylimidazolidin-4-one (210)

A solution of **(144)** (1.3g, 5mmol) in THF (20ml) was slowly added (*via cannula*) to a solution of diisopropylamine (0.70ml, 5mmol) and 1.6M butyllithium (3.87ml, 5mmol) in THF (25ml) at -78°C and left to stir at -78°C for 15min. The temperature was lowered to -100°C for 30min and chloroacetyl chloride (1.4ml, 25mmol) was syringed into the mixture. After 5min the reaction was quenched with sat. NH_4Cl (25ml) and ether (25ml) added. The aqueous layer was extracted into Et_2O (3x25ml) and the combined organic extracts were washed with water (20ml), dried ($MgSO_4$) and evaporated to give a yellow oil which was not characterised but was dissolved directly in methanol (60ml) and treated with sodium borohydride (50mg, 1.2mmol). The reaction was left to stir at room temperature for 5min and then quenched to neutral pH by addition of 1N HCl. The volatiles were removed under reduced pressure and the residue was suspended in H_2O (20-30ml) and extracted into Et_2O (3x25ml). Removal of the solvent left a yellow gum which was purified by flash chromatography (ethyl acetate/ petrol, 3:2) to afford the product as a yellow oil (0.2g, 11.8%). IR (KBr): 3340m (br), 2962s, 1683s, 1661m, 1410m, 1110m. ^{1}H-NMR ($CDCl_3$): 7.43-8.04 (5H, m, Ar), 5.51 (1H, m, H-COBz), 4.29 (1H, m, H-C(5)), 4.20 (1H, d, J=2.0, H-C(2)), 3.98 (2H, d, J=6.4, H_2C-Cl), 2.92 (3H, s, N-Me), 1.02 (9H, s, t-Bu). ^{13}C-NMR ($CDCl_3$): 171.3 (C-OPh), 163.4 (C-4), 134.1 (arom), 129.9 (arom), 129.2 (arom), 128.7 (arom), 84.9 (C-2), 72.9 (C-2'), 68.8 (C-1'), 58.1 (C-5), 39.5 (-C(Me)$_3$), 33.5 (N-Me), 23.9 ((Me)$_3$). MS: (EI); 340 (M^++2, 2.3%), 339 (M^++1, 14.8%), 281 (18.9%), 161 (30.6%), 159 (95.7%), 105 (100%), 77 (36.4%), 42 (30.4%). CHN found C 60.39 % H 6.63% N 8.24% $C_{17}H_{23}N_2O_3Cl$ requires C 60.26% H 6.79% N 8.27% .

Experimental

(Part II)

5.30 Biological methods

5.30.1 General preparation of suspension cultures of *S. cattleya*

S. cattleya NRRL 8057 was supplied by Queen's University of Belfast and initiated onto agar slants. Suspension cutltures of *S. cattleya* were grown using defined or complex media of nutrients. However in most cases, the defined medium was used. Cells of *S. cattleya* were grown in the defined medium (90ml) dispensed into 250ml Erlenmeyer flasks stoppered with cotton wool and incubated on an orbital shaker (200rpm) at 28°C. Production cultures were initiated by inoculation (2ml) from the first generation culture stock. After 14 days a production medium was subcultured. Approximately 4-5 generations were grown before returning to the 'authentic' frozen stock. In order to achieve asepsis, all relevant apparatus was sterilised using a portable gas heated autoclave maintaining a temperature of 120°C for 20min at 15psi. The rims of bottles and other vessels for dispensing materials were rendered sterile by flaming. All experiments were handled in a laminer flow hood, prewashed with 70% ethanol. Presterilised disposable instruments were used as often as required.

5.30.1.1 Defined culture medium composition [107]

Suspension cultures grown on defined medium consisted of (g/ 500ml of H_2O) ; glycerol (5), mono sodium L-glutamate monohydrate (2.5), KH_2PO_4 (1), NH_4Cl (0.75), $MgSO_4.7H_2O$ (0.25), NaCl (0.25), inositol (0.2), NaF (0.042), $FeSO_47H_2O$ (0.012),

$ZnSO_4.7H_2O$ (0.005), $CoCl_2.6H_2O$ (0.005), $CaCO_3$ (0.125) and *p*-aminobenzoic acid (1 x 10^{-5}). The pH of the resulting solution was adjusted to pH 7.0 with 1N NaOH.

5.30.1.2 Complex culture medium composition [24]

Suspension cultures of *S. cattleya* grown on the complex medium consisted of (g/ 500ml of H_2O) ; D-(+)-glucose (5), Yeast extract (1), $NaNO_3$ (1), $MgSO_4.7H_2O$ (0.25), KCl (0.25), $CaCO_3$ (anhyd) (0.25), NaF (0.05), $FeSO_47H_2O$ (0.005). The pH of the resulting solution was adjusted to pH 7.0 with 1N NaOH.

5.31 Preparation of various culture media used to investigate the production of fluorinated metabolites by *Streptomyces sp OH 5093*

Solid agar plates were initially inoculated with *Streptomyces sp. OH 5093* obtained from Prof. S. Omura at the Kitasato Institute in Japan. The agar medium was composed of (g/ 500ml of H_2O) ; Yeast extract (2), malt extract (5), glucose (2), agar (7.5). The pH of the resulting solution was adjusted to pH 7.0 with 1N NaOH. The liquid agar medium (4 Erlenmeyer flasks x 90ml) was subsequently sterilised in an autoclave at 100°C for 20min at 15psi. The agar solutions were allowed to cool to 30-35°C and then poured onto petri-dishes to set. Growth of *Streptomyces sp. OH 5093* was clearly visible after 7days incubation at 28°C.

Production cultures were initiated by loop transfer of spores to five different types of culture media, two of which are detailed in section 5.28. The remaining three media were denoted as complex (II), complex (III) and Omura (I). The composition of ;

(a) *complex (II)* culture medium (g/ 500ml of H_2O) is ; yeast extract (2), malt extract (5) and glucose (2). The pH of the resulting solution was adjusted to pH 7.0.

(b) *complex (III)* culture medium (g/ 500ml of H_2O) is ; glucose (4.5), soybean flour (13.5), $CaCO_3$ (2.7), $FeSO_4.7H_2O$ (4.94) and MgCl (0.027). The pH of the resulting solution was adjusted to pH 7.0 with 1N NaOH.

(c) *Omura (I)* culture medium (500ml of H_2O) is ; glucose (0.1%), starch (2.4%), peptone (0.3%), yeast extract (0.5%) and $CaCO_3$ (0.4%). The pH of the resulting solution was adjusted to pH 7.0 with 1N NaOH.

Each of the five types of culture media was incubated with *Streptomyces sp. OH 5093* spores in an orbital shaker (200rpm) at 28°C for 28days. Aliquots (1ml) of supernatant were extracted, at intervals of 3days, from each of the five types of media and filtered through hyflo supercell, and subsequently concentrated and redissolved in ^2H_2O (0.5ml) for ^{19}F-NMR (200MHz) analysis.

5.32 Preparation of resting cells of *S. cattleya*

Six day old batch culture cells of *S. cattleya* grown on the defined medium were harvested by centrifugation (Beckman J2-21M/ E Centrifuge at 14000 rpm for 15min), washed with 50mM MES pH 6.5 buffer (3x30ml) and resuspended in this buffer at a concentration of 0.15g wet weight ml^{-1}. The resting cells were used directly for incubation experiments.

5.33 General procedure for feeding experiments (conducted in Belfast) with ^{13}C/ ^{2}H labelled precursors

The precursor (200mM, 1ml) was added to a mixture of resting cells (0.75g wet weight) of *S. cattleya* already suspended in 50mM MES buffer (pH 6.5, 20.25ml) and 40mM fluoride (1ml) contained in a 100ml conical flask, plugged with a cotton wool stopper. This gave a final concentration of precursor at 10mM. The conical flasks were subsequently incubated at 29°C with shaking at 180 rpm for 24 and 48 hours. Two flasks of each treatment (24h and 48h) were removed, centrifuged and the supernatants stored at 4°C pending analysis.

5.34 Analysis of feeding experiments conducted with resting cells of *S. cattleya*

5.34.1 ^{19}F-NMR spectroscopy

Fluoroacetate and 4-fluorothreonine in the culture supernatant were determined by ^{19}F-NMR and $^{19}F\{^{1}H\}$-NMR at 471MHz. The freeze dried supernatant, from a feeding experiment, was dissolved in $^{2}H_2O$ (1ml) and the resulting solution was filtered through glass wool to remove any particulate matter. Spectra were obtained with an acquisition time of ~8-10 hours at ambient temperature. Chemical shifts were measured relative to the fluoride signal (-119ppm) present in all NMR samples. It must be noted that under the decoupling conditions, the protons are irradiated with a separate radiofrequency that causes indirect enhancement of the fluorine signals. The area under the fluorine peaks is

no longer an accurate representation of the proportion of the labelled and unlabelled fluorinated metabolites, thus generally ^{19}F-NMR spectra are not integrated.

5.34.1.1 ^{19}F{^{1}H}-NMR data of supernatant from feeding experiments with :

[2-^{2}H]-glycolate

^{19}F-NMR (D_2O): -119 (s, fluoride); -216.8 (t, J=46.7, fluoroacetate); -217.4 (dt, J=47.7, β-shift = 0.058ppm); -229.54 (dt, J=46.8, 24.8, 4-fluorothreonine)

^{19}F{^{1}H}-NMR ($^{2}H_2O$): -119.0 (s, fluoride); -218.2 (s, fluoroacetate); -218.8 (s*, ^{19}F-^{12}C-^{2}H, β-shift = 0.60ppm); -232.4 (s, 4-fluorothreonine); -233.0 (s*, ^{19}F-^{12}C-^{2}H, β-shift = 0.60ppm).

(Expect a broad triplet but the signal is not resolved sufficiently)*

[2,2-$^{2}H_2$]-glycolate (*refer to Fig. 3.5*)

^{19}F{^{1}H}-NMR ($^{2}H_2O$): -119.0 (s, fluoride); -218.8 (s, fluoroacetate); -219.4 (s*, ^{19}F-^{12}C-^{2}H, β-shift = 0.60ppm); -233.2 (s, 4-fluorothreonine); -233.7 (s*, ^{19}F-^{12}C-^{2}H, β-shift = 0.50ppm).

(Expect a broad triplet but the signal is not resolved sufficiently)*

[2-^{13}C]-glycolate (*refer to Fig. 3.6*)

^{19}F{^{1}H}-NMR ($^{2}H_2O$): -119.0 (s, fluoride); -213.45 (s, unidentified); -214.69 (s, fluoroacetate); -214.78 (d, J=178.9, ^{19}F-^{13}C-^{12}C, α-shift = 0.09ppm); -214.79 (dd, J=178.9, 17.4, ^{19}F-^{13}C-^{13}C, α+β-shift = 0.11ppm); -229.24 (s, 4-fluorothreonine); -229.26 (d, J=18, ^{19}F-^{12}C-^{13}C, β-shift = 0.02ppm); -229.32 (d, J=170.0, ^{19}F-^{13}C-^{12}C, α-shift = 0.080ppm); -229.34 (dd, J=167.9, 19.5, ^{19}F-^{13}C-^{13}C, α + β-shift = 0.10ppm).

[1-^{13}C]-glycine (*refer to Fig. 3.7*)

$^{19}F\{^{1}H\}$-NMR ($^{2}H_2O$): -119.0 (s, fluoride); -215.68 (s, fluoroacetate); -223.24 (s, 4-fluorothreonine).

[1,2-$^{13}C_2$]-glycine (*refer to Fig. 3.8*)

$^{19}F\{^{1}H\}$-NMR ($^{2}H_2O$): -119.0 (s, fluoride); -214.96 (s, fluoroacetate); -214.98 (d, J=18, ^{19}F-^{12}C-^{13}C, β-shift = 0.02ppm); -215.05 (d, J=177.6, ^{19}F-^{13}C-^{12}C, α-shift = 0.085ppm); -215.07 (dd, J=178, 17.4, ^{19}F-^{13}C-^{13}C, α + β-shift = 0.10ppm); -229.51 (s, 4-fluorothreonine); -229.53 (d, J=18, ^{19}F-^{12}C-^{13}C, β-shift = 0.02ppm); -229.59 (d, J=169.6, ^{19}F-^{13}C-^{12}C, α-shift = 0.083ppm); -229.61 (dd, J=167.9, 17.9, ^{19}F-^{13}C-^{13}C, α + β-shift = 0.10ppm).

[2-^{13}C]-glycine (*refer to Fig. 3.9*)

$^{19}F\{^{1}H\}$-NMR ($^{2}H_2O$): -119.0 (s, fluoride); -215.71 (s, fluoroacetate); -215.73 (d, J=18, ^{19}F-^{12}C-^{13}C, β-shift = 0.02ppm); -215.80 (d, J=179, ^{19}F-^{13}C-^{12}C, α-shift = 0.086ppm); -215.82 (dd, J=179, 17.6, ^{19}F-^{13}C-^{13}C, α + β-shift = 0.10ppm); -230.23 (s, 4-fluorothreonine); -230.25 (d, J=18, ^{19}F-^{12}C-^{13}C, β-shift = 0.02ppm); -230.31 (d, J=166.3, ^{19}F-^{13}C-^{12}C, α-shift = 0.083ppm); -230.41 (dd, J=166.3, 18.4, ^{19}F-^{13}C-^{13}C, α + β-shift = 0.10ppm).

[1,2-$^{2}H_5$]-glycine

$^{19}F\{^{1}H\}$-NMR ($^{2}H_2O$): -119.0 (s, fluoride); -215.0 (s, fluoroacetate); -215.80 (t, J=6.6, ^{19}F-^{12}C-^{2}H, β-shift = 0,058ppm); -216.16 (p, ^{19}F-^{12}C-$(^{2}H)_2$, 2 x β-shift = 1.16ppm); -229.53 (s, 4-fluorothreonine); -230.11 (t, β-shift = 0.58ppm).

[3-^{13}C]-Serine (*refer to Fig. 3.14*)

$^{19}F\{^{1}H\}$-NMR ($^{2}H_2O$): -119.0 (s, fluoride); -215.61 (s, fluoroacetate); -215.70 (d, J=177.6, ^{19}F-^{13}C-^{12}C, α-shift = 0.089ppm); -230,16 (s, 4-fluorothreonine); -230.25 (d, J=167.2, ^{19}F-^{13}C-^{12}C, α-shift = 0.083ppm).

[1-^{13}C]-pyruvate (*refer to Fig. 3.15*)

$^{19}F\{^{1}H\}$-NMR ($^{2}H_2O$): -119.0 (s, fluoride); -215.63 (s, fluoroacetate); -230.10 (s, 4-fluorothreonine)

[2-^{13}C]-pyruvate (*refer to Fig. 3.16*)

$^{19}F\{^{1}H\}$-NMR ($^{2}H_2O$): -119.0 (s, fluoride); -215.67 (s, fluoroacetate); -215.69 (d, J=18.8, ^{19}F-^{12}C-^{13}C, β-shift = 0.02ppm); -215.77 (d, J=178.9, ^{19}F-^{13}C-^{12}C, α-shift = 0.080ppm), -230.12 (s, 4-fluorothreonine); -230.14 (d, J=18.3, ^{19}F-^{12}C-^{13}C, β-shift = 0.02ppm); -230.20 (d, J=179, ^{19}F-^{13}C-^{12}C, α-shift = 0.080ppm)

[3-^{13}C]-pyruvate (*refer to Fig. 3.17*)

$^{19}F\{^{1}H\}$-NMR ($^{2}H_2O$): -119.0 (s, fluoride); -214.85 (s, fluoroacetate); -214.93 (d, J=178.0, ^{19}F-^{13}C-^{12}C, α-shift = 0.09ppm), -229.26 (s, 4-fluorothreonine); -229.34 (d, J=168.1, ^{19}F-^{13}C-^{12}C, α-shift = 0.082ppm

[3-^{13}C]-alanine (*refer to Fig. 3.19*)

$^{19}F\{^{1}H\}$-NMR ($^{2}H_2O$): -119.0 (s, fluoride); -215.50 (s, fluoroacetate); -215.52 (d, J=18,, ^{19}F-^{12}C-^{13}C, β-shift = 0.02ppm); -215.59 (d, J=177.6, ^{19}F-^{13}C-^{12}C, α-shift = 0.09ppm); -215.60 (dd, J=178, 14.6, ^{19}F-^{13}C-^{13}C, α + β-shift = 0.11ppm), -229.94 (s, 4-fluorothreonine); -229.96 (d, J=18, ^{19}F-^{12}C-^{13}C, β-shift = 0.02ppm); -230.02 (d, J=168.1, ^{19}F-^{13}C-^{12}C, α-shift = 0.084ppm)

3-^{13}C-3,3,3-$^{2}H_3$]-alanine (*refer to Fig. 3.20*)

^{19}F-NMR ($^{2}H_2O$): -119.0 (s, fluoride); -216.40 (t, J=47.2, fluoroacetate); -217.60 (dp, J=164.8, ^{19}F-^{13}C-($^{2}H)_2$, α + 2β-shift = 1.28ppm); -230.92 (dt, J=25.0, 47.4, 4-fluorothreonine); -232.20 (dp, J=167.0, ^{19}F-^{13}C-($^{2}H)_2$, α + 2β-shift = 1.28ppm)

^{19}F{^{1}H}-NMR ($^{2}H_2O$): -119.0 (s, fluoride); -215.24 (s. fluoroacetate); -215.33 (d, J=177.3, ^{19}F-^{13}C-^{12}C, α-shift = 0.088ppm); -215.90 (dt, J=173.5, ^{19}F-^{13}C-^{2}H, α + β-shift = 0.66ppm); -216.49 (dp, J=173.5, ^{19}F-^{13}C-($^{2}H)_2$, α + 2β-shift = 1.25ppm); -229.78 (s. 4-fluorothreonine); -229.87 (d, J=166.0, ^{19}F-^{13}C-^{12}C, α-shift = 0.08ppm); -230.44 (dt, J=171.7, ^{19}F-^{13}C-^{2}H, α + β-shift = 0.66ppm); -231.02 (dp, J=166.0, ^{19}F-^{13}C-($^{2}H)_2$, α + 2β-shift = 1.24ppm)

[2,2,3,3-$^{2}H_4$]-succinate (*refer to Fig. 3.21*)

^{19}F{^{1}H}-NMR ($^{2}H_2O$): -119.0 (s, fluoride); -214.71 (s, fluoroacetate); -215.28 (s* (br), ^{19}F-^{12}C-^{2}H, β-shift = 0.58ppm); -229.26 (s, 4-fluorothreonine); -229.84 (s* (br), ^{19}F-^{12}C-^{2}H, β-shift = 0.58ppm).

(Expect a broad triplet but the signal is not resolved sufficiently)*

[2-^{13}C]-acetate (*refer to Fig. 3.23*)

^{19}F{^{1}H}-NMR ($^{2}H_2O$): -119.0 (s, fluoride); -214.37 (s, fluoroacetate); -214.39 (d, J=18, ^{19}F-^{12}C-^{13}C, β-shift = 0.02ppm); -214.46 (d, J=177.6, ^{19}F-^{13}C-^{12}C, α-shift = 0.09ppm); -214.48 (dd, J=177.6, 17.4, ^{19}F-^{13}C-^{13}C, α + β-shift = 0.11ppm), -228.88 (s, 4-fluorothreonine); -228.90 (d, J=18, ^{19}F-^{12}C-^{13}C, β-shift = 0.02ppm); -228.96 (d, J=168.1, ^{19}F-^{13}C-^{12}C, α-shift = 0.082ppm); -228.98 (dd, J=167.0, 18.1, ^{19}F-^{13}C-^{13}C, α + β-shift = 0.10ppm).

[2,3,3-$^{2}H_3$]-aspartate (*refer to Fig. 3.22*)

$^{19}F\{^{1}H\}$-NMR ($^{2}H_2O$): -119.0 (s, fluoride); -214.59 (s, fluoroacetate); -215.17 (t, J=7.5, ^{19}F-^{12}C-^{2}H, β-shift = 0.58ppm); -215.76 (m, [2,2-$^{2}H_2$]-fluoroacetate, ^{19}F-^{12}C-($^{2}H)_2$, 2β-shift = 1.16ppm); -229.21 (s, 4-fluorothreonine); -229.79 (t, J=7.5, [4-^{2}H]-4-fluorothreonine, ^{19}F-^{12}C-^{2}H, β-shift = 0.58ppm); -230.36 (m, [4-^{2}H]-4-fluorothreonine, ^{19}F-^{12}C-($^{2}H)_2$, , 2β-shift = 1.14ppm).

[2-^{13}C]-glycerol (*refer to Fig. 3.25*)

$^{19}F\{^{1}H\}$-NMR ($^{2}H_2O$): -119.0 (s, fluoride); -215.96 (s, fluoroacetate); -215.98 (d, J=18, ^{19}F-^{12}C-^{13}C, β-shift = 0.02ppm); -216.00 (d, J=176.6, ^{19}F-^{13}C-^{12}C, α-shift = 0.060ppm); -216.03 (dd, J=170.0, 24.0, ^{19}F-^{13}C-^{13}C, α + β-shift = 0.070ppm); -230.66 (s, 4-fluorothreonine); -230.68 (d, J=18, ^{19}F-^{12}C-^{13}C, β-shift = 0.02ppm); -230.73 (d, J=165.8, ^{19}F-^{13}C-^{12}C, α-shift = 0.070ppm); -230.75 (dd, J=145.0, 20.7, ^{19}F-^{13}C-^{13}C, α + β-shift = 0.090ppm).

5.34.2 ^{14}C-Radiochemical experimental procedure

*** *Sodium fluoroacetate is toxic and must be handled with great caution.*

The precursor (20 μCi) was added to a mixture of resting cells (3g wet weight) of *S. cattleya* already suspended in 50mM MES buffer (pH 6.5, 20.25ml) and 40mM fluoride (1ml) contained in a 100ml conical flask, plugged with a cotton wool stopper. The conical flasks were subsequently incubated at 29°C with shaking at 180 rpm for 24 and 48 hours. Two flasks of each treatment (24h and 48h) were removed, centrifuged and the supernatants stored at 4°C pending analysis.

Sodium fluoroacetate (30mg) was added to the supernatant solution (2ml) from a radiochemical feeding experiment and subsequently freeze dried to a powder. 4-Phenylphenacyl bromide (100mg, 1.25equiv) and 18-crown-6 (18mg) were added to this powder and the mixture suspended in toluene/ acetonitrile (1:1, v/v, 20ml) and heated under reflux for 12h at 75°C. The cooled solution was filtered and the solvent removed by evaporation using a stream of nitrogen gas. The remaining solid was purified by preparative tlc using silica gel GF_{254} as the adsorbate with toluene as the eluant. The band containing the 4-phenylacetophenone derivative of fluoroacetate was identified under UV light and scraped off the glass plate, and extracted with DCM (10ml). After filtration and removal of the solvent, again using a stream of nitrogen gas, the derivative (Mp. 138°C) was recrystallised from petroleum/ diethylether. An accurately weighed sample of the recrystallised derivative was dissolved in 'Ecoscint' scintillation fluid (5ml) and the radioactivity recorded as counts in dpm were recorded on a Packard 200CA liquid scintillation counter

5.35 Preparation of 4-phenyphenacyl-fluoroacetate (87)

*** *Sodium fluoroacetate is toxic and must be handled with great caution.*

Sodium fluoroacetate (30mg) was added to a mixture of 4-phenylphenacyl bromide (86) (100mg, 1.25equiv) and 18-crown-6 (18mg) suspended in toluene/ acetonitrile (1:1, v/v, 20ml) and heated under reflux for 12h at 75°C. The cooled reaction mixture was filtered and the solvent was concentrated under reduced pressure to leave a yellow solution (1-2ml). To follow, this yellow solution (~1ml) was purified by preparative tlc using silica gel GF_{254} as the adsorbate and toluene as the eluant. The single band containing the derivative (87) was scraped off the glass plate and extracted with DCM (10ml). Filtration and removal of the solvent afforded 4-phenyphenacyl-fluoroacetate which was

recrystallised from petrol/ Et_2O (40-60°C). Mp. 138°C. IR (KBr): 3547br, 3407br, 1684s, 1620s, 1316m, 1097s, 804m, 600m. ^{1}H-NMR ($CDCl_3$): 8.00-7.45 (9H, m, arom), 5.51 (2H, s, H_2CO), 5.07 (2H, d, J=47.7, $C\underline{H}_2F$). ^{13}C-NMR ($CDCl_3$): 190.9 (CO), 167.5 (CO_2, d, J=18.2), 142.1 (C-CO, arom), 139.5 (C-4-(PhCO), 132.5 (C-1-(Ph-Ph-CO), 129.0 (arom), 128.5 (arom), 128.3 (arom), 127.6 (arom), 127.2 (arom), 75.9 (CO), 68.4 ($\underline{C}H_2F$, d, J=251.1). ^{19}F-NMR ($CDCl_3$): -231.10 (t, J=46.4). MS: (EI); 272 (M^+, 2.5%), 182 (11.9%), 180 (100%), 152 (27.7%), 84 (8%), 69 (5.8%), 57 (5.5%), 43 (3.5%). CHN found C 70.71% H 4.73% $C_{16}H_{13}O_3F$ requires C 70.59% H 4.78%.

5.36 Feeding experiment of calcium [2-^{2}H]-glycolate with suspensions cultures of *S. cattleya*

A solution of calcium [2-^{2}H]-glycolate (200mg, 1.29mM) in water (30ml) was administered to cultures (2 x 90ml) of *S. cattleya via* a micropore filter on the 6th, 8th and 10th days (5ml pulsed into each flask on each day). The cultures were harvested after 28 days, filtered through hyflo supercell and the volume reduced to 2ml. The dark solution was refiltered through glass wool and the resulting filtrate was analysed for incorporation into both fluoroacetate or 4-fluorothreonine by ^{19}F{^{1}H}-NMR.

5.37 Feeding experiment of sodium [2,2-$^2H_2$]-glycolate with suspensions cultures of *S. cattleya*

A solution of sodium [2,2-$^2H_2$]-glycolate (200mg, 1.29mM) in water (30ml) was administered to cultures (2 x 90ml) of *S. cattleya via* a sterile micropore filter on the 6th, 8th and 10th days (5ml pulsed into each flask on each day). The cultures were harvested after 28 days, filtered through hyflo supercell and the volume reduced to 2ml. The dark

solution was refiltered through glass wool and the resulting filtrate was analysed by high field $^{19}F\{^{1}H\}$-NMR (see Fig. 3.5, Chapter 3).

5.38 Feeding experiment [2-$^{2}H_2$]-glycine of with suspensions cultures of *S. cattleya*

[2-$^{2}H_2$]-Glycine (200mg, 1.29mM) was dissolved in water (15ml) and administered to a culture (90ml) of *S. cattleya via* a micropore filter on the 6th, 8th and 10th days (5ml pulsed into the flask on each day). The culture was harvested after 28 days, filtered through hyflo supercell and the volume reduced to 2ml. The dark solution was refiltered through glass wool and the resulting filtrate was analysed for incorporation into both fluoroacetate or 4-fluorothreonine by $^{19}F\{^{1}H\}$-NMR.

5.39 Suspension culture of *S. cattleya* in $^{2}H_2O$

A suspension culture (90ml) of *S. cattleya* was administered with $^{2}H_2O$ (9ml) *via* a sterile micropore filter. The experiment was conducted with both defined and complex media. For each experiment the $^{2}H_2O$ (3x3ml) was pulsed into the system starting on day 6 and then another pulse on day 8 and the final volume on day 10 and then the cultures were incubated in a shaker for 28 days. The culture broths were filtered through hyflo supercell and the volume reduced to 2ml and refiltered through glass wool. The supernatant was subsequently analysed by $^{19}F\{^{1}H\}$-NMR (see Fig. 3.1, Chapter 3).

5.40 Resting cell suspensions of *S. cattleya* in $^{2}H_2O$

Resting cells of *S. cattleya* (3g wet weight) suspended in 50 mM MES buffer (pH 6.5, 18ml) and sodium fluoride (2mM) were treated with $^{2}H_2O$ (2ml). Each flask was

plugged with cotton wool and subsequently incubated at 29°C with shaking at 120rpm for 48h. After 48h incubation, the resting cells were centrifuged and the supernatant collected and evaporated to dryness prior to analysis by $^{19}F\{^{1}H\}$-NMR.

5.41 Incubation of [2-$^{2}H_2$]-glycine with resting cells of *S. cattleya*

A solution of [2-$^{2}H_2$]-glycine (200mM, 1ml) was added to resting cells of *S. cattleya* (0.75g wet weight) suspended in 50 mM MES buffer (pH 6.5, 20.25) and 40mM sodium fluoride (1ml). The flask was stoppered with cotton wool and subsequently incubated at 29°C with shaking at 120rpm for 48h. After 48h incubation, the resting cells were centrifuged and the supernatant collected and evaporated to dryness prior to analysis by ^{19}F-NMR.

5.42 Incubation of [2,2,3,3-$^{2}H_4$]-succinate with resting cells of *S. cattleya*

A solution of [2,2,3,3-$^{2}H_4$]-succinate (200mM, 1ml) was added to resting cells of *S. cattleya* (0.75g wet weight) suspended in 50 mM MES buffer (pH 6.5, 20.25) and 40mM sodium fluoride (1ml). The flask was stoppered with cotton wool and subsequently incubated at 29°C with shaking at 120rpm for 48h. After 48h incubation, the resting cells were centrifuged and the supernatant collected and evaporated to dryness prior to $^{19}F\{^{1}H\}$-NMR analysis (see Fig. 3.21, Chapter 3).

APPENDIX A

Crystal Structures & Data

A.1 5-(*2S,3S*)-(2'-Fluoroacet-1'-one)-2-(tert-butyl)-3-methylimidazolidin-4-one **(186)**

A.2 4-(*2S,3S*)-Fluorothreonine **(202)**

A.3 Packing diagram of 4-(*2S,3S*)-fluorothreonine

A.4 5-(*2S,3S*)-(1'-Keto-2'-methyl)-2-(tert-butyl)-3-methylimidazolidin-4-one **(212)**

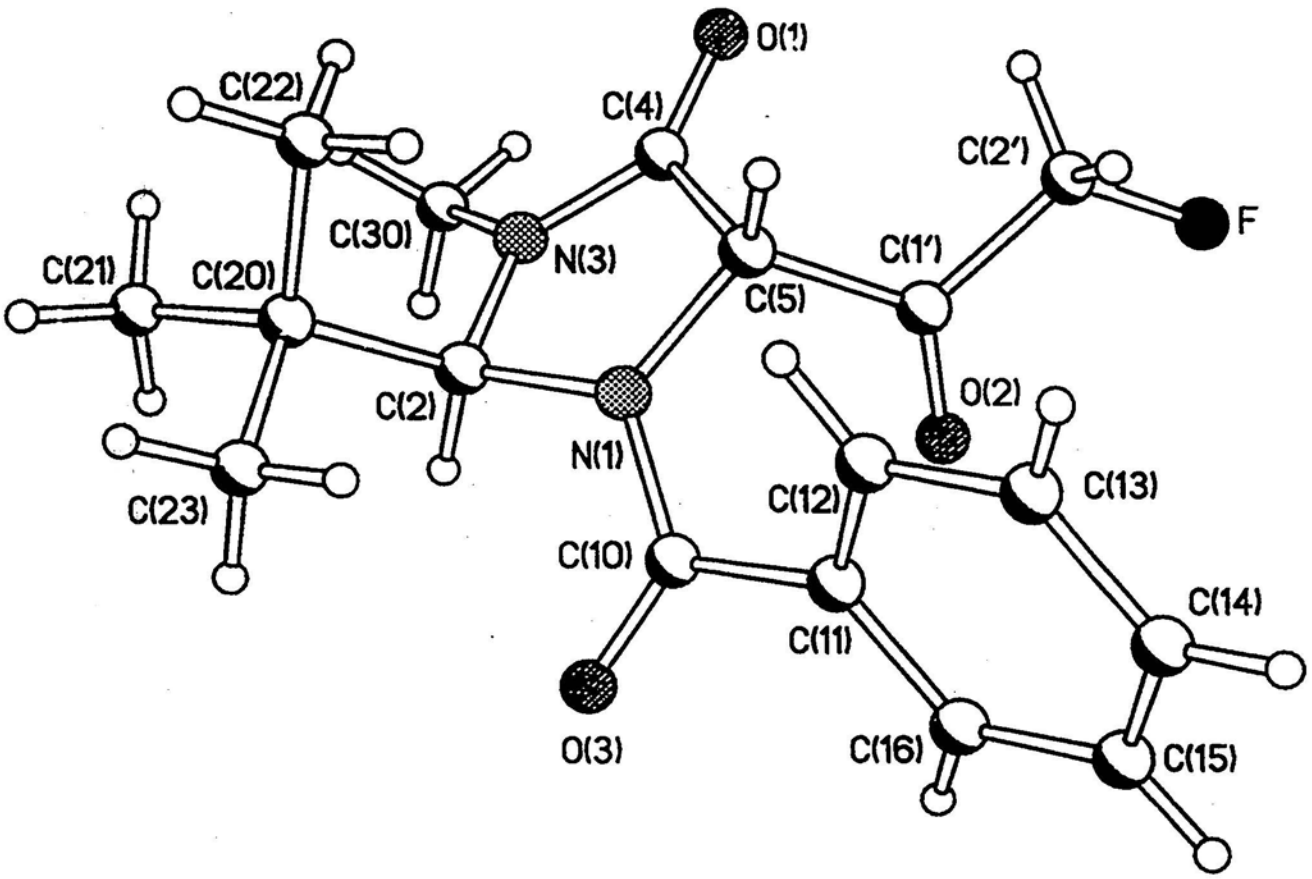

A.1 Crystal structure of 5-(2S,3S)-(2'-fluoroacet-1'-one)-2-(tert-butyl)-3-methylimidazolidin-4-one ***(186)***

A.1 Crystal data

Identification code	96srv186
Empirical formula	C17 H21 F N2 O3
Formula weight	320.36
Temperature	296(2) K
Wavelength	0.71073 A
Crystal system	Orthorhombic
Space group	P2(1)2(1)2
Unit cell dimensions	a = 13.294(1) A alpha = 90 deg. b = 21.437(2) A beta = 90 deg. c = 6.037(1) A gamma = 90 deg.
Volume	1720.5(3) A^3
Z	4
Density (calculated)	1.237 g/cm^3
Absorption coefficient	0.092 mm^-1
F(000)	680
Crystal size	0.4 x 0.2 x 0.15 mm
Theta range for data collection	1.80 to 27.48 deg.
Index ranges	-12<=h<=17, -27<=k<=27, -6<=l<=7
Reflections collected	12388
Independent reflections	3936 [R(int) = 0.0408]
Absorption correction	None
Refinement method	Full-matrix least-squares on F^2
Data / restraints / parameters	3916 / 0 / 225
Goodness-of-fit on F^2	1.141
Final R indices [I>2sigma(I)]	R1 = 0.0503, wR2 = 0.1130
R indices (all data)	R1 = 0.0782, wR2 = 0.1416
Absolute structure parameter	-1(2)
Largest diff. peak and hole	0.188 and -0.190 e.A^-3

Atomic coordinates (x 10 4) and equivalent isotropic displacement parameters (A^2 x 10^3) for 1. U(eq) is defined as one third of the trace of the orthogonalized Uij tensor.

	x	y	z	U(eq)
O(1)	7070(2)	7561(1)	9571(4)	77(1)
O(2)	8707(1)	6417(1)	6661(4)	69(1)
O(3)	6858(2)	5691(1)	3102(3)	73(1)
F	9681(1)	6600(1)	10448(4)	135(1)
N(1)	6608(1)	6232(1)	6290(3)	46(1)
C(2)	5999(2)	6711(1)	5158(4)	51(1)
N(3)	6320(2)	7277(1)	6288(3)	54(1)
C(4)	6809(2)	7176(1)	8199(4)	54(1)
C(5)	7067(2)	6476(1)	8303(4)	46(1)
C(1')	8214(2)	6452(1)	8321(5)	54(1)
C(2')	8666(2)	6499(2)	10588(6)	86(1)
C(10)	6983(2)	5734(1)	5111(4)	52(1)
C(11)	7495(2)	5226(1)	6390(4)	52(1)
C(12)	7120(2)	5020(1)	8411(4)	61(1)
C(13)	7569(3)	4521(1)	9498(6)	83(1)
C(14)	8395(3)	4241(1)	8609(7)	93(1)
C(15)	8786(3)	4443(1)	6639(7)	88(1)
C(16)	8325(2)	4934(1)	5483(5)	70(1)
C(20)	4855(2)	6577(1)	5352(5)	66(1)
C(21)	4262(3)	7070(2)	4017(8)	106(1)
C(22)	4529(3)	6598(2)	7768(6)	93(1)
C(23)	4622(3)	5934(2)	4375(6)	90(1)
C(30)	6170(3)	7907(1)	5400(6)	76(1)

Anisotropic displacement parameters (A^2 x 10^3) for 1. The anisotropic displacement factor exponent takes the form: -2 pi^2 [h^2 a*^2 U11 + ... + 2 h k a* b* U12]

	U11	U22	U33	U23	U13	U12
O(1)	91(1)	56(1)	84(1)	-28(1)	-7(1)	6(1)
O(2)	62(1)	64(1)	81(1)	-7(1)	19(1)	-7(1)
O(3)	113(2)	62(1)	44(1)	-7(1)	-3(1)	18(1)
F	57(1)	200(3)	147(2)	-57(2)	-24(1)	-2(1)
N(1)	55(1)	40(1)	43(1)	-1(1)	-2(1)	5(1)
C(2)	66(2)	42(1)	45(1)	5(1)	2(1)	7(1)
N(3)	65(1)	39(1)	59(1)	3(1)	4(1)	5(1)
C(4)	55(1)	46(1)	63(2)	-7(1)	7(1)	3(1)
C(5)	50(1)	43(1)	45(1)	-3(1)	3(1)	-2(1)
C(1')	55(1)	42(1)	66(2)	-3(1)	4(1)	-3(1)
C(2')	58(2)	112(3)	87(2)	-19(2)	-16(2)	0(2)
C(10)	66(2)	42(1)	47(1)	-2(1)	0(1)	2(1)
C(11)	64(2)	36(1)	57(1)	-8(1)	-8(1)	1(1)
C(12)	85(2)	43(1)	56(1)	-1(1)	-8(1)	1(1)
C(13)	122(3)	54(2)	74(2)	6(1)	-28(2)	5(2)
C(14)	119(3)	55(2)	106(3)	4(2)	-37(2)	16(2)
C(15)	77(2)	52(2)	136(3)	-19(2)	-9(2)	17(1)
C(16)	75(2)	48(1)	86(2)	-10(1)	8(2)	7(1)
C(20)	62(2)	64(2)	71(2)	8(1)	-11(1)	3(1)
C(21)	87(2)	95(2)	135(4)	21(2)	-37(2)	20(2)
C(22)	65(2)	121(3)	93(2)	5(2)	21(2)	-8(2)
C(23)	80(2)	84(2)	105(3)	2(2)	-25(2)	-15(2)
C(30)	93(2)	42(1)	92(2)	10(1)	7(2)	10(1)

Hydrogen coordinates (x 10^4) and isotropic displacement parameters (A^2 x 10^3) for 1.

	x	y	z	U(eq)
H(2)	6191(2)	6733(1)	3592(4)	50(6)
H(5)	6783(2)	6279(1)	9628(4)	47(6)
H(21')	8541(2)	6117(2)	11398(6)	99(12)
H(22')	8353(2)	6840(2)	11390(6)	117(13)
H(12)	6567(2)	5217(1)	9040(4)	82(10)
H(13)	7305(3)	4378(1)	10832(6)	108(13)
H(14)	8697(3)	3910(1)	9348(7)	110(12)
H(15)	9358(3)	4254(1)	6063(7)	106(12)
H(16)	8577(2)	5062(1)	4119(5)	61(8)
H(211)	4230(20)	7451(5)	4845(23)	146(10)
H(212)	4595(13)	7144(11)	2631(23)	146(10)
H(213)	3593(8)	6920(6)	3746(45)	146(10)
H(221)	4693(16)	6999(4)	8384(12)	119(8)
H(222)	3816(4)	6532(11)	7863(7)	119(8)
H(223)	4873(13)	6278(7)	8582(10)	119(8)
H(231)	3912(3)	5857(5)	4458(35)	112(7)
H(232)	4833(16)	5922(4)	2855(13)	112(7)
H(233)	4975(14)	5620(2)	5199(25)	112(7)
H(301)	6338(16)	7912(3)	3854(10)	115(7)
H(302)	5478(5)	8026(4)	5584(33)	115(7)
H(303)	6593(13)	8195(2)	6180(25)	115(7)

Hydrogen coordinates (x 10^4) and isotropic displacement parameters (A^2 x 10^3) for 1.

	x	y	z	U(eq)
H(2)	6191(2)	6733(1)	3592(4)	50(6)
H(5)	6783(2)	6279(1)	9628(4)	47(6)
H(21')	8541(2)	6117(2)	11398(6)	99(12)
H(22')	8353(2)	6840(2)	11390(6)	117(13)
H(12)	6567(2)	5217(1)	9040(4)	82(10)
H(13)	7305(3)	4378(1)	10832(6)	108(13)
H(14)	8697(3)	3910(1)	9348(7)	110(12)
H(15)	9358(3)	4254(1)	6063(7)	106(12)
H(16)	8577(2)	5062(1)	4119(5)	61(8)
H(211)	4230(20)	7451(5)	4845(23)	146(10)
H(212)	4595(13)	7144(11)	2631(23)	146(10)
H(213)	3593(8)	6920(6)	3746(45)	146(10)
H(221)	4693(16)	6999(4)	8384(12)	119(8)
H(222)	3816(4)	6532(11)	7863(7)	119(8)
H(223)	4873(13)	6278(7)	8582(10)	119(8)
H(231)	3912(3)	5857(5)	4458(35)	112(7)
H(232)	4833(16)	5922(4)	2855(13)	112(7)
H(233)	4975(14)	5620(2)	5199(25)	112(7)
H(301)	6338(16)	7912(3)	3854(10)	115(7)
H(302)	5478(5)	8026(4)	5584(33)	115(7)
H(303)	6593(13)	8195(2)	6180(25)	115(7)

Bond lengths [A] and angles [deg] for 1.

O(1)-C(4)	1.221(3)	O(2)-C(1')	1.200(3)
O(3)-C(10)	1.227(3)	F-C(2')	1.368(4)
N(1)-C(10)	1.376(3)	N(1)-C(5)	1.457(3)
N(1)-C(2)	1.476(3)	C(2)-N(3)	1.456(3)
C(2)-C(20)	1.553(4)	N(3)-C(4)	1.341(3)
N(3)-C(30)	1.467(3)	C(4)-C(5)	1.541(3)
C(5)-C(1')	1.526(3)	C(1')-C(2')	1.498(4)
C(10)-C(11)	1.498(3)	C(11)-C(16)	1.382(4)
C(11)-C(12)	1.390(4)	C(12)-C(13)	1.390(4)
C(13)-C(14)	1.361(5)	C(14)-C(15)	1.368(5)
C(15)-C(16)	1.404(4)	C(20)-C(22)	1.522(4)
C(20)-C(23)	1.532(4)	C(20)-C(21)	1.544(4)
C(10)-N(1)-C(5)	123.9(2)	C(10)-N(1)-C(2)	119.9(2)
C(5)-N(1)-C(2)	111.5(2)	N(3)-C(2)-N(1)	101.7(2)
N(3)-C(2)-C(20)	113.9(2)	N(1)-C(2)-C(20)	111.9(2)
C(4)-N(3)-C(2)	114.2(2)	C(4)-N(3)-C(30)	122.0(2)
C(2)-N(3)-C(30)	123.8(2)	O(1)-C(4)-N(3)	127.7(2)
O(1)-C(4)-C(5)	124.6(2)	N(3)-C(4)-C(5)	107.5(2)
N(1)-C(5)-C(1')	114.4(2)	N(1)-C(5)-C(4)	102.8(2)
C(1')-C(5)-C(4)	104.8(2)	O(2)-C(1')-C(2')	123.3(2)
O(2)-C(1')-C(5)	122.8(3)	C(2')-C(1')-C(5)	113.9(2)
F-C(2')-C(1')	110.5(3)	O(3)-C(10)-N(1)	121.3(2)
O(3)-C(10)-C(11)	121.1(2)	N(1)-C(10)-C(11)	117.5(2)
C(16)-C(11)-C(12)	119.3(2)	C(16)-C(11)-C(10)	119.2(2)
C(12)-C(11)-C(10)	121.4(2)	C(13)-C(12)-C(11)	120.4(3)
C(14)-C(13)-C(12)	119.9(3)	C(13)-C(14)-C(15)	120.6(3)
C(14)-C(15)-C(16)	120.3(3)	C(11)-C(16)-C(15)	119.4(3)
C(22)-C(20)-C(23)	109.8(3)	C(22)-C(20)-C(21)	109.6(3)
C(23)-C(20)-C(21)	108.1(3)	C(22)-C(20)-C(2)	110.2(2)
C(23)-C(20)-C(2)	109.6(2)	C(21)-C(20)-C(2)	109.5(2)

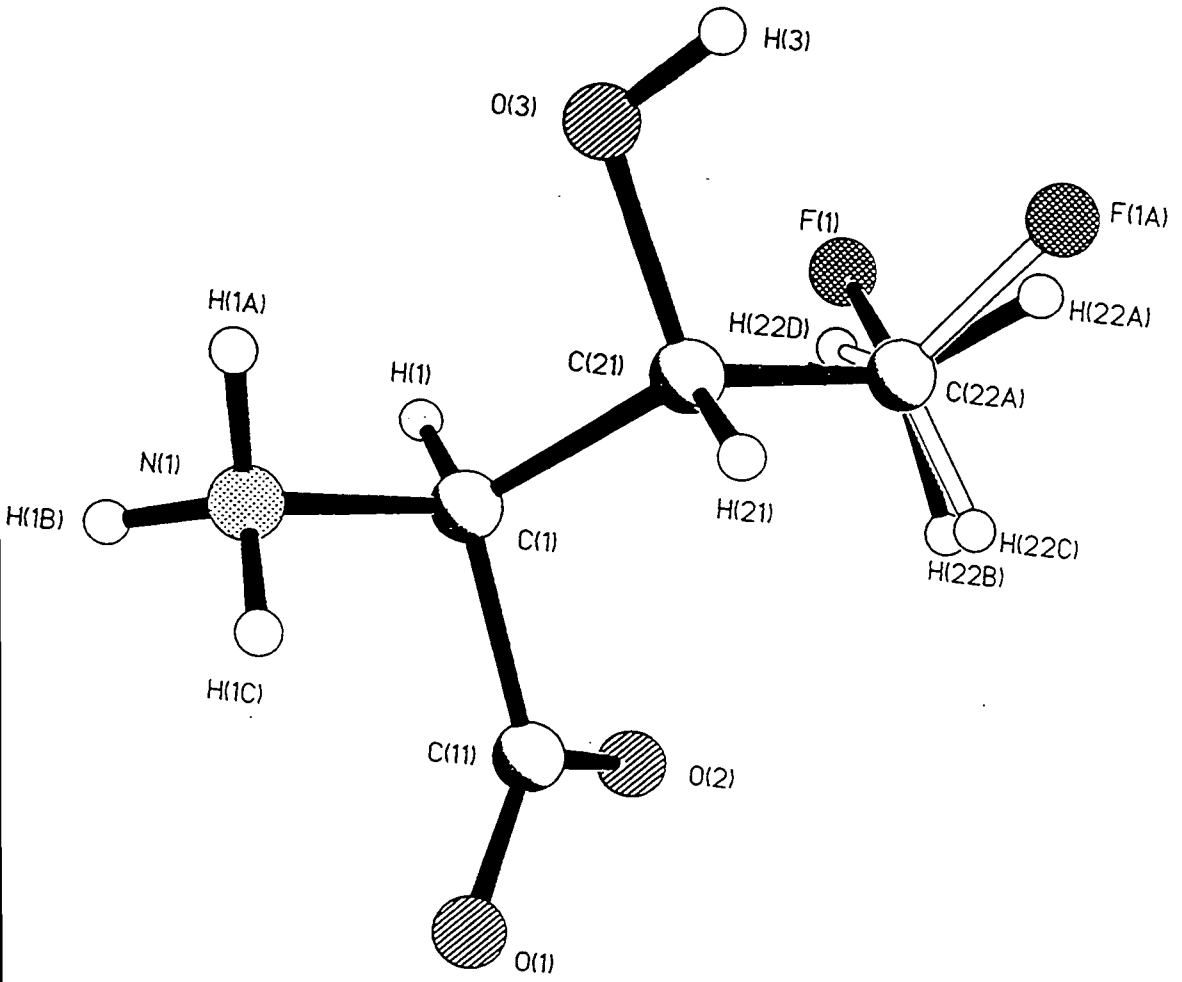

A.2 Crystal structure of 4-(2S,3S)-fluorothreonine ***(202)***

Identification code	97srv025
Empirical formula	C4 H8 F N O3
Formula weight	137.11
Temperature	296(2) K
Wavelength	1.54178 A
Crystal system	Orthorhombic
Space group	P2(1)2(1)2(1)
Unit cell dimensions	a = 5.2313(10) A alpha = 90 deg. b = 7.870(2) A beta = 90 deg. c = 13.603(3) A gamma = 90 deg.
Volume	560.0(2) A^3
Z	4
Number of reflexions used	573 Unique, 549 Used.
Crystal description	Hexagonal plate
Crystal colour	Colourless
Density (calculated)	1.626 Mg/m^3
Absorption coefficient	1.391 mm^-1
F(000)	288
Crystal size	0.15 x 0.15 x 0.05 mm
Theta range for data collection	6.50 to 49.95 deg.
Index ranges	-5<=h<=5, -8<=k<=8, -15<=l<=15
Experiment device	RIGAKU AFC6S
Experiment methods	Omega scans
Number of standard reflexions	3
Interval Counts	147
Reflections collected	730
Independent reflections	573 [R(int) = 0.0293]
Refinement method	Full-matrix least-squares on F^2
Data restraints / parameters	549 / 0 / 93
Goodness-of-fit on F^2	1.023
Final R indices [I>2sigma(I)]	R1 = 0.0589, wR2 = 0.1413
R indices (all data)	R1 = 0.0807, wR2 = 0.1625
Absolute structure parameter	-0.2(11)
Largest diff. peak and hole	0.271 and -0.215 e.A^-3

Atomic coordinates (x 10^4) and equivalent isotropic displacement parameters (A^2 x 10^3) for 1. U(eq) is defined as one third of the trace of the orthogonalized Uij tensor.

	x	y	z	U(eq)
N(1)	6241(10)	7621(6)	1622(4)	27(2)
O(3)	7496(10)	8929(7)	-186(3)	45(2)
C(11)	9575(14)	9344(8)	2424(5)	31(2)
O(2)	11950(8)	9673(6)	2475(4)	42(2)
C(22A)	10582(18)	10932(13)	427(7)	56(2)
F(1)	12449(13)	10004(11)	108(6)	62(3)
C(22B)	10582(18)	10932(13)	427(7)	56(2)
F(1A)	10517(27)	11714(17)	-387(10)	59(6)
C(1)	8668(13)	8553(8)	1466(5)	25(2)
C(21)	8231(13)	9865(9)	661(4)	36(2)
O(1)	7998(10)	9613(8)	3068(4)	55(2)

Anisotropic displacement parameters (A^2 x 10^3) for 1. The anisotropic displacement factor exponent takes the form: -2 pi^2 [h^2 a*^2 U11 + ... + 2 h k a* b* U12]

	U11	U22	U33	U23	U13	U12
N(1)	33(3)	15(3)	34(3)	2(3)	2(3)	-2(3)
O(3)	66(4)	40(3)	29(3)	6(2)	-16(3)	-16(3)
C(11)	35(4)	21(4)	36(4)	-1(4)	-3(4)	4(4)
O(2)	33(3)	41(3)	52(3)	-11(3)	-9(3)	3(3)
C(22A)	54(6)	51(5)	65(7)	0(6)	-2(5)	-13(6)
F(1)	44(5)	60(5)	83(5)	9(4)	15(4)	-6(4)
C(22B)	54(6)	51(5)	65(7)	0(6)	-2(5)	-13(6)
F(1A)	79(11)	56(10)	42(9)	36(7)	-5(8)	-24(8)
C(1)	25(4)	17(4)	34(4)	-3(3)	2(3)	6(3)
C(21)	43(5)	36(4)	30(4)	-1(4)	-7(3)	-1(4)
O(1)	41(3)	82(5)	43(3)	-24(3)	6(3)	-6(3)

Hydrogen coordinates (x 10^4) and isotropic displacement parameters (A^2 x 10^3) for 1.

	x	y	z	U(eq)
H(1B)	6568(12)	6625(21)	1905(25)	33
H(1A)	5477(35)	7450(41)	1046(5)	33
H(1C)	5220(30)	8229(22)	2010(22)	33
H(3)	7238(10)	9585(7)	-644(3)	67
H(22A)	10145(18)	11772(13)	-67(7)	68
H(22B)	11121(18)	11531(13)	1014(7)	68
H(22C)	10809(27)	11759(17)	948(10)	68
H(22D)	12067(27)	10194(17)	430(10)	68
H(1)	9967(13)	7745(8)	1240(5)	30
H(21)	6826(13)	10617(9)	855(4)	44

Bond lengths [A] and angles [deg] for 1.

N(1)-C(1)	1.482(8)
N(1)-H(1B)	0.89
N(1)-H(1A)	0.89
N(1)-H(1C)	0.89
O(3)-C(21)	1.420(8)
O(3)-H(3)	0.82
C(11)-O(1)	1.222(9)
C(11)-O(2)	1.271(8)
C(11)-C(1)	1.521(9)
C(22A)-F(1)	1.294(10)
C(22A)-C(21)	1.523(11)
C(22A)-H(22A)	0.97
C(22A)-H(22B)	0.97
C(22B)-F(1A)	1.27(2)
C(22B)-C(21)	1.523(11)
C(22B)-H(22C)	0.97(2)
C(22B)-H(22D)	0.97(2)
C(1)-C(21)	1.522(10)
C(1)-H(1)	0.98
C(21)-H(21)	0.98

C(1)-N(1)-H(1B)	109.5(3)
C(1)-N(1)-H(1A)	109.5(3)
H(1B)-N(1)-H(1A)	109.5
C(1)-N(1)-H(1C)	109.5(3)
H(1B)-N(1)-H(1C)	109.5
H(1A)-N(1)-H(1C)	109.5
C(21)-O(3)-H(3)	109.5(3)
O(1)-C(11)-O(2)	125.9(7)
O(1)-C(11)-C(1)	118.3(6)
O(2)-C(11)-C(1)	115.8(6)
F(1)-C(22A)-C(21)	111.6(8)
F(1)-C(22A)-H(22A)	109.3(6)
C(21)-C(22A)-H(22A)	109.3(5)
F(1)-C(22A)-H(22B)	109.3(5)
C(21)-C(22A)-H(22B)	109.3(4)
H(22A)-C(22A)-H(22B)	108.0
F(1A)-C(22B)-C(21)	115.4(10)
F(1A)-C(22B)-H(22C)	108.4(14)
C(21)-C(22B)-H(22C)	108.4(11)
F(1A)-C(22B)-H(22D)	108(2)
C(21)-C(22B)-H(22D)	108.4(11)
H(22C)-C(22B)-H(22D)	108(2)
N(1)-C(1)-C(21)	108.1(5)
N(1)-C(1)-C(11)	110.3(5)
C(21)-C(1)-C(11)	112.7(5)
N(1)-C(1)-H(1)	108.6(3)
C(21)-C(1)-H(1)	108.6(4)
C(11)-C(1)-H(1)	108.6(4)
O(3)-C(21)-C(1)	105.8(6)
O(3)-C(21)-C(22A)	109.6(6)
C(1)-C(21)-C(22A)	113.8(6)
O(3)-C(21)-C(22B)	109.6(6)
C(1)-C(21)-C(22B)	113.8(6)
O(3)-C(21)-H(21)	109.2(4)
C(1)-C(21)-H(21)	109.2(4)
C(22A)-C(21)-H(21)	109.2(5)

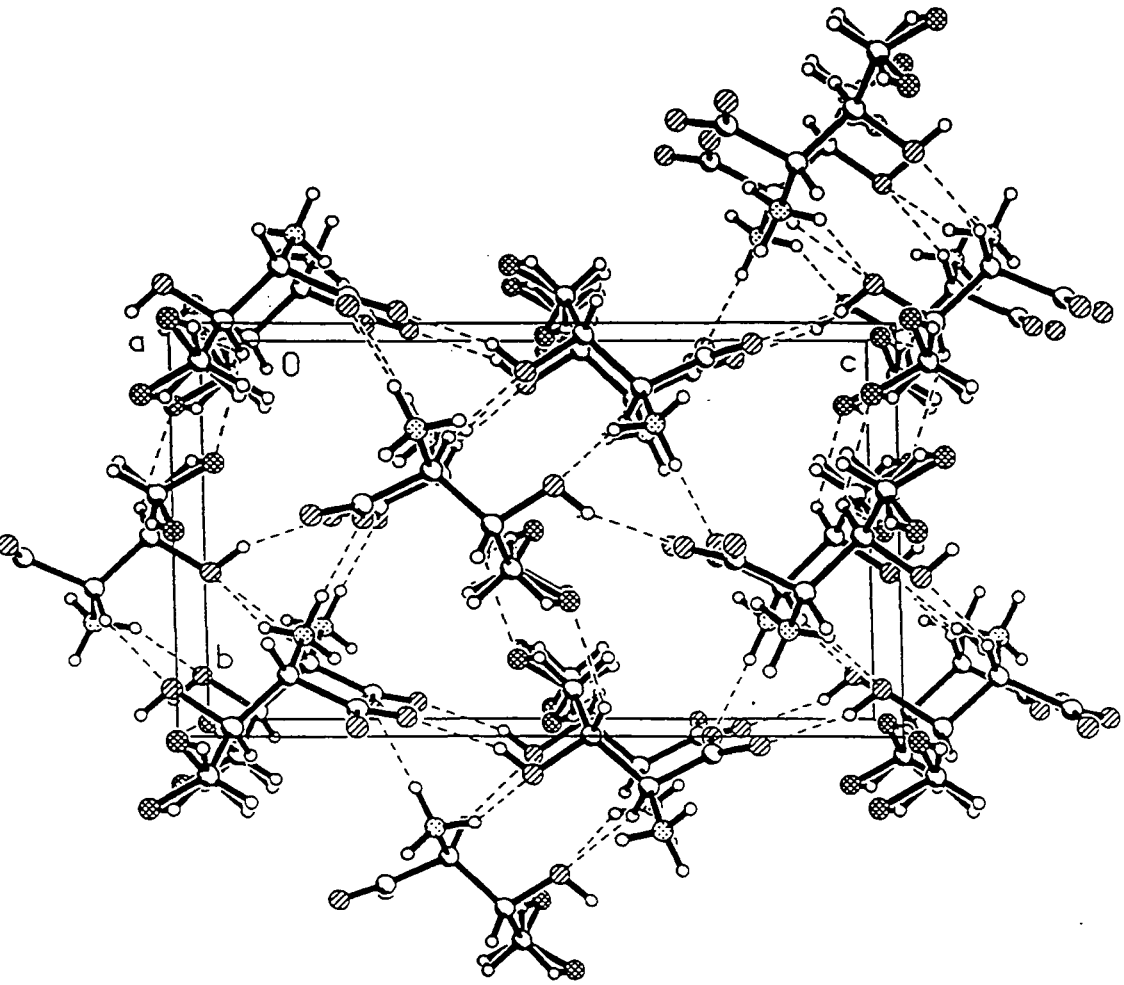

A.3 Diagram showing the 3-D network of hydrogen-bonded interactions between molecules of 4-(2S,3S)-fluorothreonine.

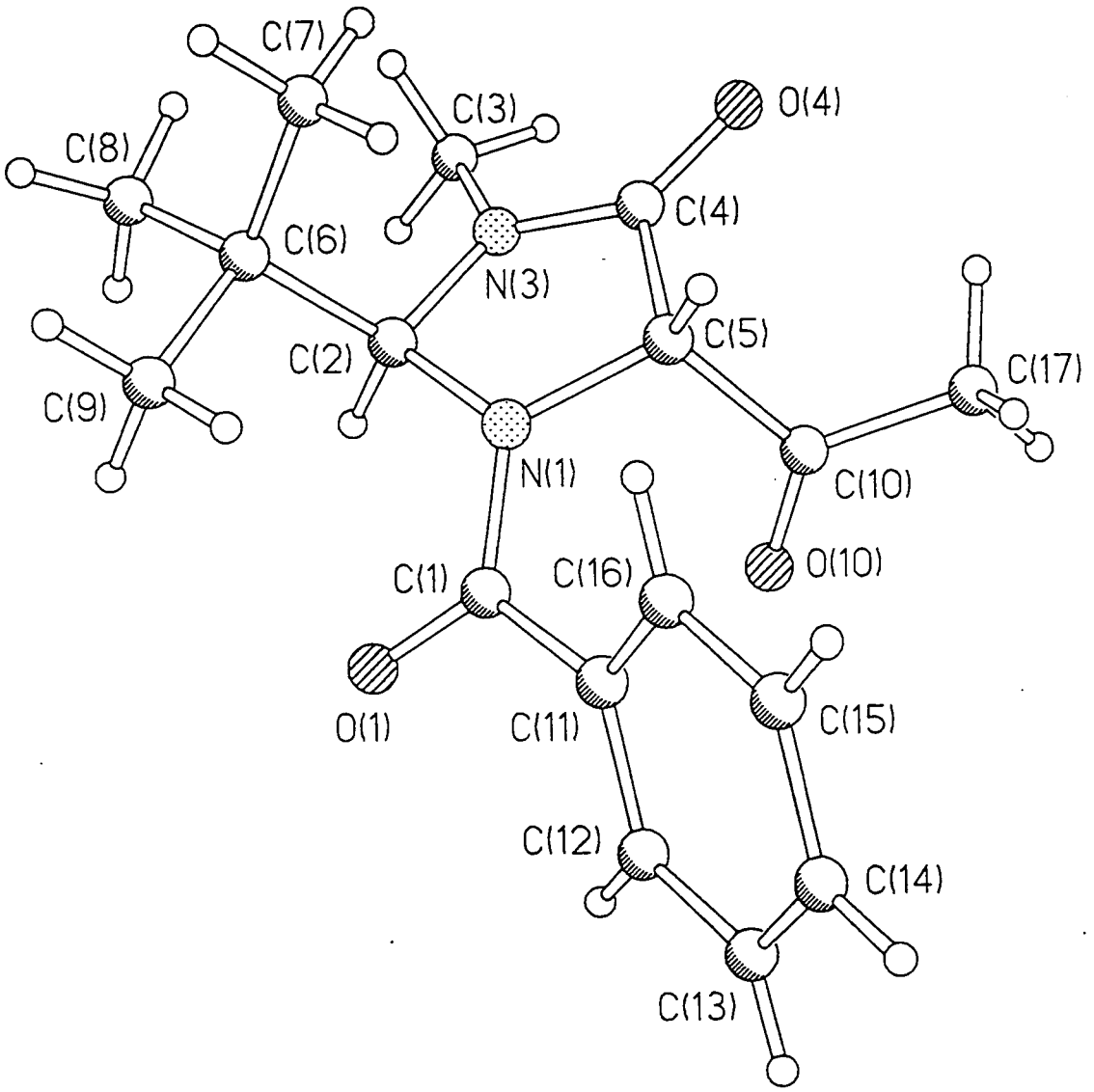

A.4 Crystal structure of 5-(2S,3S)-(1'-keto-2'-methyl)-2-(tert-butyl)-3-methylimidazolidin-4-one ***(212)***

Identification code	97srv068
Empirical formula	C17 H22 N2 O3
Formula weight	302.37
Temperature	150(2) K
Wavelength	0.71073 A
Crystal system	Orthorhombic
Space group	P2(1)2(1)2
Unit cell dimensions	a = 12.636(1) A alpha = 90 deg. b = 21.459(2) A beta = 90 deg. c = 6.059(1) A gamma = 90 deg.
Volume	1642.9(4) A^3
Z	4
Density (calculated)	1.222 g/cm^3
Absorption coefficient	0.084 mm^-1
F(000)	648
Crystal size	0.40 x 0.20 x 0.10 mm
Theta range for data collection	1.87 to 25.00 deg.
Index ranges	-16<=h<=16, -27<=k<=25, -7<=l<=7
Reflections collected	9842
Independent reflections	2905 [R(int) = 0.0641]
Observed reflections, I>2sigma(I)	2289
Absorption correction	None
Refinement method	Full-matrix least-squares on F^2
Data / restraints / parameters	2866 / 0 / 216
Goodness-of-fit on F^2	1.143
Final R indices [I>2sigma(I)]	R1 = 0.0504, wR2 = 0.0978
R indices (all data)	R1 = 0.0768, wR2 = 0.1149
Absolute structure parameter	0(2)
Largest diff. peak and hole	0.148 and -0.193 e.A^-3

Atomic coordinates (x 10^4) and equivalent isotropic displacement parameters (A^2 x 10^3) for 1. U(eq) is defined as one third of the trace of the orthogonalized Uij tensor.

	x	y	z	U(eq)
N(1)	6577(2)	1205(1)	6287(4)	25(1)
N(3)	6237(2)	2251(1)	6259(4)	27(1)
O(1)	6925(2)	673(1)	3129(3)	38(1)
O(4)	6845(2)	2535(1)	9691(3)	37(1)
O(10)	8737(2)	1421(1)	6681(4)	36(1)
C(1)	7023(2)	716(1)	5144(5)	28(1)
C(2)	5979(2)	1686(1)	5040(5)	27(1)
C(3)	6041(3)	2881(1)	5426(5)	36(1)
C(4)	6675(2)	2149(1)	8246(5)	27(1)
C(5)	7014(2)	1460(1)	8338(5)	24(1)
C(6)	4768(2)	1540(1)	4950(5)	31(1)
C(7)	4296(3)	1587(2)	7274(6)	45(1)
C(8)	4221(3)	2001(1)	3387(6)	47(1)
C(9)	4586(3)	879(1)	4066(6)	47(1)
C(10)	8239(2)	1472(1)	8376(5)	28(1)
C(11)	7559(2)	212(1)	6433(5)	26(1)
C(12)	8418(2)	-90(1)	5459(5)	33(1)
C(13)	8906(2)	-582(1)	6555(6)	39(1)
C(14)	8530(3)	-780(1)	8583(6)	44(1)
C(15)	7670(3)	-485(1)	9539(5)	38(1)
C(16)	7187(2)	14(1)	8478(5)	30(1)
C(17)	8724(3)	1568(2)	10594(5)	45(1)

Bond lengths [A] and angles [deg] for 1.

N(1)-C(1)	1.377(3)	N(1)-C(5)	1.466(3)
N(1)-C(2)	1.486(3)	N(3)-C(4)	1.343(4)
N(3)-C(2)	1.456(3)	N(3)-C(3)	1.466(3)
O(1)-C(1)	1.231(3)	O(4)-C(4)	1.226(3)
O(10)-C(10)	1.210(3)	C(1)-C(11)	1.497(4)
C(2)-C(6)	1.562(4)	C(4)-C(5)	1.539(4)
C(5)-C(10)	1.548(4)	C(6)-C(7)	1.533(5)
C(6)-C(9)	1.533(4)	C(6)-C(8)	1.535(4)
C(10)-C(17)	1.492(4)	C(11)-C(16)	1.391(4)
C(11)-C(12)	1.395(4)	C(12)-C(13)	1.391(4)
C(13)-C(14)	1.385(5)	C(14)-C(15)	1.386(4)
C(15)-C(16)	1.389(4)		
C(1)-N(1)-C(5)	123.8(2)	C(1)-N(1)-C(2)	118.8(2)
C(5)-N(1)-C(2)	111.3(2)	C(4)-N(3)-C(2)	114.3(2)
C(4)-N(3)-C(3)	121.9(2)	C(2)-N(3)-C(3)	123.8(2)
O(1)-C(1)-N(1)	121.0(3)	O(1)-C(1)-C(11)	120.6(3)
N(1)-C(1)-C(11)	118.3(2)	N(3)-C(2)-N(1)	101.9(2)
N(3)-C(2)-C(6)	113.9(2)	N(1)-C(2)-C(6)	112.1(2)
O(4)-C(4)-N(3)	127.1(2)	O(4)-C(4)-C(5)	125.1(3)
N(3)-C(4)-C(5)	107.7(2)	N(1)-C(5)-C(4)	102.9(2)
N(1)-C(5)-C(10)	113.3(2)	C(4)-C(5)-C(10)	105.3(2)
C(7)-C(6)-C(9)	108.9(3)	C(7)-C(6)-C(8)	110.4(3)
C(9)-C(6)-C(8)	108.2(3)	C(7)-C(6)-C(2)	109.7(2)
C(9)-C(6)-C(2)	110.2(2)	C(8)-C(6)-C(2)	109.5(2)
O(10)-C(10)-C(17)	124.3(3)	O(10)-C(10)-C(5)	120.4(3)
C(17)-C(10)-C(5)	115.3(3)	C(16)-C(11)-C(12)	119.8(3)
C(16)-C(11)-C(1)	122.2(2)	C(12)-C(11)-C(1)	117.8(2)
C(13)-C(12)-C(11)	119.7(3)	C(14)-C(13)-C(12)	120.3(3)
C(13)-C(14)-C(15)	120.0(3)	C(14)-C(15)-C(16)	120.2(3)
C(15)-C(16)-C(11)	120.0(3)		

Hydrogen coordinates (x 10^4) and isotropic displacement parameters (A^2 x 10^3) for 1.

	x	y	z	U(eq)
H(2)	6265(2)	1717(1)	3506(5)	27(7)
H(3A)	6182(13)	2895(2)	3836(7)	45(5)
H(3B)	5301(5)	2994(3)	5701(26)	45(5)
H(3C)	6506(10)	3177(2)	6186(21)	45(5)
H(5)	6716(2)	1245(1)	9663(5)	27(7)
H(71)	4646(12)	1286(7)	8248(10)	68(7)
H(72)	4401(15)	2009(3)	7849(15)	68(7)
H(73)	3537(4)	1494(10)	7210(8)	68(7)
H(81)	4164(15)	2409(3)	4103(15)	65(7)
H(82)	4642(9)	2040(8)	2036(16)	65(7)
H(83)	3512(7)	1848(5)	3017(28)	65(7)
H(91)	4873(14)	846(3)	2568(14)	54(6)
H(92)	4942(14)	577(2)	5026(20)	54(6)
H(93)	3825(3)	791(4)	4038(32)	54(6)
H(12)	8667(2)	40(1)	4054(5)	35(8)
H(13)	9505(2)	-779(1)	5916(6)	28(8)
H(14)	8858(3)	-1121(1)	9311(6)	56(10)
H(15)	7408(3)	-622(1)	10926(5)	46(9)
H(16)	6602(2)	219(1)	9143(5)	36(8)
H(171)	8348(11)	1902(7)	11368(15)	67(7)
H(172)	9470(5)	1683(10)	10420(6)	67(7)
H(173)	8673(15)	1182(3)	11452(13)	67(7)

Anisotropic displacement parameters (A^2 x 10^3) for 1. The anisotropic displacement factor exponent takes the form: -2 pi^2 [h^2 a*^2 U11 + ... + 2 h k a* b* U12]

	U11	U22	U33	U23	U13	U12
N(1)	29(1)	22(1)	24(1)	-2(1)	-1(1)	4(1)
N(3)	35(1)	19(1)	28(1)	1(1)	-1(1)	2(1)
O(1)	55(1)	35(1)	24(1)	-3(1)	1(1)	10(1)
O(4)	46(1)	29(1)	35(1)	-10(1)	-1(1)	1(1)
O(10)	32(1)	32(1)	42(1)	1(1)	9(1)	-2(1)
C(1)	32(2)	25(2)	27(2)	2(1)	3(1)	1(1)
C(2)	33(2)	22(1)	25(2)	2(1)	1(1)	3(1)
C(3)	45(2)	22(2)	40(2)	6(1)	-1(2)	3(1)
C(4)	28(2)	25(2)	28(2)	2(1)	6(1)	0(1)
C(5)	28(1)	23(1)	20(1)	-2(1)	3(1)	-2(1)
C(6)	33(2)	27(2)	34(2)	3(1)	-7(1)	2(1)
C(7)	31(2)	56(2)	48(2)	5(2)	8(2)	-5(2)
C(8)	43(2)	41(2)	56(2)	7(2)	-18(2)	4(2)
C(9)	39(2)	36(2)	66(3)	1(2)	-18(2)	-4(2)
C(10)	31(2)	16(1)	36(2)	2(1)	-2(2)	0(1)
C(11)	28(2)	21(1)	28(2)	-2(1)	-4(1)	-2(1)
C(12)	35(2)	24(2)	38(2)	-6(1)	4(2)	0(1)
C(13)	32(2)	26(2)	59(2)	-8(2)	-3(2)	7(1)
C(14)	49(2)	28(2)	54(2)	4(2)	-20(2)	3(2)
C(15)	53(2)	27(2)	34(2)	4(1)	-6(2)	0(2)
C(16)	36(2)	22(1)	32(2)	-4(1)	-3(2)	2(1)
C(17)	39(2)	53(2)	44(2)	-3(2)	-11(2)	-5(2)

APPENDIX B

Colloquia, Presentations & Conferences

B.1 Colloquia, lectures and seminars from invited speakers

B.2 Research Conferences attended

B.3 Seminars and Poster presentations given

B.4 Papers published and submitted

B.1 Colloquia, seminars and lectures from invited speakers

1993

October 14	Dr. P. Hubberstey, University of Nottingham, *Alkali metals: Alchemist's Nightmare, Biochemist's Puzzle and Technologist's Dream*
October 20	Dr. P. Quale, University of Manchester, *Aspects of Aqueous ROMP Chemistry*
December 1	Prof. M.A. Mckervey, Queen's University, Belfast *Synthesis and Applications of Chemically Modified Calixarenes.*

1994

February 9	Prof. D. Young, University of Sussex *Chemical and Biological Studies on the Co-enzyme Tetrahydrofolic acid*
March 9	Prof. F. Wilkinson, Loughborough University of Technology *Nanosecond and Picosecond Laser Flash Photolysis*
March 10	Prof. S.V. Ley, University of Cambridge *New Methods for Organic Synthesis*
October 19	Prof. N. Bartlett, University of California *Some Aspects of Ag(II) and Ag(III) Chemistry*
November 10	Dr. M. Block, Zeneca Pharmaceuticals, Macclesfield *Large Scale Manufacture of ZD1542, a Thromboxane Antagonist Synthase Inhibitor*
November 16	Prof. M. Page, University of Huddersfield Four-membered Rings and β-Lactamase

1995

January 11	Prof. P. Parsons, University of Reading
	Applications of Tandem Reactions in Organic Synthesis
January 25	Dr. D.A. Roberts, Zeneca Pharmaceuticals
	The Design and Synthesis of Inhibitors of the Renin-Angiotensin System
February 16	Prof. H. Kroto
	C_{60} - The Celestial Sphere that Fell to Earth
February 22	Prof. E. Schaumann, University of Clausthal
	Silicon and Sulphur mediated Ring-Opening Reactions of Epoxides
March 1	Dr. M. Rosseinsky, Oxford University
	Fullerene Intercalation Chemistry
May 4	Prof. A.K. Kresge, University of Toronto
	The Ingold Lecture: Reactive Intermediates; Carboxylic acid Enols and Other Unstable Species
November 1	Prof. W. Motherwell, UCL London
	New Reactions for Organic Synthesis
November 8	Dr. D. Craig, Imperial College, London
	New Strategies for the Assembly of Heterocyclic Systems
December 8	Prof. M.T. Reetz, Max Planck Institut, Mullheim
	Perkin Regional Meeting

1996

January 17	Prof. J.W. Emsley, Southampton University
	Liquid crystals, More than Meets the Eye
January 24	Dr. A. Armstrong, Nottingham University
	Alkene Oxidation and Natural Product Synthesis
February 21	Dr. C.R. Pulham, University of Edinburgh
	Heavy Metal Hydrides- an exploration of the chemistry of stannanes and plumbanes
February 28	Prof. E.W. Randall, Queen Mary & Westfield College
	New Perspectives in NMR Imaging
March 13	Prof. D. Garner, Manchester University
	Mushrooming in Chemistry

B.2 Research Conferences Attended

December 1993	Bio-Organic Group Postgraduate Symposium, Exeter University
December 1994	Bio-Organic Group Postgraduate Symposium, Durham University
December 1995	Recent Developments in Stereochemistry, Sheffield University
March 1995	SCI Novel Organic Chemistry, 6th Graduate Symposium, York University
July 1995	Biological Challenges for Organic Chemistry, University of St. Andrews
May 1996	Isotopes Conference, Glaxo-Wellcome Foundation, Stevenage
December 1996	Bio-Organic Group Postgraduate Symposium, Liverpool University

B.3 Seminars and poster presentations given

December 1994	ICI/Zeneca Postgraduate Chemistry Poster Competition, University of Durham
December 1995	Bio-Organic Postgraduate Group Symposium, University of Southampton (poster presentation)
April 1996	North East Universities Postgraduate Chemistry Symposium, University of Sunderland (oral presentation)
June 1996	Postgraduate Chemistry Seminars, University of Durham (oral presentation)
September 1996	Scottish Highlands Meeting, Postgraduate Bio-Organic Symposium, Crieff, Scotland (poster presentation)

B.4 Papers published and submitted

K.A. Reid, J.T.G. Hamilton, R.D. Bowden, D.O'Hagan, L. Dasaradhi, **M.R. Amin**, D.B. Harper, *Microbiology*, 1995, **141**, 1385

"*Biosynthesis of Fluoroacetate and 4-Fluorothreonine by Streptomyces cattleya. Glycine and Pyruvate as Precursors*", J.T.G. Hamilton, **M.R. Amin**, D.B. Harper, D. O'Hagan, *J. Chem. Soc., Chem. Comm.*, 1997, 797

"*The Biosynthetic Origin of Fluoroacetate and 4-Fluorothreonine in S. cattleya*", J.T.G. Hamilton, C.D. Murphy, **M.R. Amin**, D. O'Hagan, D.B. Harper, *Microbiol.*, 1997, (submitted)

" *A Short Highly Stereoselective Synthesis of the Fluorinated Natural Product 4-(2S,3S)-Fluorothreonine*", **M.R. Amin**, D.B. Harper, J.B. Moloney, C.D. Murphy, J.A.K. Howard, D. O'Hagan, *J. Chem. Soc., Chem. Comm.*, 1997 (submitted)

APPENDIX C

Bibliography

References

1. J.A. Timbrell, Introduction to Toxicology, Taylor and Francis, 1989

2. J. Mann, Secondary Metabolism, Oxford University Press, Oxford, 1987

3. R.H. Whittaker, P.P. Feeney, *Science*, 1971, **171**, 757-770.

4. P. Krogsgaard-Larsen, S.B. Christensen, H. Kofod, Natural Products & Drug Developement, Munksgaard, Copenhagen, 1984

5. J.D. Bu'Lock, D. Hamilton, M.A. Hulme, A.J. Powell, H.M. Smalley, D. Shepherd, G.N. Smith, *Can J. Microbiol*, 1965, **11**, 765

6. J.B. Walker, *J. Biol. Chem*, 1974, **249**, 2397

7. R.B. Herbert, Biosynthesis of secondary metabolites, 2nd Ed., Chapman and Hall, London, 1989

8. G.S. Fraenkel, *Science*, 1959, **129**, 1466

9. E. Soundheimer, J.B. Simeone, Eds., Chemical Ecology, Academic Press, New York, 1970

10. M. Luckner, Secondary metabolism in micro-organisms, plants and animals, Springer Verlag, 3rd Ed., Berlin, 1990

11. T. Swain, Secondary compounds as protective agents, *Ann. Rev. Plant Physiol.*, 1977, **28**, 479

12. J.B. Harbone, Recent Advances in Chemical Ecology, *Nat. Prod. Rep*, 1986, **3**, 323

13. E.L. Rice, Allelopathy, Acad. Press, London, 1983.

14. M.S. Edenborough, R.B. Herbert, *Nat. Prod. Rep.*, 1988, **5**, 229

15. C.J.W. Brooks, D.G. Watson, *Nat. Prod. Rep.*, 1985, **2**, 427

16. M.S. Kemp, R.S. Burden, *Phytochemistry*, 1986, **25**, 1261

17. R.P. Schoffer, R.S. Livingston, *Science*, 1984, **223**, 17

18. A.M. Mayer, *Phytochemistry*, 1989, **28**, 311

19. A. Nahrstedt, Recent developments in chemistry, distribution and biology of cyanogenic glycosides, Clarendon Press, Oxford, 1987, pp213-234.

20. M.L. Delapuente, S.V. Ley, M.S.J. Simmonds, W.M. Blaney, *J. Chem. Soc., Perkin Trans. 1*, 1996,**13**, 1523

21. R.L. Metcalfe, 1987, *CRC Crit Rev. Plant Sci*, 1987, **5**, 251

22. R. Baker, R.B. Herbert, *Nat. Prod. Rep*, 1984, **1**, 299

23. T.J. Grinsteiner, Y. Kishi, *Tetrahedron Lett.*, 1994, **35**, 8333

24 K. Reid, "Biochemical Studies of Fluoroacetate and 4-Fluorothreonine Biosynthesis in *Streptomyces cattleya*", PhD Thesis, 1994, Queen's University of Belfast

25. W.A. Emboden, Narcotic plants of the World, Macmillan, NewYork, 1979.

26. K. Bloch, *Ann Rev. Biochem,* 1977, **46**, 263

27. F.D. Gunstone, *Nat. Prod. Rep.* 1984, **1**, 483

28. F.D. Gunstone, *Nat. Prod. Rep.* 1987, **4**, 95

29. J.L. Harwood, *Ann. Rev. Plant Physiol, Plant Mol Biol.,* 1988, **39**, 101.

30. D.O'Hagan, Polyketides, Ellis Harwood, Chichester, 1991

31. D.O'Hagan, *Nat. Prod. Rep.*, 1995, **10**. 1

32. M. Murata, N. Naoki, T. Iwashita, S. Matsunaga, M. Sasoki, A. Yokoyama, T. Yasumoto, *J. Am. Chem.Soc.*, 1993, **115**, 2060

33. D.V. Banthorpe, S.A. Branch, (1984-1987), *Nat. Prod. Rep.*, **1**, 443; **2**, 513; **4**, 157..

34. J.R. Hanson, *Nat. Prod. Rep.,* 1984, **1**, 443

35. R. Croteau, *Chem Rev.*, 1987, **87**, 929.

36. D.H. Grayson, *Nat. Prod. Rep.,* 1984-1987, **1**, 319; **3**,251; **4**, 377

37. J.R. Hanson, *Nat. Prod. Rep.,* 1984-1988, **1**, 171; **3**, 307; **4**, 399; **5**, 211.

38. J.R. Hanson, *Nat. Prod. Rep.*, 1986. **3**, 123

39. G.A. Cordell, *Prog. Phytochem.*, 1977, **4**, 209

40. D.M. Harrison, *Nat. Prod. Rep.,* 1985, **2**, 525

41. W.J. Baas, *Phytochemistry*, 1985, **24**, 1875.

42. P.M Dewick, *Nat. Prod. Rep.,* 1984-1988, **1**, 451; **2**, 495; **3**, 565; **5**, 73

43. G.A. Swan, An Introduction to the alkaloids, Blackwell Scientific Publications, Oxford, 1967.

44. J. Mann. R.S. Davidson, J.B. Hobles, D.V. Barnthorpe, J.B. Harbone, Natural products, their chemistry and biological significance, J. Wiley and Sons, Inc., 1994

45. D.J. Robins, *Prog. Chem. Org. Nat. Prod.* 1982, **41**, 115.

46. D.J. Robins, *Nat. Prod. Rep.,* 1984-1987, **1**, 235; **2**, 213; **3**, 297; **4**, 577

47. J.E. Saxton, *Nat. Prod. Rep.,* 1984-1986, **1**, 21; **2**, 49; **3**, 353

48. J.B. Harbone, Introduction to Ecological Biochemistry, 3rd Ed., Academic Press, London, 1988.

49. E.A. Evans, D.C. Warrell, J,A, Elridge, J.R. Jones, 'Handbook of Tritium NMR spectroscopy and its applications'. Wiley, Chichester 1985.

50. K.O' Neill, C.P. Richards: Biological ^{31}P NMR spectroscopy, *Annual reports on NMR spectroscopy*, G.A. Web (Ed.), 1980, **10A**, 133.

51. J.C. Vederas, *Nat. Prod. Rep.*, 1987, **4**, 277.

52. M.J. Garson, J. Staunton, *Chem. Soc. Rev.*, 1979, 539.

53. J. Mason, *Chem. Br.,* 1983, **19**, 654.

54. W. Philipsborn, von, R. Muller ^{15}N-NMR spectroscopy- new methods and applications, *Angew Chem Int. Ed. Engl.* (1986) **25**: 383.

55. L. Cavali, *Annual reports on NMR Spectroscopy.*, Ed. E.F. Mooney, **6B**, Academic Press, 1976

56. C.R. Hutchinson, Biological methods for studying the biosynthesis of natural products. *Nat. Prod. Rep.*, 1986. **3** :133-152.

57. S. Itoh, Y. Odakura, H. Kase, 1984, *J. Antibiot.*, **37**, 1664 and 1670.

58. A. J. Rudge, 'Fluorine, manufacture and uses', Oxford University Press, 1962

59. B.E. Smart, Organofluorine chemistry: Principles and commercial applications, Chapter 3, pp57, Plenum Press, New York, 1994.

60. J. T. Welch, *Tetrahedron,* 1987, **43**, 3123

61. J.A.K. Howard, V. J. Hoy, D. O'Hagan, G. T. Smith, *Tretrahedron*, 1996, **52**, 12613.

62. D. Seebach, *Angew. Chem., Int. Ed. Engl.* 1990, **29**, 1320.

63. M.R.C. Gerstenberger, A. Haas, *Angew. Chem., Int. Ed. Engl.*, 1981, 20, 647

64. J.G. Riess, M. Le Blanc, *Angew Chem.*, 1978, **90**, 654, *Angew Chem., Int, Ed. Engl.*, 1978, **17**, 621.

65. S. Bernstein, R.H. Lenhard, W.S. Allen, M. Heller, R. Littell, S.M. Stolar, L.J. Feldman, R.H. Blank, *J. Am. Chem. Soc.*, 1956, **78**, 569.

66. E. Klauke, E. Kuhle, F. Grewe, H. Kaspers, R. Wegler, *Chem. Abstr.* 1963, **58**, 9093.

67. E.A. Paul, P.M. Huang, 'Handbook of Environmental Chemistry' ed. O. Hutzinger, Springer-Verlag, Berlin, 1980, **1**, 69.

68. J. Cooke, 'Fluoride compounds in plants, their occurrence, distribution and effects'; PhD thesis, 1972, University of Newcastle-upon-Tyne.

69. D.B. Harper, D.O' Hagan, *Nat. Prod. Rep.*, 1994, **11**, 23

70. R.P. Gregson, B.A. Baldo, P.G. Thomas, R.J. Quinn, P.R. Bergquist, J.F. Stephens, A.R. Horne, *Science,* 1979, **206**, 1108.

71. P. Venkateswarlu, W.D. Armstrong, L. Singer, *Plant Physiol.*, 1965, **40**, 255.

72. S.M. Andrews, J.A. Cooke, M.S. Johnson, *Environ. Pollut.*, 1989, **60**, 165.

73. K.C. Engvild, *Phytochemistry*, 1986, **25**, 781

74. L. Pauling, 'The nature of the chemical bond,' Cornell University Press, Ithaca, New York, 1960, p82.

75. J.C.S. Marais, *Onderstepoort. J. Vet. Sci. Anim. Ind.*, 1943, **18**, 203.

76. J.C.S. Marais, *Onderstepoort. J. Vet. Sci. Anim. Ind.*, 1944, **20**, 67.

77. F.L.M. Pattison, 'Toxic aliphatic fluorine compounds', Elsvier Publishing Company, Amsterdam, 1959.

78. E. Nel, P.J. Robbertse, N. Grobbelaar, *S. Afri. J. Bot.* 1982, **1**, 14-17.

79. J Tannock, *Rhod. J. Agric. Res.*, 1975, **13**, 67-70.

80. E.G Bollard, G.W. Butler, *Ann. Rev. Plant. Physiol.*, 1966. **17**, 77-112.

81. D.O' Hagan, R. Perry, J.M. Lock, J.J.M. Meyer, L. Dasaradhi, J.T.G. Hamilton. D.B. Harper, *Phytochemistry*, 1993, **33**, 1043.

82. T.E.H. Aplin, *J. Agric. West. Aust.*, 1971, **12**, 154.

83. P.B. Oelrichs, T. McEwan, *Nature*, 1961, **190**, 808.

84. T. Vartiainen, J. Gynther, *Fd. Chem. Toxic.*, 1984, **22**, 307.

85. R.J. Hall, *New Phytol.*, 1972, **71**, 855.

86. B. Vickery. M.L. Vickery, *Phytochemistry*, 1972, **11**, 1905.

87. R.A.Peters, R.J. Hall, *Biochemical Pharmacology*, 1959, **2**, 25.

88. P.F.V. Ward, R.J. Hall, R.A. Peters, *Nature*, 1964, **201**, 611.

89. J.T.G. Hamilton, D.B. Harper, *Phytochemistry*, 1997, **44**, 1129.

90. R.A. Peters, M. Shorthouse, *Nature,* 1967, **216**, 80.

91. R.A. Peters, M. Shorthouse, *Nature*, 1971, **231**, 123.

92. R.A. Peters, M. Shorthouse, *Phytochemistry*, 1972, **11**, 1337.

93. R. Keck, M. Haas, J. Retey, *FEBS Lett.*, 1980, **114**, 287.

94. C. Walsh, *Adv. in Enzymology*, 1982, **55**, 197

95. D. O'Hagan, H. S. Rzepa, *J. Chem. Soc. Chem. Comm.*, 1994, 2029

96. E.R. Kalmbach, *Science*, 1945, **102**, 232.

97. J.W.E. Harrison, J.L. Ambrus, C.M. Ambrus, E.W. Rees, R.H. Peters Jr., L.C. Reese, T. Baker, *J. Amer. Med. Assoc.* 1952, **149**, 1520.

98. E. Kirsten, M.L. Sherman, E. Kun, *Mol. Pharmacol.,* 1978, **14**, 172.

99. Lauble, M.C. Kennedy, M.H. Emptage, H. Beinert, C.D. Stout, *Proc. Natl. Acad. Sci. USA,* 1996, **93**, 13699

100. S. Matura, N. Kokubu, S. Watanabe, Y. Samesima. *Mem. Fac. Sci. Kyushu. Uni. Ser.C.* 1955, **2**, 75.

101. M. Meyer, D.O' Hagan, *Chem. Brit.*, 1992, **28**, 785.

102. W.S. Guy, D.R. Taves, W.S. Brey, 'Organic Fluoro-compounds in Human Plasma: Prevalence and Characterisation' (Ciba Foundation Symposium), ed. K. Elliott and J. Birch, Associated Scientific Publishers, Amsterdam, 1972, p.117.

103. L.E. Twig, D.R. King, OIKOS 1991, **61**, 412

104. S.O. Thomas, V.L. Singleton, J.A. Lowery, R.W. Sharpe, L.M. Pruess, J.N. Poster, J.H. Mowat, N. Bohonos, *Antibiotics Ann.*, 1956-1957, 716.

105. C.W. Waller, J.B. Patrick, W. Fulmer, W.E. Meyer, *J. Am. Chem. Soc.*, 1957, **79**, 1011.

106 I.D. Jenkins, J.P.H. Verheyden, J.G. Maffot, *J. Am. Chem. Soc.*, 1976, **98**, 3346.

107. M. Sanada, T. Miyano, S. Iwadare, J.M. Williamson, B.H. Arison, J.L. Smith, A.W. Douglas, J.M. Liesch, E. Inamine, *J. Antibiotics,* 1986, **39**, 259.

108. M. Sanada, T. Miyano, S. Iwadare, *J. Antibiotics*, 1986, **39**, 304.

109. H. Yoshida, N. Arai, M. Sugoh, J. Iwabuchi, K. Shiomi, M. Shinose, Y. Tanaka, S. Omura, *J. Antibiotics*, 1994, **47**, 1165

110. J.J.M. Meyer, N. Grobbelaar, unpublished observation.

111. D.H. Treble, D.T.A. Lamport, R.A. Peters, *Biochem. J.* 1962, **85**, 113

112. J.J.M. Meyer., N. Grobbelaar, R. Vleggaar, A.J. Louw, *J. Plant Physiol.* 1992, **139**, 369

113. P. Goldman, *J. Biol Chem.,* 1965, **8**, 3434.

114. J.J.M. Meyer, N. Grobbelaar, P.L. Steyn. *Appl. Environ. Microbiol.* 1990, **56**, 2152

115. P. Goldman, G.W.A. Milne, *J. Biol. Chem.* 1966, 241, 5557.

116. H. Kawasaki, K. Miyashi, K. Tonomura, *Agric. Biol. Chem.*, 1981, **45**, 543.

117. A.I. Soiefer, P.J. Kostyniak, *J. Biol. Chem*, 1984, 259, 10787.

118. S. Blumenthal, H.R. Hendrickson, Y.P. Abrol, E.E. Conn, *J. Biol. Chem.*, 1968, 243, 5302.

119. R..J. Mead, W. Segal, *Aust. J. Biol. Sci.*, 1972, **25**, 327.

120. J.J.M. Meyer, D.O' Hagan, *Phytochemistry*, 1992, **31**, 499.

121. J.N. Eloff, N. Grobbelaar, *Joernaal van die Suid-Afrikaanse Chemiese Institute*, 1972, **25**, 109.

122. R.A. Peters, M. Shorthouse, *Life Sci.*, 1967, **6**, 1505.

123. J.H. Dodds, S.K. Musa, P.H. Jerie, M.A. Hall, *Plant Sci., Lett.*, 1979, **17**, 109.

124. R.A. Peters, L.R. Murray, M. Shorthouse, *Biochem J.*, 1965, **95**, 724.

125. B. Vickery, F. Kaberia, *Experientia.* 1979, **35**, 299.

126. L.M. Prescott, J.P. Harley, D.A. Klein, Microbiology, 2nd ed., Wm.C. Brown Publishers, 1990.

127. J.S. Kahan, F.M. Kahan, R. Goegelman, S.A. Currie, M. Jackson, E.O. Stapley, T.W. Miller, A.K. Miller, D. Hendlin, S. Mochales, S. Hernandez, H.M. Woodruff, J. Birnbaum, *J. Antibiotics*, 1979, **32**, 1.

128. Albers-Schonberg, G.B.H. Arison, E. Kaczka, F.M. Kahan. J.S. Kahan, B. Lago, W.M. Maiese, R.E. Rhodes, J.L. Smith, *Abst. Intersci. Conf. Antimicrob. Agents. Chemother.*, 1976, **16**, 229.

129. M. Noble, D. Noble, R.A. Fletton, *J. Antibiotics*, 1978. **31**, 15.

130. T. Tamura, M. Wada, N. Esaki, K. Soda, 1995, *J. Bacteriol.*, **177**, 2265.

131. G.O. Morton, J.E. Lancaster, G.E. Van Lear, W. Fulmor, W.E. Meyer, *J. Am. Chem. Soc.*, 1969, **91**, 1535.

132. K.A. Reid, J.T.G. Hamilton, R.D. Bowden, D.O'Hagan, L. Dasaradhi, M.R. Amin, D.B. Harper, *Microbiology*, 1995, **141**, 1385.

133. G. Gish, T. Smyth, R. Kluger, *J. Am. Chem. Soc.*, 1988, **110**, 6230.

134. G.K. Darland, R. Hadju, H. Kropp, F.M. Kahan, R.W. Walker, W.J.A. Vand enheurel, *Drug. Met. Dispos.*, 1986, **14**, 668.

135. N. Louw, Floorometabolisme in *D. cymosum*, MSc. thesis, University of Pretoria, 1968.

136. J.A. Peters, K.J. Baxter, *Bull. Environ. Contam. Toxicol.*, 1974, **11**, 177.

137. H.M. Stahr, W.B. Buck, P.F. Ross, *J. Assoc. Off. Anal. Chem.*, 1974, **57**, 405.

138. R. J. Hall, 'Carbon-fluorine compounds; Chemistry, biochemistry and biological activities, (Ciba Foundation Symposium), p. 164, Elsvier, Amsterdam, 1972.

139. M.L. Baron, C.M. Bothroyd, G.I. Rogers, A. Staffa, I.D. Rae, *Phytochemistry*, 1987, **26**, 2293.

140. J.E. Peterson, *Bull Environ. Contam. Toxicol.*, 1975, **13**, 751.

141. I. Okuno, G.E. Connolly, P.J. Savarie, C.P. Breidenstein, *J. Assoc. Off. Anal. Chem.*, 1984, **67**, 549.

142. A.C. Ray, L.O. Post, J.C. Reagor, *J. Assoc. Off. Anal. Chem.*, 1981, **64**, 19.

143. T. Vartiainen, P. Kauranen, *Anal. Chim. Acta* 1984, **157**, 91.

144. D.G. Burke, D.K.T. Lew, X. Cominos., *J. Assoc. Off. Anal. Chem.,* 1989, **72**, 503.

145. M. W. Hunkapiller, J.E. Strickler, K.J. Wilson, *Science*, 1984, **226**, 309.

146. J.T.G. Hamilton, C.D. Murphy, M.R. Amin, D. O'Hagan, D.B. Harper, *Appl. Environ. Microbiol.*, 1997, (submitted).

147. P.K. Rathod, J.H. Fellman, *Arch. Biochem. Biophys.*, 1985, **235**, 435.

148. G. Zubay, Biochemistry (3rd ed.), Wm. C. Brown Publishers, 1993.

149. D.M. Hughes, R. Ostwald, B.M. Tolbert, *J. Am. Chem. Soc.,* 1952, **74**, 2434.

150. J.T.G. Hamilton, M.R. Amin, D.B. Harper, D. O'Hagan, *J. Chem. Soc., Chem. Comm.,* 1997, 797.

151. S.M. Klein, R.D. Sagers, *J. Bacteriol.*, 1962, **83**, 121.

152. E.B. Cunningham, Biochemistry, Mechanisms of Metabolism, McGraw-Hill Book Company, 1978.

153. C.A.Snith, E.J. Wood, Molecular and cell biochemistry, Biosynthesis, Chapman and Hall, 1992.

154. R. Naef, D. Seebach, *Helv. Chim. Acta*, 1985, **68**, 135.

155. J. Nielschalk, R.D. Bowden, D.B. Harper, J.T.G. Hamilton, C.D. Murphy, D. O'Hagan, *J. Chem. Soc., Chem. Comm.,* 1997 (submitted).

156. T. Kitazume, J.T. Lin, T. Yamazaki, *Tetrahedron Asymmetry*, 1991, **4**, 235.

157. C. Scolastico, E. Conca, L. Prati, G. Guanti, L. Banfi, A. Berti, P. Farina, U. Valcavi, *Synthesis*, 1985, 850

158. M. Shimizu, T. Yokota, K. Fujimori, T. Fugisawa, *Tetrahedron Asymmetry*, 1993, **4**, 835.

159. D. Seebach, J. Golinski, *Helv. Chim. Acta,* 1981, **64**, 1413

160. *Cf*.P. Caramella, N.G. Rondan, M.N. Paddon-Row, K.N. Houk, *J. Am. Chem. Soc.,* 1981, **103**, 2438

161. R. Fitzi, D. Seebach, *Angew. Chem., Int. Ed. Engl.*, 1986, **25**, 345

162. D. O'Hagan, J. White, D.A. Jones, *J. Label. Cpds. Radiopharm.*, 1994, **34**, 871

163 H. Yoshida, N. Arai, M. Sugoh, J. Iwabuchi, K. Shiomi, M. Shinose, Y. Tanaka, S. Omura, *J. Antibiot.,* 1994, **47**, 1165.

164. N. Fukuchi, A. Isogai, J. Nakayama, S. Takayama, S. Yamashita, K. Suyama, A. Suzuki, *J. Chem. Soc. Perkin Trans. 1*, 1992, 875.

165. N. Fukuchi, A. Isogai, J. Nakayama, S. Takayama, S. Yamashita, K. Suyama, J.Y. Takemoto, A. Suzuki, *J. Chem. Soc. Perkin Trans. 1*, 1992, 1149.